UNIVERSITÀ
DEGLI STUDI
DI PADOVA

UNIVERSITA' DEGLI STUDI DI PADOVA

FACOLTA' DI INGEGNERIA

DIPARTIMENTO DI PROCESSI CHIMICI DELL' INGEGNERIA

UNIVERSITE DE NICE-SOPHIA ANTIPOLIS

UFR SCIENCES

EQUIPE CHIMIE ORGANIQUE AUX INTERFACES

SCUOLA DI DOTTORATO DI RICERCA IN INGEGNERIA INDUSTRIALE

INDIRIZZO: Ingegneria Chimica

XXIV CICLO

ECOLE DOCTORALE DE SCIENCES FONDAMENTALES ET APPLIQUEES

DISCIPLINE: Chimie

SYNTHESIS OF FLUORINATED COMPOUNDS FOR BIOMEDICAL APPLICATIONS

Director of the School: Prof. Paolo Bariani

Director of the School: Prof. Hélène Politano

Supervisor :Prof. Lino Conte

Supervisor: Prof. Frédéric Guittard

PhD Student: Gennifer Padoan

To my Family

ABSTRACT

The aim of this work thesis was born by the importance of fluorinated compounds in biomedical field. The intrinsic properties of luorine provide to the fluorinated molecules extraordinary characteristics incomparable with the hydrocarbons pairs. An overview of the most important industrial biomedical applications of fluorinated amphiphilic and their evolution in the current years are provided and more particularly on blood substitutes, diagnostic agents, liquid ventilation, ophthalmic disorders. In the last years, the growth of retinal disorders in diabetic patients leads to investigate on the new products with the aim to improve long-term intraocular biocompatibility to use as vitreous tamponades after vitrectomy. Therefore, the first part of this work has been focalized on the search of ideal vitreous substitute to suitable in retinal detachment diseases.

Hence, a straight and economical methodology for the preparation of highly pure PFEs with general formula $F(CF_2)_m(CH_2)_2O(CH_2)_nH$ (m = 4, 6, 8 and n = 2, 3, 5, 8, 14, 18, 21) obtained by reaction of 1H,1,H,2H,2H-perfluoro-1-alkanols with 1-bromoalkanes under basic conditions were studied. This procedure have provided high pure products with yields than more that 65 %.

Then, physico-chemical properties such as specific gravity, refractive index, viscosity, solubility and amphiphile surface activity in a variety of solvents were evaluated. Therefore, their comparison with semifluorinated n-alkanes was estimated in order to investigate the role of both the ratio m / n and the ether linkage in determining the self-organizing behavior of these compounds. However, significant results in biomedical fields were obtained in particular for 4 of partially fluorinated ethers leading to industrial enterprise (Al.Chi.Mi.A S.r.l) to register a patent.

In fact, molecules with high purity degree, high biocompatibility, and suitable specific gravity values were obtained to use alone (short-term tamponade) or in mixtures of silicone oils (long-term tamponades) in ophthalmology field.

The growth of resistance displayed by many organisms to the bactericidal action of quaternary ammonium salts had also been leaded to develop new biocide agents having original chemical structures. The proposed mechanisms of bacterial action of these compounds are numerous and not completely clarified. However, the first step in all the presented mechanisms is related to the amphiphilic character of these molecules which allows them to strongly interact with the cellular membrane. Length of the aliphatic chain, number of carbon atoms in the aliphatic groups, introduction of fluorinated chain are also all

significant factors to provide specific amphiphilic properties in order to study the antimicrobial activity of Quats.

Therefore, in the second part of this work I have focalized my attention to the research of one structure that improves the physico-chemical properties in order to provide the adsorption on bacterial cell.

Hence, a series of hybrid surfactants F_nH_ms with general formula $F(CF_2)_nCH_2CH(OH)CH_2N(CH_2)_mH(CH_2)_mHX^-$ (with X= I, Br) obtained by reaction of semifluorinated tertiary ammine with iodoalkane in acetonitrile as solvent were synthesized.

Therefore, the influence of fluorocarbon / hydrocarbon chain lengths and counter-ion on physic-chemical properties and antibacterial activity were investigated.

An intensive physico-chemical characterization of amphiphilic molecules were carried out determining the critical micellar concentration, the superficial tension, the surface excess, the area per molecule, the hydrodynamic diameter, the micellar structures and shape of micelles by optical microscopy observations.

Rheological study by oscillatory-shear measurements were carried out in order to investigate the viscoelastic properties of some surfactants hydrogel solutions obtained as function of temperature, concentration, frequency, etc. Interesting results, in particular a thermo-responsive behavior, for some solutions were found leading to the use of these molecules in important industrial applications as drag reduction fluids.

RIASSUNTO

Lo scopo di questo lavoro di tesi è nato dall'importanza dei composti fluorurati in applicazioni biomediche. Le intrinseche proprietà del fluoro impartiscono alle molecole straordinarie caratteristiche, incomparabili con le omologhe idrocarburiche. Viene fornita, quindi, una panoramica delle più importanti applicazioni biomediche industriali di molecole fluorurate amfifiliche e la loro evoluzione nei correnti anni, in particolare riguardo i sostituti del sangue, agenti diagnostici, liquidi per la ventilazione assistita, malattie oftalmiche. Inoltre, negli ultimi anni, la crescita di malattie retinee in pazienti diabetici ha spinto a investigare su nuovi prodotti con lunga biocompatibilità intraoculare per una loro utilizzazione come tamponanti vitrei dopo vitrectomia. Quindi, nella prima parte il lavoro è focalizzato sulla ricerca di un sostituto vitreo ideale da sfruttare nelle malattie del distacco della retina. Pertanto, è stata fornita una rapida ed economica procedura per la preparazione di PFEs dotati di alta purezza di generica formula $F(CF_2)_m(CH_2)_2O(CH_2)_nH$ (m = 4, 6, 8 e n = 2, 3, 5, 8, 14, 18, 21) ottenuti dalla reazione di 1H,1,H,2H,2H-perfluoro-1-alkanoli con 1-bromoalkani in condizioni basiche. Questa procedura ha permesso di ottenere prodotti con rese superiori al 65%. Inoltre, sono state valutate proprietà fisico-chimiche come la densità, l'indice di rifrazione, la viscosità, la solubilità, l'attività superficiale in una serie di solventi. È stata effettuata anche una comparazione con n-alkani semifluorurati per investigare sia il ruolo del rapporto m / n sia il legame etereo nel determinare il comportamento di auto-organizzazione di questi composti. Quindi, sono stati ottenuti significativi risultati in campo biomedico in particolare per 4 eteri parzialmente fluorurati che hanno indotto una azienda industriale (Al.Chi.Mi.A S.r.l) a depositare un brevetto. Infatti, il lavoro ha permesso di ottenere molecole con alto grado di purezza, alta biocompatibilità e idonei valori di densità da poter essere utilizzati da soli (tamponanti a breve permanenza) o in miscele di olii di silicone (tamponanti a lunga permanenza) in campo oftalmico.

La crescita della resistenza mostrata da molti microrganismi all'azione dei sali di ammonio quaternari conduce inoltre lo sviluppo di nuovi agenti biocidi con una struttura chimica originale. I meccanismi proposti per l'azione battericida di questi composti sono numerosi e non completamente chiariti. Comunque, il primo passo in tutti i meccanismi presentati è relativo al carattere anfifilico di queste molecole che permette loro di interagire fortemente con la membrana cellulare. Lunghezza della catena alifatica, numero di atomi di carbonio in gruppi alifatici, introduzione di una catena fluorurata sono tutti significativi fattori per fornire specifiche proprietà anfifiliche per lo studio dell'attività antimicrobica dei

Quats. Pertanto, nella seconda parte il lavoro è improntato sulla ricerca di una struttura tale da fornire proprietà chimico-fisiche per favorire l'assorbimento sulla cellula batterica.

Quindi, è stata sintetizzata una serie di tensioattivi ibridi F_nH_ms di generica formula $F(CF_2)_nCH_2CH(OH)CH_2N(CH_2)_mH(CH_2)_mHX^-$ (con X= I, Br) ottenuti dalla reazione di un'ammina terziaria parzialmente fluorurata con iodoalkani in acetonitrile come solvente.

In seguito, sono stati studiati l'influenza delle catene fluorurate / idrocarburiche e il contro ione sulle proprietà chimico-fisiche e l'attività antibatterica. È stata condotta inoltre un'intensa caratterizzazione delle molecole amfifiliche determinando la concentrazione micellare critica, la tensione superficiale, la superficie di eccesso, l'area per molecola, il diametro idrodinamico, la struttura e la forma delle micelle, osservazioni microscopiche.

È stato compiuto uno studio reologico attraverso misure di taglio-oscillatorio per investigare le proprietà viscoelastiche di alcune soluzioni di tensioattivi in forma di idrogel, effettuate in funzione della temperatura, concentrazione, frequenza, etc. Interessanti risultati, in particolare un comportamento termo-reattivo, sono stati trovati per alcune soluzioni tali da poterli indicare in importanti applicazioni industriali quali i fluidi di riduzione alla resistenza di attrito in un flusso turbolento.

RESUME

L’objectif de cet travail de thèse est né de l’importance de composés fluorées dans le domaine biomédical. Les propriétés intrinsèques du fluor fournissent des caractéristiques extraordinaires à des molécules fluorées incomparables à ceux des molécules hydrocarburés.

Un aperçu des plus importantes applications biomédicales industrielles des molécules amphiphiliques fluorées et leur évolution pendant les années en cours on été étudiées et plus en détail sur les remplaçants de sang, agents diagnostiques, ventilation liquide et maladies ophtalmiques.

Pendant les dernières années, la croissance des maladies rétiniens dans le patients diabétiques a conduis à étudier des nouveaux produits dans le but de améliorer la biocompatibilité intraoculaire à long terme pour la leur utilisation comme tamponnages vitreux après vitrectomie.

Par conséquence, dans la premier partie le travail de thèse a été focalisé sur la recherche du substituts vitreux idéaux pour leur utilisation dans les maladies du détachement rétinien.

En fait, une méthodologie rapide et économique pour la préparation des PFEs avec la formule général $(CF_2)_m(CH_2)_2O(CH_2)_nH$ (m = 4, 6, 8 et n = 2, 3, 5, 8, 14, 18, 21) obtenus par réaction du 1H,1,H,2H,2H-perfluoro-1-alkanols avec 1-bromoalkanes sous conditionnes basiques est fourni. Cet procédure a fournis des produits très pures avec des rendements de plus de 65 %. Ensuite, les propriétés physico-chimiques telles que la densité, l’indice de réfraction, la viscosité, la solubilité et l’activité superficiel amphiphilique dans un grand choix de solvants ont été étudiées. Ensuite, leur comparaison avec des n-alkanes partiellement fluorées ont été évalués afin d’étudier le rôle du rapport m / n et de le liaison éther en déterminant le comportement à organisation autonome de ces derniers composés. Puis, dés résultats significatifs dans le domaine biomédical ont été obtenus en particulier pour 4 éthers partiellement fluorés en collaboration avec une entreprise industrielle (Al. Chi. Mia S. r. l) pour enregistrer un brevet. En fait, des molécules avec un degré très élevé, haut biocompatibilité et valeurs appropriées de densité ont été obtenus pour employer seul (tamponnage à court terme) ou dans les mélanges des huiles de silicone (tamponnages à long terme) dans le domaine ophtalmologie.

La croissance de la résistance montrée par beaucoup d'organismes à l'action bactéricide des sels d'ammonium quaternaire a eu également lieu pour développer des nouveaux agents de biocide ayant des constituants chimiques originales. Les mécanismes proposés de l'action bactérienne de ces composés sont nombreux et pas complètement clarifiés. Cependant, la première étape dans tous les mécanismes présentés est liée au caractère amphiphilique de

ces molécules qui leur permet d'agir l'un sur l'autre fortement avec la membrane cellulaire. La longueur de la chaîne aliphatique, le nombre d'atomes de carbone dans les groupes aliphatiques, introduction de chaîne fluorée sont également tous des facteurs significatifs pour fournir des propriétés amphiphiliques spécifiques afin d'étudier l'activité antimicrobienne de Quats.

Par conséquence, dans la deuxième partie de mon travail de thèse a été focalisé sur la recherche d'une structure capable d'avoir des propriétés physico-chimiques pour améliorer l'adsorption des molécules sur la surface de la cellule bactérienne. Par conséquence, une série d'agents tensio-actifs hybrides F_nH_ms avec la formule général $F(CF_2)_nCH_2CH(OH)CH_2N(CH_2)_mH(CH_2)$ (avec X= I, Br) obtenu par la réaction de l'amine tertiaire semi-fluorée avec l'iode-alkane en acetonitrile comme dissolvant a été synthétisée. Par conséquence, l'influence des portées de fluorocarbure/hydrocarbure et du compteur-ion sur des propriétés de médicament-produit chimique et de l'activité antibactérienne ont été étudiées. Une caractérisation physico-chimique intensive des molécules amphiphilique a été effectuée pour déterminer la concentration micellaire critique, la tension superficielle, l'excès extérieur, le secteur par molécule, le diamètre hydrodynamique, les structures micellaires et la forme des micelles par observations optiques de microscopie.

L'étude rhéologique par des mesures d'oscillant-cisaillement ont été effectuées afin d'étudier les propriétés viscoélastiques des solutions d'hydrogel de quelques agents tensio-actifs obtenues comme fonction de la température, de la concentration, de la fréquence, etc. Intéressants résultats, en particulier un comportement thermo responsive, pour quelques solutions ont été trouvés ce qui peut conduire à l'utilisation des ces molécules dans des applications industrielles telles que des fluides de réductions.

INTRODUCTION

FLUORINATED COMPOUNDS FOR BIOMEDICAL APPLICATIONS

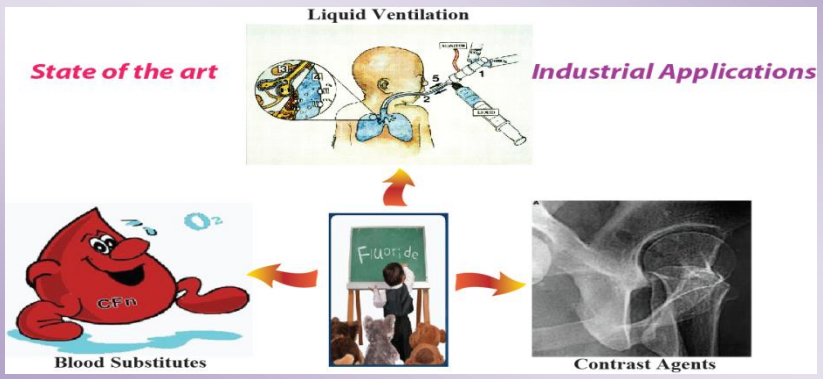

CHAPTER 1

PARTIALLY FLUORINATED ETHERS

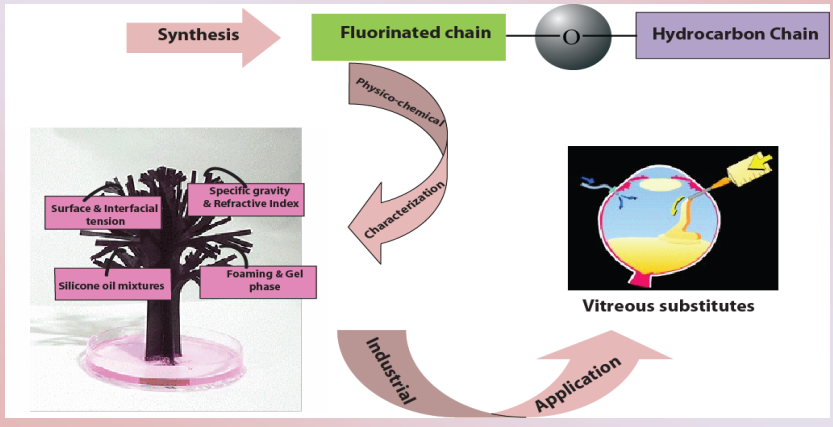

CHAPTER 2

PARTIALLY FLUORINATED QUATERNARY AMMONIUM SALTS

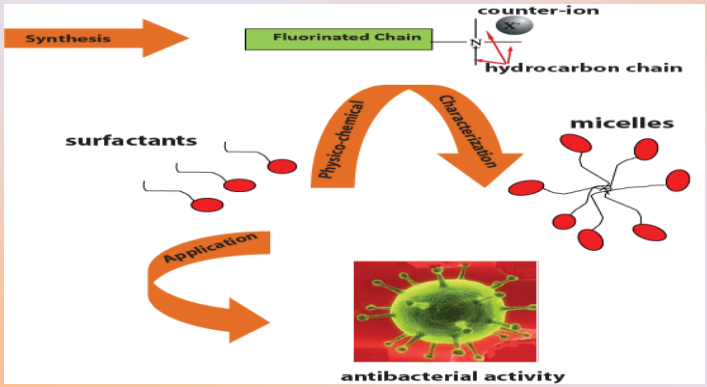

Contents

Introduction

1 Fluorine and fluorinated compounds

Fluorine is one of the most abundant halogens ranking 13th in order of frequency of the elements in the earth's crust (carbon ranks 14th). It is seldom found in mineral compounds, as fluorite, in plants as mono or di-fluorinated toxic compounds. Otherwise, no natural perfluorocompounds or fluorinated moieties have, as yet, been found. Consequently, Nature left a wide field open for chemists to develop their own.

Abundant literature exists on investigations about perfluorocarbons (PFCs) in relation to life sciences and biomedical issues. Highly fluorinated compounds and moieties can allow unique functional modifications of natural compounds and offer surrogate means of molecular recognition and selection, as well as provide unique microenvironments unknown to nature.

The unexpected potential of molecules containing fluorine in medicinal chemistry was recognized by researchers. However, the replacement of C–H or C–O bonds with C-F has extraordinary advantages. Introducing fluorine into a molecule tends to generate novel behaviors with unmatched performances.

The importance of fluorine in medicine born in 1953 by the publication of pioneer work of E. Fried [1] about the preparation 9α-fluoro idrocortisone acetate: it is the first application of selective fluorination to modify biological activity of substances [2]. He demonstrated the potential importance of fluorine substituent in order to enhance the efficacy of drugs throughout a number of noteworthy studies. Then, Sir Rudolph Peters was one of the first to study the toxic effects of fluoroacetic acid. Its mechanism of action is based on inhibition of the citric acid cycle, the main source of metabolic energy in all animals.

The high reactivity of fluorine demanded special experts and technologies, obstructing a rapid expansion [3]. Thereafter, the invention of electrophilic fluorinating agents and the strategies to tame high reactive have contributed to the rapid evolution of this field.

In this chapter, characteristic physico-chemical properties associated with the incorporation fluorine-containing groups to organic molecules are described in detail based on the most updated literature sources.

1.1 Physico-Chemical properties of C-F bond

The driving force of fluorinated compounds are imputable to the intrinsic characteristics of the fluorine. As seen from its position on the periodic table of elements, fluorine atom is

bigger, more electronegative (4.1 for fluorine versus 2.2 of hydrogen) and less polarizable than hydrogen atom.

The C-F bond (van der Waal radius estimated at 1.47 Å) is more isosteric that the C-O bond (van der Waal radius estimated at 1.52 Å) and the C-H bond (van der Waal radius estimated at 1.20 Å). Perfluorocarbon chains are more rigid than hydrocarbons and their cross section (30 $Å^2$ versus 20 $Å^2$ of hydrogen) leads to have helical structures rather than planar zig-zag structures of hydocarbons. The mean volume of CF_2, CF_3 groups are 92 $Å^3$, 38 $Å^3$ respectively, versus 27 $Å^3$ of CH_2 and 54 $Å^3$of CH_3.

The presence of fluorinated chains in molecules increases the polarity because the strong electron-withdrawing of F-chains creates or amplifies a dipole [4].

Free conformation of PFCs is very strongly reduced with high trans / gauche interchange energy (4.6 kJ mol^{-1} versus 2.0 kJ $mol^{-1}$of hydrogen) which facilitates stacking and ordering.

The chemical structure and the weak intermolecular interaction are responsible for the particular properties of fluorinated compounds including low surface tension, dielectric constant, refractive index, high densities (due to their high molecular weight), viscosity and gas solubility that are the largest known especially for fluorinated liquids. The very low cohesiveness provides also lower van der Waals interactions between pairs of CF_2 groups and leads the liquid fluorinated compounds like nearly ideal gas.

Therefore, the structure of fluorocarbon / hydrocarbon liquids depends essentially on the molecular shape of fluorinated chains because the presence of fluorine atoms, bigger than hydrogen atoms into a carbon chain, leads to irregular molecular shape. Hence, it produces numerous large-sized cavities in the liquid, providing lower boiling points and higher viscosity of these compounds, and their ability to dissolve large quantity of gases compared with hydrocarbon pairs [5].

The high electronegativity of fluorine was used also to develop enzyme inhibitors and to render molecules resistant to chemical degradation. In fact, the replacement of fluorine into a molecule introduces minimal steric alterations leading to facilitate interactions of a fluorinated biomolecules with enzyme active sites, receptor recognition sites, transport mechanisms, and other biological systems [5, 6].

1.2 Production of fluorinated compounds

Perfluorocarbons were obtained initially by the reaction of graphite with fluorine gas. In fact, on the laboratory scale the production of PFCs occurs with the control of radical reactions by appropriate solvents leading to a selective fluorination.

Instead, they were synthesized industrially by substitution of hydrogen atoms with fluorine atoms in an organic compound, using electrochemical fluorination, halogens exchange between chlorocarbons and hydrogen, reaction with heavy metal fluorides (CoF_3, AgF_2 or MnF_3) or by direct action of molecular difluorine.

During the Manhattan Project the industrial scale procedure was developed for the synthesis of perfluorocarbons using cobalt trifluoride [7]. This process is commercialized now by F_2 Chemicals as "Flutec" process [8]. These are all exothermal processes that can lead to a lot of mixtures. Industrially, halogen exchange method, called *Finkelstein synthesis*, provides only products with 98 % of purity. Electrochemical fluorination was also developed during the Manhattan Project by J. H. Simons and coworkers and provides, also now, products with high purity.

Another method to obtain highly pure materials is telomerization: this technique consists of tetrafluoethylene polymerization [3]. Then, the precursors obtained are assembling in small building blocks.

2 Fluorinated compounds in biomedical field

Fluorinated molecules and their derivatives represent a very interesting and stimulating class of chemicals in the physical chemistry and polymer science due to their specific and unusual properties. In fact, fluorinated chains are more hydrophobic, lipophobic than the hydrocarbon analogs leading to a favorable self-aggregation, molecular organization, phase separation and the exclusion of non-highly fluorinated solutes. Due to all these properties PFCs are used in a wide area of industrial applications as surfactants in supercritical solvents [9, 10], environmental probes [8], anticorrosive [11] and antifriction components [12], as flame retardants [13], water repellents [14], in paints and coatings [15], polymer technology [16], metal working [17]. Then, the combination of low polarizability, electroattracting character of fluorine and the strenght of C-F bond lead to high thermal stability and chemical inertness, candidating these molecules for biomedical applications. However, in the biomedical areas most of the relevant applications are based on the large gas solubility of fluorinated compounds: in fact, perfluorocarbons dissolve relatively high concentrations of gases, for example, 100 mL of perfluorodecalin at 25 °C will dissolve 49 mL of oxygen at STP (standard temperature-pressure). However, the ability to dissolve high concentrations of oxygen has also led to the use of perfluorocarbons in so-called "artificial blood" as oxygen therapeutics which function as artificial erythrocytes, serving to transport and deliver oxygen in the body. In fact, perfluorocarbons accelerate nitrogen washout after venous gas emboli. Success in the treatment of decompression sickness has been shown in rat, swine, and hamster models. This treatment shows great potential as a future adjunctive therapy for decompression sickness in humans.

Therefore, perfluorocarbons have been used in "liquid breathing" where the perfluorocarbon is breathed into the lungs instead of air. Several perfluorocarbons were also commercialized as medical purposes including ultrasound diagnostic imaging [18], ophthalmic applications [19], magnetic resonance image [20], etc.

Anti-tumoral agents, and lubrication and cushioning for articular disorders, drug and cosmetic formulations and delivery are other biomedical applications.

Therefore, the interesting increase of fluorine compounds in diagnostic field is due because in human body there is no fluorine. Then, the introduction of fluorinated compound permits to determine exactly where the product has gone and to use the intrinsic properties of fluorinated compounds to analyze in a better manner specific zones of human body. Furthermore, in radiographic imaging the perfluorocarbon derivative, as

perfluorooctylbromide (PFOB), is employed as this is more opaque to X-rays. Hence, fluorine is a valuable probe for structure determination due to favorable X-ray scattering and NMR.

Perfluorocarbons are also used in contrast ultrasounds to improve ultrasound signal backscatter. Then, perfluorocarbons can be used in magnetic resonance imaging (MRI), though this is not as common. Usually MRI is set up to detect hydrogen nuclei, but it is also possible to use MRI for 19-fluorine nuclei.

In particular, NMR studies show that the structure of the fluid, rather than attractive oxygen-fluorine forces, seems to play a predominant part in oxygen solubility.

The specific properties of perfluorocarbons, fluoro-chains, fluoro-surfactants, F_nH_m diblocks and fluorinated colloids relevant into biomedical purposes include chemical and biological inertness, strong hydrophobic and lipophobic properties, high gas solubilities, low lipid solubilities and very low water solubility, and outstanding surface characteristics.

These properties are discussed in detail for the most important applications, as well as the biochemical and biomedical uses of PFCs and highly fluorinated amphiphiles, and more particularly oxygen delivery (blood substitutes), diagnostic agents, liquid ventilation. The principal industrial products are also reported and their evolution in the current years.

2.1 Blood substitutes

Blood substitutes are fluids used to transport oxygen around the body. They are used as cell-free oxygen carriers, oxygen therapeutics, red cell substitutes [21, 22]. The useful shelf-life of blood or red cells is only 42 days max (35 days in the UK); this have served as a stimulus to develop a synthetic substitute for human blood, more specifically for development of a red blood cell substitute.

These efforts have essentially focused on the ability of red blood cells to carry oxygen. Today, we need blood substitutes for an increase in the number of elective surgeries, for public opinions on virus transmission (HIV), for life insurance issues, for new blood born diseases and also the cost of safe transfusion in developing world.

We can use blood substitutes as coupling with autologous blood, as supporting transfusion service in developing countries or alternative to blood transfusion for patients with religious objections.

There are essentially two categories of blood substitutes: biometric and abiotic. Biometric (hemoglobin-based) compounds mimics nature’s way of delivering oxygen to the body’s tissues. Hemoglobin (human, bovine or genetically engineered), usually modified with intra-

molecular cross-linked, polymerized, grafted onto polymers or encapsulated, is used in order to give the essential biological properties of natural hemoglobin in red blood cells [23, 24].

Figure 1: rat breaths normally in a satured PFC solution

Abiotics are synthetic chemicals compounds able to deliver oxygen to the tissues. Among abiotics compounds, the most important are perfluorocarbons (PFCs). They are chemically inert, heat stable, linear, cyclic or polycyclic fluorine substitutes. The hyperfluorination of organic compounds leads also a complete lack of metabolism *in vivo* [25]. The interest in PFCs as blood substitutes was born in 1966 when Leland C. Clark, Jr. and Frank Golan [26, 27] discovered the capacity of PFCs to dissolve gases with covalent binding. In their work they demonstrated that a rat can breathe normally if it is immersed in a saturated solution of PFC at atmospheric pressure.

PFCs are able to dissolve large volumes of O_2 (45 mL per 100 mL), CO_2 (>200 mL per 100 mL), N_2 and other non polar gases.

PFC liquids are immiscible with aqueous systems, blood and other body fluids, but can be injected intravenous in an emulsified form containing a dispersion of fine particles, suspended an isotonic electrolyte solution.

Solubility of O_2 is independent of temperature and the quantity of gas dissolved in PFC emulsions is linearly related with partial pressure pO_2 approximating to Henry's Law [25].

While blood exhibits a sigmoidal oxygen dissociation, perfluorocarbon emulsions are characterized by a linear relationship between oxygen partial pressure and oxygen content. Elevated arterial oxygen partial pressures are thus beneficial to maximize the oxygen transport capacity of perfluorocarbon emulsions [28].

The unloading at the tissues is facilitated because they are O_2 carriers without chemical bonding and they transport a lot of oxygen like blood under hyperoxic conditions.

To use PFCs as blood substitutes, it is important that the compounds have a similar viscosity to blood, an adequate arterial pH and intravascular persistence, a long-term storage and easy to use. PFC emulsions injected in bloodstream also increase solubility of oxygen in plasma phase [27].

Another fundamental condition to apply PFC emulsions is the stability for long periods. The stability of an emulsion, surface area available for a gas exchange, the viscosity, intravascular half-life are influenced by the proportion of the various components and by the size of the particles.

Ostwald ripening is responsible for the irreversible particle growth in PFC emulsions and the low interfacial tension and low solubility of PFCs can counteract the growth of particle.

However, the smaller droplets of PFC have higher chemical potential due to higher curvature and grow to form larger droplets with smaller curvature.

The Lifshitz–Slezov equation (eq. 1) control droplet growth though molecular diffusion [29]:

$$\omega = \frac{d\overline{r^3}}{dt} = \frac{8V_m CD\gamma_i}{9RT} f(\varphi) \quad (1)$$

where $\overline{r}^3$ is the droplet volume, C the solubility, γ_i the interfacial tension and D the diffusibility of the PFC in the aqueous phase with V_m mole volume of the PFC and f (φ) is volume fraction. In this way, size of particle plays important role also in the efficacy of fluorocarbon.

In order to improve the stability of fluorinated emulsions at room temperature, two PFCs are used. The second PFC added is a perfluorocarbon (perfluorodecylbromide [27]) with a higher molecular weight. The former fluorocarbon is less soluble in the continuous aqueous phase than the latter, and has nevertheless an acceptably fast excretion rate [30]. Also, fluorosurfactants agents can be used to improve emulsion stability but a large dose cause excessive organ retention. Then, fluorocarbon-hydrocarbon diblocks used with phospholipids lead to an effective stabilization of emulsions [31], primarily locating at the interface between the fluorocarbon droplets and the film of phospholipids that surrounds them.

US Food and Drug Administration identified specific clinical targets for potential blood substitutes and approved the use of fluoro-octyl bromide, called also Perflubron ($C_8F_{17}Br$), perfluorooctylethane ($C_8F_{17}C_2H_4$), perfluorodecaline ($C_{10}F_{18}$) bis(perfluoro-butyl)ethene ($C_4F_9CH{=}CHC_4F_9$), perfluorodichlorooctane ($C_8F_{16}Cl_2$), perfluoro-methylisoquinoline ($C_{10}F_{19}N$) even with the use of modern nutrient additives (e.g. mannitol, glucose, adenine). Principal linear perfluorocarbon used is Perflubron; it dissolves oxygen more effectively than cyclic molecules as perfluorodecaline [22, 32]. Perflubron and perfluorodecalin are synthesized to a very high degree of purity in good yields; they present specially low levelly of toxic impurities reducing the risk of unwanted side-effect and physiological response frequently attributed to partially-fluorinated contaminants [21].

Fluosol (GreenCross, Japon) was the first generation of PFC emulsions. It was composed by 14 % (w/v) perfluodecalin, 6 % (w/v) perfluorotri-n-propylamine and Pluronic F-68 egg yolk phospholipids and potassium oleate as surfactants.

The second-generation of perfluorocarbon emulsions was developed by Alliance Pharmaceutical Corporation (San Diego, California, USA). The concentrated (60 % w/v) called Oxygent, composes of 58 % w/v perfluorooctyl bromide and 2 % w/v perfluorodecyl bromide, with an average particle size of 0.16–0.18 μm diameter. Oxygent has a 2-year shelf life and a 12 – 48 hours half-life at standard refrigeration temperature (SRT = 5 - 10 °C) [33]. Oxyfluor, a concentrated (40 % v / v), was developed by Hemagen / perfluorocarbon (St Louis, Missouri, USA). It is composed by perfluorodichlorooctane, egg yolk phospholipid and triglycerid with an average particle size of 0.22 – 0.25 μm diameter [34].

A new generation of PFC are the Ftoran® type (Ftoremulsion III) developed by Russian Academy of Natural Sciences [35]. Ftoremulsion III composed by 20 vol % PFC concentration has a total oxygen capacity (gas-dissolution 7 vol %) 2.5 times less than O_2 capacity of blood but it is a positive blood - tissue gas balance between the total mass flow of O_2 from blood into tissue and of CO_2 in the reverse direction. In this way, PFCs contribute to extract CO_2 from tissues and to transport it to the lungs for adjusting blood gas-transport properties. PFCs with a lipophilic function, as a halogen or short hydrocarbon segment in the molecule, can accelerate the excretion, which increased by an exponential function of molecular weight.

To improve a reduction of particle's size, a new generation of microemulsion was developed using mixed fluorinated and hydrogenated oil along with biocompatible hydrogenated surfactant (Montanox 80) [31] which increased solubility of oxygen more than Fluosol.

The new technique uses the properties of surfactants to form micellar aggregates in water and oils resulting in stable microemulsions.

Over the last few years there were a continuous research toward developing new emulsifying agents having great stability and broader utility in many medical issues.

2.2 Liquid ventilation

In patients with inhalation injury and with the risk of iatrogenic injury, mechanical ventilation is necessary [36-38]. The use of conventional mechanical ventilation in this setting requires the use of high rate-pressure products to attain adequate minute ventilation. The unique chemical-physic properties candidate perfluorocarbons as liquids ventilation in a treatment for respiratory distress syndrome in adults and may thus be useful in lung surfactant replacement compositions for neonates [39, 40]. In partial liquid technique, the

perfluorocarbon is installed into the lung via trachea that is ventilated by gas. The PFC acts as an alveolar-capillary membrane through which oxygen and carbon dioxide diffuse. The fundamental properties to apply PFC as liquid ventilation are low kinematic viscosity, immiscibility with water and a low surface tension. PFC have very low surface tension (15-20 mN m^{-1}) but the value become lower in conjunction with lung surfactants (2-5 mN m^{-1}) [41]. In fact, a less cohesive material, such as a PFC takes less energy to create a hole and the cohesive energy density, called Hildebrand parameter, is very low and very similar to Oxygen (5.7 for O_2 and 6 for PFC, 7-9 for HCs and 23.5 for water) [29]. Hence, PFCs behave like gas-like fluids.

Perfluorooctylbromide was used as liquid ventilation allowing an efficient and homogeneous gas exchange at low inflating pressures and the administration of drugs by the pulmonary route. It has a positive spreading coefficient on saline dispersing spontaneously over the pulmonary membrane.

It can use to remove edema fluids while improving gas exchange and lung mechanism.

Costa-Gomez was able to measure O_2 solubility as in several fluorinated liquids of medical grade as a function of range temperature biomedical applications [42]. However, only the combination of O_2 / CO_2 solubilities and biological inertness candidate PFC as O_2 carries.

An emulsion of dodecafluorepentane, called ‘phase-shift’, with a very low boiling point (29 °C) initially used as a contrast agent for ultrasound imaging, is now being investigated for O_2-delivery [43]. It turns into gaseous microbubbles at body temperature leading to a fast permeating gases inside the bubble and a good equilibrium between the gas exchange (O_2 and CO_2) allowing the transport of O_2 from the lungs to the tissues. PFCs were used also to prevent formation of a liquid condensed phase in a phospholipid film.

In the last decade PFCs are used also as lung surfactant substitutes to pulmonary surfactant (PS) preparations for therapy distress syndrome [44]. Pulmonary surfactants are located into alveolus surface of mammalian lungs and are necessary to create an interfacial barrier against pathogens and a biophysic activity across the alveolar fluid. This biophysic activity consists into exhibit a rate of surface adsorption matching the rapid expansion of air–liquid interfaces in the lung during the first breaths, and subsequently during the inspiration phase of each ventilator cycle throughout life. The adsorption process should generate an equilibrium surface tension of about 25 mN m^{-2}. Second, the surfactant film should reduce surface tension to nearly 0 mN m^{-2} during surface compression, to prevent alveolar collapse and maintain the patency of terminal bronchioles at end-expiration. Third,

they must be effective replenishment of surfactant molecules at the air–liquid interfaces during surface expansion, ensuring that maximum surface tension does not rise much above the equilibrium level (low maximum surface tension reduces the work of breathing). These properties of lung surfactant, originally defined on the basis of *in vitro* surface tension measurements and theoretical considerations, are indeed expressed in the terminal air spaces, as can be shown by placing droplets of test fluids with known surface tension on the alveolar surface and observing changes in the shape of the droplets during various phases of a 'quasistatic' ventilatory cycle. PS are used to prevent alveolar collapses at the end of expiration and to minimize of work of breathing by reducing surface tension at the alveolar surface during the respiration activity. During surface compression the pulmonary surfactants can reduce surface tension at very low values. There is a formation of a surface balance in which surface tension is recorded as traction force on a dipping plate or by pulsating bubble surfactometer measuring contractile forces recorded in an open bubble oscillating in the sample fluid. Surface area can be changed with a moveable barrier. This surface balance is called *Langmuir–Wilhelmy balance* [45]. However, the significative low value (2 - 5 mN m^{-1}) of surface tension demonstrates the very hydrophobic character of pulmonary surfactants [41, 46].

Neonatal respiratory distress syndrome is caused by deficiency of these surfactants. Gerber and co-workers have recently examined the fluidization of dipalmitoylphosphatidylcholin, formed by a semi-crystalline monolayer during compression of a monolayer of the phospholipids, using perfluorooctylethane [47]. Recently Biochemicals Inc. (Ontario, Canada) developed BLES® surfactant, Chiesi Farmaceutici (Parma, Italy) Curosurf® surfactant. Both these surfactants have showed very optimal biocompatible and biophysical properties [48, 49].

The miscibility between fluorinated surfactants and biological surfactants are extensively studied because it can have deleterious effects during respiration. A lot of investigations are carried out about the influence of dipalmitoyphosphatidylcholines (DPPC) chain length on miscibility binary lung surfactants mixtures [50-52]. DPPC is one of the surfactants components necessary to low surface tension. Recently, it is studied the use of partially fluorinated amphiphiles ((perfluorooctyl) pentanol / undecanol) to improve the efficiency of the PS preparation for treatment of neonatal respiratory distress syndrome (NRDS) [53-55]. More recently fluorocarbon hydrocarbon cationic lipid and its mixtures with a phospholipid were investigated in the formulation of lung surfactants [39].

In this way, the water in the lungs can be sucked out because it is lighter than perfluorocarbon.

2.3 Contrast agents for ultrasound imaging

Ultrasound is the low cost, non-invasive imaging technique and most frequently used for diagnostic of numerous pathologies. An elevate activity is currently focused on perfluorocarbon-based microbubbles thanks to a large market of medical products commercially available [56].

Since the end of 1970s PFCs are tested as ultrasounds contrast agents (USCa) and magnetic resonance imaging (MRI). Ultrasound contrast agents are useful when contrast between tissues is insufficient to allow reliable and accurate diagnosis. In 1977 perfluorooctylbromide was used as contrast agent for gastroenterography [57].

The contrast agent is injected through a peripheral vein and has the ability to pass unimpeded through the pulmonary circulation. The agent must remain intact in the blood stream for an extended period of time to allow adequate scanning of the organ of interest. Since the average diameter of lung capillaries is between 4 μm to 7 μm, in order to avoid potential capillary embolism, the size of bubbles contrast agents should be smaller than approximately 4 μm.

The injectable sound scattered is a little gas bubble, which is highly compressible and reflects sound waves several orders of magnitude more effectively than red blood cells.

One of the first ultrasound fluorinated contrast agent, in the form of microbubbles, was *Optison*® launched in 1998 by Molecular Biosystems, Inc. (San Diego, CA). It was constituted by a suspension of perfluoropropane microspheres (2 - 4.5 μm) and a shell of human albumin [58]. Another perfluoropropane dispersion (1 - 3.3 μm), *Definity*®, with a phospholipid coating constituted by dipalmitoylphosphatidylcholine (DPPC), a methylPEG dipalmitoylphosphatidylethanolamine and a minor amount of negatively charged dipalmitoylphosphatidic acid, has been licenzed in 2001 by Dupont Phamaceutical Co. (North Billerica, Ma, USA). An aqueous suspension of stabilized SF_6 microbubbles, called Sonovue® was developed by Bracco (Milan, Italy) [33, 59].

A microbubble based-fluorohexane constituted of phospholipids-coated nitrogen is Imagent® developed by Alliance Pharmaceutical Corp. [60].

The combined action of arterial blood pressure and surface tension γ forces the air out of bubble leading to collapse of the micro-size bubbles. It need to control the bubble size and inhibit the growth. Hence, they must be highly deformable soft shell.

Fluorocarbons provide the unique combination of low solubility in water and high vapor pressure necessary to achieve bubble stabilization.

When microbubbles are injected into the circulation, they dissolve rapidly in the blood under the combined actions of the blood pressure and the Laplace pressure.

Fluorocarbon can oppose the dissolution of gaseous bubbles in the blood providing to the osmotic equilibrium between the Laplace pressure ($\Delta P = 2\gamma / r$), arterial pressure, oxygen metabolism, and ultrasound waves. In this way, the combined action of air and PFCs lead to a stable micro-bubbles due to counterbalances between the partial pressure of fluorocarbon, surface pressure and blood pressure (Figure 2). Hence, the rates of water-soluble gases in and out of bubble become equal and an osmotic equilibrium is formed.

The osmotic agents used must have a low water solubility and high saturated vapor pressure at body temperature. The gas inside the bubble must be less soluble in the blood than air leading perfluorocarbons to be obvious candidates. However, the micro-bubbles must be stable enough to provide an accurate imaging and they must have an adequate diameter to provide effective scattering intensity and to cross capillary beds.

Kabalnov *et al.* have developed a model to predict the stability of emulsions [60]. The stability depends critically on the nature of the surfactant and it is controlled by the free penalty energy E_p, associated with nucleation of a critical hole in an emulsion film (eq. 2):

$$E_p = -4\pi\bar{k} + 7.0k + \frac{35{,}7k^{\frac{3}{2}}}{\gamma_i^{\frac{1}{2}}} H_0 \qquad (2)$$

The free energy penalty is dipendent to the monolayer spontaneus curvature H_0, created by surfactant, to interfacial tension (γ_i) equilibrium between the oil and water phases at the balance point (H_0= 0), to monolayer bending k and saddle splay moduli $\bar{k}$. However, the emulsion will be unstable for negative values of H_0 and stable for positive values. Hence, the surfactants with a rigid structure can enhance the stability near of balance point H_0= 0. The spontaneus curvature of natural phospholipids at oil/water interface can be modify by fluorinated compounds to reach the balance. Porous microspheres, constituted by dimyristoyl phosphatidylcholine, hydroxyethylstarch, sodium chloride and phosphate buffers under a nitrogen-diluted fluoro-hexane atmosphere, were used as contrast agent by Alliance and Schering AG (Berlin, Germany). Microbubble contrast agents have a unique property to interact with sound waves. The response of these microbubbles to ultrasound is constituted of an harmonic and sub-harmonic sound waves in opposite of the blood or other tissues that have a linear response.

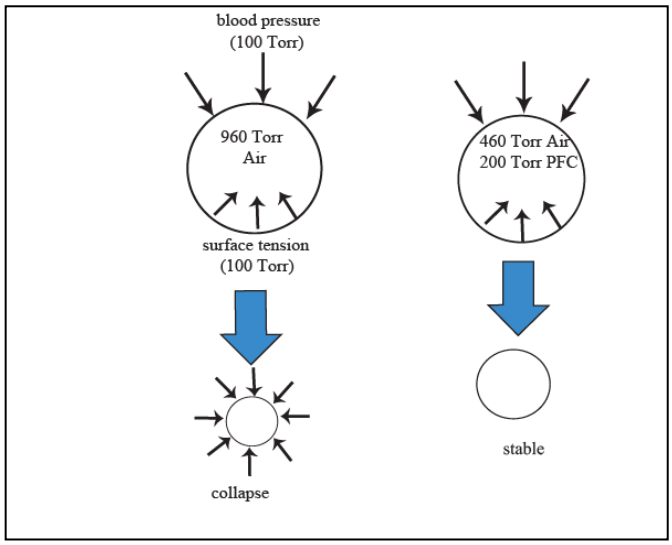

Figure 2 counterbalances between the partial pressure of fluorocarbon, surface pressure and blood pressure

A lot of works focus on gaseous PFCs, but the difficulty to control the size of bubbles leads recently to use also liquid PFCs; they are more resistant to pressure changes and mechanical stresses. Most of radiopaque agents are hydrosoluble and they have a very short intravascular persistence owing their rapid diffusion in the tissues but it is very short time to deep examinations. Hence, for accurate examination of numerous pathologies, for instance lymph node imaging, and to improve accurate treatment, it is necessary to use fluorocarbon emulsions. They accumulate in the regional lymph nodes and the different degree of contrast allow the distinction of normal, hyperplastic and neoplastic nodes.

A limit of these compounds is the fluorophilicity rendering them insoluble and potentially toxic in aqueous environments. They must be injected as emulsions. The formulation of stable emulsions in aqueous environments is thus with lipid surfactants and must be necessary easily to apply and with a long-term storage.

However, an emulsion of perfluoropentane, called EchoGen®, was developed by Pharmaceutical® in 1994. It was very efficient to produce opacification of the left ventricule and myocardium with a very low dose. Emulsions of perfluorohexane with a mixture of phospolipides were also used to detect macrophages that play a crucial role in the development of atherosclerotic. However, an efficacy product, Fluosol-DA, was developed by Green Cross Corp (Osaka, Japan) but it must be stored frozen and the emulsion must be mixed immediately before use. Another formulation, PHER O_2, very stable and easier to inject, was developed by Sanguine Corp. (Pasadena, Ca) [61]. Some works focused on the substitution of lipid coating with a polymeric coating (PLGA) to encapsulate and stabilize the PFC. In this way, the polymeric coating, already approved for human use, is degraded and metabolized in vivo; there is the possibility to create specific covalent bond or other active agents targeted in vivo by antibodies or ligands, retaining large PFC payloads [62]. In the last years the focus of researchers is on to find emulsions with a diameter much less than 4-5 μm. In fact, it was thought emulsions of large size remain trapped in pulmonary

capillaries and could not pass from the right side to the left side of the heart. It is developed nanoemulsions of PFCs offering the potential for extravascular diagnosis [63]. Novel nanoemulsions with particle size of 160-190 nm were used for cellular imaging, labed a wide range of cell types and the cell trafficking can be monitored in vivo by ^{19}FMRI [64].

2.4 Biocompatibility

Medical applications of PFCs require high purity perfluorocarbons. Hence, infrared spectroscopy, nuclear magnetic resonance and cell cultures can be used to test the biocompatibility of the perfluorocarbons.

Particular attention is used to environmental issues associated to the use of fluorinated compounds since if they are injected in the vascular space, they are not metabolized and excreted unmodified in the air. Because of there are also no microorganisms developed against the fluorinated compounds injected, the environment protection agency retains the risk of these products insignificant.

Chapter 1: partially fluorinated ethers

1 Ophthalmic agents

Perfluorocarbon compounds are commonly used as material in ophthalmology and reconstructive surgery [65]. Various gaseous (perfluoropropane, SF_6) and liquids (perfluoroctane, perfluorodecaline, perfluoroperhydrophenanthrene) are being used as ophthalmic agents for ocular tamponades, vitreous substitutes, intraocular washes to remove silicone oil [66]. Recently, the use of fluorosilicones, diblock semifluorinated alkanes and diethers especially as intraocular tamponades are investigated in vitreoretinal surgery [40].

The chemical and physical properties that make PFCLs appear promising as temporary intraoperative vitreous substitutes including good surface tension in an aqueous environment, high specific gravity, transparency, low viscosity, optical clarity. Their high densities, low viscosity and immiscibility with water, silicone, or blood, allow the surgeon to use PFCLs for relatively atraumatic tissue manipulation during vitrectomy. Their molecular weight permits to have high vapor pressure favorable to a good evaporation of residual droplets from eye. However, fluorinated polymer as perfluoropolyethers, fluorosilicones are also used to soften contact lenses showing an increase of oxygen permeability and reduced liphophilicity.

This chapter describes the principal characteristics of human eye and the most common ophthalmic disorders. Then, an intensive discussion is effected on importance of the vitreous substitutes and the materials used in the past and in the currently years.

After the description of the principal physico-chemical characteristics necessary for an ideal vitreous substitute suitable, in particular, for retinal detachment, the new approach of partially fluorinated compounds with an ether linkage in the molecule is presented.

Therefore, the experimental section and physico-chemical characterizations are described. Finally, a brief description on biocompatibility and the comparison of some partially fluorinated ethers with some commercial products are reported.

1.1 Human eye

In a cavity in the skull of anterior head is located a spherical organ, human eye (Figure 3). The human eye consists of two parts, an anterior and a posterior segment. Cornea and lens constitute the smaller part. In the posterior part is located the sclera, the choroid and the retina. The sclera is a coat connective tissue with a protective function and a support of the shape of eyeball resisting intraocular pressure. The choroid is a vascular layer that provides the blood supply that supports the retinal cells. Bruch's membrane, a sensory inner coat of

the posterior segment of the eye, separates the choroid to the retina. Visual impressions are created by the brain via optical nerve focusing the ambient light onto the photoreceptor cells of the retina. There are two type of photoreceptors [67], rods and cones localized adjacent retinal pigment epithelium and their distribution varies in different regions of the retina. The cones are especially in the macula (central region), whereas the rods are in the peripheral region of retina. The pigment epithelium of retina, vascular systems of the choroid and the glial cells provide a support. In particular, the cells of epithelium are often phagocytic and stationary cells providing a protection for the photoreceptors. They become broblastic and mobile during a trauma or infection and they form a opaque membrane upon the retina.

However, an acute loss of vision is caused by retina's damage, whereas a loss of visual fields is caused by peripheral retina's damage.

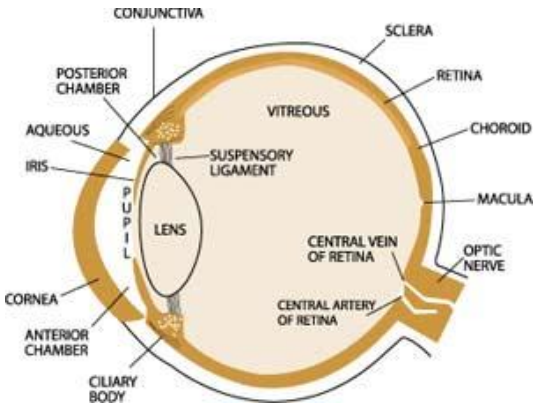

Figure 3: human eye

The light, refracted in the cornea and crystalline lens, passes through the innermost layer of the retina, named vitreous body or vitreous, and then in the neural component of the retina. Vitreous cavity consists of 98 - 99 % water with a scaffold of collagen fibers, proteoglycans and macromolecules of hyaluronic acid winding through the scaffold. His function is to act as a shock absorber supporting the shape of the eye and positioning the retina at against Bruch's membrane. It has refractive index of 1.33 and a consistency to that of egg white.

With increasing age the human vitreous became more liquid and the retinal detachment can arrive permitting vitreous to enter the subretinal space.

1.2 Vitreoretinal disorders

There are various posterior segment disorders that can arise spontaneously, as trauma accidental and surgical, or caused by infection as toxocara, syphilis, or degeneration as diabetic retinopathy and ARMD, or diseases as tumors.

Opacification, hemorrhage, inflammation and retinal detachment are common diseases in diabetic patients. In this case, there is an elevated level of glucose in the vitreous leading to an increase in non-enzymatic glycation products and advanced glycationend products which

may affect vitreous collagen fibers [68].The diabetic retinopathy can lead blindness and may require vitrectomy.

There are two type of retinopathy, non proliferative and proliferative (proliferative vitreous retinopathy (PVR)). Non proliferative is characterized by intraretinal microaneurysms, hemorrhages, nerve-fiber layer infarcts, hard exudates and microvascular abnormalities. The proliferative retinopathy detachment, named PDR, is constituted by neovascularization arising either from the disk or from retinal vessels. It is characterized by abnormal growth of membranes on the outer as well as on the inner side of the detached retina and proliferation of new blood vessels in the affected area.

Retinal detachment is characterized by the separation of the neural retina from the underlying retinal pigment epithelium inducing to the patient a dark curtain or shadow interfering with vision. There are three type of retinal detachment that must be treated differently [69].

Tractional retinal detachment is a late-stage complication of diabetic retinopathy. In this case, there is a traction upon the retina from contractile membranes. It causes the neural retina to be pulled off the retina epithelium. It is often observed in the PVR and in the PDR (rhegmatogenous retinal detachment).

In the *exudative* detachment there is the formation of fluid in the subretinal space, caused by the disruption of choroid, leading to the elevation and detachment of retina from the retinal pigment epithelium. In *rhegmatogenous* type, the detachment is caused by influx of fluid vitreous in the subretinal space thought a retinal tear or a hole.

The patient is subjected to a specific treatment depending of type of retinal detachment.

The prevention of neovascularization involves treatment with lasers [70, 71], whereas a retinal detachment complicated by neovascularization requires a surgery and materials to be treated [72].

1.2.1 Rhegmatogenous retinal detachment

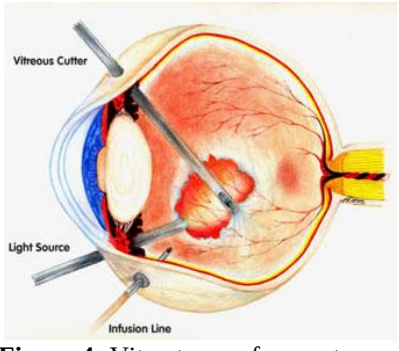

Figure 4: Vitrectomy of regmatous detachment

Rhegmatogenous detachment is most complex and most difficult to treat. In rhegmatogenous detachment the fluid accumulation into the subretinal space induces separation of neurosensoryn retina from the retinal pigmentary epithelium. The shrinkage of these membranes may lead to further detachments and additional holes creating vitreous hemorrhages and additional fibrous epiretinal proliferations.

Retina Society and more recently the Silicone Study Group declare that the incidence of pathology is as low as 1/10,000 per year and it can lead to blindness if surgical repair fails. Vitreoretinal surgery, named vitrectomy, therefore involves the use of various methods and materials to position the retina and to maintain it in position.

A standard treatment consists in performing a cut through the pars plana with subsequent alternating cuts and aspiration steps to remove the vitreous gel from the eye (Figure 4). It results a retinal scar around the tear. Then, the removed volume has to be replaced with a balanced salt solution to avoid ocular hypotension.

Hence, after a full or partial vitrectomy, it is necessary the replacement of human vitreous by gas or perfluorocarbon liquids or silicone oil injecting intravitreally the tamponade material in order to position the retina against the retinal pigment. An exchange with other fluid/gas material can be necessary depending on the final tamponade material and the gravity of detachment. These surgical techniques use the hydrodynamic force created by the high specific gravity of the substances. However, particular material and procedure are used as function of lifetime for tamponade effect of material.

1.3 Vitreous substitutes

In the 21th Century the search for an ideal tamponade biocompatibility replacement is continually in expansion.

An ideal vitreous substitute should have some characteristics including non-toxicity and biocompatibility with ocular tissues, clearness and transparency with refractive index and density similar to those of natural vitreous, biological and chemical inertness, sufficiently rigid to act as an effective tamponade agent, able to allow the transfer of metabolites and proteins, preferably non-absorbable and non-biodegradable in order to be maintained in the vitreous cavity for as long as possible, preferably hydrophilic and insoluble in water, injectable through a small-gauge needle, able to maintain its properties after injection, storable and sterilizable.

An intensive research is turn towards the elimination of deficiencies of current substitutes.

In fact, the ophthalmic use of PFCs like perfluorooctane [73, 74] and perfluorodecalin [75] are been known and their chemical inertness is undeniable. Nevertheless, some undesirable side effects have been observed during long-term treatment probably for insufficient purity of the compounds [76, 77]. PFCs are made in extreme reaction conditions, and can produce toxic by-products, like hydrogen containing fluorine

compounds or fluoroolefins. These by-products must be removed completely to avoid inflammatory effects in the eye.

The ideal vitreous substitute should have all positive qualities of vitreous: transparency, elasticity, buffer capacity, high purity and biocompatible with the tissues [78].

It is worth mentioning that the first selection criterion for a material is its optical properties, as a potential vitreous substitute, must primarily be clear and transparent to the light. Besides the optical suitability, other properties should be taken into account to evaluate if a specific compound is a good candidate for vitreous substitution.

Vitreous substitutes are currently used to maintain intraocular pressure, the biomechanical and optical properties of the vitreous space.

The materials in clinical use include perfluorinated gases, silicone oils, various perfluorocarbon liquid, hydrogels and polymers [79].

The functionality of the tissues can be inhibited by the different polarity, electrical resistance and insolubility of tamponades, compared to aqueous material. As with any biomaterial, vitreous substitutes need to be tested for a variety of properties, such as cytotoxicity, hemocompatibility, mutagenicity, and pyrogenicity.

Therefore, only generic toxicological tests in vitro don't justify the biocompatibility of the materials. Hence, European Medical Device Directive exudes specific requests for ocular endotamponades as classical medical devices. They must be non-toxic, sterile ultra-purity and mostly need also of tests in vivo to be defined "biocompatibilities tamponades". Special controls during the manufacturing (as well as for the release of finished products) and a risk management only on physical–mechanical contact must be made, to prevent some inflammatory or immune reactions and the functionality's loss due to bad management of the products.

1.4 Physico-chemical characteristics

The vitreous substitutes must have some characteristics to maintain the form and the function of native vitreous but it also must be easy to manipulate during surgery. It must have similar viscoelastic properties in other to maintain an adequate intraocular pressure, which support the intraocular tissues and retina in proper position. It must be useful to allow movements of ions and electrolytes. It must be clear, permanent and requiring one time implantation. It must be biocompatible, not biodegradable, easy to available, stable during storage, injectable through a small syringe and available a reasonable cost.

There are some fundamental physico-chemical characteristic that modulate the behavior of substitutes and they must be considered for the project of new substitutes.

1.4.1 Interfacial tension

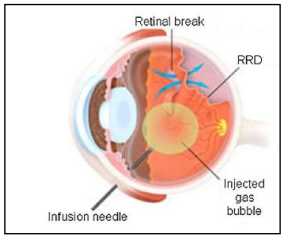

Figure 5: retinal break

The interfacial tension against water is a parameter to control to obtain a good retinal tamponade.

In fact, the balanced salt solution into the internal cavity of eye having a minimal interfacial tension against the fluid leads their passage thought the retinal break (Figure 5) to subretinal space resulting difficult for the chirurgic removes completely the liquid after vitrectomy. In this way, the vitreous tamponade having higher interfacial tension avoids the passage of the liquid into subretinal space. Hence, after injection of a gas or liquid (Figure 6) to seal retinal break, the subretinal fluid is re-adsorbed allowing to the retina to reattach and resume normal position [80].

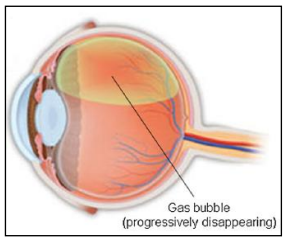

Figure 6: gas into retinal cavity

1.4.2 Viscosity

Viscosity is a parameter to modulate to provide a good tamponade agent. It is a parameter related to the molecular weight and so as function of the chain length, leading oils with short chain length and low molecular weight to have low viscosity.

It is important to have a suitable viscosity. It must not be too low to ensure the tamponade effect. It must not be too high to help the chirurgic to manipulate easily the tamponade.

1.4.3 Density

Density is a important parameter to modulate for specific applications. For instance, silicone oils have a density slightly inferior to water and they are effective for a retinal detachment in superior position of eye with a patient in upright position. Instead, for a retinal detachment in the posterior position is necessary that the patient remains in a prone position for several hours every day.

Some authors consider that PFCs with a density twice as high as of water can cause a mechanical damage by increasing pressure on the retina vessels [81]: in fact, the normal ocular pressure is 20 Torr and the increase of 3 - 6 Torr introducing a tamponade agent is a physiological limit tolerated by the eye.

1.4.4 Oxygen content

PFCs can dissolve high volumes of gases as CO_2 and O_2 but this property is not used extensively for ophthalmic applications. During vitrectomy the oxygen partial pressure increases from 15 Torr to 160 Torr and the carbon oxide partial pressure decreases from 150 Torr to 3 Torr. Hence, there is an equilibrium provided by intraocular diffusion processes. However, an increase of the retinal constriction vessel and the blood flow can alterate this equilibrium and to induce a damage of the retina. Therefore, the use of controlled levels of gases can be useable to restore the equilibrium pressure.

1.4.5 Shape of the droplet / contact angle

The differences in the interfacial tension and density of tamponades lead to a difference in drop shape and contact angle between the medium and the retina. The retinal damage and the emulsification of perfluorocarbons were attributed to the combination of low viscosity and high density. This parameter is useful on the maneuver during the drainage of the aqueous solution before removing perfluorocarbon. Because of the formation of a perfluorocarbon's layer that coats the retina for a long time, disarrangements can be created with a toxicological effect. Silicone oils create this layer but they have no direct contact with the retina and the movement of the eye can compensate the insulating effect of the tamponade.

2 Materials

Vitreous substitutes can be classified as function of the permanence into the eye's cavity. There are short-term tamponades and long-term tamponades.

The first category includes gases (air, SF_6), liquids (balanced salt solutions, perfluorocarbon liquids). Then, the second group is constituted by semifluorinated alkanes, silicone oils and natural or synthetic polymers. Current substitutes satisfy mainly the biomechanical aspects, but there are some characteristic to modulate in order to improve a long-term or short-term non toxic replacement. An overview of the principal compounds used as replacement in ophthalmic field is provided.

2.1 Natural materials

The first vitreous substitutes, used by Deutschmann in human patients, was an animal donor vitreous. Then, human donor vitreous was used [82]. They were suitable only for immediate treatment, but used as long-term post-tamponades they provided inflammation, cataracts and other several complications. They presented, also, rapid bioabsorption and biodegradation in vivo to inhibit a complete reattachment.

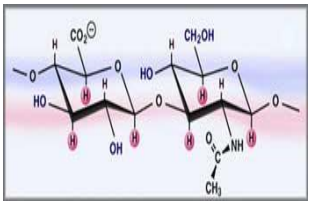

Figure 7: hyaluronic acid

Then, the research progressively aimed towards semisynthetic polymers, as modified natural polymers, to mimic nature.

In 1960 hyaluronic acid (Figure 7) and its derivatives were chosen as vitreous substitutes [83, 84] because they constituted, with the collagen, the biopolymers of natural vitreous. They presented an excellent biocompatibility but a short residence time (only two weeks). In 1993 Larsen et al. developed "hylan gel biopolymer", a cross-linking sodium hyaluronate with divynil sulfone or formaldehyde but without interesting results [85].

Solutions of different polysaccharides including dextrin, alginic acid and chondroitin sulfate, were also tested as vitreous substitutes in rabbits and humans [86]. They induced several inflammations and opacifications leading to the failure of reattachment.

In order to use another component of natural vitreous, Pruett et al. used collagen gel in human patients. It provided several inflammation, complications, no good retinal reattachment and only partial vision was recovered [87]. Methylated-collagen mixture was also used by Liang et al., without inflammations but with a too high surface tension inhibiting a good tamponade effect [88]. Then, it was tested several collagen derivative, including gelatin, polygeline [89], with a good tolerance and without adverse reactions but too short retention times and rapid decrease in viscosity inhibiting the reattachments.

Recently, a modified gelatin hydrogel was tested by Lai [90] with a good biocompatibility and tolerance without large side effects.

2.2 Gas-based substitutes

In 1911 Ohm used air to repair retinal detachments. It is an inexpensive and with no need to be removed but it has some limits. It remains in intra-vitreal cavity only for some days, Then, his refractive index is 1.0008 and it is very difficult to distinguish from the other tissues.

In 1970, Norton used sulfur hexafluoride for pneumatic retinopexy and found the persistence of gas and its expansive features superior to air [91]. In 1980 Lincoff *et al.* [92] proposed the use of perfluorocarbon gases as C_2F_6, C_3F_8, C_4F_8 and C_5F_{12}. These gas were more advantageous than SF_6 thanks to a lower requirement of intravitreal injected volumes due to increased expansion and longer persistence thanks to their low solubility [93].

Others gases, as xenon, argon, helium, N_2O, CO_2, were tested in animal and human models, but they disappeared rapidly [94].

Only in 1993 Food and Drug Administration approved the use of some fluorinated gases, as SF_6 and perfluoropropane, for pneumatic retinopexy and tamponade agents. They are five or six times heavier than air, colorless, odorless and inert. Gases have most high surface tension and high diffusion than other gases, as oxygen and carbon oxide, then liquid replacements is useful to maintain a tamponade effect. They are a residential time from 6 to 80 days depending on perfluoro percentage avoiding to be replace with humor vitreous.

An abrupt increasing of intraocular pressure due to their expansible nature can provide a central retinal occlusion [95]. Hence, the patients must prevent high altitudes in order to avoid dangerous gas expansion and maintain face-down position for several days until breaks close and retinal fluid is reabsorbed. They have a density inferior of vitreous, so they cannot be used in inferior retinal detachment and their refractive index is only 1.17, lower of cornea, fluid and lents. Then, in the last years they are retained responsible for some side effects as cataract formation and corneal endothelial changes [96].

Hence, these gases are useful only for short-term vitreous substitutes and for selected retinal detachments.

2.3 Silicone based oils

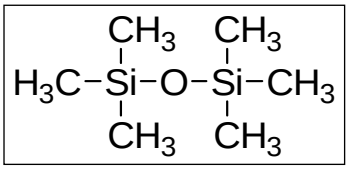

Figure 8:hexamethyldisiloxane

Silicones are polymers constituted by repeating silicon-oxygen bonds with 2 organic radicals attached to each silicon atom except in the terminal silicon atoms that have 3 organic radicals.

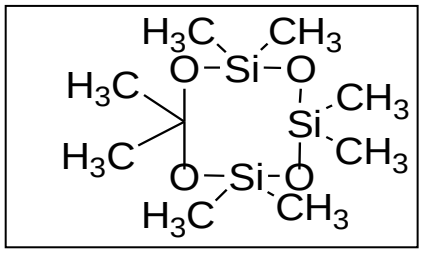

Figure 9: Octamethylcyclotetrasiloxane

Methyl radical is the most used in biomedical silicone. The properties of the silicones depend on the size of the molecules and on the nature of the radicals attached to the silicon atom. Figures 8 - 10, show examples of silicones

used in ophthalmic field.

In 1962 silicone oils have been in use by Cibis as a vitreous substitute [97], but only in 1994 the Food and Drug Administration approved their use as tamponade agents. They are synthetic polymers belonging to the class polydimethylsiloxanes, hydrophobic substance with a density near water (0.97 g mL^{-1}) and a refractive index near vitreal body (1.4).

Silicone oil was initially used as stabilization of retina and to unroll the flaps of retinal tears, but there are substituted by perfluorocarbon with higher surface tension.

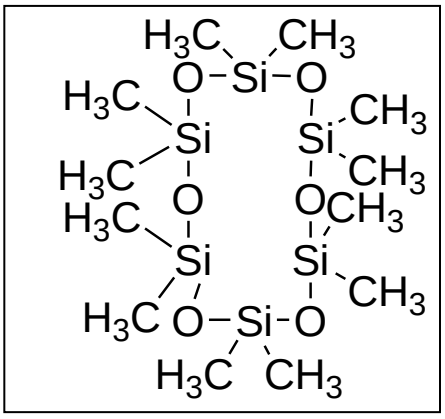

Figure 10: Dodecamethylcyclohexasiloxane

Now, they are used as long or short-term tamponades for complied retinal detachment.

The use of dimethylsiloxanes of different viscosities (multiples of centistokes 1000 - 5000) was tested for clinical employs [98]. They cannot cover all vitreous cavity because of their low viscosity ant that is responsible to float upon residual vitreal fluid leading to a bad or no tamponade effect in inferior retinal detachment [99]. They are removed from retinal space after 3 - 6 months when retina is reattached but they are stable for 6 to 24 mouths leading to ideal long-term substitutes. Silicone oil is preferable to SF_6 in complicated retinal detachment. It has low toxicity, easy to remove, and transparency. Silicone oils are candidates as long term retinal tamponade because they remain in the eye until they are removed, whereas perfluorocarbon gases and polymer solutions are reabsorbed in relatively short periods of time. Their high surface tension and density permit a good tamponade on superior retina. They are used primary in children patients or adults with physical impairment to facilitate the post operative position. They are used also if an airplane travel is planned [100]. They have a refractive index of 1.4 and their use requires optical adjustment. However, in the superior retinal detachment, their low density causes them to float upon the residual vitreous, with a reduced tamponade effect and thus the patient in the prone position is required [80].

Therefore, the use of silicone oil is retained responsible of corneal abnormalities, cataracts and emulsification due to low viscosity [101]. Furthermore, the patients must be followed a lot for possible complications after vitrectomy. Then, sometimes occurs the phenomenon of “sticky oil” and his removal can also create complications because it remains adherent to retina.

In the last years oil purification technologies have allowed to eliminate the residual components of polymerization reactions (monomers and polymerization residues) reducing

various side effects as emulsification and dispersion of silicone [102]. The emulsification also depends from interfacial tension of materials. This phenomenon was found higher in silicone with a low interfacial tension between two immiscible liquids and with low viscosities. The emulsification can be due to incorporation of vesicles interfering with the transport of metabolites. The emulsification rate is also reduced using a silicone with higher viscosity.

Then, a second generation of silicone oils were introduced in 2000. Poly(methyl-3,3,3-trifluoro)propylsiloxane and poly(methyl-3,3,3-trifluoro)propylsiloxane–co-dimethylsiloxane silicone/fluorosilicone co-polymer oils can mentioned. They are fluorosilicone oils, in which the fluoro-alkyl group is covalently bound to the Si-O-Si backbone. Fluorosilicones have a density higher than water and thanks to the difference in density, they can be used to flatten retina with the patient in a prone position displacing subretinal fluid. Nevertheless, they present a lower intramolecular tolerance with side effects in a shorter period [102]. Therefore, although the interfacial tensions of silicone and fluorosilicone in water are similar, the fluorinated compounds emulsify more readily than hydrocarbon pairs. In fact, the polarity given by the high electronegative fluorine provides higher adsorption of intramolecular proteins at the interface between fluorosilicone and water (vitreous) leading to the lower interfacial tension that promote emulsification [80].

Doi et al. [103] investigated the use of mixtures of silicone and fluorosilicone co-polymer oils to several employs as retina fixation, short –term vitreous substitute, release of drugs to prevent proliferative vitreous retinopathy. They have a lower viscosity permitting an easy injection and also an easy removal but the side effects are similar or more serious than those observed in other hydrocarbon silicones. Their use is suggested only for a period inferior to two mouths.

2.4 Perfluorocarbon liquids

Water with a balanced of salts solution was the first liquid used as tamponade [104]. Nowadays, water-based balanced salt solutions are used only for intravitreal washes in the course of vitreoretinal surgery procedures or after removing other vitreous substitutes.

In 1982 for the first time, Haidt et al. [105] evaluated the use of liquid perfluorocarbon as a vitreous substitutes. Then, Zimmerman and Faris reported the use of PFCs as intraoperative tools to retina’s surgery [106]. They are synthetic fluorinated liquids, clear, colorless and odorless.

Interfacial tension and specific gravity establish the shape of the intraocular substance-droplet, providing to a easy rolling bubble or a quickly sinking mass with a horizontal liquid level [107]. Therefore, water immiscibility of perfluorocarbons is useful to prevent tissue reabsorption through pynocitic mechanisms [108].

They have a specific gravity twice higher than water (1.7-2.1 g cm^{-3}) and are used for temporary tamponades and mechanical fixation of the retina. In fact, a good quality smooth surface is provided because their high specific gravity can break the micro-membranes on the surface of retina facilitating reattachment considerably [109]. They have an extensive capacity for transporting and releasing oxygen and carbon oxide (capacity very used initially in blood substitutes). They have a refractive index near water permitting their visualization with a conventional contact lens during vitreous surgery.

They have not pharmacological action in the eye, and their action is purely mechanical. Therefore, any pure PFCL can be used as an intraoperative device. Therefore, their use can facilitate the stabilization of retina and epiretinal removal and traction release. They can flatten the retina temporarily during surgery of complex retinal detachment and their low viscosity allows a facilitate use intraoperatively. They can be used as alternative to oil silicone as long-term tamponades without to force the patients to a face-down position.

While the stability of the carbon-fluorine bond [110] provides fluorinated compounds very inert, the difficulty to synthesize highly pure products causes to their toxicity for long period of permanence into the eye leading to irreversible cell damages. The major impurities in perfluorocarbon are hydrocarbon, due to incomplete fluorination. Their persistence over more than four days postoperatively leads to severe complications. These impurities lead to the formation and the adhesion of a thin protein film. In fact, Keese and Giaever [66, 111] demonstrated that a protein film sufficiently strong to support cell growth cannot occur on purified fluorocarbon liquids, but requires the presence of trace amounts of polar, surface active compounds. Hence, there is the formation of a moisture on the tissues and the surface of retina. The residuals of the layer can be remain inside the eye with the formation of micro-bubble leading to emulsification with the plasma or cell components and then side effects. Therefore, at the end of surgical procedure may remain some residuals of products and this can be detected by ultrasounds. Nevertheless, it is very complicated to remove completely the residuals of perfluorocarbon because they are no soluble in conventional solvents. Then, it is necessary to remove the residuals with additional procedures in order to avoid other side effects.

The high density is retained responsible for post-operative complications, rather that the toxicity of the materials. For instance, Vitreon®, a perfluoro-perhydrophenanthrene, has a viscosity that rends difficult to withdraw from the eye and an refractive index of 1.334 very similar to water (1.333). However, the perfluorocarbons should have a refractive index different of water to facilitate their visibility. Hence, residuals of droplets remaining in the eyes proving a disorganization of retinal cell growth pattern, loss of neuritis probably also due to high specific gravity [108].

In fact, some researchers retain that the high density of PFCL is responsible of mechanical damage to cells through the compression and the extensive emulsification, rather than the intrinsic material toxicity [66, 111]. Among these substances the most wide used are perfluorodecalin, perfluorooctane, perfluorohexyloctane, perfluoroperhydrophenanthrene, and octafluoropropane (Figures 11 - 14).

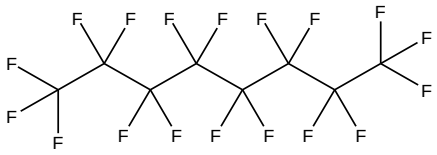

Figure 11: perfluorooctane

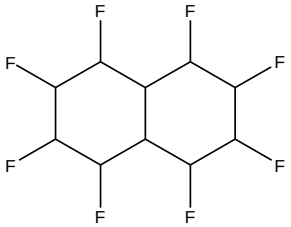

Figure 12: perfluorodecalin

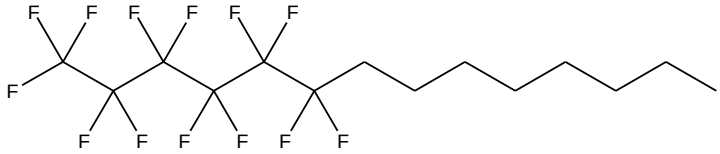

Figure 13: perfluorohexyloctane

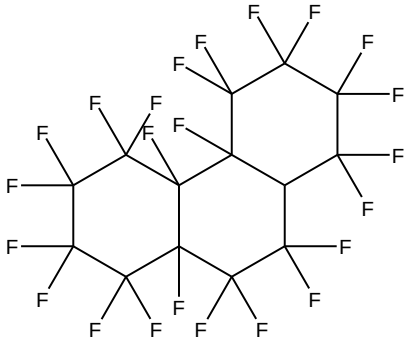

Figure 14: perfluoroperhydrophenanthrene

2.5 Semifluorinated alkanes (R_FR_H)

In the last years, the search for a vitreous substitute was addressed to find a biocompatible fluid, primarily as long-term tamponade agent. The objective is a formulation that can be in situ without long-term clinical complications, such as compressive damage to cells, intraocular pressure rise (IOP) and postoperative glaucoma. An ideal artificial vitreous should closely mimic the light transmittance of natural vitreous humor, as well as its physical and mechanical properties. In fact, it was observed that high specific gravity of perfluorocarbon is the principal cause to create intraocular tissue damage. In this way, the search was addressed to new tamponades with a reduced specific gravity. This reduction may be reach with a partial replacement of hydrogen atoms in perfluorocarbon compounds. With their different rations of hydrocarbon and fluorinated chain were introduced to amplify the performance of PFCs increasing the tamponade effect with a reduction of density of mixtures. These materials are colorless, immiscible with water and physically, chemically, physiologically inert. They have a specific gravity of 1.35 g mL^{-1} and a refractive index of 1.3-1.4 [112].

Recently, candidates for this purpose are semifluorinated alkanes. Partial fluorination leads to a stepwise reduction in specific gravity, from 2.03 g cm^{-3} for perfluorophenanthren to 1.32 g cm^{-3} for perfluorohexyl-octane [107].

Simultaneously, hydrogenation causes the increase of polarisation and an increasing of lipophilic character.

The general formula of these compounds is $F(CF_2)_n(CH_2)_mH$ and $F(CF_2)_n(CH_2)_m(CF_2)_nF$ (n, m =3 - 20 in both cases), respectively. Hence, they are named R_FR_H (di-block) and $R_FR_HR_F$ (tri-block) and have an hybrid character combining the behaviors of alkanes and perfluoroalkanes.

In the 1970 Mahler synthesized and characterized for the first time semifluorinated alkanes, low-molecular weight diblock copolymers of the general structure $F(CF_2)_m(CH_2)_nH$ (abbreviated F_mH_n) but without publication. Then, he reported thermal and optical characterization of F_mH_n with different block lengths m and n [113].

Therefore, semifluorinated alkanes have physico-chemical properties including polar character, strong dipole moment due to CF_2-CH_2 dipole, surface tensions and dielectric constant higher than perfluorinated and hydrogenated compounds [114].

They have an interfacial tension against water of 50 - 58 mN m^{-1} at 20 °C tending to form spontaneously emulsions between immiscible liquids. They have very low surface tensions

against air (15 - 25 mN m^{-1} at 20 °C). They are soluble, as function of the length of the R_F part, in perfluorocarbons or their derivatives and as function of the length of the R_H part, in hydrocarbons or their derivatives [115, 116].

Semifluorinated alkanes are amphiphilic compounds, because of their exceptional aptitude at developing both hydrophobic and lipophobic effects in relation of length of R_F and R_H parts. Then, the mutual incompatibility between R_F and R_H generates a set of interesting phenomena in all states of matter. These are expression in micro-phase separation, segregation and Langmuir monolayer formation at the water–air interface, self-assembly. Turberg and Brady attributed the particular conformation of these molecules the "chemical antipathy" of head and the tail and on their opposite 'sympathy' for water molecules leading to the mutual repulsion of two parts [117].

Hence, they also can form aggregates micelles or fibrous gels [118], depending on the length of hydrocarbon or fluorocarbon chain, in solutions. Therefore, they are highly effective in generating stable, organized, and compartmented molecular systems with controlled complexity. In fact, due to formation of F-H bridges between the R_F and R_H parts of neighboring molecules, the formation of alternate lamellar arrangements in relation to R_F and R_H segments is been observed [119].

They can also be used as surface active agents in selected organic liquids including methanol, fluorocarbons, hydrocarbons, dimethyl-sulfoxide, dimethylformamide, toluene, tetrahydrofuran and so on [120, 121]. In fact, three interactions are involved in relation of R_H-R_H, R_F-R_F and R_H-R_F linkage, instead of the six in general surfactant-water system (water-water, head-water, tail-water, head-head, tail-head, tail-tail) [122].

Recently, surface activity of semifluorinated alkane compounds in apolar solvents has been studied. Semifluorinated alkanes dissolved in hydrocarbon media are also surface active. The free energy of transfer of one CH_2 from a hydrocarbon solvent to a perfluorinated alkane (1.1 kJ mol L^{-1}) is about one-third the energy needed to transfer a CH_2 group from alkane to water [122, 123].

Semifluorinated alkanes are miscible only in a limited composition and temperature range in the hydrocarbon solvents [124]. They are also surface active in a limitated concentration range in perfluoroalkanes and hydrocarbon solvents with a very low aggregations number.

Therefore, semifluorinated alkanes show high chemical and biological stability due to the CF_2-CH_2-connection. According to Conte et al. [110] semifluorinated linear alkanes do not eliminate hydrogen fluoride in presence of bases and are stable under cleaning-up conditions for perfluorocarbons. This element of discontinuity in the structure permits to use

them in biomedical field. From biological point of view, they have a behavior close to perfluorinated analogs. In fact, they cause no inhibition of proliferation concerning DNA and protein synthesis and undergo neither catabolism nor metabolism in the human body. Then, no effect on cell cultures is been observed.

The use of semifluorinated alkanes in vitreoretinal surgery is relatively new and they have the potential to act as long-term vitreous substitutes. Except for short perfluorinated parts CF_3- and C_2F_5-, semifluorinated alkanes are completely biocompatible [115]. Semifluorinated alkanes with a short perfluoroalkyl chain and long hydrocarbon chain can be toxic because they are closer to the alkanes.

Therefore, they present an excretion velocity from human body dependent on block sizes [114].

Semifluorinated alkanes may also allow the removal of silicone oil remaining from the eye or wash out contaminations of silicone oil from intraocular lenses. Then, perfluorocarbon, semifluorinated alkanes and silicone oil in succession intra-operatively, “silicone oil in fluorinated solutions” were tested, but dense opacification, which obscure the vision of the surgeons, and the difficult removal were observed [107]. Like the perfluorocarbons and hydrocarbons, the semifluorinated alkanes are scarcely or not soluble in silicone oil. While some authors found encouraging results [125, 126] other groups reported a plethora of complications and discouraged the use of semifluorinated alkanes as a vitreous substitute [127, 128].

Semifluorinated alkanes are less viscous than silicone oil, with a viscosity of 2500 cSt and then more easy to handle. Their low specific gravity (1.1 - 1.7 g cm^{-3}), compared to PFCLs, produces less retinal damage.

They are soluble in PFCLs, hydrocarbons, and silicone oils and have a preferred refractive index, a higher interface tension than silicone oil. Initially, they were used as a biocompatible solvent for silicone oil in inferior retinal detachment. Then, their use for special retinal detachment in place of silicone oils was tested. Their solubilization in silicone brings to particular different shapes of the droplet facilitating special maneuvers or the removal of residual silicone oil. Then, from the biological standpoint, there is no effect on cell cultures, very low acute toxicity, absence of metabolism and excretion rate dependent on block sizes.

Therefore, the inert perfluorinated part cannot compensate always the hydrocarbon part. So, it is necessary to test every single compound to see his toxicological behavior and ensure its suitability as an ophthalmic agent. In addition, semifluorinated alkanes were used

successfully as intraoperative tools to unfold and long-term tamponades [115]. One example is 1-perfluorooctyl-5-methylhex-2-en, named RMN_3. It is a partially fluorinated compound with a low molecular weight, thus it can easily penetrate tissues.

Another example of the semifluorinated alkanes, perfluorohexyloctane, was tested in animal experiments as long-term vitreous substitute and it was found to be well tolerated [126]. Then, his low specific gravity of 1.35 causes less damage to the underlying retina as internal tamponade agent. However, a common important complication of the perfluorohexyloctane is the formation of droplets due to the his low viscosity. Clinical trials have shown their tolerance in the eye for 2 - 3 months but some problems of cataract and emulsion were verified.

Since 2000 partially fluorinated alkanes or fluorinated alkanes, were developed as tamponated agents "heavier than water".

2.5.1 Silicone oil and fluorinated compounds mixtures

The research was focalized to create a silicone oil "heavier than water". Hence, new, less toxic substitutes are developed combining silicone oil with other liquids.

The combination of two liquids, silicone oil and fluorinated compounds was investigated and recently approved for biomedical use. They represent the third generation of silicone oils and are called "heavy oils". In this way, the specific gravity can be increasing maintaining a characteristic viscosity to produce a vitreous substitute with a good tamponade effect and minimal emulsification. Their typical densities are in the range 1.0 – 1.3 g cm^{-3} and they have also been successfully tested in the treatment of complicated retinal detachment.

Depending on the ratio of the two liquids, there are two type of mixtures. The "heavy silicone oils" is an homogeneous, clear solution, while "double fills" is a separated solution.

In the first case, partially fluorinated compounds are enclosed by a silicone oil matrix and they have no direct contact with retina permitting to mask their side effects.

An example of heavy solution of partially fluorinated olefine with silicone oil 5700, named Oxane Hd® was developed in 2003 by Bausch and Lomb (Toulouse, France) to treat the lower quadrant of retina [129-131]. It had a density of 1.02 g mL^{-1}. Recently, Oxane Hd® was found to be unsuitable for clinical use due to the incidence of adverse effects, including oil emulsification, glaucoma and cataract.

In the meantime, different mixtures of perfluoralkyl-alkanes with silicone oil, named Densiron 68®, was developed by Fluoron GmbH (Neu-Ulm, Germany). It was found to be

effective and safe in inferior retinal detachment and in the surgery of persistent macular holes [85]. It results in an optimal tool with high anatomical success because it leaded functional improvements in the patients' visual acuity [131, 132].

In recent year (2007) has been developed HWS 46-3000 by [133, 134]. It is well tolerated by tissues, effective in the inferior quadrants with a low incidence of membrane development. The main complication was the high rate of tamponade-related cataract formation.

Instead, double fill mixtures have the light support of silicone oil on the superior retina, while the heavier fluorinated alkane on inferior retina, reducing complications than each liquid alone.

It is demonstrated a reduce emulsification compared with using silicone oil alone, but in the superior detachment it does not provide a good support: the bubble are no homogeneous and a bubble of pure fluorinated compound is located inferiorly, whereas a lighter solution superiorly. Bottoni et al. shown that a double-fill silicone mixture of silicone and fluorosilicone lead to the formation of a residual fluid between silicone and fluorosilicone obstructing a complete fill of vitreous cavity [126].

Meinert and Roy believe that semifluorinated alkane are good candidates for use as solvents for long-term tamponades and for intravitreal drugs released in situ post-surgery [115]. They have attractive characteristics because they are very tolerated and have a reduced emulsification rather than silicone oil.

2.6 Hydrofluorocarbon oligomers

In 2001 new hydrocarbon oligomers with higher viscosity were developed by Hennings et al. [107] to provide tamponades with a decrease of emulsification and to reduce some intraocular complications. These hydrocarbons present a viscosity from 90 to 1750 mPa·s, guaranteeing an easy handing and injectability. Then, they have high stability reducing the formation of droplets. They have a specific gravity of 1.6 g cm^{-3} and a refractive index identical to body vitreous. This last aspect is convenient for the patient but for the surgeon is more difficult to distinguish the oligomer from intraocular fluid. Hence, the oligomer must be mix with a perfluorocarbon to modify the refractive index.

3 Towards an ideal vitreous substitute

Ether-linked fluorocarbon hydrocarbon compounds as ideal candidate for substitutes vitreous

The search for an ideal vitreous substitute, able to actually mimic the features of natural vitreous, is currently in progress.

We have investigated a new series of ether-linked fluorocarbon hydrocarbon compounds to overcome the "defects" of semifluorinated alkanes.

The overall goal of work is to synthesize and characterize different series of partially fluorinated ethers with general formula R_F-O-R_H and to study the influence of ethers linked on physico-chemical properties. Simultaneous optimization of the physico-chemical and biocompatibility properties to improve adequate mechanical and solution characteristics of vitreous substitutes have led to the synthesis of a series of partially fluorinated ethers (PFEs) with general formula $F(CF_2)_m(CH_2)_2O(CH_2)_nH$, (m = 4, 6, 8 and n = 2, 3, 5, 8, 14, 18, 21). In these compounds *m* is the number of carbon atoms in the perfluorinated moiety and *n* is the number of carbon atoms in the hydrocarbon segment. Then, they must have high biocompatibility, high purity degree and suitable specific physico-chemical values to use as tamponade liquids in ophthalmology field, in particular in retinal detachment. In fact, they must have some specific characteristics to exert a sufficient pressure during said operation so as to enable a correct repositioning and a sufficient adhesion of the retina to the adjacent eye components. They must have a high purity degree and biocompatibility to remain an undetermined lapse of time without damaging the retina and provide serious sides effects. They must also have an adequate refractive index to be easily visible to surgeon. They must have high solubility in unfluorinated liquids, to use as long-term tamponades in addiction to silicone oils. Then, to be effective as a tamponade, they must be immiscible with water which it will form an interface.

3.1 Methods of synthesis of semifluorinated ethers

Many old methods were reported in literature to synthesize PFEs. The typical methods are fluorination of the ether compound by F_2 gas [135, 136], fluorination of the ether compound by metal fluoride [137], electro-chemical fluorination of the ether compound [138], addition reaction of alcohol to fluorinated olefin under basic conditions [104, 139] and nucleophilic reaction of fluorinated alkoxide [140-143]. These reactions were carried out with or without an organic solvent [139, 144-146]. Sometimes unsaturated ether might be formed besides

fluorinated ether, probably due to solvent effect. Therefore, the mixture must be treated with bromide and distillated to remove the unsatured ethers, with a lower of yields of satured ethers [145, 146]. In this way, Mutara et al. [144] demonstrated the existence of an unique mechanism for the production of semifluorinated ethers, except for 1,4-dioxane solvent.

In Scheme 1 the two plausible mechanisms for the production of semifluorinated ethers were reported.

The *path 1* is the dehydrofluorination of alcohol, while the *path 2* is the elimination of fluoride anion from the carbanion intermediate.

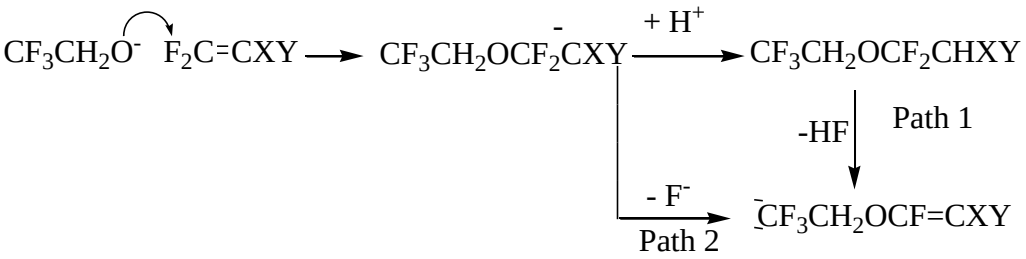

Scheme 1: dehydrofluorination of alcohol (Path 1) and the elimination of fluoride anion from the carbanion intermediate (Path 2)

The path 2 is inhibited by increasing of the proton source in the medium, for instance water or alcohol [144].

Then, Murata experimented a green process for the preparation of fluorinated ether by the addition of alcohols to fluorinated olefins under basic conditions (Scheme 2):

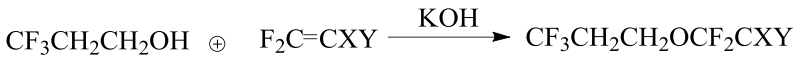

Scheme 2: addition of alcohols to fluorinated olefins under basic conditions

In 2003 Prakash et al. prepared fluorinated ethers from nucleophilic alkylation of fluorinated alkoxides [147]. They used a strong alkylating agent [148], as dimethyl sulfate, methyl, ethyl, hexyl triflate, methyl mesylate and methyl tosylate, for the methylation of a nucleophile (Scheme 3).

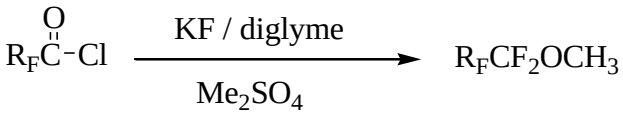

Scheme 3: nucleophilic alkylation of fluorinated alkoxides

In the Scheme 4 is reported the mechanism of reaction, where fluoroacyl chloride is fluorinated by KF to fluoroacyl fluoride and transformed into fluoroalkoxide. A solvent with high polarity is needed and an excellent solvation power as diglyme.

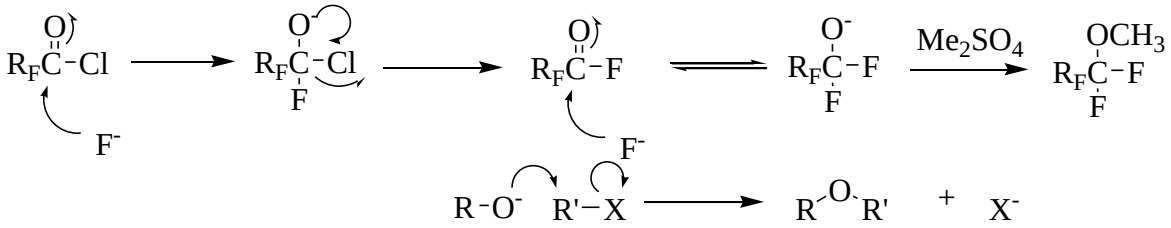

Scheme 4: mechanism of reaction of nucleophil alkylation

However, addition of perfluoroalkyl iodides to allyl-ether glycosides followed by reductive deiodination [149, 150] (Scheme 5), or perfluoroalkymethyl-oxiranes with galactopyranose and xylitol [151] (Scheme 6) lead to ether surfactants with high hemocompatibility.

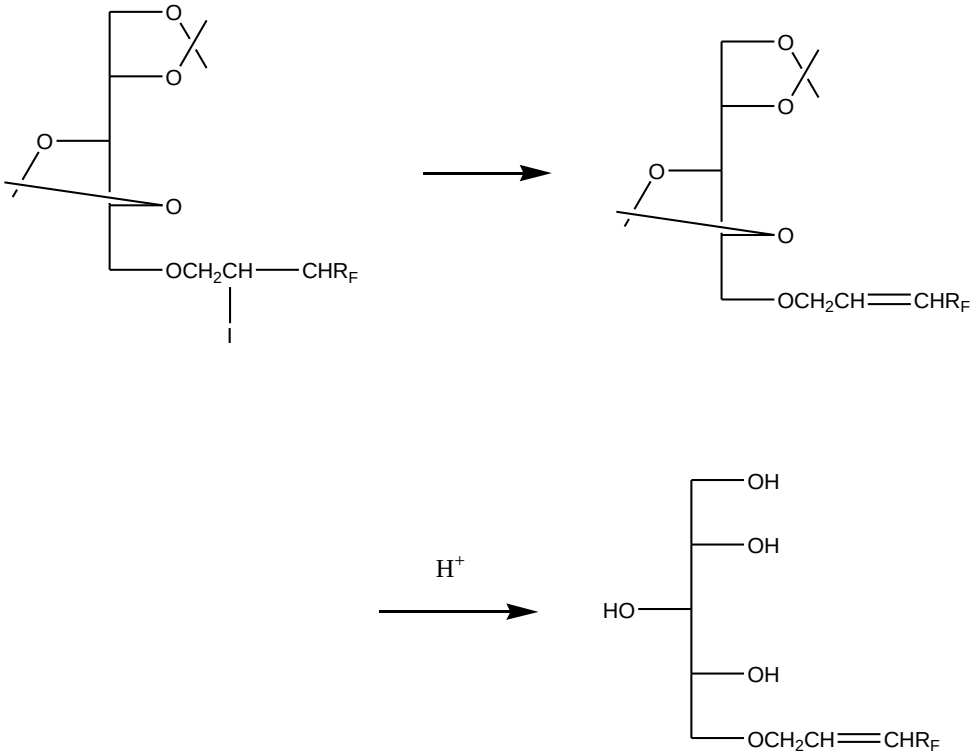

Scheme 5: perfluoroalkyl iodides to allyl-ether glycosides followed by reductive deiodination

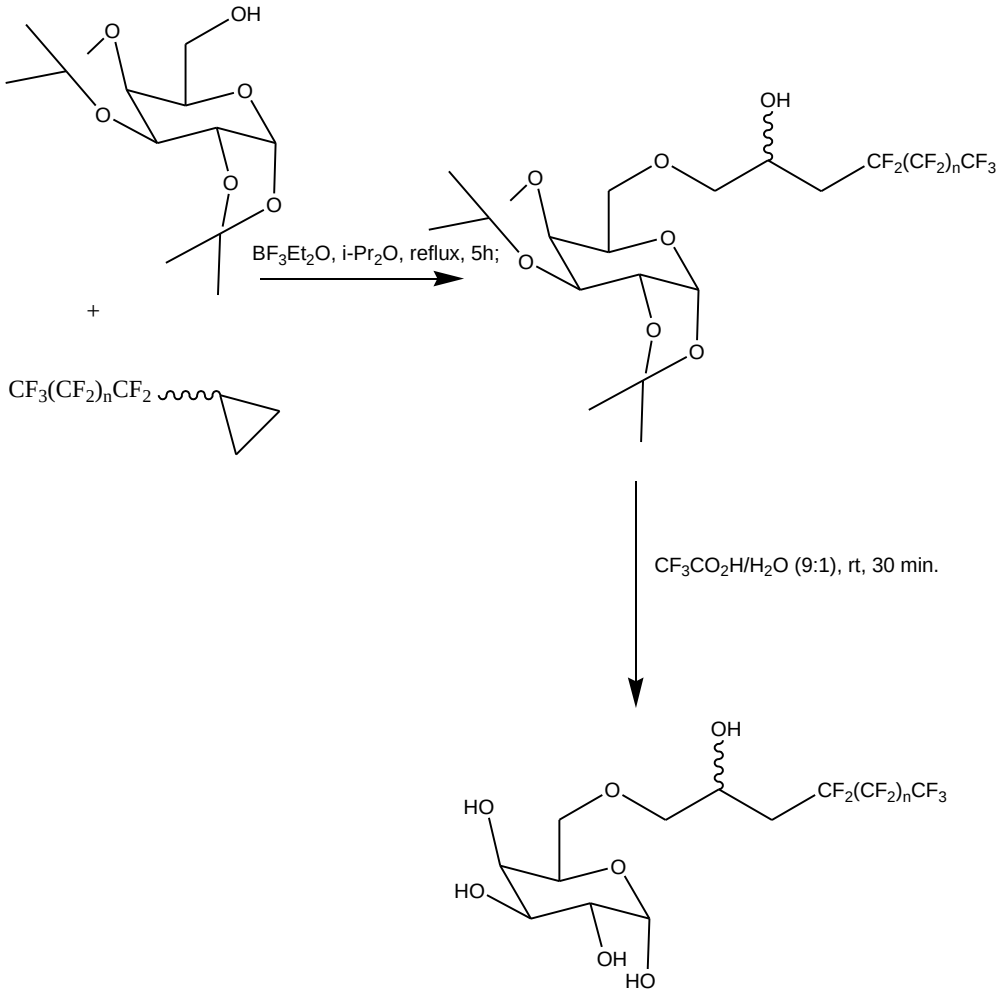

Scheme 6: Preparation of perfluoroalkylated derivatives of D-galactopyranose

Then, in the patent US 6060626 (2000) is reported the fluorination of alcohol with aldehydes and Pd-C as catalyst (pH 7.2) under hydrogen pressure to obtain PFEs [152].

$$R_F - (CH_2) - O - R_H$$

PFEs were also successfully synthesized by Huang et al. using the Williamson ether synthesis under basic conditions to couple commercially available fluorocarbons with α-bromo alkanes [153]. In this reaction perfluoroalkanols and 1-halogen-alkanes were mixed in aqueous solution of sodium or potassium hydroxide in the presence of a phase-transfer catalyst (tetrabutylammonium hydrogen sulfate or tetrabutylammonium bromide) and benzene or THF or DMSO as solvents.

3.2 Synthesis of $PFE_{n,m}$

The present work aimes to give a straight and economical methodology for the preparation of highly pure $PFE_{m,n}$ with different fluorocarbon–hydrocarbon ratio (m / n).

Of the variety of techniques now available to couple the perfluoroalcohol and bromo-alkyl segments, in a first test we have relied upon the well-known synthesis of Williamson

et the procedure of Huang [148]. The Williamson reaction was discovered in 1850 and involves treatment of the fluoro-halide with alkoxide ion prepared from an alcohol, although methylation via an S_N2 reaction [148].

The general reaction mechanism is reported in Scheme 7:

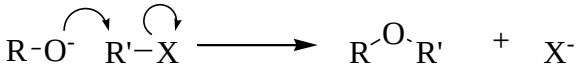

Scheme 7: mechanism of reaction of fluoro-halide treatment with alkoxide ion prepared from an alcohol

The reaction needs an anion dissolved in an organic solvent to increase the kinetic of reaction. Anions of sodium and potassium salts can be dissolved in organic solvents but there is no effect on the rate. They need of an appropriate phase-transfer catalyst to increase the rate of reaction. In fact, the anions exist in the solvent as ion pairs Na^+ or K^+ and are not free to attack the substrate [148].

In quaternary ammonium salts the ion paring is more weak leading them to be easily attack by “naked anions”.

PFEs can be efficiently prepared with the use of appropriate phase-transfer catalysis. Some experimentations are often required to find the optimum catalyst.

4 Experimental Section

4.1 Synthesis of $PFE_{n,m}$ (first procedure)

The procedure reported in Scheme 8 was used initially for the synthesis of partially fluorinated ethers. In this reaction 1H,1H,2H,2H-perfluoro-1-alkanols $F(CF_2)_{m(}CH_2)_2OH$ and 1-bromoalkanes $Br(CH_2)_nH$ were mixed in 50 % aqueous solution of sodium or potassium hydroxide in the presence of a phase-transfer catalyst, tetrabutylammonium hydrogen sulfate or tetrabutylammonium bromide (BTAC) using a mix of cyclohexane-THF as solvents.

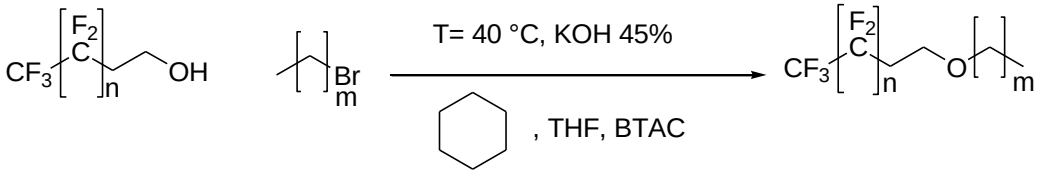

Scheme 8: first procedure synthesis of partially fluorinated ether

The mixture was stirred for 1.7 h at 10 °C, followed by the addition of 1- bromoalkane (31.2 mmol); then, the mixture was stirred at 40-70 °C for several days. After dilution with

hexane and washing with water, the crude product was dried over sodium sulfate. The solvent removed and partially fluorinated ether was recovered by distillation under reduced pressure.

Synthesis of 1,1,1,2,2,3,3,4,4-Nonafluoro-6-oxy-propane ($PFE_{4,3}$)

In a 1000 mL round-bottom flask, 100.0 g (0.38 mol) of 1H,1H,2H,2H-nonafluoro-1-ol, 150 mL of cyclohexane and 150 mL of tetrahydrofuran were stirred vigorously for 2 h at room temperature, drop-wising an aqueous solution of 50 % NaOH (400 mL). Then, 10.0 g (0.11 mol) of tetrabutylammonium bromide (BTAB), the phase transfer catalyst, and 170.0 g of bromopropane (1.38 mol) were added. The reaction mixture was kept under stirring at 40 °C for 40 h, then at 70 °C for 8 h. The water/organic solution was extracted five times with deionized water. Then, the solvents were evaporated. The organic phase was then purified by distillation in a kugelrohr apparatus under reduced pressure to give colorless liquids. 15.0 g of $PFE_{4,3}$ were obtained with 13 % of yield.

Synthesis of 1,1,1,2,2,3,3,4,4-Nonafluoro-6-oxy-penthane ($PFE_{4,5}$)

In a 1000 mL round-bottom flask, 200.0 g (0.757 mol) of 1H,1H,2H,2H-nonafluoro-1-ol, 300 mL of cyclohexane and 350 mL of tetrahydrofuran were stirred vigorously for 2 h at room temperature, drop-wising an aqueous solution of 50 % NaOH (400 mL). Then, 25.0 g (0.11 mol) of benzyltriethyl ammonium chloride, the phase transfer catalyst, and 200 g of bromopentane (1.32 mol) were added. The reaction mixture was kept under stirring at 40 °C for 40 h, then at 70 °C for 8 h. The water/organic solution was extracted five times with water. Then, the solvents were evaporated. The organic phase was then purified by distillation in a kugelrohr apparatus under reduced pressure to give colorless liquids. 23.0 g of $PFE_{6,5}$ were obtained with 15 % of yield.

Synthesis of 1,1,1,2,2,3,3,4,4-trideca-6-oxy-ethane ($PFE_{6,3}$)

In a 1000 mL round-bottom flask, 252.0 g (0.687 mol) 1H,1H,2H,2H-tridecafluoro-1-ol, 300 mL of cyclohexane and 350 mL of tetrahydrofuran were stirred vigorously for 2 h at room temperature, drop-wising an aqueous solution of 50 % NaOH (400 mL). Then, 25.0 g (0.11 mol) of benzyltriethyl ammonium chloride, the phase transfer catalyst, and 170.0 g of bromopropane (1.38 mol) were added. The reaction mixture was kept under stirring at 40 °C for 40 h, then at 70 °C for 8 h. The water/organic solution was extracted five times water. Then, the solvents were evaporated. The organic phase was then purified by

distillation in a kugelrohr apparatus under reduced pressure to give colorless liquids. 55.0 g of $PFE_{6,3}$ were obtained with 20 % of yield.

Synthesis of 1,1,1,2,2,3,3,4,4,5,5,6,6 Tridecafluoro-8-oxy-pentane ($PFE_{6,5}$)

In a 1000 mL round-bottom flask, 252.0 g (0.692 mol) of 1H,1H,2H,2H-tridecafluoro-1-ol, 300 mL of cyclohexane and 350 mL of tetrahydrofuran were stirred vigorously for 2 h at room temperature, drop-wising an aqueous solution of 50 % NaOH (400 mL). Then, 25.0 g (0.11 mol) of benzyltriethyl ammonium chloride, the phase transfer catalyst, and 209.0 g (1.38 mol) were added. The reaction mixture was kept under stirring at 40 °C for 40 h, then at 70 °C for 8 h. The water/organic solution was extracted five times water. Then, the solvents were evaporated. The organic phase was then purified by distillation in a kugelrohr apparatus under reduced pressure to give colorless liquids. 37.0 g of $PFE_{6,5}$ were obtained with 12 % of yield.

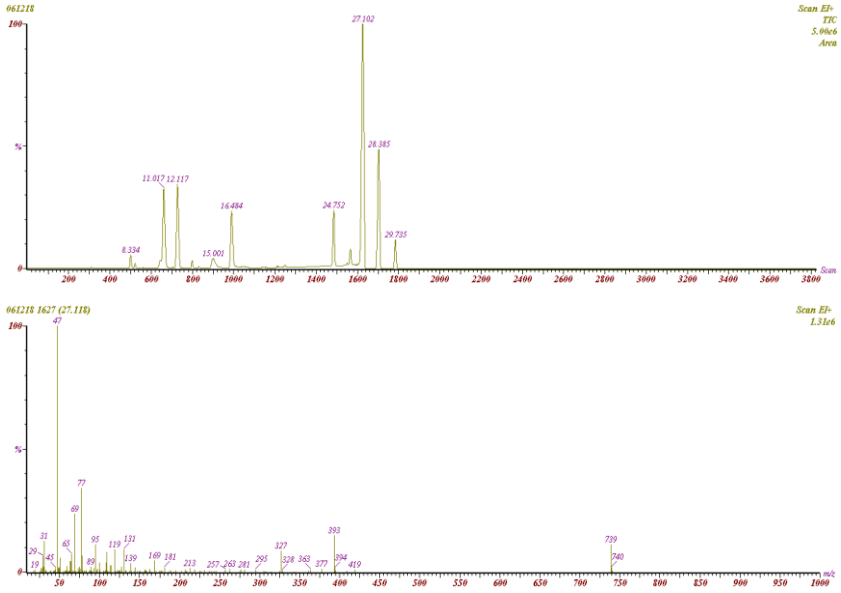

Figure 15 :GC-MS of $PFE_{6,5}$ before distillation.

The use of phase-transfer catalyst leads to no increase of reaction's rate and the formation of several byproducts as showed by Gas chromatography-mass spectrometry (GC-MS) in Figure 15.

The final products are accompanied by traces of contaminants of very similar boiling point which makes the separation by distillation without excessive losses in yield difficult.

Also, the impurities are often not efficiently removed by recrystallization since their solubilities are very similar to the desired product. The most abundant byproducts are symmetric fully hydrogenated ether as $H(CH_2)_5O(CH_2)_5H$.

The phase transfer probably promotes first a nucleophilic substitution on a molecule of 1-bromoalkane with the formation of a linear alcohol, which further reacts with a second molecule of 1-bromoalkane to give a hydrogenated ethers.

Then, attributed to the phase-transfer the formation of several byproducts, a different way of synthesis was developed in order to obtain high pure PFEs with a straight and economical methodology.

4.2 Optimization procedure of reaction: control parameters

We tested another procedure to synthesize $PFE_{n,m}$, without phase-transfer catalysis, using addition of fluorinated alcohols to bromo-alkanes under basic conditions, as Murata's procedure [144]. To formulate a straight and economic procedure for an industrial application, it necessary to test different conditions of the fundamental control parameters including temperature, solvent, basic conditions, etc.

4.2.1 Solvent

The requirement of a solvent with an excellent solvation power and also with an economic cost carried out to change different solvents. At the first time, acetone was used but it leaded to several byproducts and low yields. Then, 1-3 dioxalane was used with the same results. Another attempt was made with N,N-dimethylformamide. It is reported the synthesis using N,N-dimethylformamide as solvent. It leaded to good yield (as demonstrated in previous paragraph) but this solvent can't be used because as demonstrated by spectra GC-MS in Figure 16, there was the formation of a byproduct between alcohol and solvent (Scheme 9).

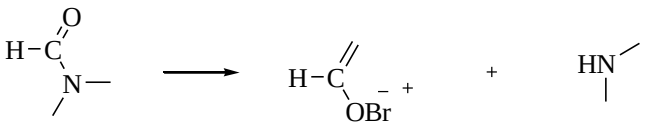

Scheme 9: formation of a byproduct between alcohol and solvent

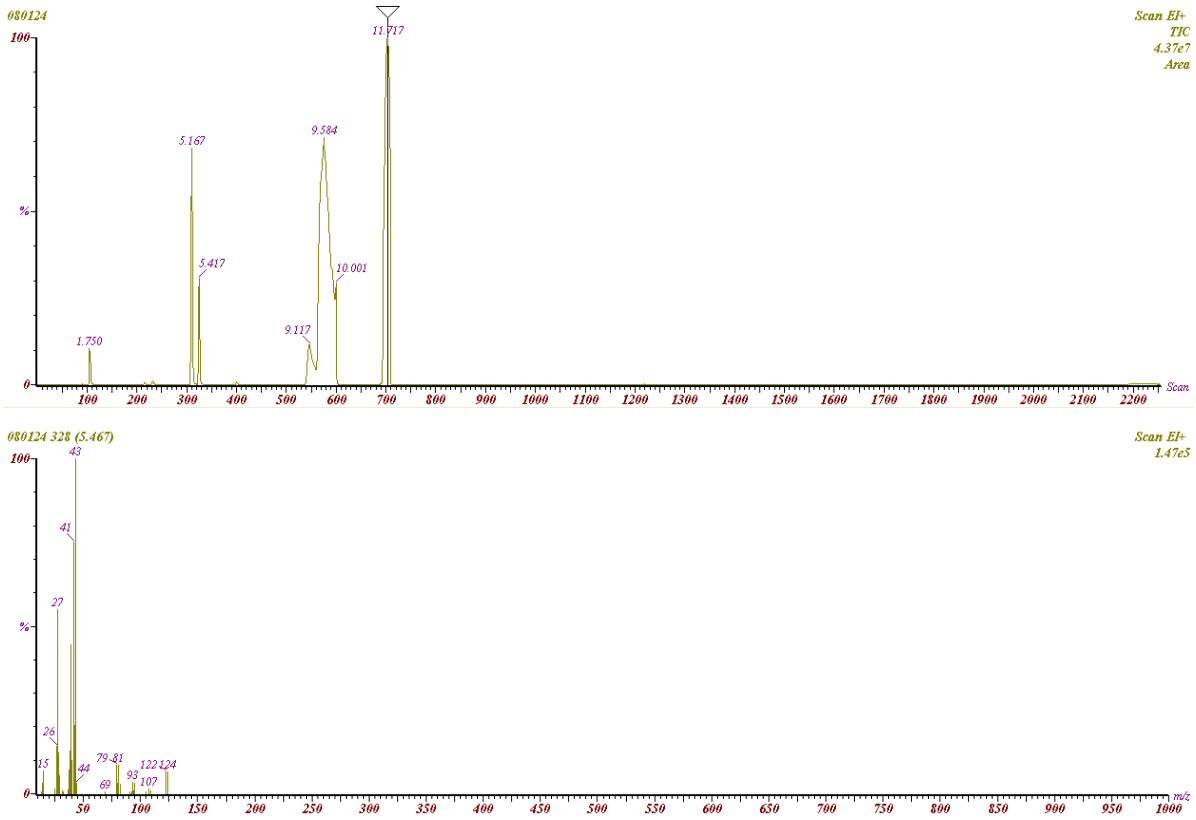

Figure 16: GC-MS of product synthesized with N-N dimethylformamide as solvent of reaction

Finally, N-methyl-pyrrolidone was used. It was an industrial candidate: in fact, the use of solvent leads to good yield and its removal, at the end of reaction, is very simple by water extraction.

The following paragraphs report examples of synthesis using 1-3 dioxalane and N,N-dimethylformamide as solvent of reaction.

Synthesis of 1,1,1,2,2,3,3,4,4-Nonafluoro-6-oxy-propane ($PFE_{4,3}$)

A mixture comprising of 30 g (0.11 mol) 1H,1H,2H,2H-nonafluoro-1-ol, 100 mL of 1-3 dioxalane and 27.0 g (0.22 mol) of bromopropane, dropwising for 20 minutes 15.5 g of a 45 % aqueous solution KOH, was heated under stirring for 23 h at room temperature and 14 h at 70 °C. Then, the raw reaction mixture was filtered so as to remove the formed KBr and the washed for several times with deionized water to eliminate traces of solvent. At the end, the organic phase of $PFE_{4,3}$ were purified by distillation in a kugelrohr apparatus under reduced pressure to give colorless liquid. It obtained with a 57 % of yield.

Synthesis of 1,1,1,2,2,3,3,4,4,5,5,6,6 Tridecafluoro-8-oxy-propane ($PFE_{6,3}$)

A mixture comprising of 30.0 g (0.08 mol) of 1H,1H,2H,2H-tridecafluoro-1-ol, 50.0 g of N,N-dimethylformamide and 19.68 g (0.16 mol) of bromopropane, dropwising for 30

minutes 31.1 g of a 45 % aqueous solution KOH, was heated under stirring for 5 h at 90 °C. Then, the raw reaction mixture was filtered so as to remove the formed KBr and the washed for several times to eliminate traces of solvent. At the end, 23.8 g of $PFE_{6,3}$ were obtained with a 73 % of yield.

4.2.2 Temperature

The reaction was carried out at several temperatures (10 - 90 °C) controlling the formation of byproducts and the yields. The reaction was carried out for 2.5 h at 90 °C with a good yield (80 %) initially but with the formation of several byproducts. In this case the formation of a byproduct due to opening of N-methyl pyrrolidone molecule was observed. Finally, the reaction was carried out at 30 °C leading to good yields and the decrease of formation of byproducts.

4.2.3 Basic conditions

Initially the basic conditions were created by sodium methoxide. In this case, a low rate reaction was obtained. Then, sodium hydroxide was used. It leaded a degradation of mixture also to low temperatures. Finally, potassium hydroxide was chosen.

4.2.4 Purification

The biomedical application requires high purity of products because some impurities can give inflammation response. In fact, the use of R_FR_H is progressively abandoned to the difficulty of purification.

Therefore, a industrial purification process to eliminate all impurities was carried out. The most abundant impurity to eliminate was the alcohol unreacted.

Hence, the second step of reaction consists of a treatment with a derivative of toluene diisocyanate-based (Desmodur®) to eliminate residue alcohol. After distillation, $PFE_{m,n}$ result very pure products as demonstrated by NMR and GC-MS spectra (Figure 17).

Toxicological in vitro tests were performed by Al.Chi.Mi.A S.r.l. to evaluate biocompatibility of the $PFE_{m,n}$ with m= 4, 6 and n= 3, 5, destined to ophthalmic use.

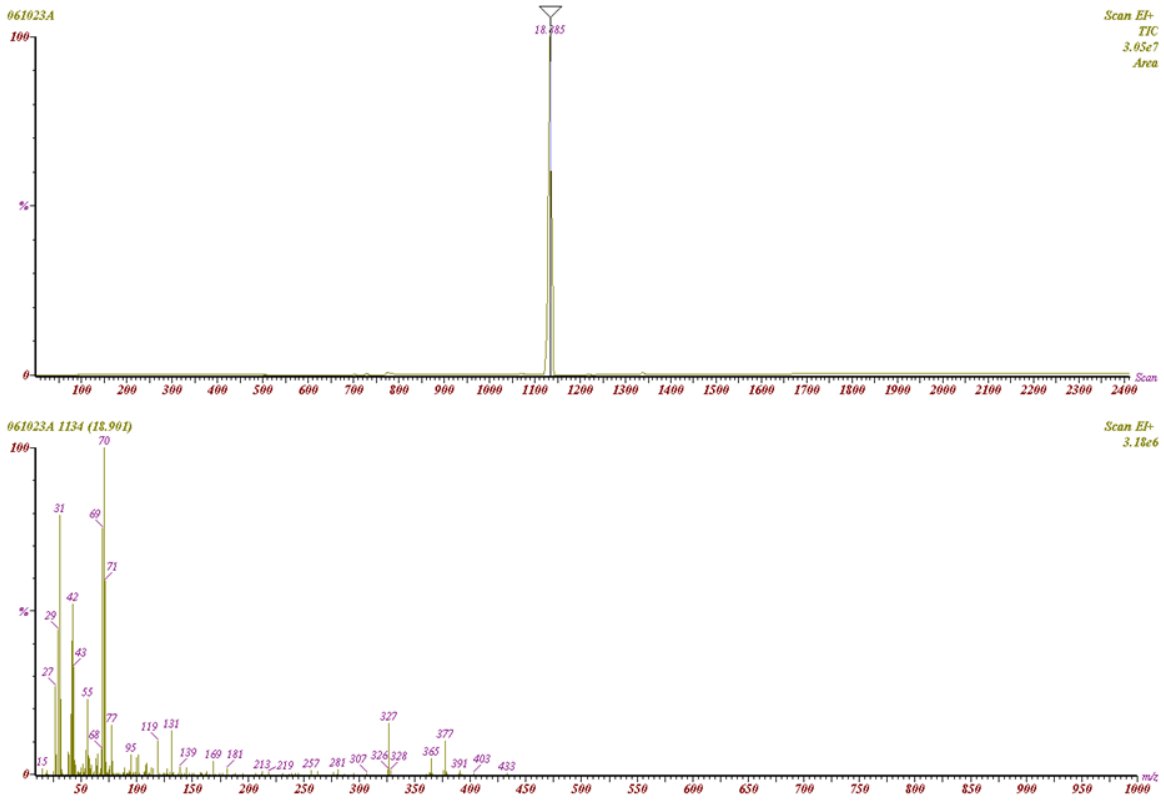

Figure 17: GC-MS $PFE_{6,5}$ after treatment of Desmodur®

In this case the presence of toxicological compounds (traces of heavy metal derived by use of Desmodur®) leaded to think to a new technology for the purification of the partially fluorinated ethers destined to ophthalmic use. Therefore, the treatment with Desmodur®, to eliminate the residue alcohol, is a good and rapid technology that can be used for partially fluorinated ethers with a long fluorocarbon hydrocarbon chains destined, for instance, as lubricants in sky-wax products, in substitution of R_FR_H products.

4.2.5 Purification via flash column chromatography

It is necessary to find a treatment of purification industrially applicable.

The partially fluorinated ethers $PFE_{n,m}$ with n= 4, 6 and m= 3, 5 designated to ophthalmic use were purified via flash column chromatography on alumina with diethyl ether as the eluent to eliminate traces of alcohol un-reacted. This is a convenient industrial method because it permits also to recovery of fluorinated alcohol.

The presence of other impurities of symmetric ethers in particular on $PFE_{n,m}$ with n= 4, 6 and m= 3, 5 is very difficult to eliminate with a distillation method because they have a boiling point very close to fluorinated ethers synthesized. Therefore, another treatment in column chromatography was performed.

The products were treated via flash column chromatography on Fluorisil® using n-hexane as eluent without good results. Then, it was used a flash column chromatography on silica gel with diethyl-ether as eluent.

Then, another passage in carbon column with methanol as eluent was performed.

Two types of carbon (Norit® S-A2 and Darco® G-60) were tested.

STEP A: $PFE_{6,5}$ with a 1.38 % of penthilic ether was treated via flash column chromatography on Norit® S-A2. A partially fluorinated ether was obtained with 0.55 % of impurities. Then, further steps are necessary to obtained a very high pure product.

Therefore, an other carbon column was tested.

STEP B: $PFE_{6,5}$ with 1.12 % of penthilic ether was treated by flash column chromatography on Darco® G-60, 100 mesh using methanol as eluent. The yield was 75 %.

The use of Darco® G-60 allows to obtain highly pure products with only one passage in carbon column.

This method was used to purify $PFE_{4,3}$, $PFE_{4,5}$, $PFE_{6,3,}$ $PFE_{6,5}$ with a yields of 96 %, 93 % and 82 %, 79 % respectively.

4.2.6 Conclusion

The general procedure for an economical and straight synthesis is:

1° STEP: dropping a 45 % aqueous solution of potassium hydroxide in a mixture composed by N-methyl- 2-pyrrolidone, 1H,1H,2H,2H-perfluoro-1-alkanols and 1-bromoalkane at 30 °C for 7 - 35 h as function of hydrocarbon and fluorocarbon length.

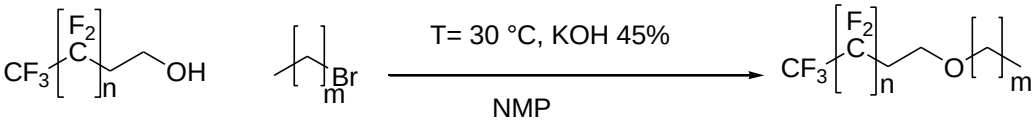

Scheme 10: second procedure to synthesis of partially fluorinated ethers

Therefore, the purification of $PFE_{n,m}$ was carried out by Desmodur® 3400 or 3600 as reported in STEP 2. In alternative, if the compounds are destined to biomedical use the purification was carried out using flash column chromatography as reported in STEP 3.

2° STEP: The mixture $PFE_{n,m}$ is treated with Desmodur® N 3600 (toluene isocyanate based compound) to eliminate un-reacted alcohol using drops of dibutyltin laureate, as catalyst. It is heated at 90-100 °C for several minutes. Then, a distillation was carried out.

3° STEP: The mixture of $PFE_{n,m}$ was purified by a flash column chromatography on silica gel with diethyl-ether as eluent. Then, the ether was treated by flash column chromatography on Darco® G-60 (100 mesh) using methanol as eluent.

Synthesis of 1,1,1,2,2,3,3,4,4-Nonafluoro-6-oxy-ethane ($PFE_{4,2}$)

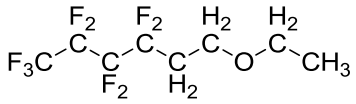

1° STEP: A mixture of 20 g (0.075 mol) 1H,1H,2H,2H-nonafluoro-1-ol, 40 g of N-methyl-pirrolidinone was adjunct to 16.5 g (0.17 mol) of bromoethane, dropwising for 30 minutes 20 g of a 45 % aqueous solution KOH. Then, it was heated under stirring for 17 h at room temperature. Then, the raw reaction mixture was filtered so as to remove the formed KBr and then washed for several times to eliminate traces of solvent. At the end, 20.2 g of crude $PFE_{4,2}$ were obtained with a 97.5 % of yield.

2° STEP: The mixture was treated with Desmodur® N 3600 (toluene isocyanate based compound) to eliminate un-reacted alcohol (2 %). Therefore, 20.2 g of $PFE_{4,2}$ and 0.7 g of Desmodur® N 3600 and 1 drops of dibutyltin laureate, as catalyst, were heated at 90-100 °C for several minutes. Then, a distillation was carried out. 19.8 g of fluorinated ether were obtained with a 95.6 % of yield.

Colourless liquid;

spectral data: MS *m/z* (rel. ab. %): 292 ($[M]^+$, 10 %); 277 ($[M\text{-}CH_3]^+$, 30 %), 263 ($[M\text{-}CH_3CH_2]^+$, 5 %), 73 ($[M\text{-}CF_3(CF_2)_3]^+$, 10 %), 59 ($[M\text{-}CF_3(CF_2)_3, \text{-}CH_2]^+$, 100 %), 29 ($[M\text{-}CF_3(CF_2)_3CH_2CH_2O]^+$, 100 %); FTIR: $\nu_{C\text{-}F}$ 1122-1321 cm^{-1}, $\nu_{C\text{-}H}$ 2851-2923 cm^{-1}.

^{1}H NMR (CD_3OD) : δ = 0.90 (t, $CH_3(\alpha)$, 3H); 3.35 (t, $CH_2(\beta)$, 2H); 3.73 (t, $CH_2(x)$, 2H); 2.49 (ttt, $CH_2(y)$, 2H);

^{19}F NMR (CD_3OD): δ = -84.2 (t, $CF_3(a)$, 3F); -128.9 (m, $CF_2(b)$, 2F); -127.3 (m, $CF_2(c)$, 2F); -116.2 (m, $CF_2(d)$, 2F).

Anal. calcd for $C_8H_9F_9O$: C, 32.9 %; F, 58.6 %; H, 3.1 %. Found: C, 32.1 %; F, 58.1 %; H, 2.9 %.

Synthesis of 1,1,1,2,2,3,3,4,4,5,5,6,6-Tridecafluoro-8-oxy-ethane ($PFE_{6,2}$)

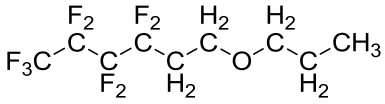

1° STEP: A mixture of 20.0 g (0.054 mol) 1H,1H,2H,2H-tridecafluoro-1-ol, 40 g of N-methylpyrrolidinone and was adjunct to 12.0 g (0.11 mol) of bromoethane, dropwising for 30 minutes 50 g of a 45 % aqueous solution KOH. Then, it was heated under stirring for 14 h at room temperature. Then, the raw reaction mixture was filtered so as to remove the formed KBr and the washed for several times to eliminate traces of solvent. At the end, 20.0 g of crude $PFE_{6,2}$ were obtained with 98.5 % of yield.

2° STEP: The mixture was treated with Desmodur® N 3600 (toluene isocyanate based compound) to eliminate un-reacted alcohol (1.35 %). Therefore, 20.0 g of $PFE_{6,2}$ and 0.7 g of Desmodur® N 3600 and 2 drops of dibutyltin laureate, as catalyst, were heated at 90-100 °C for several minutes. Then, a distillation was carried out. 19.5 g fluorinated ether were obtained with a 95 % of yield.

Colourless liquid;

spectral data: MS *m/z* (rel. ab. %): 392 ($[M]^+$, 5 %); 277 ($[M\text{-}CH_3]^+$, 30 %), 363 ($[M\text{-}CH_3CH_2]^+$, 5 %), 73 ($[M\text{-}CF_3(CF_2)_5]^+$, 5 %), 59 ($[M\text{-}CF_3(CF_2)_5, \text{-}CH_2]^+$, 100 %), 29 ($[M\text{-}CF_3(CF_2)_5CH_2CH_2O]^+$, 100 %);

FTIR: $\nu_{C\text{-}F}$ 1120-1325 cm^{-1}, $\nu_{C\text{-}H}$ 2860-2900 cm^{-1}.

^{1}H NMR (CD_3OD): δ = 0.90 (t, $CH_3(\alpha)$, 3H); 3.36 (t, $CH_2(\beta)$, 2H); 3.74 (t, CH_2(x), 2H); 2.50 (ttt, CH_2(y), 2H);

^{19}FNMR (CD_3OD): δ = -83.9 (t, CF_3(a), 3F); -129.1 (m, CF_2(b), 2F); -126.3 (m, CF_2(c), 2F); -125.6 (m, CF_2(d), 2F); -124.6 (m, CF_2(e), 2F); -116.0 (m, CF_2(f), 2F).

Anal. calcd for $C_{10}H_9F_{13}O$: C, 30.6 %; F, 63.0 %; H, 2.3 %. Found: C, 30.9 %; F, 62.6 %; H, 2.1 %.

Synthesis of 1,1,1,2,2,3,3,4,4,5,5,6,6,7,7,8,8-Heptadecafluoro-10-oxy-ethane ($PFE_{8,2}$)

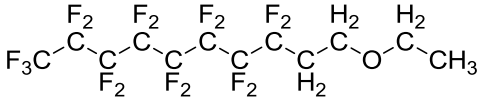

1° STEP: A mixture of 20.0 g (0.043 mol) 1H,1H,2H,2H-heptadecafluoro-1-ol, 40.0 g of N-methylpyrrolidinone was adjunct to 6.9 g (0.064 mol) of bromoethane, dropwising for 30 minutes 20.0 g of a 45 % aqueous solution KOH. Then, it was heated under stirring for 23 h at room temperature. Then, the raw reaction mixture was filtered so as to remove the formed

KBr and then washed for several times to eliminate traces of solvent. At the end, 20.3 g of crude $PFE_{8,2}$ were obtained with 98.5 % of yield.

2° STEP: The mixture was treated with Desmodur® N 3600 (toluene isocyanate based compound) to eliminate un-reacted alcohol (0.31 %). Therefore, 20.3 g of $PFE_{8,2}$ and 0.7 g of Desmodur® N 3600 and 2 drops of dibutyltin laureate, as catalyst, were heated at 90-100 °C for several minutes. Then, a distillation was carried out. 20.2 g of fluorinated ether were obtained with a 98 % of yield.

Colourless liquid;

spectral data: MS *m/z* (rel. ab. %): 492 ($[M]^+$, 5 %); 377 ($[M\text{-}CH_3]^+$, 20 %), 463 ($[M\text{-}CH_3CH_2]^+$, 10 %), 73 ($[M\text{-}CF_3(CF_2)_7]^+$, 10 %), 59 ($[M\text{-}CF_3(CF_2)_7, \text{-}CH_2]^+$, 100 %), 29 ($[M\text{-}CF_3(CF_2)_8CH_2CH_2O]^+$, 100 %);

FTIR: $\nu_{C\text{-}F}$ 1125-1320 cm^{-1}, $\nu_{C\text{-}H}$ 2870-2910 cm^{-1}.

^{1}H NMR (CD_3OD): δ = 0.90 (t, $CH_3(\alpha)$, 3H); 3.38 (t, $CH_2(\beta)$, 2H); 3.73 (t, $CH_2(\gamma)$, 2H); 2.48 (ttt, $CH_2(\delta)$, 2H);

^{19}F NMR (CD_3OD): δ = -83.6 (t, CF_3(a), 3F); -128.5 (m, CF_2(b), 2F); -126.4 (m, CF_2(c), 2F); -125.4 (m, CF_2(d), 2F); -124.6 (m, CF_2(e), 2F); -123.1 (m, CF_2(f), 2F); -122.5 (m, CF_2(g), 2F); -115.4 (m, CF_2(h), 2F).

Anal. calcd for $C_{12}H_9F_{17}O$: C, 29.3 %; F, 65.6 %; H, 1.8 %. Found: C, 29.8 %; F, 66.4 %; H, 1.9 %.

Synthesis of 1,1,1,2,2,3,3,4,4-Nonafluoro-7-oxadecane ($PFE_{4,3}$)

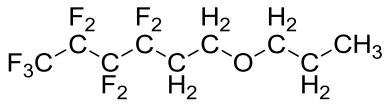

1° STEP: A mixture comprising of 30.0 g (0.11 mol) 1H,1H,2H,2H-nonafluoro-1-ol, 40.0 g of N-methylpyrrolidinone was adjunct to 21.3 g (0.17 mol) of bromopropane, dropwising for 30 minutes 50.0 g of a 45 % aqueous solution KOH. Then, it was heated under stirring for 23 h at room temperature. Then, the raw reaction mixture was filtered so as to remove the formed KBr and the washed for several times to eliminate traces of solvent. At the end, 30.3 g of crude $PFE_{4,3}$ were obtained with 90.2 % of yield.

2° STEP: The mixture was treated with Desmodur® N 3600 (toluene isocyanate based compound) to eliminate un-reacted alcohol (1.05 %). Therefore, 30.3 g of $PFE_{4,3}$ and 0.7 g of Desmodur® N 3600 and 2 drops of dibutyltin laureate, as catalyst, were heated at 90-100 °C for several minutes. Then, a distillation was carried out. 28.3 g of fluorinated ether were obtained with a 84 % of yield.

Colourless liquid;

spectral data: MS *m/z* (rel. ab. %): 306 ($[M]^+$, 10 %), 291 ($[M\text{-}CH_3]^+$, 30 %), 277 ($[M\text{-}CH_2CH_3]^+$, 30 %), 263 ($[M\text{-}CH_3CH_2CH_2]^+$, 10 %), 87 ($[M\text{-}CF_3(CF_2)_3]^+$, 5 %), 73 ($[M\text{-}CF_3(CF_2)_3, \text{-}CH_2]^+$, 90 %), 43 ($[M\text{-}CF_3(CF_2)_3CH_2CH_2O]^+$, 100 %);

FTIR: $\nu_{C\text{-}F}$ 1118-1305 cm^{-1}, $\nu_{C\text{-}H}$ 2880-2930 cm^{-1}.

^{1}H NMR (CD_3OD): δ = 0.90 (t, $CH_3(\alpha)$, 3H); 1.56 (t, $CH_2(\beta)$, 2H); 3.41 (t, $CH_2(\gamma)$, 2H); 3.73 (t, CH_2(x), 2H); 2.49 (ttt, $CH_2(\delta)$, 2H);

^{19}F NMR (CD_3OD): δ = -84.2 (t, CF_3(a), 3F); -128.8 (m, CF_2(b), 2F); -127.4 (m, CF_2(c), 2F); -116.1 (m, CF_2(d), 2F).

Anal. calcd for $C_9H_{11}F_9O$: C, 35.3 %; F, 55.6 %; H, 3.6 %. Found: C, 35.9 %; F, 55.0 %; H, 3.3 %.

Synthesis of 1,1,1,2,2,3,3,4,4,5,5,6,6 Tridecafluoro-8-oxy-propane ($PFE_{6,3}$)

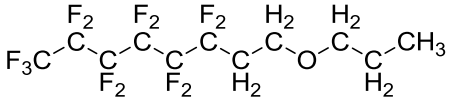

1° STEP: A mixture of 100.0 g (0.27 mol) of 1H,1H,2H,2H-tridecafluoro-1-ol, 110.0 g of N-methylpyrrolidinone was adjunct to 61.5 g (0.5 mol) of bromopropane, dropwising for 30 minutes 100.0 g of a 45 % aqueous solution KOH, was heated under stirring for 32 h at room temperature. Then, the raw reaction mixture was filtered so as to remove the formed KBr and then washed for several times to eliminate traces of solvent. At the end, 107.6 g of crude $PFE_{6,3}$ were obtained with 98.1 % of yield.

2° STEP: The mixture was treated with Desmodur® N 3600 (isocyanate) to eliminate un-reacted alcohol (4.3 %). Therefore, 107.6 g of $PFE_{4,5}$ and 5.3 g of Desmodur® N 3600 and 3 drops of dibutyltin laureate, as catalyst, were heated at 90-100 °C for several minutes. Then, a distillation was carried out. 93.2 g of fluorinated ether were obtained with a 85 % of yield.

Colourless liquid;

spectral data: MS *m/z* (rel. ab. %): 406 ($[M]^+$, 5 %), 391 ($[M\text{-}CH_3]^+$, 25 %), 377 ($[M\text{-}CH_2CH_3]^+$, 20 %), 363 ($[M\text{-}CH_3CH_2CH_2]^+$, 15 %), 87 ($[M\text{-}CF_3(CF_2)_5]^+$, 10 %), 73 ($[M\text{-}CF_3(CF_2)_5, \text{-}CH_2]^+$, 100 %), 43 ($[M\text{-}CF_3(CF_2)_5CH_2CH_2O]^+$, 100 %);

FTIR: $\nu_{C\text{-}F}$ 1125-1310 cm^{-1}, $\nu_{C\text{-}H}$ 2890-2910 cm^{-1}.

^{1}H NMR (CD_3OD): δ = 0.90 (t, $CH_3(\alpha)$, 3H); 1.55 (t, $CH_2(\beta)$, 2H); 3.42 (t, $CH_2(\gamma)$, 2H); 3.74 (t, $CH_2(\delta)$, 2H); 2.50 (ttt, $CH_2(\varepsilon)$, 2H);

^{19}F NMR (CD_3OD): δ = -83.9 (t, CF_3(a), 3F); -129.1 (m, CF_2(b), 2F); -126.3 (m, CF_2(c), 2F); -125.6 (m, CF_2(d), 2F); -124.6 (m, CF_2(e), 2F); -116.0 (m, CF_2(f), 2F).

Anal. calcd for $C_{11}H_{11}F_{13}O$: C, 32.5 %; F, 60.8 %; H, 2.7 %. Found: C, 31.9 %; F, 61.2 %; H, 2.5 %.

Synthesis of 1,1,1,2,2,3,3,4,4,5,5,6,6,7,7,8,8-Heptadecafluoro-10-oxy-propane ($PFE_{8,3}$).

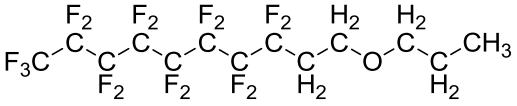

1° STEP: A mixture of 10.0 g (0.021 mol) 1H,1H,2H,2H-heptadecafluoro-1-ol, 30.0 g of N-methylpyrrolidinone was adjunct to 5.14 g (0.042 mol) of bromopropane, dropwising for 30 minutes 16.0 g of a 45 % aqueous solution KOH. Then, it was heated under stirring for 8 h at room temperature. Then, the raw reaction mixture was filtered so as to remove the formed KBr and then washed for several times to eliminate traces of solvent. At the end, 9.1 g of crude $PFE_{8,3}$ were obtained with 85.4 % of yield.

2° STEP: The mixture was treated with Desmodur® N 3600 (toluene isocyanate based compound) to eliminate un-reacted alcohol (2.1 %). Therefore, 9.1 g of $PFE_{8,3}$ and 0.7 g of Desmodur® N 3600 and 2 drops of dibutyltin laureate, as catalyst, were heated at 90-100 °C for several minutes. Then, a distillation was carried out. 8.7 g of fluorinated ether were obtained with a 82 % of yield.

Colourless liquid;

spectral data: MS *m/z* (rel. ab. %): 506 ($[M]^+$, 5 %); 491 ($[M\text{-}CH_3]^+$, 20 %), 377 ($[M\text{-}CH_3CH_2]^+$, 15 %), 463 ($[M\text{-}CH_3CH_2CH_2]^+$, 10 %), 87 ($[M\text{-}CF_3(CF_2)_7]^+$, 10 %), 73 ($[M\text{-}CF_3(CF_2)_7, \text{-}CH_2]^+$, 100 %), 43 ($[M\text{-}CF_3(CF_2)_8CH_2CH_2O]^+$, 100 %);

FTIR: $\nu_{C\text{-}F}$ 1120-1320 cm^{-1}, $\nu_{C\text{-}H}$ 2890-2920 cm^{-1}.

^{1}H NMR (CD_3OD): δ = 0.90 (t, $CH_3(\alpha)$, 3H); 1.54 (t, $CH_2(\beta)$, 2H); 3.41 (t, $CH_2(\gamma)$, 2H); 3.73 (t, $CH_2(\delta)$, 2H); 2.51 (ttt, $CH_2(\varepsilon)$, 2H);

^{19}F NMR (CD_3OD): δ = -83.7 (t, CF_3(a), 3F); -128.4 (m, CF_2(b), 2F); -126.2 (m, CF_2(c), 2F); -125.6 (m, CF_2(d), 2F); -124.8 (m, CF_2(e), 2F); -123.3 (m, CF_2(f), 2F); -122.7 (m, CF_2(g), 2F); -115.2 (m, CF_2(h), 2F).

Anal. calcd for $C_{13}H_{11}F_{17}O$: C, 30.8 %; F, 63.8 %; H, 2.2 %. Found: C, 30.2 %; F, 63.4 %; H, 2.3 %.

Synthesis of 1,1,1,2,2,3,3,4,4 Nonafluoro-6-oxy-pentane ($PFE_{4,5}$)

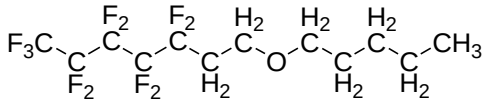

1° STEP: A mixture of 59.0 g (0.22 mol) 1H,1H,2H,2H-nonafluoro-1-ol, 70.0 g of N-methylpyrrolidinone was adjunct to 60.0 g (0.17 mol) of bromopentane, dropwising for 30 minutes 70.0 g of a 45 % aqueous solution KOH. Then, it was heated under stirring for 27 h at room temperature. Then, the raw reaction mixture was filtered so as to remove the formed KBr and then washed for several times to eliminate traces of solvent. At the end, 70.5 g of crude $PFE_{4,5}$ were obtained 95.7 % of yield.

2° STEP: The mixture was treated with Desmodur® N 3600 (isocianate) to eliminate un-reacted alcohol (4,96 %). Therefore, 70.5 g of $PFE_{4,5}$ and 3.5 g of Desmodur® N 3600 and 2 drops of dibutyltin laureate, as catalyst, were heated at 90-100 °C per several minutes. Then, a distillation was carried out. 66.2 g of fluorinated ether were obtained with a 90 % of yield.

Colourless liquid;

spectral data: MS *m/z* (rel. ab. %): 334 ($[M]^+$, 10 %), 319 ($[M\text{-}CH_3]^+$, 20 %), 305 ($[M\text{-}CH_2CH_3]^+$, 20 %), 291 ($[M\text{-}CH_3CH_2CH_2]^+$, 10 %), 277 ($[M\text{-}CH_3CH_2CH_2CH_2]^+$, 10 %); 115 ($[M\text{-}CF_3(CF_2)_3]^+$, 5 %), 101 ($[M\text{-}CF_3(CF_2)_3, \text{-}CH_2]^+$, 70 %), 71 ($[M\text{-}CF_3(CF_2)_3CH_2CH_2O]^+$, 100 %);

FTIR: $\nu_{C\text{-}F}$ 1110-1290 cm^{-1}, $\nu_{C\text{-}H}$ 2870-2920 cm^{-1}.

^{1}H NMR (CD_3OD): δ = 0.88 (t, $CH_3(\alpha)$, 3H); 1.33 (m, $CH_2(\beta)\div CH_2(\gamma)$, 4H); 1.56 (m, $CH_2(\delta)$, 2H); 3.45 (t, $CH_2(\varepsilon)$, 2H); 3.73 (t, $CH_2(\zeta)$, 2H); 2.49 (ttt, $CH_2(\eta)$, 2H).

^{19}F NMR (CD_3OD): δ = -84.2 (t, CF_3(a), 3F); -128.9 (m, CF_2(b), 2F); -127.4 (m, CF_2(c), 2F); -116.3 (m, CF_2(d), 2F).

Anal. calcd for $C_{11}H_{15}F_9O$: C, 39.5 %; F, 51.2 %; H, 4.5 %. Found: C, 39.2 %; F, 50.5 %; H, 4.2 %.

Synthesis of 1,1,1,2,2,3,3,4,4 tridecafluoro-6-oxy-pentane ($PFE_{6,5}$)

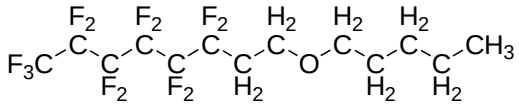

A mixture of 130.0 g (0.35 mol) of 1H,1H,2H,2H-tridecafluoro-1-ol, 130.0 g of N-methylpyrrolidinone was adjunct to 105.7 g (0.70 mol) of bromopentane, dropwising for 30 minutes 130.0 g of a 45 % aqueous solution KOH. It was heated under stirring for 35 h at room temperature. Then, the raw reaction mixture was filtered so as to remove the formed

KBr and then washed for several times to eliminate traces of solvent. At the end, 143.4 g of crude $PFE_{6,5}$ were obtained with 94.4 % of yield.

2° STEP: The mixture was treated with Desmodur® N 3600 (toluene isocyanate based compound) to eliminate un-reacted alcohol (4.96 %). Therefore, 143.4 g of $PFE_{6,5}$ and 5.5 g of Desmodur® N 3400 and 3 drops of dibutyltin laureate, as catalyst, were heated at 90-100 °C for several minutes. Then, a distillation was carried out. 125.0 g fluorinated ether were obtained with a 82 % of yield.

Colourless liquid;

spectral data: MS *m/z* (rel. ab. %): 334 ($[M]^+$, 10 %), 319 ($[M\text{-}CH_3]^+$, 20 %), 305 ($[M\text{-}CH_2CH_3]^+$, 20 %), 291 ($[M\text{-}CH_3CH_2CH_2]^+$, 10 %), 277 ($[M\text{-}CH_3CH_2CH_2CH_2]^+$, 10 %); 115 ($[M\text{-}CF_3(CF_2)_3]^+$, 5 %), 101 ($[M\text{-}CF_3(CF_2)_3, \text{-}CH_2]^+$, 70 %), 71 ($[M\text{-}CF_3(CF_2)_3CH_2CH_2O]^+$, 100 %);

FTIR: $\nu_{C\text{-}F}$ 1110-1290 cm^{-1}, $\nu_{C\text{-}H}$ 2870-2920 cm^{-1}.

^{1}H NMR (CD_3OD): δ = 0.88 (t, $CH_3(\alpha)$, 3H); 1.33 (m, $CH_2(\beta)\div CH_2(\gamma)$, 4H); 1.56 (m, $CH_2(\delta)$, 2H); 3.45 (t, $CH_2(\varepsilon)$, 2H); 3.73 (t, $CH_2(\zeta)$, 2H); 2.49 (ttt, $CH_2(\eta)$, 2H).

^{19}F NMR (CD_3OD): δ = -84.2 (t, CF_3(a), 3F); -128.9 (m, CF_2(b), 2F); -127.4 (m, CF_2(c), 2F); -116.3 (m, CF_2(d), 2F).

Anal. calcd for $C_{11}H_{15}F_9O$: C, 39.5 %; F, 51.2 %; H, 4.5 %. Found: C, 39.2 %; F, 50.5 %; H, 4.2 %.

Synthesis of 1,1,1,2,2,3,3,4,4,5,5,6,6,7,7,8,8 Heptadecafluoro-10-oxy-pentane ($PFE_{8,5}$)

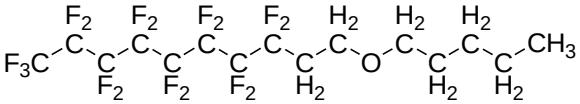

A mixture of 50.0 g (0.107 mol) of 1H,1H,2H,2H-heptadecafluoro-1-ol, 50 g of N-methylpyrrolidinone was adjunct to 31.7 g (0.21 mol) of bromopentane, dropwising for 30 minutes 50 g of a 45 % aqueous solution KOH. It was heated under stirring for 10h at room temperature. Then, the raw reaction mixture was filtered so as to remove the formed KBr and then washed for several times to eliminate traces of solvent. At the end, 53 g of crude $PFE_{8,5}$ was obtained with 92 % of yield.

2° STEP: The mixture was treated with Desmodur® N 3600 (toluene isocyanate based compound) to eliminate un-reacted alcohol (3 %). Therefore, 53 g of $PFE_{8,5}$ and 5.0 g of Desmodur® N 3400 and 3 drops of dibutyltin laureate, as catalyst, were heated at 90-100 °C

per several minutes. Then, a distillation was carried out. 46.8 g of fluorinated ether were obtained with a 82 % of yield.

Colourless liquid;

spectral data: MS *m/z* (rel. ab. %): 534 ($[M]^+$, 10 %), 519 ($[M\text{-}CH_3]^+$, 15 %), 505 ($[M\text{-}CH_2CH_3]^+$, 20 %), 491 ($[M\text{-}CH_3CH_2CH_2]^+$, 10 %), 477 ($[M\text{-}CH_3CH_2CH_2CH_2]^+$, 10 %); 115 ($[M\text{-}CF_3(CF_2)_7]^+$, 5 %), 101 ($[M\text{-}CF_3(CF_2)_7, \text{-}CH_2]^+$, 70 %), 71 ($[M\text{-}CF_3(CF_2)_7CH_2CH_2O]^+$, 100 %);

FTIR: $\nu_{C\text{-}F}$ 1120-1300 cm^{-1}, $\nu_{C\text{-}H}$ 2810-2930 cm^{-1}.

^{1}H NMR (CD_3OD): δ = 0.88 (t, $CH_3(\alpha)$, 3H); 1.33 (m, $CH_2(\beta)\div CH_2(\gamma)$, 4H); 1.56 (m, $CH_2(\delta)$, 2H); 3.45 (t, $CH_2(\varepsilon)$, 2H); 3.73 (t, $CH_2(\zeta)$, 2H); 2.49 (ttt, $CH_2(\eta)$, 2H).

^{19}F NMR (CD_3OD): δ = -83.5 (t, CF_3(a), 3F); -128.2 (m, CF_2(b), 2F); -126.5 (m, CF_2(c), 2F); -125.2 (m, CF_2(d), 2F); -124.6 (m, CF_2(e), 2F); -123.1 (m, CF_2(f), 2F); -122.3 (m, CF_2(g), 2F); -115.1 (m, CF_2(h), 2F).

Anal. calcd for $C_{15}H_{15}F_{17}O$: C, 33.7 %; F, 60.5 %; H, 2.8 %. Found: C, 33.1 %; F, 60.9 %; H, 2.3 %.

Synthesis of 1,1,1,2,2,3,3,4,4 Nonafluoro-6-oxy-octane ($PFE_{4,8}$)

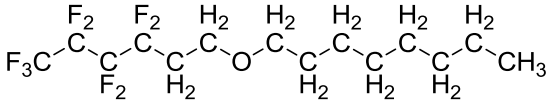

A mixture of 10.0 g (0.037 mol) 1H,1H,2H,2H-nanofluoro-1-ol, 10.0 g di N-methylpyrrolidinone was adjunct to 14.6 g (0.075 mol) of bromopentane, dropwising for 30 minutes 10 g of a 45 % aqueous solution KOH. It was heated under stirring for 26h at room temperature. Then, the raw reaction mixture was filtered so as to remove the formed KBr and then washed for several times to eliminate traces of solvent.

At the end, 11.5 g of crude $PFE_{4,8}$ were obtained with 82.7 % of yield.

2° STEP: The mixture was treated with Desmodur® N 3600 (toluene isocianate based compound) to eliminate un-reacted alcohol (2.4 %). Therefore, 11.5 g of $PFE_{4,5}$ and 0.5 g of Desmodur® N 3400 and 1 drop of dibutyltin laureate, as catalyst, were heated at 90-100 °C per several minutes. Then, a distillation was carried out. 9.7 g fluorinated ether were obtained with a 70 % of yield.

Colourless liquid;

spectral data: MS *m/z* (rel. ab. %): 397 ($[M]^+$, 5 %), 382 ($[M\text{-}CH_3]^+$, 15 %), 368 ($[M\text{-}CH_2CH_3]^+$, 15 %), 353 ($[M\text{-}CH_3CH_2CH_2]^+$, 5 %), 339 ($[M\text{-}CH_3CH_2CH_2CH_2]^+$, 5 %); 178

([M-$CF_3(CF_2)_3$]$^+$, 10 %), 164 ([M-$CF_3(CF_2)_3$, -CH_2]$^+$, 80 %), 134 ([M-$CF_3(CF_2)_3CH_2CH_2O$]$^+$, 100 %);

FTIR: ν_{C-F} 1100-1260 cm^{-1}, ν_{C-H} 2850-2910 cm^{-1}.

^{1}H NMR (CD_3OD): δ = 0.88 (t, CH_3(α), 3H); 1.36 (m, CH_2(β)÷CH_2(ζ), 8H); 1.56 (m, CH_2(η), 2H); 3.45 (t, CH_2(θ), 2H); 3.75 (t, CH_2(ι), 2H); 2.51 (ttt, CH_2(κ), 2H).

^{19}F NMR (CD_3OD): δ = -84.1 (t, CF_3(a), 3F); -128.8 (m, CF_2(b), 2F); -127.5 (m, CF_2(c), 2F); -116.1 (m, CF_2(d), 2F).

Anal. calcd for $C_{14}H_{21}F_9O$: C, 42.3 %; F, 43.1 %; H, 5.2 %. Found: C, 41.8 %; F, 42.1 %; H, 5.5 %.

Synthesis of 1,1,1,2,2,3,3,4,4,5,5,6,6 Tridecafluoro-8-oxy-octane ($PFE_{6,8}$)

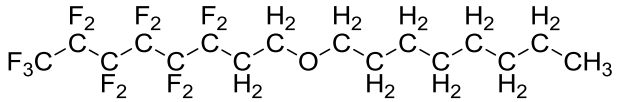

A mixture of 10.0 g (0.027 mol) 1H,1H,2H,2H-tridecafluoro-1-ol, 130.0 g of N-methylpyrrolidinone was adjunct to 10.6 g (0.054 mol) of bromopentane, dropwising for 30 minutes 10 g of a 45 % aqueous solution KOH. It was heated under stirring for 18h at room temperature. Then, the raw reaction mixture was filtered so as to remove the formed KBr and then washed for several times to eliminate traces of solvent.

At the end, 11.8 g of crude $PFE_{6,8}$ were obtained with 91.8 % of yield.

2° STEP: The mixture was treated with Desmodur® N 3600 (toluene isocianate based compound) to eliminate un-reacted alcohol (3.15 %). Therefore, 11.8g of $PFE_{4,5}$ and 0.5 g of Desmodur® N 3400 and 1 drops of dibutyltin laureate, as catalyst, were heated at 90-100 °C for several minutes. Then, a distillation was carried out. 9.1 g of fluorinated ether were obtained with a 71 % of yield.

Colourless liquid;

spectral data: MS *m/z* (rel. ab. %): 497 ([M]$^+$, 5 %), 482 ([M-CH_3]$^+$, 10 %), 468 ([M-CH_2CH_3]$^+$, 20 %), 453 ([M-$CH_3CH_2CH_2$]$^+$, 10 %), 439 ([M-$CH_3CH_2CH_2CH_2$]$^+$, 10 %); 178 ([M-$CF_3(CF_2)_5$]$^+$, 15 %), 164 ([M-$CF_3(CF_2)_5$, -CH_2]$^+$, 70 %), 134 ([M-$CF_3(CF_2)_5CH_2CH_2O$]$^+$, 100 %);

FTIR: ν_{C-F} 1120-1280 cm^{-1}, ν_{C-H} 2810-2920 cm^{-1}.

^{1}H NMR (CD_3OD): δ = 0.88 (t, CH_3(α), 3H); 1.36 (m, CH_2(β)÷CH_2(ζ), 8H); 1.56 (m, CH_2(η), 2H); 3.45 (t, CH_2(θ), 2H); 3.75 (t, CH_2(ι), 2H); 2.51 (ttt, CH_2(κ), 2H).

^{19}F NMR (CD_3OD): δ = -83.7 (t, CF_3(a), 3F); -129.3 (m, CF_2(b), 2F); -126.3 (m, CF_2(c), 2F); -125.9 (m, CF_2(d), 2F); -124.7 (m, CF_2(e), 2F); -116.2 (m, CF_2(f), 2F).

Anal. calcd for $C_{16}H_{21}F_{13}O$: C, 38.6 %; F, 34.4 %; H, 4.2 %. Found: C, 38.1 %; F, 33.2 %; H, 3.9 %.

Synthesis 1,1,1,2,2,3,3,4,4,5,5,6,6,8,8,9,9 Heptadecafluoro-10-oxy-octane ($PFE_{8,8}$)

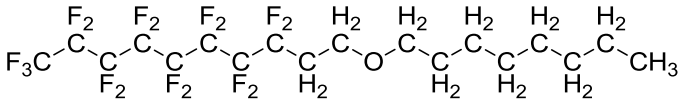

A mixture of 15.0 g (0.032 mol) of 1H,1H,2H,2H-heptadecafluoro-1-ol, 25.0 g of N-methylpyrrolidinone was adjunct to 12.35 g (0.064 mol) of bromooctane, dropwising for 60 minutes 17.7 g of a 45 % aqueous solution KOH. It was heated under stirring for 15h at room temperature. Then, the raw reaction mixture was filtered so as to remove the formed KBr and then washed for several times to eliminate traces of solvent.

At the end, 18 g of crude $PFE_{8,8}$ were obtained with 97.8 % of yield.

2° STEP: The mixture was treated with Desmodur® N 3600 (toluene isocyanate based compound) to eliminate un-reacted alcohol (2.76 %). Therefore, 18.0 g of $PFE_{8,8}$ and 0.5 g of Desmodur® N 3400 and 1 drops of dibutyltin laureate, as catalyst, were heated at 90-100 °C per several minutes. Then, a distillation was carried out. 13.3 g fluorinated ether were obtained with a 72 % of yield.

Colourless viscous liquid;

spectral data: MS *m/z* (rel. ab. %): 597 ($[M]^+$, 10 %), 582 ($[M\text{-}CH_3]^+$, 5 %), 568 ($[M\text{-}CH_2CH_3]^+$, 10 %), 553 ($[M\text{-}CH_3CH_2CH_2]^+$, 15 %), 539 ($[M\text{-}CH_3CH_2CH_2CH_2]^+$, 5 %); 178 ($[M\text{-}CF_3(CF_2)_7]^+$, 10 %), 164 ($[M\text{-}CF_3(CF_2)_7, \text{-}CH_2]^+$, 90 %), 134 ($[M\text{-}CF_3(CF_2)_7CH_2CH_2O]^+$, 100 %);

FTIR: $\nu_{C\text{-}F}$ 1110-1290 cm^{-1}, $\nu_{C\text{-}H}$ 2800-2900 cm^{-1}.

^{1}H NMR (CD_3OD): δ = 0.88 (t, CH_3(α), 3H); 1.36 (m, CH_2(β)÷CH_2(ζ), 8H); 1.56 (m, CH_2(η), 2H); 3.45 (t, CH_2(θ), 2H); 3.75 (t, CH_2(ι), 2H); 2.51 (ttt, CH_2(κ), 2H).

^{19}F NMR (CD_3OD): δ = -83.3 (t, CF_3(a), 3F); -128.1 (m, CF_2(b), 2F); -126.4 (m, CF_2(c), 2F); -125.3 (m, CF_2(d), 2F); -124.8 (m, CF_2(e), 2F); -123.0 (m, CF_2(f), 2F); -122.5 (m, CF_2(g), 2F); -115.0 (m, CF_2(h), 2F). Anal. calcd for $C_{18}H_{21}F_{17}O$: C, 36.2 %; F, 28.6 %; H, 3.5 %. Found: C, 36.9 %; F, 29.2 %; H, 3.8 %.

Synthesis of 1,1,1,2,2,3,3,4,4 Nonafluoro-6-oxy-tetradecane ($PFE_{4,14}$)

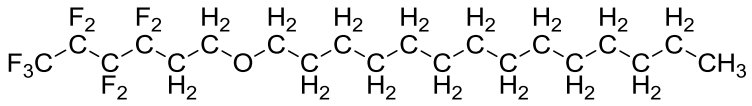

A mixture of 5.0 g (0.019 mol) 1H,1H,2H,2H-nonafluoro-1-ol, 5.0 g of N-methylpyrrolidinone was adjunct to 10.5 g (0.037 mol) of bromotetradecane, dropwising for 30 minutes 5 g of a 45 % aqueous solution KOH. It was heated under stirring for 40 h at room temperature. Then, the raw reaction mixture was filtered so as to remove the formed KBr and then washed for several times to eliminate traces of solvent.

At the end, 7.8 g of crude $PFE_{4,14}$ were obtained with 89.2 % of yield.

2° STEP: The mixture was treated with Desmodur® N 3600 (toluene isocyanate based compound) to eliminate un-reacted alcohol (2.4 %). Therefore, 7.8 g of $PFE_{4,14}$ and 0.5 g of Desmodur® N 3400 and 1 drops of dibutyltin laureate, as catalyst, were heated at 90-100 °C per several minutes. Then, a distillation was carried out. 6.2 g fluorinated ether were obtained with a 71 % of yield.

White solid;

spectral data: MS *m/z* (rel. ab. %): 536 ($[M]^+$, 10 %), 521 ($[M\text{-}CH_3]^+$, 10 %), 507 ($[M\text{-}CH_2CH_3]^+$, 15 %), 493 ($[M\text{-}CH_3CH_2CH_2]^+$, 10 %), 479 ($[M\text{-}CH_3CH_2CH_2CH_2]^+$, 10 %); 317 ($[M\text{-}CF_3(CF_2)_3]^+$, 15 %), 303 ($[M\text{-}CF_3(CF_2)_3, \text{-}CH_2]^+$, 100 %), 273 ($[M\text{-}CF_3(CF_2)_3CH_2CH_2O]^+$, 100 %);

FTIR: $\nu_{C\text{-}F}$ 1105-1270 cm^{-1}, $\nu_{C\text{-}H}$ 2840-2920 cm^{-1}.

^{1}H NMR (CD_3OD): δ = 0.90 (t, $CH_3(\alpha)$, 3H); 1.31 (m, $CH_2(\beta)\div CH_2(\mu)$, 22H); 1.54 (m, $CH_2(\nu)$, 2H); 3.41 (t, $CH_2(\xi)$, 2H); 3.72 (t, $CH_2(o)$, 2H); 2.49 (ttt, $CH_2(\pi)$, 2H.

^{19}F NMR (CD_3OD): δ = -84.2 (t, CF_3(a), 3F); -128.9 (m, CF_2(b), 2F); -127.1 (m, CF_2(c), 2F); -116.8 (m, CF_2(d), 2F).

Anal. calcd for $C_{20}H_{33}F_9O$: C, 44.8 %; F, 32.0 %; H, 6.1 %. Found: C, 44.2 %; F, 31.5 %; H, 5.9 %.

Synthesis of 1,1,1,2,2,3,3,4,4,5,5,6,6 Tridecafluoro-8-oxy-tetradecane ($PFE_{6,14}$)

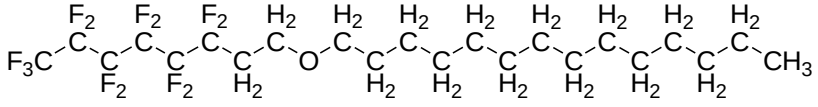

A mixture of 10.0 g (0.027 mol) 1H,1H,2H,2H-tridecafluoro-1-ol, 10.0 g of N-methylpyrrolidinone was adjunct to 15.2 g (0.055 mol) of bromotetradecane, dropwising for 30 minutes 10.0 g of a 45 % aqueous solution KOH. It was heated under stirring for 40 h at

room temperature. Then, the raw reaction mixture was filtered so as to remove the formed KBr and then washed for several times to eliminate traces of solvent.

At the end, 13.4 g of crude $PFE_{6,14}$ were obtained with 74.2 % of yield.

2° STEP: The mixture was treated with Desmodur® N 3600 (toluene isocyanate based compound) to eliminate un-reacted alcohol (3.72 %). Therefore, 13.4 g of $PFE_{6,14}$ and 0.5 g of Desmodur® N 3400 and 1 drops of dibutyltin laureate, as catalyst, were heated at 90-100 °C for several minutes. Then, a distillation was carried out. 10.3 g of fluorinated ether were obtained with a 68 % of yield.

White solid;

spectral data: MS *m/z* (rel. ab. %): 636 ($[M]^+$, 5 %), 621 ($[M\text{-}CH_3]^+$, 15 %), 607 ($[M\text{-}CH_2CH_3]^+$, 15 %), 593 ($[M\text{-}CH_3CH_2CH_2]^+$, 5 %), 579 ($[M\text{-}CH_3CH_2CH_2CH_2]^+$, 15 %); 317 ($[M\text{-}CF_3(CF_2)_5]^+$, 10 %), 303 ($[M\text{-}CF_3(CF_2)_5$, $\text{-}CH_2]^+$, 100 %), 273 ($[M\text{-}CF_3(CF_2)_5CH_2CH_2O]^+$, 100 %);

FTIR: $\nu_{C\text{-}F}$ 1100-1250 cm^{-1}, $\nu_{C\text{-}H}$ 2830-2930 cm^{-1}.

^{1}H NMR (CD_3OD): δ = 0.90 (t, $CH_3(\alpha)$, 3H); 1.31 (m, $CH_2(\beta)\div CH_2(\mu)$, 22H); 1.54 (m, $CH_2(\nu)$, 2H); 3.41 (t, $CH_2(\xi)$, 2H); 3.72 (t, $CH_2(o)$, 2H); 2.49 (ttt, $CH_2(\pi)$, 2H.

^{19}F NMR (CD_3OD): δ = -83.5 (t, CF_3(a), 3F); -129.1 (m, CF_2(b), 2F); -126.4 (m, CF_2(c), 2F); -125.8 (m, CF_2(d), 2F); -124.5 (m, CF_2(e), 2F); -116.3 (m, CF_2(f), 2F).

Anal. calcd for $C_{22}H_{33}F_{13}O$: C, 41.5 %; F, 38.8 %; H, 5.2 %. Found: C, 40.8 %; F, 38.1 %; H, 5.4 %.

Synthesis of 1,1,1,2,2,3,3,4,4,5,5,6,6,8,8 Heptadecafluoro-10-oxy-tetradecane ($PFE_{8,14}$)

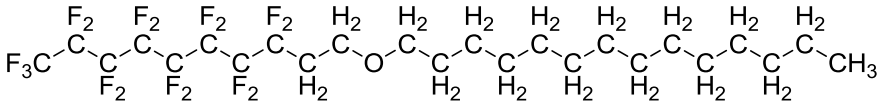

A mixture of 10.0 g (0.02 mol) of 1H,1H,2H,2H-heptadecafluoro-1-ol, 20.0 g of N-methylpyrrolidinone was adjunct to 6.1 g (0.022 mol) of bromotetradecane, dropwising for 30 minutes 10.0 g of a 45 % aqueous solution KOH. It was heated under stirring for 35 h at room temperature. Then, the raw reaction mixture was filtered so as to remove the formed KBr and then washed for several times to eliminate traces of solvent. At the end, 12.7 g of crude $PFE_{8,14}$ were obtained with 96.2 % of yield.

2° STEP: The mixture was treated with Desmodur® N 3600 (isocyanate) to eliminate un-reacted alcohol (2.92 %). Therefore, 12.7 g of $PFE_{8,14}$ and 0.5 g of Desmodur® N 3600 and 1

drop of dibutyltin laureate, as catalyst, were heated at 90-100 °C for several minutes. Then, a distillation was carried out. 9.0 g of fluorinated ether were obtained with a 68 % of yield.

White solid;

spectral data: MS *m/z* (rel. ab. %): 736 ($[M]^+$, 5 %), 721 ($[M\text{-}CH_3]^+$, 15 %), 707 ($[M\text{-}CH_2CH_3]^+$, 10 %), 693 ($[M\text{-}CH_3CH_2CH_2]^+$, 10 %), 679 ($[M\text{-}CH_3CH_2CH_2CH_2]^+$, 10 %); 317 ($[M\text{-}CF_3(CF_2)_7]^+$, 5 %), 303 ($[M\text{-}CF_3(CF_2)_7, \text{-}CH_2]^+$, 100 %), 273 ($[M\text{-}CF_3(CF_2)_7CH_2CH_2O]^+$, 90 %);

FTIR: $\nu_{C\text{-}F}$ 1150-1270 cm^{-1}, $\nu_{C\text{-}H}$ 2880-2910 cm^{-1}.

^{1}H NMR (CD_3OD): δ = 0.90 (t, $CH_3(\alpha)$, 3H); 1.31 (m, $CH_2(\beta)\div CH_2(\mu)$, 22H); 1.54 (m, $CH_2(\nu)$, 2H); 3.41 (t, $CH_2(\xi)$, 2H); 3.72 (t, $CH_2(o)$, 2H); 2.49 (ttt, $CH_2(\pi)$, 2H.

^{19}F NMR (CD_3OD): δ = -83.2 (t, CF_3(a), 3F); -128.4 (m, CF_2(b), 2F); -126.1 (m, CF_2(c), 2F); -125.6 (m, CF_2(d), 2F); -124.3 (m, CF_2(e), 2F); -123.5 (m, CF_2(f), 2F); -122.1 (m, CF_2(g), 2F); -115.5 (m, CF_2(h), 2F).

Anal. calcd for $C_{24}H_{33}F_{17}O$: C, 39.1 %; F, 43.9 %; H, 4.5 %. Found: C, 38.5 %; F, 42.7 %; H, 4.2 %.

Synthesis of 1,1,1,2,2,3,3,4,4 Nonafluoro-6-oxy-octadecane ($PFE_{4,18}$)

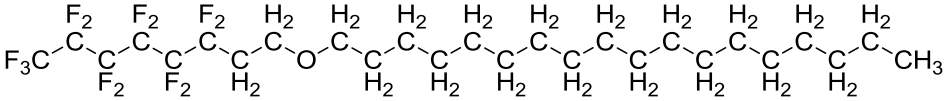

A mixture of 5.0 g (0.019 mol) of 1H,1H,2H,2H-nonafluoro-1-ol, 10.0 g of N-methylpyrrolidinone and 11.3 g (0.038 mol) of bromooctadecane, dropwising for 30 minutes 5 g of a 45 % aqueous solution KOH. It was heated under stirring for 35 h at 35 °C. Then, the raw reaction mixture was filtered so as to remove the formed KBr and then washed for several times to eliminate traces of solvent. At the end, 8.5 g of crude $PFE_{4,18}$ were obtained with 86.7 % of yield.

2° STEP: The mixture was treated with Desmodur® N 3600 (toluene isocyanate based compound) to eliminate un-reacted alcohol (5.2 %). Therefore, 8.5 g of $PFE_{4,18}$ and 1 g of Desmodur® N 3600 and 2 drops of dibutyltin laureate, as catalyst, were heated at 90-100 for several minutes. Then, a distillation was carried out. 6.0 g fluorinated ether were obtained with a 65 % of yield.

White solid;

spectral data: MS *m/z* (rel. ab. %): 516 ($[M]^+$, 10 %), 501 ($[M\text{-}CH_3]^+$, 15 %), 487 ($[M\text{-}CH_2CH_3]^+$, 10 %), 473 ($[M\text{-}CH_3CH_2CH_2]^+$, 5 %), 459 ($[M\text{-}CH_3CH_2CH_2CH_2]^+$, 5 %); 297

([M-$CF_3(CF_2)_3$]$^+$, 10 %), 383 ([M-$CF_3(CF_2)_3$, -CH_2]$^+$, 100 %), 253 ([M-$CF_3(CF_2)_3CH_2CH_2O$]$^+$, 90 %);

FTIR: $\nu_{C\text{-}F}$ 1100-1260 cm^{-1}, $\nu_{C\text{-}H}$ 2850-2910 cm^{-1}.

^{1}H NMR (CD_3OD): δ = 0.88 (t, $CH_3(\alpha)$, 3H); 1.28 (m, $CH_2(\beta)\div CH_2(\pi)$, 30H); 1.58 (m, $CH_2(\rho)$, 2H); 3.50 (t, $CH_2(\sigma)$, 2H); 3.80 (t, $CH_2(\tau)$, 2H); 2.52 (ttt, $CH_2(\upsilon)$, 2H).

^{19}F NMR (CD_3OD): δ = -84.2 (t, CF_3(a), 3F); -128.5 (m, CF_2(b), 2F); -127.8 (m, CF_2(c), 2F); -116.2 (m, CF_2(d), 2F).

Anal. calcd for $C_{24}H_{41}F_9O$: C, 55.8 %; F, 33.1 %; H, 7.9 %. Found: C, 55.4 %; F, 33.9 %; H, 7.4 %.

Synthesis of 1,1,1,2,2,3,3,4,4,5,5,6,6 Tridecafluoro-8-oxy-octadecane ($PFE_{6,18}$)

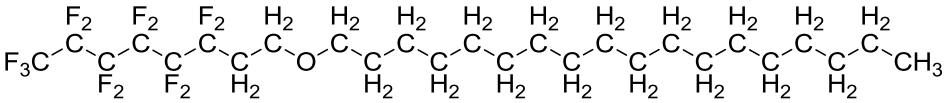

A mixture of 15.0 g (0.041 mol) of 1H,1H,2H,2H-tridecafluoro-1-ol, 30.0 g of N-methylpyrrolidinone and 24.6 g (0.082 mol) of bromooctadecane, dropwising for 30 minutes 15.0 g of a 45 % aqueous solution KOH, was heated under stirring for 35 h at 35 °C. Then, the raw reaction mixture was filtered so as to remove the formed KBr and then washed for several times to eliminate traces of solvent. At the end, 23.0 g of crude $PFE_{6,18}$ were obtained with 91.2 % of yield.

2° STEP: The mixture was treated with Desmodur® N 3600 (toluene isocyanate based compound) to eliminate un-reacted alcohol (3.94 %). Therefore, 23 g of $PFE_{6,18}$ and 1 g of Desmodur® N 3600 and 2 drops of dibutyltin laureate, as catalyst, were heated at 90-100 °C for several minutes. Then, a distillation was carried out. 16.0 g of fluorinated ether were obtained with a 67 % of yield.

White solid;

spectral data: MS *m/z* (rel. ab. %): 616 ([M]$^+$, 10 %), 601 ([M-CH_3]$^+$, 10 %), 587 ([M-CH_2CH_3]$^+$, 5 %), 573 ([M-$CH_3CH_2CH_2$]$^+$, 10 %), 559 ([M-$CH_3CH_2CH_2CH_2$]$^+$, 10 %); 297 ([M-$CF_3(CF_2)_5$]$^+$, 10 %), 383 ([M-$CF_3(CF_2)_5$, -CH_2]$^+$, 100 %), 253 ([M-$CF_3(CF_2)_5CH_2CH_2O$]$^+$, 80 %); FTIR: $\nu_{C\text{-}F}$ 1080-1250 cm^{-1}, $\nu_{C\text{-}H}$ 2800-2880 cm^{-1}.

^{1}H NMR (CD_3OD): δ = 0.88 (t, $CH_3(\alpha)$, 3H); 1.28 (m, $CH_2(\beta)\div CH_2(\pi)$, 30H); 1.58 (m, $CH_2(\rho)$, 2H); 3.50 (t, $CH_2(\sigma)$, 2H); 3.80 (t, $CH_2(\tau)$, 2H); 2.52 (ttt, $CH_2(\upsilon)$, 2H).

^{19}F NMR (CD_3OD): δ = -83.0 (t, CF_3(a), 3F); -129.8 (m, CF_2(b), 2F); -127.1 (m, CF_2(c), 2F); -126.2 (m, CF_2(d), 2F); -125.0 (m, CF_2(e), 2F); -116.8 (m, CF_2(f), 2F).

Anal. calcd for $C_{26}H_{41}F_{13}O$: C, 50.6 %; F, 40.0 %; H, 6.6 %. Found: C, 50.0 %; F, 39.2 %; H, 6.1 %.

Synthesis of 1,1,1,2,2,3,3,4,4,5,5,6,6,7,7,8,8 Heptadecafluoro-10-oxy-octadecane ($PFE_{8,18}$)

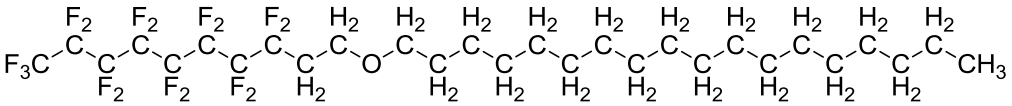

A mixture of 15.0 g (0.03 mol) of 1H,1H,2H,2H-heptadecafluoro-1-ol, 20.0 g of N-methylpyrrolidinone was adjunct to 12.0 g (0.036 mol) of bromooctadecane, dropwising for 30 minutes 21.6 g of a 45 % aqueous solution KOH. It was heated under stirring for 35 h at 35 °C. Then, the raw reaction mixture was filtered so as to remove the formed KBr and the washed for several times to eliminate traces of solvent. At the end, 19.5 g of crude $PFE_{8,18}$ were obtained with 90.6 % of yield.

2° STEP: The mixture was treated with Desmodur® N 3600 (toluene isocyanate based compound) to eliminate un-reacted alcohol (4.71 %). Therefore, 19.5 g of $PFE_{8,18}$ and 1.0 g of Desmodur® N 3600 and 2 drops of dibutyltin laureate, as catalyst, were heated at 90-100 °C per several minutes. Then, a distillation was carried out. 13.3 g of fluorinated ether were obtained with a 65 % of yield.

White solid;

spectral data: MS *m/z* (rel. ab. %): 716 ($[M]^+$, 10 %), 701 ($[M\text{-}CH_3]^+$, 5 %), 687 ($[M\text{-}CH_2CH_3]^+$, 10 %), 673 ($[M\text{-}CH_3CH_2CH_2]^+$, 5 %), 659 ($[M\text{-}CH_3CH_2CH_2CH_2]^+$, 15 %); 297 ($[M\text{-}CF_3(CF_2)_7]^+$, 5 %), 383 ($[M\text{-}CF_3(CF_2)_7, \text{-}CH_2]^+$, 90 %), 253 ($[M\text{-}CF_3(CF_2)_7CH_2CH_2O]^+$, 100 %);

FTIR: $\nu_{C\text{-}F}$ 1120-1280 cm^{-1}, $\nu_{C\text{-}H}$ 2840-2920 cm^{-1}.

^{1}H NMR (CD_3OD): δ = 0.88 (t, $CH_3(\alpha)$, 3H); 1.28 (m, $CH_2(\beta)\div CH_2(\pi)$, 30H); 1.58 (m, $CH_2(\rho)$, 2H); 3.50 (t, $CH_2(\sigma)$, 2H); 3.80 (t, $CH_2(\tau)$, 2H); 2.52 (ttt, $CH_2(\upsilon)$, 2H).

^{19}F NMR(CD_3OD): δ = -83.9 (t, CF_3(a), 3F); -128.9 (m, CF_2(b), 2F); -126.6 (m, CF_2(c), 2F); -125.9 (m, CF_2(d), 2F); -125.0 (m, CF_2(e), 2F); -124.0 (m, CF_2(f), 2F); -122.0 (m, CF_2(g), 2F); -115.8 (m, CF_2(h), 2F).

Anal. calcd for $C_{28}H_{41}F_{17}O$: C, 46.9 %; F, 45.1 %; H, 5.7 %. Found: C, 46.0 %; F, 30.0 %; H, 6.1 %.

Synthesis of 1,1,1,2,2,3,3,4,4 Nonafluoro-6-oxy-docosane ($PFE_{4,21}$)

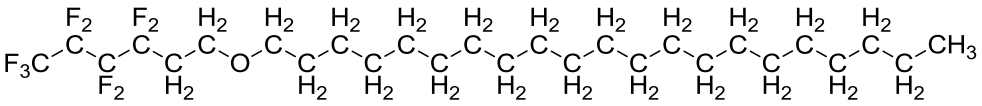

A mixture comprising of 5.0 g (0.018 mol) of 1H,1H,2H,2H-nonafluoro-1-ol, 10.0 g of N-methylpyrrolidinone was adjunct to 13.5 g (0.036 mol) of bromooctadecane, dropwising for 30 minutes 15.0 g of a 45 % aqueous solution KOH. It was heated under stirring for 35 h at 30 °C. Then, the raw reaction mixture was filtered so as to remove the formed KBr and then washed for several times to eliminate traces of solvent. At the end, 8.1 g of crude $PFE_{4,21}$ were obtained with 81 % of yield.

2° STEP: The mixture was treated with Desmodur® N 3600 (toluene isocyanate based compound) to eliminate un-reacted alcohol (3.94 %). Therefore, 8.1 g of $PFE_{4,21}$ and 1.0 g of Desmodur® N 3600 and 2 drops of dibutyltin laureate, as catalyst, were heated at 90-100 °C for several minutes. Then, a distillation was carried out. 6.9 g of fluorinated ether were obtained with a 69 % of yield.

White solid;

spectral data: MS *m/z* (rel. ab. %): 558 ($[M]^+$, 10 %), 543 ($[M\text{-}CH_3]^+$, 10 %), 529 ($[M\text{-}CH_2CH_3]^+$, 15 %), 515 ($[M\text{-}CH_3CH_2CH_2]^+$, 10 %), 501 ($[M\text{-}CH_3CH_2CH_2CH_2]^+$, 10 %); 339 ($[M\text{-}CF_3(CF_2)_3]^+$, 15 %), 325 ($[M\text{-}CF_3(CF_2)_3, \text{-}CH_2]^+$, 90 %), 295 ($[M\text{-}CF_3(CF_2)_3CH_2CH_2O]^+$, 100 %);

FTIR: $\nu_{C\text{-}F}$ 1150-1250 cm^{-1}, $\nu_{C\text{-}H}$ 2820-2950 cm^{-1}.

^{1}H NMR (CD_3OD): δ = 0.90 (t, $CH_3(\alpha)$, 3H); 1.30 (m, $CH_2(\beta)\div CH_2(\tau)$, 38H); 1.60 (m, $CH_2(\upsilon)$, 2H); 3.55 (t, $CH_2(\phi)$, 2H); 3.82 (t, $CH_2(\chi)$, 2H); 2.54 (ttt, $CH_2(\psi)$, 2H).

^{19}F NMR (CD_3OD): δ = -84.5 (t, CF_3(a), 3F); -128.9 (m, CF_2(b), 2F); -128.0 (m, CF_2(c), 2F); -116.7 (m, CF_2(d), 2F).

Anal. calcd for $C_{27}H_{47}F_9O$: C, 58.1 %; F, 30.6 %; H, 8.4 %. Found: C, 57.0 %; F, 31.4 %; H, 8.0 %.

Synthesis of 1,1,1,2,2,3,3,4,4,5,5,6,6 Tridecafluoro-8-oxy-docosane ($PFE_{6,21}$)

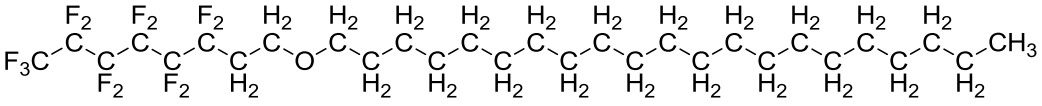

A mixture of 5.0 g (0.013 mol) of 1H,1H,2H,2H-tridecafluoro-1-ol, 10.0 g of N-methylpyrrolidinone was adjunct to 10.3 g (0.027 mol) of bromooctadecane, dropwising for 30 minutes 15.0 g of a 45 % aqueous solution KOH. It was heated under stirring for 35 h at

30 °C. Then, the raw reaction mixture was filtered so as to remove the formed KBr and then washed for several times to eliminate traces of solvent. At the end, 7.5 g of crude $PFE_{6,21}$ were obtained with 87.7 % of yield.

2° STEP: The mixture was treated with Desmodur® N 3600 (toluene isocyanate based compound) to eliminate un-reacted alcohol (2.93 %). Therefore, 7.5 g of $PFE_{6,21}$ and 1.0 g of Desmodur® N 3600 and 2 drops of dibutyltin laureate, as catalyst, were heated at 90-100 °C for several minutes. Then, a distillation was carried out. 6.2 g fluorinated ether were obtained with a 72.5 % of yield.

White solid;

spectral data: MS *m/z* (rel. ab. %): 658 ($[M]^+$, 10 %), 643 ($[M\text{-}CH_3]^+$, 15 %), 629 ($[M\text{-}CH_2CH_3]^+$, 10 %), 615 ($[M\text{-}CH_3CH_2CH_2]^+$, 5 %), 601 ($[M\text{-}CH_3CH_2CH_2CH_2]^+$, 15 %); 339 ($[M\text{-}CF_3(CF_2)_5]^+$, 10 %), 325 ($[M\text{-}CF_3(CF_2)_5$, $\text{-}CH_2]^+$, 95 %), 295 ($[M\text{-}CF_3(CF_2)_5CH_2CH_2O]^+$, 100 %);

FTIR: $\nu_{C\text{-}F}$ 1160-1270 cm^{-1}, $\nu_{C\text{-}H}$ 2840-2930 cm^{-1}.

^{1}H NMR (CD_3OD): δ = 0.90 (t, $CH_3(\alpha)$, 3H); 1.30 (m, $CH_2(\beta)\div CH_2(\tau)$, 38H); 1.60 (m, $CH_2(\upsilon)$, 2H); 3.55 (t, $CH_2(\phi)$, 2H); 3.82 (t, $CH_2(\chi)$, 2H); 2.54 (ttt, $CH_2(\psi)$, 2H).

^{19}F NMR (CD_3OD): δ = -82.9 (t, CF_3(a), 3F); -129.2 (m, CF_2(b), 2F); -126.9 (m, CF_2(c), 2F); -126.0 (m, CF_2(d), 2F); -124.9 (m, CF_2(e), 2F); -116.2 (m, CF_2(f), 2F).

Anal. calcd for $C_{29}H_{47}F_{13}O$: C, 52.9 %; F, 37.5 %; H, 7.1 %. Found: C, 51.8 %; F, 36.7 %; H, 7.5 %.

Synthesis of 1,1,1,2,2,3,3,4,4,5,5,6,6,7,7,8,8 Heptadecafluoro-10-oxy-docosane ($PFE_{8,21}$)

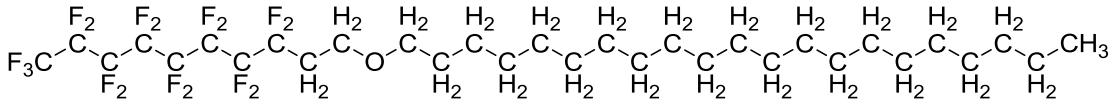

A mixture of 7.0 g (0.015 mol) of 1H,1H,2H,2H-heptadecafluoro-1-ol, 15.0 g of N-methylpyrrolidinone was adjunct to 11.3 g (0.03 mol) of bromooctadecane, dropwising for 30 minutes 15.0 g of a 45 % aqueous solution KOH. It was heated under stirring for 35 h at 35 °C. Then, the raw reaction mixture was filtered so as to remove the formed KBr and then washed for several times to eliminate traces of solvent. At the end, 9.2 g of crude $PFE_{8,21}$ were obtained with 80.9 % of yield.

2° STEP: The mixture was treated with Desmodur® N 3600 (toluene isocianate based compound) to eliminate un-reacted alcohol (2.7 %). Therefore, 9.2 g of $PFE_{8,21}$ and 1.0 g of Desmodur® N 3600 and 2 drops of dibutyltin laureate, as catalyst, were heated at 90-100 °C

per several minutes. Then, a distillation was carried out. 7.0 g fluorinated ether were obtained with a 60 % of yield.

White solid;

spectral data: MS *m/z* (rel. ab. %): 758 ($[M]^+$, 5 %), 743 ($[M\text{-}CH_3]^+$, 10 %), 729 ($[M\text{-}CH_2CH_3]^+$, 5 %), 715 ($[M\text{-}CH_3CH_2CH_2]^+$, 10 %), 701 ($[M\text{-}CH_3CH_2CH_2CH_2]^+$, 10 %); 339 ($[M\text{-}CF_3(CF_2)_7]^+$, 15 %), 325 ($[M\text{-}CF_3(CF_2)_7, \text{-}CH_2]^+$, 90 %), 295 ($[M\text{-}CF_3(CF_2)_7CH_2CH_2O]^+$, 100 %); FTIR: $\nu_{C\text{-}F}$ 1150-1210 cm^{-1}, $\nu_{C\text{-}H}$ 2820-2910 cm^{-1}.

^{1}H NMR (CD_3OD): δ = 0.90 (t, $CH_3(\alpha)$, 3H); 1.30 (m, $CH_2(\beta)\div CH_2(\tau)$, 38H); 1.60 (m, $CH_2(\upsilon)$, 2H); 3.55 (t, $CH_2(\phi)$, 2H); 3.82 (t, $CH_2(\chi)$, 2H); 2.54 (ttt, $CH_2(\psi)$, 2H).

^{19}F NMR (CD_3OD): δ = -83.4 (t, CF_3(a), 3F); -128.3 (m, CF_2(b), 2F); -126.2 (m, CF_2(c), 2F); -125.1 (m, CF_2(d), 2F); -124.5 (m, CF_2(e), 2F); -123.8 (m, CF_2(f), 2F); -122.1 (m, CF_2(g), 2F); -115.1 (m, CF_2(h), 2F).

Anal. calcd for $C_{31}H_{47}F_{17}O$: C, 49.1 %; F, 42.6 %; H, 6.2 %. Found: C, 48.4 %; F, 41.2 %; H, 5.8 %.

4.3 Conclusions

Partially fluorinated ethers are synthesized as procedure reported in Scheme 10. The yields varied from 97 % for $PFE_{6,2}$ and $PFE_{8,2}$ to 60 % for $PFE_{8,21}$ as reported in Table 1.

Under these conditions, we observed a remarkable increase in the reaction yield and a shortening in the reaction time.

However, by a combination of simple fractional Kugelrohr distillations and recrystallizations, the materials used in this study have all been obtained in greater than 98 % purity. Therefore, the residue alcohol is eliminated via flash column chromatography on alumina with diethyl ethers as eluent.

Then, another treatment is effectuated in column chromatography on Darco® G-60 using methanol as eluent to eliminate some impurities.

This procedure provides high pure products. In vitro tests of $PFE_{n,m}$ effectuated by Al.Chi.Mi.A S.r.l demonstrated no toxicological effects and the biocompatibility of products.

Therefore, the work was patented with the title “fluoroalkyloxy alkanes, process for production and uses thereof by Al.Chi.Mi.A S.r.l, with inventors L. Conte, A. Zaggia, M. Beccaro, E. Bettini, P. Signori [154].

Table 1: yields of $PFE_{n,m}$ synthesized.

Compound	Yield %	Compound	Yield %	Compound	Yield %	Compound	Yield %
$PFE_{4,2}$	95.6	$PFE_{4,5}$	90	$PFE_{4,14}$	71	$PFE_{4,21}$	69
$PFE_{6,2}$	95	$PFE_{6,5}$	82	$PFE_{6,14}$	68	$PFE_{6,21}$	72
$PFE_{8,2}$	98	$PFE_{8,5}$	82	$PFE_{8,14}$	68	$PFE_{8,21}$	60
$PFE_{4,3}$	84	$PFE_{4,8}$	70	$PFE_{4,18}$	65		
$PFE_{6,3}$	85	$PFE_{6,8}$	71	$PFE_{6,18}$	67		
$PFE_{8,3}$	82	$PFE_{8,8}$	72	$PFE_{8,18}$	65		

5 Physico-chemical characterizations

Fluoro-alkylated compounds exhibit unique properties as self-assembling materials. They can form micellar and bilayer structures in aqueous [155, 156], hydrocarbon [157], and fluorocarbon solvents [120, 158], supercritical fluids (CO_2) as well as having thermotropic liquid crystalline properties in the absence of solvents [159, 160]. The fluorocarbon part provides a low surface tension leading to excellent properties for lubrification. The hydrocarbon part provides an adequate interfacial tension leading to ideal candidates products to biomedical use, including oxygen carriers, drug delivery vehicles, liquid ventilation [161], vitreous substitutes [162].

It is difficult to draw a close analogy between the molecular organization of fluoroalkylated compounds in solvents because of the complexity of molecular interactions that need to be considered, together with the large numbers of molecule and limited number and structural diversity of semifluorinated compounds found in literature. In fact, fluorinated compounds as well as assemble through solvophobic and van der Waals interactions, they are also capable to forming intermolecular hydrogen bonding leading to supramolecular structures in organic solvents [163, 164]. Semifluorinated alkanes have the basic block-architecture required for these molecules to operate as surfactants in hydrocarbon plus fluorocarbon systems. Moreover, semifluorinated alkanes are able to stabilize perfluorocarbon emulsions [155] producing both micelles in hydrocarbons [165] and reversed micelles in fluorocarbons [166] at very low concentrations. Semifluorinated alkanes were also used as gelling and foaming agents in solvent systems [167].

In order to compare the properties of $PFE_{m,n}$ with semifluorinated alkanes, the surface active properties of $PFE_{m,n}$ were assessed by the following tests:

(1) surface tension measurements;

(2) foaming tendency in different organic solvents [168];

(3) maximum surface tension reduction;

(4) detecting gel-phase formation in binary mixtures;

(5) interfacial tension measurements;

(6) specific gravity;

(7) refractive index;

(8) miscibility in silicone oil;

(9) stability;

(10) biocompatibility studies.

5.1 Surface tension measurements

The air/solution surface tensions were measured with a Du Nouy ring tensiometer (K10, Kruss). Prior to use the ring, it was rinsed copiously with pure water and ethanol. Before to each measurement, the Pt–Ir ring was heated until glowing. The surface tension was taken as the average of the 10 repeat measurements. In Table 2 are summarized the values of $PFE_{n,m}$.

The reference value of surface tensions found for the solvents were the following: γ_{hex}=18.4 mN m^{-1}, γ_{dod} = 25.4 mN m^{-1}; $\gamma_{perfdec}$ = 19.4 mN m^{-1}.

Table 2: Foaming tendency, solvent surface tension depression, for $PFE_{m,n}$ synthesized.

Compound	Surface tension [$mN \cdot m^{-1}$]	Foaming tendency[a]			Solvent surface tension depression[b]		
		n-hexane	*n*-dodecane	perfluoro decalin	*n*-hexane	*n*-dodecane	perfluoro decalin
$PFE_{4,2}$	18.5				18.2	25.2	19.1
$PFE_{6,2}$	18.0				18.3	24.9	19.4
$PFE_{8,2}$	18.4				18.2	25.1	19.4
$PFE_{4,3}$	21.1				18.1	25.1	18.9
$PFE_{6,3}$	18.7				17.9	24.9	19.3
$PFE_{8,3}$	20.4				17.8	23.1	19.4
$PFE_{4,5}$	21.8				18.2	24.5	18.8
$PFE_{6,5}$	21.7				18.1	23.9	18.7
$PFE_{8,5}$	18.5				17.6	24.1	18.8
$PFE_{4,8}$	19.7				17.5	24.5	19.1
$PFE_{6,8}$	19.3	n.f.o.	n.f.o.	n.f.o.	17.8	24.2	19.2
$PFE_{8,8}$	18.8				17.6	23.9	18.9
$PFE_{4,14}$	24.5				17.9	23.5	18.5
$PFE_{6,14}$	24.0				18.1	23.9	18.6
$PFE_{8,14}$	23.6				18.4	23.9	18.5
$PFE_{4,18}$	28.9				18.5	24.3	18.9
$PFE_{6,18}$	23.2				18.4	24.1	19.4
$PFE_{8,18}$	21.4				18.6	24.2	19.5
$PFE_{4,21}$	28.8				18.2	23.4	19.1
$PFE_{6,21}$	22.5				17.9	22.9	19.3
$PFE_{8,21}$	21.6				18.1	22.8	18.7

a: 10 mL solution of 10 mM of $PFE_{m,n}$

b: 200 mM solutions of $PFE_{m,n}$

5.2 Foaming tendency

Procedures: to determine the foaming action of the $PFE_{m,n}$, 10 mL of a 10 mM solution in organic solvent (n-hexane, n-dodecane, perfluorodecalin) was shaken for 10 s by hand for a few seconds and the persistence of bubbles formed was monitored and the time recorded.

If any foam was noted the sample was considered foaming and marked with a F and the time for the breakdown of the foam was recorded. Non-foaming $PFE_{m,n}$ solutions were marked with a n.f.o (no foam in organic solvent).

All $PFE_{m,n}$ have only limited surface activity being completely soluble and showing no foaming ability in the organic solvents tested, as reported in Table 2.

5.3 Surface tension reduction

An important guide to whether or not adsorption of molecules will occur from any given solvent is the difference between surface tension of pure solvent and surface tension of the complete monolayer. It is defined as *surfactant effectiveness*, that is the point at which the surface tension of the mixture at its critical micelle concentration, γ_{cmc}, is a minimum.

The effectiveness of a surfactant in reducing surface tension can be measured by the amount of reduction, or surface pressure,

$\pi_{cmc} = \gamma_0 - \gamma_{cmc}$

attained at the critical micelle concentration, since the reduction of the tension beyond the cmc is relatively insignificant [169]. To induce adsorption γ has to be large enough, typically about $5 mNm^{-1}$; hence, adsorption of a monolayer is thermodynamically favorable, thereby lowering the effective surface energy.

In different organic solvents including n-hexane, n-dodecane, perfluorodecaline, regardless of the concentration of the $PFE_{m,n}$ surface tensions are measured.

Tensiometric measurements, irrespective of the type of the solvent, showed the inability of $PFE_{m,n}$ to lower significantly the surface tension even up to 200 mM concentration. The limiting surface tension appears to be essentially constant for all the systems and the values are quite similar, displaying only minor variations, indicating that the limiting surface energies are broadly independent of solvent type.

It is noteworthy that an increase in n has virtually no effect on surface tension reduction of solutions. For instance, $PFE_{8,3}$ lowers the surface tension of n-dodecane from 25.4 mN m^{-1} down to 23.1 mN m^{-1}; $PFE_{8,21}$ performs similarly lowering the surface tension to 22.8 mN m^{-1}. The increase in m from 4 to 8 results in a mild surface tension reduction: while $PFE_{4,3}$ virtually does not affect the surface tension of n-dodecane, $PFE_{8,3}$ reduces it from 26.5 down to 23.1 mN m^{-1}.

5.4 Gel-phase formation in binary mixtures

In the presence of a suitable solvent, semifluorinated alkanes form gel phases that exhibit a first-order phase transition at a specific temperature (T_c), depending on the nature and concentration of the solute. Heating a mixture of a semifluorinated n-alkane in hydrocarbon solvents above its melting point and allowing it to cool, a gel phase forms. It is a reversible

phenomenon, where non-covalent forces dominate, as opposed to chemical gels, the component interact though covalent interactions.

The temperature T_c at which the gel phase begins to form (gel point) strongly depends on the molecular structure, and on process variables such as concentration and the heating/cooling rate [170]. In fact the strong incompatibility between the fluorinated and hydrogenated parts of molecules draw the self-assembly of gelator amphiphiles [168].

It is interesting to investigate this behavior for ophthalmology applications, cancer therapy, bone therapy, oxygen-rich liquid, etc. [171, 172].

In order to investigate whether $PFE_{n,m}$ have the ability to form gel phases, gel point tests were performed.

Procedures: the mixtures of $PFE_{m,n,}$ constituted by 10 mL of different solvents (n-dodecane, methanol, perfluorodecalin) per gram of semifluorinated ethers, were cooled at fixed concentration. The temperature of the mixture was measured and plotted as a function of time. If gelation occurred the temperature of the mixture was expected to remain nearly constant for a period.

As shown in Table 3, mixtures of $PFE_{m,n}$ in non-polar, polar and fluorinated organic solvents are isotropic solutions failing to exhibit any transition to gel-like phases.

Table 3: solvent gel-phase formation for $PFE_{n,m}$

compound	Solvent gel-phase formation [a]			Silicone oil solubility [b]
	n-dodecane	methanol	perfluorodecalin	(wt/wt) %
$PFE_{4,2}$	n.g.o	n.g.o	n.g.o	98
$PFE_{6,2}$				64
$PFE_{8,2}$				41
$PFE_{4,3}$				96
$PFE_{6,3}$				52
$PFE_{8,3}$				35
$PFE_{4,5}$				93
$PFE_{6,5}$				43
$PFE_{8,5}$				31
$PFE_{4,8}$				91
$PFE_{6,8}$				40
$PFE_{8,8}$				28
$PFE_{4,14}$				87
$PFE_{6,14}$				38
$PFE_{8,14}$				24
$PFE_{4,18}$				78
$PFE_{6,18}$				31
$PFE_{8,18}$				23
$PFE_{4,21}$				65
$PFE_{6,21}$				21
$PFE_{8,21}$				14

a: composition of mixtures tested. 10 mL of solvent per gram of $PFE_{m,n}$, cooling rate 2 °C min^{-1}.

b: the values refers to the percentages of $PFE_{m,n}$ in RS-OIL 5000 at which the onset of turbidity (25 °C) is observed. n.g.o= no gel observed.

5.5 Interfacial tension measurements

Interfacial tension between a compound and water is the energy derived from the van der Waal's interaction on the bubbles surface. The higher is interfacial tension, the greater is a substance's tendency to stay as a single bubble. In ophthalmic application, the interfacial tension must prevent the tamponade going through the break. It is another parameter to control.

The water/solution interfacial tension measurements were conducted by pendant drop method. A selected plane method was used to calculate interfacial values from a digital video image. In Table 3 are reported the values of PFEs with n= 4, 6, 8 and m= 2, 3, 5, 8.

The synthesized compounds present low interfacial tension and have the preferred properties of the vitreous substitutes in regard to their interfacial tension against water (41.8 - 55.2 mN m^{-1} at 25 °C). The values are close to semifluorinated alkanes.

5.6 Specific gravity

The high density of PFCs is retained to cause mechanical damage by increasing pressure on the retina vessels. The goal is obtaining the compounds with a density slightly higher than water. From Table 4 it is seen that the specific gravity of PFEs is in the desiderated range (1.1 - 1.6). Then, the specific gravity increases as the length of hydrocarbon segment increases.

Table 4: Physical-chemical properties of PFEs compared to commercial vitreous substitutes

compound	Interfacial tension [mN m^{-1}] at 25 °C	Specific gravity [g cm^{-3}] at 25 °C	Refractive Index n_D^{20}
Human vitreous humor	-	1.00	1.3345
Silicone oil (1000 cSt)	23.3	0.97	1.3800
Silicone oil (5000 cSt)	35.4	0.97	1.4040
F_6H_8	49.1	1.35	1.3430
F_6H_6	49.6	1.42	1.3220
perfluorodecalin	57.6	1.93	1.3130
perfluoroctane	55	1.76	1.2700
$PFE_{4,2}$	47.2	1.12	1.3121
$PFE_{6,2}$	46.9	1.14	1.3144
$PFE_{8,2}$	45.6	1.21	1.3157
$PFE_{4,3}$	45.1	1.13	1.3201
$PFE_{6,3}$	41.8	1.18	1.3245
$PFE_{8,3}$	44.9	1.26	1.3255
$PFE_{4,5}$	43.2	1.21	1.3267
$PFE_{6,5}$	45.9	1.23	1.3385
$PFE_{8,5}$	48.4	1.31	1.3399
$PFE_{4,8}$	53.5	1.28	1.3691
$PFE_{6,8}$	54.7	1.34	1.3888
$PFE_{8,8}$	55.2	1.39	1.3920
$PFE_{4,14}$	-	1.35	n.a.
$PFE_{6,14}$	-	1.39	n.a.
$PFE_{8,14}$	-	1.41	n.a.
$PFE_{4,18}$	-	1.43	n.a.
$PFE_{6,18}$	-	1.48	n.a.
$PFE_{8,18}$	-	1.52	n.a.
$PFE_{4,21}$	-	1.47	n.a.
$PFE_{6,21}$	-	1.55	n.a.
$PFE_{8,21}$	-	1.58	n.a.

5.7 Refractive index

The refractive index are similar to that of natural vitreous. The m/n ratio plays an important role in determining the refractive index (n_D^{20}). It is showed in Table 4 that an increase in m implies an increase of the refractive index while an increase of n cause only a mild effect. The $PFE_{n,m}$ with n= 4, 6, 8 and m= 14, 18, 21 are solid compounds, so it is no possible to determine the refractive index.

5.8 PFEs - silicone oil mixtures

The use of silicone oils as tamponade liquids during ophthalmology surgery has some limitations related in particular to their low density (0.97 g cm^{-3}) leading to not sufficient pressure in the retina. In fact, they tend to come to the surface of aqueous medium constituting vitreous body. Then, emulsification phenomena are frequents due to very low interfacial tension. Emulsification is defined as the fractioning of the silicone oil bubble into variable-size droplets. It is reversely proportional to fluid viscosity and surface tension. Emulsification consequences are the loss of internal tamponade potency, poor fundus visualization, switching to anterior chamber, and others side effects.

To examine the possibility of introducing PFEs with n= 4, 6, 8 and m= 2, 3, 5, 8 as long-term tamponades in retinal detachment, their miscibility with silicone oils has been tested.

Various mixtures comprising PFEs and silicone oils having a viscosity of 1000 or 5000 cSt were prepared and homogenized by shaking.

In Table 5 there are some example of mixtures $PFE_{n,m}$ with n= 4 and m= 3, 5. The mixtures are cooled at 4 °C and after cooling was noted if the mixture remained perfectly clear (marked with "s") or phase separation (marked with "n.s"). It showed in Table 6 that all mixtures are soluble after stirring.

Table 5: mixtures of $PFE_{n,m}$ with n= 4 and m= 3, 5 in silicone oil having a viscosity of 1000 cSt

Mixture	Mix 1 (90 % $PFE_{4,5}$ 10% silicone oil 1000)	Mix 2 (90 % $PFE_{4,5}$ 10 % silicone oil 5000)	Mix 3 (90 % $PFE_{4,3}$ 10 % silicone oil 1000)	Mix 4 (90 % $PFE_{4,3}$ 10 % silicone oil 1000)
Solubility room temperature	s	s	s	n. s
Solubility after stirring	s	s	s	s

Table 6 and in Table 7 report other examples of mixtures in silicone oil 1000 cSt and 5000 cSt respectively. It notes with "s" if there is a completely solubility at room temperature, and with "o" if the mixture is opalescent after stirring but it become clear after heating at 37 °C (body temperature).

Table 6: miscibility of $PFE_{n,m}$ in silicone oil having a viscosity of 1000 cSt.

compound	33 (wt/wt) %	43 (wt/wt) %	50 (wt/wt) %
$PFE_{6,5}$	s	s	o
$PFE_{4,5}$	s	s	s
$PFE_{4,3}$	s	s	s

Table 7: miscibility of $PFE_{n,m}$ in silicone oil having a viscosity of 5000 cSt.

compound	33 (wt/wt) %	43 % (wt/wt) %	50 % (wt/wt) %
$PFE_{6,5}$	s	s	o
$PFE_{4,5}$	s	s	s
$PFE_{4,3}$	s	s	s

Then, in Table 8 it showed a comparison between the solubility of semifluorinated alkanes R_FR_H and $PFE_{m,n}$ in silicone OIL RS 5000. This comparison points out that $PFE_{n,m}$ have a solubility in silicone oils from 30 % to 56 % higher than that of R_FR_H with the same ratio m/n.

Table 8: Comparison between the solubility in silicone oil of $PFE_{n,m}$ and F_nH_m having the same values for m and n.

compound	Silicone oil solubility[a] (wt/wt) %
$PFE_{4,5}$	93
$PFE_{6,5}$	43
$PFE_{8,5}$	31
$PFE_{4,8}$	91
$PFE_{6,8}$	40
$PFE_{8,8}$	28
F_4H_5	41
F_6H_5	28
F_8H_5	16
F_4H_8	51
F_6H_8	28
F_8H_8	15

a: the values refer to the percentages of $PFE_{n,m}$ in RS-OIL 5000 at which the onset of turbidity (25 °C) is observed.

The m/n ratio plays an important role in determining the solubility of $PFE_{n,m}$ in silicone oils such as RS-OIL 5000 (with a kinematic viscosity of 5000 cSt). An increase in m implies an increase of the solubility in silicone oil while n has the opposite effect. For example, at 20 °C the solubility of $PFE_{6,5}$ in silicone oil (5000 cSt) amounts to 57 % (m/m), and the solubility of $PFE_{6,8}$ amounts to 60 % (m/m). Then, at 20 °C the solubility of $PFE_{4,5}$ in silicone oil (5000 cSt) amounts to 7 % (m/m), and the solubility of $PFE_{6,5}$ amounts to 57 % (m/m).

The introduction of a flexible ethereal bond between the rigid fluorinated moiety and the hydrocarbon chain probably increases the molecule's solubility leading to a higher affinity for silicone based solvents. Therefore, PFEs have a good solubility in silicone oils. In particular, in the silicone oils used for the silicone oil tamponade with 5000 cSt or 1000 cSt, partially fluorinated ethers are uniformly soluble. In Table 9 it showed physic-chemical properties of a mixture of $PFE_{6,3}$ and silicone oil 1000 and 5000, in comparison with other industrial formulations [173].The percentages of $PFE_{6,3}$ in silicone oil (mixture HeavySIL 350 and 1500) are the property of Al.Chi.Mi.A S.r.l [174].

Table 9: Physical and chemical properties of commercial heavy tamponades compared to HeavySIL 1500 (mixture of $PFE_{6,3}$ and RS-OIL 5000).

compound	Specific gravity [g cm^{-3}]	Interfacial tension with water [mN m^{-1}]	Surface tension [mN m^{-1}]	Refractive index n_D^{20}	Component weight %
RS-OIL 1000	0.997	38.0	23.0	1.4000	100 % silicone oil 1000cSt
RS-OIL 5000	0.997	40.0	23.6	1.4000	100 % silicone oil 5000cSt
heavySIL1500®*	1.03	41.10	20.5	1.3885	RS-OIL 5000 $PFE_{6,3}$
heavySIL350®*	1.03	40.5	21.10	1.3878	RS-OIL 1000 $PFE_{6,3}$
Densiron 68®	1.06	40.82	19.10	1.3870	30.5 % F_6H_8 69.5 % SiO 5000
Oxane HD®	1.02	44.9	20	1.4000	11.9 % RMN3 88.1 % Oxane 5700
HWS 46-3000®	1.12	41.3	18.8	1.1180	55 % F_4H_5 45 % SiO 10000

*commercial products of Al.Chi.Mi.A S.r.l.

5.9 Biocompatibility studies

J. M. Parel et al. (Department of Ophthalmology, Ophthalmic Biophysics Center, Bascom Palmer Eye Institute, University of Miami) in collaboration with Al.Chi.Mi.A S.r.l (Padova) conducted some in-vivo biocompatibility study of PFEs [175].

Varying concentrations of silicone oil combined with PFEs (Al.Chi.Mi.A, S. r. L, Italy) were randomly implanted in the rabbits. The rabbits were examined after 1 and 3, 7, 14, 21, and 28, 90 days and then monthly under the operation microscope. Histological analysis were performed on all implanted eyes.. Until to 28 days no clinical signs of infection in any rabbits were noted. All animals had a normal cornea and conjunctiva. Retinal vessels

appeared slightly tortuous after 14 days for $PFE_{4,3}$ / silicone oil mixture. Retinal vessels appeared normal until 28 days post operatory for $PFE_{6,3}$.

Histology showed mild retinal damage in eyes treated with $PFE_{4,3}$ / silicone oil mixture (Figure 19), while no retinal damage in animal implanted with $PFE_{6,3}$ / silicone oil mixture (Figure 18).

Figure 18: mixture of $PFE_{6,3}$ and silicone oil

Figure 19: mixture of $PFE_{4,3}$ and silicone oil

The pilot study indicated that the $PFE_{6,3}$ silicone oil mixture was best tolerated in the rabbit model and could potentially be effectively used in vitreous-retinal surgery as a short term vitreous substitute.

Another study was conducted by M. C. Aguilar et al. (Department of Ophthalmology, Ophthalmic Biophysics Center, Bascom Palmer Eye Institute, University of Miami) [176]. The laboratory treated three rabbit labeled with PC12, GB20, AL18 with partially fluorinated ethers-silicone oils mixtures of Al.Chi.Mi.A S.r.l..

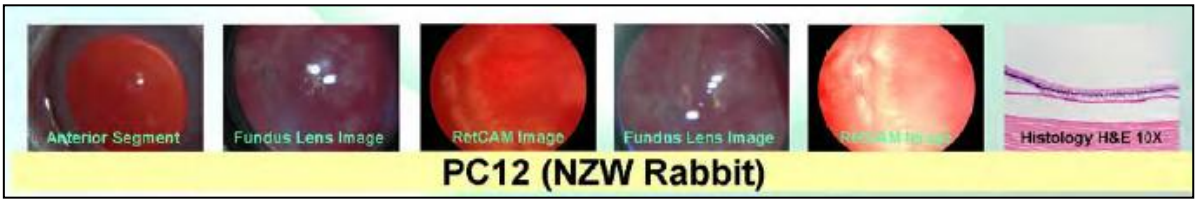

Figure 20: PC12 treated with mixture of $PFE_{4,3}$ and silicone oil.

PCL12 and GB20 (Figure 20-21) treated with mixture constituting of $PFE_{4,3}$ and $PFE_{4,5}$ respectively, caused only a mild retinal inflammation and slow emulsification.

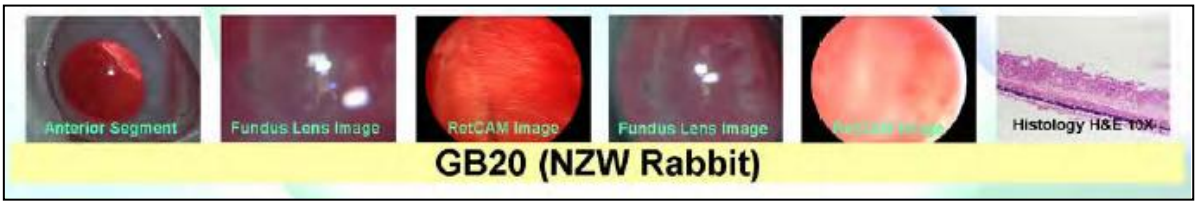

Figure 21: PC12 treated with mixture of $PFE_{4,5}$ and silicone oil.

AL18 (Figure 22) treated with mixture constituting of $PFE_{6,3}$ remained as a single large bubble and histology tests demonstrated a normal retinal morphology. However no emulsification phenomena were noticed. AL18 was also well tolerated in the rabbit for more 4 months, leading to use as long-term vitreous substitute.

Figure 22: AL18 treated with mixture of $PFE_{6,3}$ and silicone oil. Normal retinal morphology and no emulsification.

6 Conclusion

The variation of hydrocarbon-fluorocarbon ratio m/n in $PFE_{n,m}$ synthesized has enabled to control important physical parameters such as solubility in organic solvents (in particular in silicone oils), refractive index and density. $PFE_{n,m}$ synthesized show very low surface activity in solution with common organic solvents unlike semifluorinated n-alkane analogs. Further, they do not show gel-like structures and foam tendency. They present ideal physico-chemical properties to use alone as a postoperative short-term tamponades or as postoperative long-term tamponades in combination of silicone oils. In fact, $PFE_{n,m}$ with n= 4, 6, 8 and m= 2, 3, 5, 8, on account of their higher density that silicone oil and extraordinary low surface tension and interfacial tension, are suitable as a fluid for the reattachment of a detached retina. In fact, PFEs synthesized have good solubility in silicone oils, an index refractive and specific gravity close to natural vitreous. The high solubility of $PFE_{m,n}$ in silicone oils and their refractive indexes similar to those of silicone oils enable the design of soluble mixtures that can be used as long-term postoperative tamponade agents having specific gravity of 1.12 – 1.58 such that the probability of retinal damage due to weight is greatly reduced. In addition, the low surface tension of $PFE_{n,m}$ helps the uniform wetting of retina allowing its complete relaxation and proper positioning. Thus, there is a completely new application for such homogeneous solutions of PFEs in silicone oils, on account of the resultant adjustable low densities and the selectable interfacial and surface tensions. It is showed that the semifluorinated ethers are more soluble in silicone oils the higher hydrocarbon content while the fluorinated content generates the opposite effect. The solubilities decrease only slightly as the viscosity of the silicone oil increases.

All these parameters are very close to the requirements which a long-term ocular endotamponade has to fulfill.

Also, the in vivo tests in a rabbit eye model were extremely promising: no emulsification, no changes in the vascular structure of the retina and no increase of the intra-ocular pressures.

Thanks to their biocompatibility some $PFE_{n,m}$ have been recently tested as long-term postoperative tamponade agents to aid retinal reattachment after surgery to repair retinal tears or detachments.

All negative side effects, seen with the monomeric FCLs, seemed to be eliminated.

Moreover, due to their amphiphilic, boundary surface active behavior in the case of solutions silicone oils, the PFEs with n= 4, 6, 8 and m= 2, 3, 5, 8 at the boundary surfaces of these systems arrange themselves such that their hydrocarbon part reaches into the solvent containing hydrocarbons, while the oleophobic semifluorinated part reaches outward. However, such an arrangement also exists in the case of the PFEs with n= 4, 6, 8 and m= 14, 18, 21 compounds, since in the longer-chain molecules, due to the steric arrangement of the molecule, the fluorinated groups of both ends arrange themselves unilaterally against the long-chain alkane bonding link. The result is the reduction of friction on metal surfaces, ceramic surfaces, polymeric carbon fibers. Then, PFEs with n= 4, 6, 8 and m= 14, 18, 21 compounds able to use as additives in ski-wakes formulations, in lubricating oils, etc.

7 Currently

HeavySIL 1500®, a combination of silicone oil 5000 and $PFE_{6,3}$ is actually commercialize by Al.Chi.Mi.A S.r.l. It remains stable in the presence of air, water or perfluorocarbon liquid. The HeavySIL 1500® is easily removable by aspiration. Then, the advantage of using pre-warmed balanced salt solution as the infusion is that it reduces the viscosity of HeavySIL 1500 (1500 cSt). HeavySIL 1500® moreover, can present a real benefit in the treatment of complex retinal detachment. Actually clinical studies are performed. Based on the results on 24 patients in three different hospitals, anatomical success was achieved in all patients, with no significant emulsification and difficulty in oil removal. Inflammation was absent or minimal. It can conclude the HeavySIL 1500 minimizes the postoperative complications and possesses all the necessary characteristics to become an indispensable tool for vitreoretinal surgery [177].

More extensive studies are now in course [178, 179] to see the limits of in comparison with new analogues such as Densiron 68®, Oxane Hd® which has been marketed recently.

Chapter 2: partially quaternary ammonium salts

1 Surfactant agents

Surface-active agents, also named surfactants, are major industrial products with millions of metric tons produced annually throughout the world. They are *amphiphilic compounds*, where the term amphiphile comes from the Greek word "*amphi*", meaning that all surfactants molecules consist of at least two parts, one hydrophilic (water loving) and one lipophilic (oil loving). Chemically, the hydrophilic moiety of the molecule may be a carboxylate, sulphate, sulfonate, phosphate or other polar group. Then, depending on the basis of the charge or absence of ionization of the hydrophilic group, surface-active agents are classified into anionic, cationic, non-ionic and amphoteric compounds. Moreover, the lipophilic portion of the molecule is non polar group, usually of a hydrocarbon or fluorocarbon nature.

1.1 Anionic surfactants

The largest class of surfactants in general used today are the anionics, which constitute approximately 70 - 75 % of the total consumption.

The anionics group which can consist of alkaline salts of fatty acids is by far the largest compound used as in form of soaps. The major historical and economic advantage of the fatty acid soaps has always been the ready availability from natural, renewable sources. The exact properties of a given carboxylate soap will depend upon the source of the raw material.

The soaps, in addition to their cleaning and detergent characteristics, are used in pharmaceutical field to solubilize compounds. They also act as wetting and emulsifying agents in emulsion solutions.

1.2 Cationic surfactants

Cationic surfactants first became important when the commercial potential of their bacteriostatic properties was recognized with the publication of the patent of Domagk published in 1938 [74] [180].

Currently, they play an important role as antiseptic agents in cosmetics formulations, as fire-fighting agents, or corrosion inhibitors. They have also become extremely important to the textile industry as fabric softeners, waterproofing agents, and dye fixing agents.

Cationic surfactants are also used in surface treatment because of their strong tendency to adsorb on negatively charged sites, allowing the formation of a tight molecular layer with fluorinated tails protruding outwards. New uses and special requirements for surfactants evolve, their economic importance can be expected to continue to increase.

1.3 Non ionic surfactants

It is necessary to having surface active agents that are electrically neutral because, for instance, they can have a significantly lower sensitivity to the presence of electrolytes in the system or a reduced effect of pH [181, 182]. They are surface materials resistant to hard water, polyvalent metallic cations, high concentration electrolytes, soluble in water and organic solvents. Many nonionic surfactants, especially the polyoxyethylene (POE family) are generally excellent dispersing agents for carbon. Moreover, this category of surfactants is the major class of surface-actives compounds used in the pharmaceutical industry due to its very low toxicity, good compatibility and excellent stability in biological systems.

1.4 Amphoteric surfactants

The amphoteric surfactants contain, or have the potential form, both positive and negative functional groups. They are named also “betaine materials”.

Currently amphoteric compounds represent only a small fraction of the total production of surface active compounds seen of the difficulty of synthesis and the high costs of production. The most important properties of these material is the considerable synergism when they are employed with other class of surfactants. They are used in specific applications where it is required high biological contact, for instance shampoo or cream formulations, enhancing the skin tolerance.

2 Physical properties

The fundamental property of surfactants is their tendency to accumulate at the interface, such as solid-solid (suspension), liquid-liquid (emulsion), or liquid-vapor (foam). The water and oil solubility make them able to exhibit unique properties: in fact, the nonpolar group allows to the compound to be partially oil soluble and the polar group allows to the compound to be partially water soluble.

Another important characteristic is the capacity of negative or positive centers of electricity, created by an uneven distribution of electrical charge, to generate electrostatic forces, giving rise to intermolecular attractions (cohesional or adhesional forces).

These forces at interface of two immiscible liquids are called interfacial tension. Then, if the cohesional forces, which tend to hold the liquid molecules together, are stronger that the adhesional forces, which tend to pull the surface of the molecules apart, the interfacial tension will be high and the two liquids will be non mix.

To lower the interfacial tension between two immiscible liquids, the interface between the two liquids must be altered by some means. This may be accomplished by adding a substance that is capable of orienting itself between the liquid layers. On collection of a surface active substance at the interface, there is a reduction of interfacial tension.

The other important force is the surface tension of a liquid: it is the force that opposes the expansion of the surface area of the liquid. Interfacial tension is the same but it takes place at the interface of two immiscible liquid, whereas surface tension takes place between the liquid surface and the air.

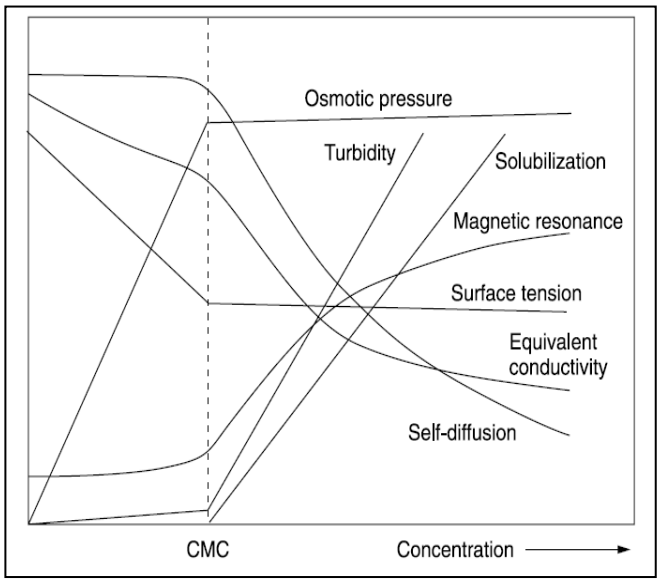

Figure 23: physico-chemical properties as function of concentration of surfactant.

Electrostatic or molecular forces are responsible together for surface and interfacial tension. These forces are the reason for the mutual attraction of the molecules each other.

Another significant property of the surfactant agents is their tendency to form micelles or aggregates of different shapes. This phenomenon of micellization reduces the free energy of system by decreasing the hydrophobic surface area exposed to water. The surfactant molecules behave differently when present in micelle's form compared with free monomers in solution. Micelles are a sort of reservoir for the surface active agent in their monomer form. The ability of surfactant molecules to lower surface tension or to be antimicrobial actives or other dynamic phenomena (wetting and foaming) is governed by the concentration of the free monomer in solution.

The self organization of amphiphilic compounds into micelles, vesicles, lamellar structures and membranes plays also a crucial role in the efficiency of many chemical and biotechnological processes.

Furthermore, the physical properties of surface active agents differ from those of smaller or non-amphipathic molecules in one major aspect, namely the abrupt changes in their properties above a critical concentration. Figure 23 illustrates with plots of several physical properties (osmotic pressure, turbidity, solubilization, magnetic resonance, surface tension, equivalent conductivity and self-diffusion) as a function of concentration. A surfactant shows an abrupt change at this particular concentration, which is consistent with the fact that at and above this concentration, surface active ions or molecules in solution associate to form larger units. These associated units are called micelles (self-assembled structures). The concentration at which this association phenomenon occurs is known as the critical micellar concentration (cmc).

Each surfactant molecules has a characteristic cmc at a given temperature and electrolyte concentration. The most common technique for measuring the cmc is by determining the surface tension, γ, which shows break at the cmc, after which it remains virtually constant with further increases in concentration. However, other techniques such as self-diffusion, conductivity, dynamic light, turbidity measurements can be used.

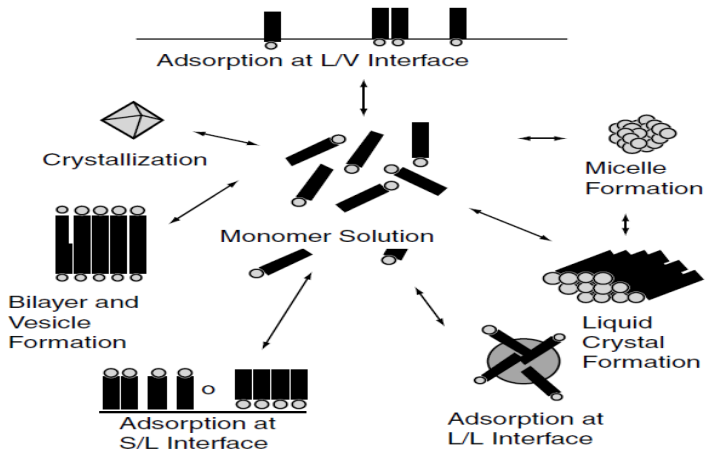

In any class of surface active agent, the cmc decreases with increasing chain length of the hydrophobic portion. As a general rule, the cmc decreases by a factor of 2 for ionics (without added salt) and by a factor of 3 for nonionics on adding one methylene group to the alkyl chain.

3 Fluorinated surfactant

An important functionality to improve hydrophobic characteristic to the design of surfactant molecule is the complete or partially substitution of hydrogen with the fluorine on the carbon chain. The introduction of a fluorinated chain in tension-active structure leads to

the enhancement of their surfactant properties, for instance to lower surface tension and critical micelle concentrations. In fact the hydrophobicity of each CF_2 unit is assumed to be equivalent to 1.5 CH_2 units [183, 184].

Therefore, fluorinated surfactants can be roughly classified into: *perfluorinated surfactants* and *partially fluorinated surfactants*. In perfluorinated surfactants all the hydrogen atoms have been replaced by fluorine atoms. In partially fluorinated surfactants the hydrophobic part of the surfactant molecule contains both fluorine and hydrogen atoms. In addition, the electronic nature of the C-F bond is such as to make perfluorinated surfactants thermally and chemically stables and to permit applications under conditions which would be too severe for conventional hydrocarbon-based surfactants [185].

The unusual properties of fluorosurfactants arise from the unique properties of elemental fluorine. Fluorocarbon compounds possess the lowest surface tensions and surface energies of any substances currently known to science. In fact, substitution of fluorine for hydrogen changes the properties of a surfactant drastically. Once again, the location and the number of fluorine atoms play a key role in determining the surface active properties of the surfactant.

The hydrophobic part of the fluorinated surfactant not only repels water but repels oil and fat as well. The perfluoroalkyl chain, which displays both hydrophobic and oleophobic properties, greatly lowers both surface and interfacial tension of aqueous solutions. Fluorinated surfactants exhibit high surface activity at much lower concentrations compared to the corresponding non-fluorinated analogs. In fact, they can lower surface tension of aqueous solutions to below 20 mN m^{-1} and are effective at very low concentration. In addition, the oleophobicity of the fluorinated chain assures a marked surface activity also in organic solvents.

The ability in lowering both surface and interface tensions makes fluorinated surfactants an essential component in fire fighting formulations, in paint and ink industries, in the formulation of agricultural additives with anti-clouding and anti-fogging properties.

The self-assembly tendency of fluorinated surfactants has been exploited for the preparation of hydrogels which show interesting properties for biomedical applications.

Unfortunately, the wide use of fluorocarbon surfactants is limited by their relatively high cost and their environmental persistence. Instead, partially fluorinated surfactants have several advantages over perfluorinated surfactants. For instance, the hydrocarbon segment provides solubility in more commonly used solvents, lowers the melting point of the

perfluorinated, reduces volatility, and decreases the acid strength of fluorinated acids and less environmental persistence.

3.1 Partially fluorinated quaternary ammonium

Synthetic perfluoroalkyl quaternary ammonium salts are cationic hybrid surfactants and they broadly comprise a fluorinated hydrophobic and oleophobic tail and three hydrocarbon moieties attached to a quaternary ammonium group.

Among the enormous number of fluorinated surfactants, fluorinated quaternary ammonium salts (Quats) display really unique physico-chemical properties. The presence of fluorinated and non-fluorinated alkyl chains on the same molecule allow simultaneously the achievement of low surface and interface tension.

The chemical structure of the surfactant dictates its cmc at a given temperature and ionic strength of the aqueous solution. Notably, cmc depends on the hydrophobe and hydrophile structure and the ionic nature of the surfactant. The cmc of partially fluorinated surfactants decreases exponentially with increasing number of carbon atoms, according to the empirical equation of Klevens [186]:

$$\ln(cmc) = A - Bn$$

where concentrations are expressed in mol L^{-1}, n is the number of carbon atoms in the hydrophobe and A and B are constants for a particular homologous series under constant conditions of temperature, pressure and other parameters. The constant A depends on the nature of the substituents in the hydrophobilic groups of surfactants, while B, the slope of the curve ln (cmc) vs. n, characterizes the variation of the cmc according to the length of the hydrophobic chains [187]. The B coefficient gives a real indication of the impact on the general hydrophobicity of the studied hydrophobic tail.

As a rule of thumb, perfluorination reduces cmc values about four times per -CF_2- group. The cmc value of a fluorinated surfactant is approximately equal to that of a hydrocarbon surfactant with a hydrocarbon chain from 1.3 to 1.7 times longer than the fluorocarbon chain.

The cmc of a fluorinated surfactant also depends on the nature of the hydrophile but only to a lesser effect than on the hydrophobe structure.

Fluorinated Quats similarly to their hydrocarbon counterpart, have the ability to form micelles in aqueous solutions. Micelles are not static structures but they are in dynamic equilibrium with non-associated surfactant molecules dissolved.

The self organization into micelles, vesicles, liposomes and lamellar structures and membranes play a key role in the efficiency of many chemical and biotechnological processes.

4 Applications of fluorinated Quats

4.1 Protein-Based Fire-Fighting Foam

Perfluoroalkyl Quaternary Ammonium Salts have been recognized as useful additives for fire-fighting foam concentrates [188]. The particular design of molecule with a lipophobic–lipophilic character and the chemical structure in different segment play a crucial rule in the formation of an insulating thin aqueous film on hydrocarbon fuels during fire-fighting foam flow. In fact, the formation of a physical barrier to prevent the creation of combustible vapors, which is the principal fire source, and the removal heat by water evaporation are the fundament characteristics required to a fire-fighting foam. In this way, fire-fighting foams must spread quickly over the burning fuel in order to cover large and inaccessible areas easily. The relationship between spreading coefficient (S_{spr}), the surface tension of the hydrocarbon burning fuel (γ_h), the surface tension of foam (γ_f), and the interfacial tension between burning fuel and foam (γ_{hf}) are shown in eq. 3:[189]

$$S_{spr} = \gamma_h - (\gamma_f - \gamma_{hf}) \qquad 3$$

It is a measure of the free-energy change for the spreading of liquid over other liquid (Figure 24).

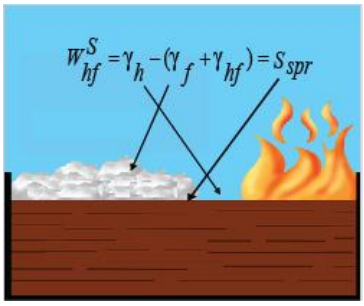

Figure 24: spreading coefficient

Indeed, it will be positive if there is a decrease in free energy on spreading (i.e., adhesive forces dominate), and the spreading process will be spontaneous [190]. If it is negative, then cohesive forces will dominate and a drop or lens will result [181].

The quaternary ammonium agents reduce the strength of the surface film because they reduce the lateral van der Waals interactions between adsorbed molecules leading to a decrease in surface tension. They may also reduce interfacial tension by the inclusion in the molecule of several hydrophilic groups along the chain, or by placing the smallest number of methylene groups in the chain consistent with the necessity for limited solubility.

Therefore, quaternary surfactants are the ideal molecules to minimize both surface and interfacial tensions conditions. In fact, the hydrocarbon moieties in the quaternary structure

are responsible for the interfacial tension reduction, while the fluorinated tail minimizes the surface tension. Finally, small amounts of a perfluoroalkyl quaternary ammonium salt in foam formulations bring surface and interfacial tensions to extremely low values, causing the spreading coefficient to become positive [13]. However, a positive value of S_{spr} is a necessary thermodynamic condition but it may not be sufficient for spontaneous spreading to occur. Because of other kinetic variables, including state of the surfaces, adsorption of foreign compounds, which may greatly hinder foam flow, specific laboratory tests are necessary to evaluate the flowing properties of foams [191].

4.2 Clay applications

Cationic fluorinated surfactants are also used for surface treatment because of their strong tendency to adsorb on negatively charged sites, allowing the formation of a tight molecular layer with fluorinated tails protruding outwards. Because most surfaces and particles are negatively charged, the adsorption can be advantageous or disadvantageous, depending on the intended use of the surfactant. For example, adsorption on clay and sludge in wastewater cleaning systems simplify the removal of cationic fluorinated surfactants from effluents [192, 193].

Quaternary fluorinated ammonium surfactants are commonly used to modify organically montmorillonite clays. Addition of cationic surfactants into an aqueous clay dispersion causes the displacement of the original interlayer cations.

Montmorillonite is a silicate clays commonly used in nanocomposites formulations since it can be exfoliated. The exfoliation process involves the separation of the layers of the clay into large, thin platelets. Often, the clay is swelled by the intercalation of surfactants or polymers between the layers and then a mechanical mixing is carried out to cleave the sheets.

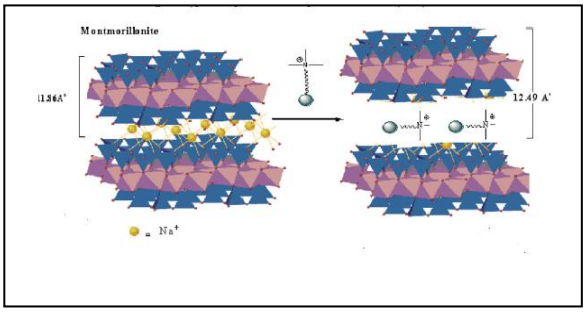

Figure 25: intercalation of Quats in nanocomposite

The swelling of the clay depends to the balance of the intermolecular forces between the layers of the clay. Montmorillonite clays (Figure 25), composed of aluminosilicate sheets of 1 nm in thickness, are negatively charged due to a charge deficiency within the layers.

Sodium or potassium ions are adsorbed between the layers and act to balance the charge. A cationic surfactant diffuses between the sheets and replaces the adsorbed ions acting to change the charge and chemistry of the montmorillonite surface.

Frequently, the intercalated molecules align themselves in an ordered structure within the interlayer space [194]. The alkyl chain of cationic surfactants is end-tethered to the surface by coulomb interaction with the negatively charged layers [195]. The arrangement of the long-chain cations in the interlayer space depends on the chain length, layer charge, and amount adsorbed [160, 196].

When an excess amount of cationic surfactants is added into the solution, surfactant adsorption occurs beyond the cation exchange capacity (CEC) of the clay mineral [165]. Excess surfactants adsorbed beyond the CEC of the clay mineral were ascribed to Van der Waals interactions [197].

The cationic surfactant adsorbs with its positively charged head group next to the negatively charged clay surface, forcing the hydrophobic surfactant tail to adsorb and be exposed to the solution. Hence, the natural montmorillonite surface is hydrophilic, but the adsorption of a small amount of surfactant on the surface renders it hydrophobic. This hydrophobic surface can more easily mix with a polymer melt to formulate nanocomposite materials. In this way, the introduction of a fluorinated chain in the molecule leads to an enhance of hydrophobic character improving an increase of the surface properties of the organically modified clay and the performance of nanocomposite.

Hence, the high thermal stability and resistance due to the hydrophobic fluorinated chain can affect in a favorable manner on the polymer processing temperatures.

4.3 Antibacterical formulations

Non-fluorinated quaternary ammonium salts have been used for many decades as disinfectant and antiseptic agents for hard surface sanitizers, cosmetics, contact lenses disinfectants. Jacobs and Heidelberger reported first the antimicrobial properties of Quats [198, 199]. The second important step was the work of Dogmak [200].

These compounds are cationic water-soluble surface-active agents, with a broad spectrum of antimicrobial activity which ranges from gram positive to gram negatives bacteria. A typical compound belonging to the first-generation of quaternary compounds is benzalkonium chloride (Figure 26) [201].

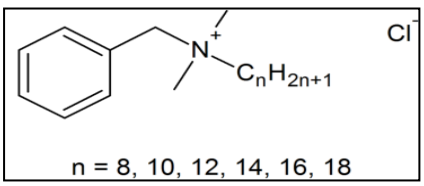

Figure 26: benzalkonium chloride

This compound was the antiseptic agent of election in disinfectant solutions for rigid contact lenses. When soft lenses was introduced, the ophthalmological community recognized the need for a disinfectant which were compatible with soft lenses which are basically made of polymethyl methacrylate (PMMA). This polymer is negatively charged and it strongly binds to benzalkonium chloride causing to increase tremendously the incidence of ocular irritation. Over the years many other classes of biocides were developed, in particular polymeric quaternaries which are less toxic than benzalkonium chloride.

Quats are very active against gram-positive bacteria and lyophylic viruses but their activity against gram-negative bacteria is less pronounced. The resistance displayed by many organisms to the bactericidal action of quaternary ammonium salts required the development of new biocide agents having original chemical structures.

However, despite widespread use, there is still much to learn about the modes of action of these compounds, and such information is vital for the rational design of optimized formulations. A large of their antimicrobial activity is conditioned by their surface active properties and by length of hydrophobic chains.

4.3.1 Molecular Structure and Antibacterial effect

A number of research programs is aimed to increase the antimicrobial performances of molecules introducing new molecular parameters such as heteroatoms [202], chemical functions [17, 171-174, 203], aromatic [204, 205] or nonaromatic cyclic substituents [206, 207], single fluorinated chains [187, 208-210], double fluorinated chains [211-213], polymerizable moieties [214]. Formulation studies are also an active field of research [215]. It is obvious that a surface-active structure plays an important role in antimicrobial performances of Quats. Length of the aliphatic chain, number of carbon atoms in the aliphatic groups, introduction of fluorinated chain are also significant factors to study the antimicrobial activity of Quats.

4.3.2 Mechanisms of action of quaternary ammonium salts

In order to explain the bactericidal activity of quaternary ammonium salts many mechanisms have been proposed over the years. The proposed action mechanisms of these compounds are numerous and not completely clarified [216-219].

One of this is the following sequence of events with microorganisms exposed to cationic agents [220]:

(i) adsorption and penetration of the agent into the cell wall;

(ii) reaction with the cytoplasmic membrane;

(iii) membrane disorganization;

(iv) leakage of intracellular low-molecular-weight material;

(v) degradation of proteins and nucleic acids;

(vi) wall lysis caused by autolytic enzymes.

Effects on the cytoplasmic membrane are the primary mode of action by these compounds.

The cytoplasmic membrane of bacterial cells is a lipid bilayer consisting of molecules such as phosphatidyl ethanolamine and phosphatidyl glycerol (Figure 27). It presumed that

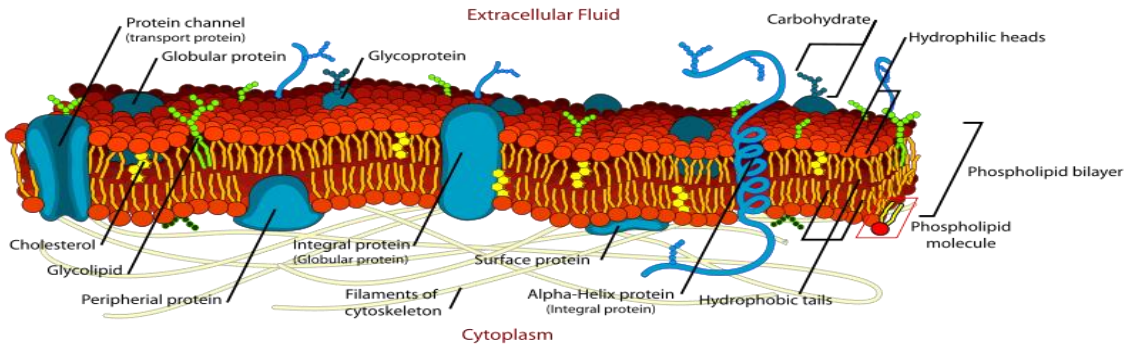

Figure 27: cell membrane

when a quaternary ammonium comes in contact with a phospholipid bilayer (Figure 27), their cations attach to the negatively charged phosphates of the lipid head-groups, while the hydrophobic side chains insert themselves into the tail region of the bilayer and result in its disorganization. Although the bacterial cell envelope is more complex than a simple bilayer structure, the antibacterial activity of ammonium quaternary compounds is believed to be due to the electrostatic interaction between the cationic molecule and the cytoplasmic membrane (plasma membrane in yeasts). These actions involve ionic interactions between positively charged biocides and negatively charged biomolecules. Hydrophobic interactions are also involved in penetration of membrane lipid bilayers and displacement of stabilizing interactions between phospholipids and proteins, and so the alkyl chain of quaternary ammonium compounds interactions with the fatty acid chains of membrane lipids.

Alterations in the membrane can lead to leakage of metabolites and coenzymes, resulting in a loss enzymatic activity. Quaternary ammonium salts interfere also with respiration and ATP synthesis and in appropriate concentration, can cause membrane leakage, release of the cellular constituents and even cell death. Quaternary ammonium compounds act by protein denaturation and disruption of membrane structure. They have the capability of killing microorganisms by promoting the uptake of these molecules by target organism.

The exact mechanism has yet to be ascertained. Ivanov et al. have proposed that disruption of the cell membrane occurs by the insertion of the hydrophobic alkyl groups, and hence, hydrophobicity was the primary determinant of activity.

Kugler et al. have also postulated a mechanism based on the release of counter-ions from the cell membrane. Mg^{2+} and Ca^{2+}, cations neutralize and bridge the phosphate groups of the phospholipid molecules, which otherwise would strongly repel each other. The removal of these cations from the outer membrane of a gram-negative bacterium such as *Escherichia coli*, in exchange for the polycation at the surface, causes destabilization of the outer membrane leading to nonviable cells.

Finally, the first step in all the presented mechanisms is related to the amphiphilic character of these compounds which allows them to strongly interact with the cell membrane.

Aggregation properties like micellization and other association patterns of amphiphilic Quacs may have important consequences for antimicrobial efficiency of these compounds [220].

Hence, the bactericidal activity of quaternary ammonium salts is related to specific structural characteristics. For example, Quats with alkyl chains below a certain length, and so with weak surfactant properties, are ineffective as antimicrobial agents.

4.3.3 Surface active properties

The efficacy in bacterial activity of these compounds is conditioned by surfactant properties. These compounds possess properties such as reduction of surface tension that promotes their adsorption onto bacteria surfaces and a well established relationship exists between cytolitic action and surface tension [221]. In fact, liquids with a very low surface tension permeate and penetrate into minute interstices more easily than liquids with an high surface tension. Then, process of diffusion and osmosis are accelerated by lowering of surface tension [170, 200]. Solutions which lower surface tension are adsorbed on the surfaces of microorganism and exist in higher concentration at the most effective point in response to the law of entropy.

Therefore, it would appear clear that surface tension plays a very important role in disinfection by chemical means, as well as in other cellular processes. The combination of very great bactericidal activity and powerful surface tension properties suggest the

importance in further investigation of the significance of surface tension factors in chemical disinfection.

4.3.4 Influence of chain length

The variation in length of the alkyl tail is thought to influence the extent of antimicrobial activity. In the antimicrobial mechanism the alkyl chain is believed integrated with the lipid bilayer of the cell membrane causing a disruption in the membrane and leakage of the cell contents. It is believed that interaction with the surface of the microorganism is a function of the polar head groups of the compounds and the alkyl chain.

The length of the alkyl chain of the surfactants is thought to contribute to the extent of this membrane disruption, because the higher chain lengths may be incorporated into the lipid bilayers of the plasma membrane.

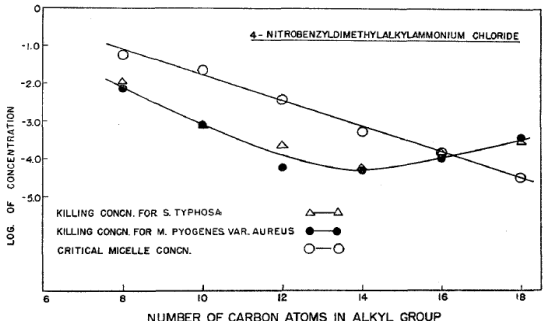

Figure 28: antimicrobial activity and cmc as function of alkyl chain

Ross et al. in 1953 [222] demonstrated that it is not possible to increase indefinitely the length of the hydrocarbon tail because the dependence of biological activity with respect to the length of the latter is usually not linear but parabolic, as shown in Figure 28, and will decrease from a given length. Then, there exists a linear relationship between activity and alkyl chain length with increased carbon number up to a maximum of between 12 and 14, at which region there could be observed a decrease in activity.

In fact, increasing of alkyl chain, the surfactant becomes more hydrophobic and values of cmc decrease [223]. However, the tendency of molecules to combine together as micelles grows exponentially as the increase of hydrophobicity. Therefore, the single molecules are increasingly removed from the solution by incorporation in the micelles, presumably at a greater rate than the rate of increase of adsorption on a hydrophobic bacterial surface leading a reduction of microbial activity.

5 Toward to a new structure

In general, quaternary surfactants are sensitive to gram-positive bacteria, in particular to staphylococci [182, 185, 224]. In order to overcome this increasing of resistance phenomenon, it is necessary to develop new molecules with an original chemical structure.

To overcome the cut-off effect of long alkyl chains on antimicrobial activity, an approach is to replace the hydrocarbon tail by a perfluoroalkylated one in order to improve the surface active properties while keeping a reasonable hydrocarbon chain length. In fact, introducing fluorine atoms on the hydrophobic chains enhances amphiphilic properties such as a significant reduce of surface tension, significant hydrophobicity, significant oleophobicity due to the intrinsic properties of fluorinated chains. Then, fluorinated surfactants have colloidal and surface active properties since the hydrocarbon pairs do not exhibit [185]. These properties are characterized by strong intramolecular bonds and weak intermolecular interactions that play in a favorable manner in antimicrobial activity.

In fact every CF_2 group in the fluorinated chain decreases the values of critical micelle concentration and surface tension leading a very low values of these parameters. Since the critical concentration or micelle formation can be determined with accuracy, its correlation with bactericidal activity is considered.

Then, it is reasonable to assume that the bactericidal action of cationic surfactant is related to the tendency to leave in solution. Therefore, aggregation properties like micellization and other association patterns of amphiphilic compounds may also have important consequences for antimicrobial efficiency of Quats.

5.1 Synthesis of partially quaternary ammonium salts

The aim of the project is the synthesis and some physicochemical properties characterizations of two series of chain-type fluorinated cationic surfactants.

These synthetic hybrid surfactants comprise a hydrophobic and oleophobic part (tail), constituted by the fluorinated alkyl chain, and by the three hydrocarbon moieties (hydrophilic part) attached to a quaternary ammonium group (cationic head). Figure 29 shows the simplified structure of partially fluorinated compounds.

The introduction of fluorinated chains in surfactants is very promising to the specific application of quaternary compounds, due to their strong surface activity, high hydrophobicity, stiffness and the formation of structures with relatively little curvature.

However, an increase hydrocarbon moieties can lead to an increase of hydrophobicity that can play in a favorable manner to the antibacterial application. Then, the hydrophobic–lipophobic-lipophilic character of the surfactants could be tuned by varying the chemical structure of the different segments; this plays a crucial role in the formation of an insulating thin aqueous film on hydrocarbon fuels during fire-fighting foam flow.

From the structure-activity relationship, it is possible to induce a variation of some molecular parameters in order to optimize these surface-active structures.

Therefore, the fluorinated, hydrocarbon and quaternizating agent chain lengths, and the counter-ion were varied.

The effects of the increase of hydrophobic and hydrophilic alkyl chain length and counter-ion on physic-chemical properties were studied.

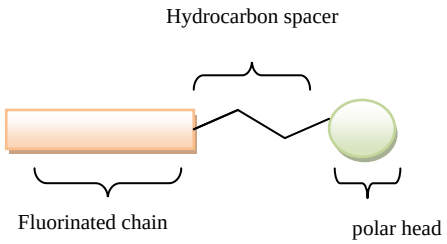

Figure 29: structure of partially fluorinated ammonium salts

The principal parameters to characterize a surface-active agent such as critical micellar concentration, superficial tension, surface excess, Area per molecule, packaging parameter, diameter hydrodynamic, micellar structures and shape of micelles were determined. Then, solutions of these surfactants have a number of peculiarity properties because their micellar chains are formed due to weak non-covalent interactions and easily change their structures in response to external actions. Therefore, optical microscopy observations and rheological measurements also carried out to investigate the viscoelastic properties of some F_nH_m solutions by oscillatory-shear measurements as function of temperature, concentration, alkyl chain length.

6 Experimental section 1

The preparation of one group synthetic perfluoroalkyl quaternary ammonium salts was performed according to the two-step reaction reported in Scheme 11.

The first group of quaternary ammonium salts is characterized by a variation of fluorinated and hydrocarbon chain and a constant alkylating agent (iodomethane).

The first step consists of the regioselective ring-opening of the (perfluoro-n-octyl)methyl oxirane. (Perfluoro-n-octyl)methyl oxirane was reacted with a dialkyl amine (methyl, ethyl, propyl, butyl, hexyl, octyl) for 3 – 24 h (in methanol as solvent) at temperature of 40-60 °C [225]. This reaction takes place by a SN2 mechanism to give the most substituted, tertiary amines. Intermediates were subsequently reacted (Step 2) with iodomethane (alkylating agent) in acetonitrile at 60 °C, obtaining the corresponding quaternary ammonium salts.

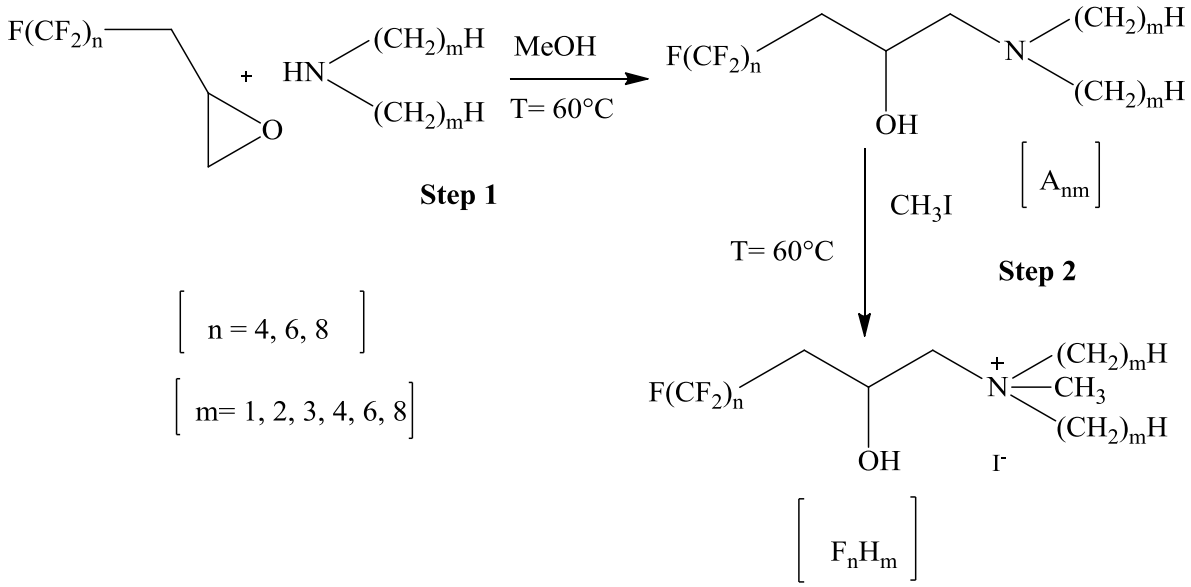

Scheme 11: synthesis of fluorinated quaternary salts F_nH_m

3-Perfluorobutyl-1,2-epoxypropane, 3-perfluorohexyl-1,2-epoxypropane, and 3-perfluorooctyl-1,2-epoxypropane are synthesized according to the previous procedure [226].

Confirmation of the structures of the intermediates and products were obtained by nuclear magnetic resonance (NMR) realized with a Bruker W-200 MHz instrument, mass spectrometry (MS) 80 using a Thermo TRACEGC instrument from Thermofischer 81 Corp. fitted with an Automass III Multi spectrometer (electron ionization at 70 eV). An example of NMR Spectra is shown in Figure 30.

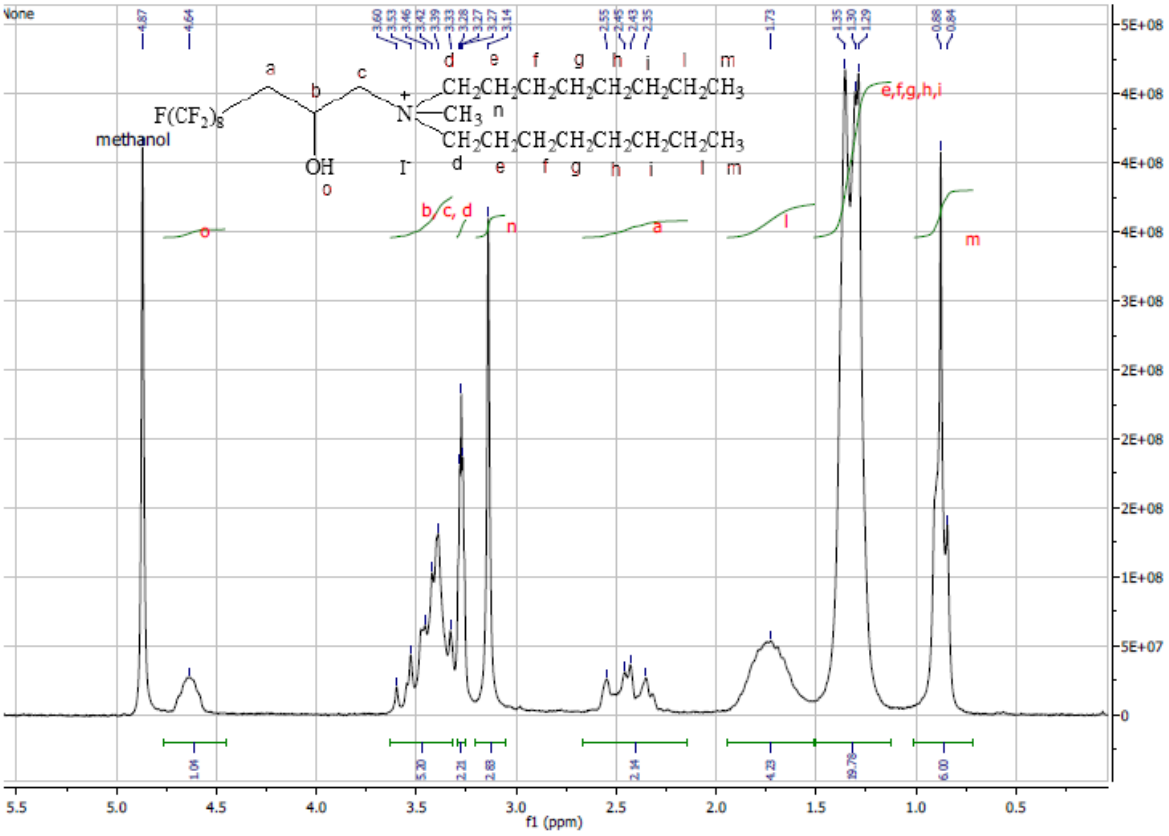

Figure 30: NMR Spectra of F_8H_8

6.1 Preparation of the Semifluorinated Tertiary Amines ($A_{n,m}$)

Synthesis 1-dymethylaminoeptadecafluoroundecan-2-ol ($A_{8,1}$)

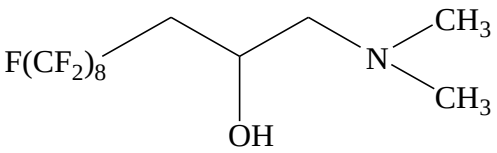

10 g (0.02 mol) of 3-perfluorooctyl-1,2 epoxypropane was added to a stirred solution of 6.5 g (0.04 mol) of dimethylammine in methanol 2 M. The mixture was refluxed for 3 h at 60 °C. After the dimethylammine and the solvent were evaporated under reduced pressure, the residue was washed several times time by deionized water to yield 1-dymethylaminoeptadecafluoroundecan-2-ol in form of white solid. The yield was 95 %.

spectral data: MS *m/z* (rel. ab. %): 521 ($[M]^{+\bullet}$, 5 %); 506 ($[M\text{-}CH_3]^+$, 20 %), 88 ($[M\text{-}CF_3(CF_2)_7, \text{-}CH_2]^+$, 10 %), 58 ($[M\text{-}CF_3(CF_2)_8CHOHCH_2]^+$, 100 %);

^{1}H NMR (CD_3OD): δ = 2.39 (m, CH_2(a), 2H); 2.6 (m, CH(b), 1H); 2.49 (d, CH_2(c), 2H); 2.29 (t, CH_3(d), 6H); 4.2 (d, OH(e), 1H).

^{19}F NMR (CD_3OD): δ = -80.9 (t, CF_3(a), 3F); -111.7 (m, CF_2CH_2(b), 2F); -126.2 (m, CF_2(c), 2F); -123.3 (m, CF_2(d), 2F);-122.8 (m, CF_2(e), 2F);-121.9 (m, CF_2(f), 2F); -121.6 (m, CF_2(g,h), 4F).

Synthesis 1-diethylaminoeptadecafluoroundecan-2-ol ($A_{8,2}$)

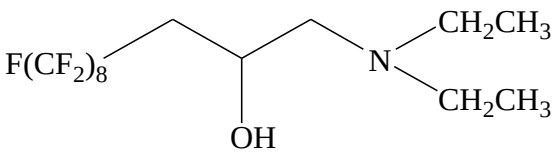

50.0 g (0.10 mol) of 3-perfluorooctyl-1,2 epoxypropane was added to a stirred solution of 8.0 g (0.11 mol) of diethylammine in 60 mL of methanol. The mixture was refluxed for 10 h at 60 °C. After the diethylammine in excess and solvent were evaporated under reduced pressure, the residue was washed three times by 100 mL of deionized water. Then, the organic phase was washed with diethyl ether, dried over anhydrous Na_2SO_4 to give a red liquid. Purification of the residue by column chromatography on silica gel (dichloromethane: methanol= 98:2) gave compound as a yellow liquid. The yield was 84 %.

spectral data: MS *m/z* (rel. ab. %): 549 ($[M]^{+\bullet}$, 3 %), 116 ($[M\text{-}CF_3(CF_2)_7, \text{-}CH_2]^+$, 30 %), 86 ($[M\text{-}CF_3(CF_2)_8CHOHCH_2]^+$, 100 %, 69 $[CF_3]^+$ 15 %;

^{1}H NMR (CD_3OD): δ = 2.18(m, CH_2(a), 1H); 2.49 (m, CH_2(a), 1H); 4.2 (d-d, CH(b), 1H); 2.49 (m, CH_2(c,d,), 6H); 1.04 (t, CH_3(e), 6H); 4.1 (d-d,OH(f), 1H).

^{19}F NMR (CD_3OD): δ = -80.9 (t, CF_3(a), 3F); -111.7 (m, CF_2CH_2(b), 2F); -126.2 (m, CF_2(c), 2F); -123.3 (m, CF_2(d), 2F);-122.8 (m, CF_2(e), 2F);-121.9 (m, CF_2(f), 2F); -121.6 (m, CF_2(g,h), 4F).

Synthesis 1-dipropylaminoeptadecafluoroundecan-2-ol ($A_{8,3}$)

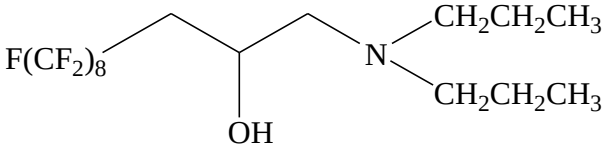

30.0 g (0.06 mol) of 3-perfluorooctyl-1,2 epoxypropane was added to a stirred solution of 7.0 g (0.069 mol) of dipropylammine in 50 mL of methanol. The mixture was refluxed for 15 h at 60 °C. After the dipropylammine in excess and solvent were evaporated under reduced pressure, the residue was washed three time by 100 mL of deionized water. Then, the organic phase was washed with diethyl ether, dried over anhydrous Na_2SO_4 to give a red liquid. Purification of the residue by column chromatography on silica gel

(dichloromethane: methanol= 98 : 2) gave compound as a yellow liquid. The yield was 84 %.

spectral data: MS *m/z* (rel. ab. %): 577 ($[M]^{+\bullet}$, 2 %); 534 ($[M\text{-}CH_2CH_2CH_3]^+$, 2 %), 144 ($[M\text{-}CF_3(CF_2)_7, \text{-}CH_2]^+$, 8 %), 114 ($[M\text{-}CF_3(CF_2)_8CHOHCH_2]^+$, 100 %), 69 $[CF_3]^+$ 15 %;

^{1}H NMR (CD_3OD): δ = 2.18 (m, CH_2(a), 1H); 2.49 (m, CH_2(a), 1H); 4.2 (d-d, CH(b), 1H); 2.49 (m, CH_2(c,d,), 6H); 1.38 (m, CH_3(e), 4H); 1.04 (d-d, CH_3(f), 6H); 4.1 (d-d, OH(g), 1H).

^{19}F NMR (CD_3OD): δ = -80.9 (t, CF_3(a), 3F); -111.7 (m, CF_2CH_2(b), 2F); -126.2 (m, CF_2(c), 2F); -123.3 (m, CF_2(d), 2F);-122.8 (m, CF_2(e), 2F);-121.9 (m, CF_2(f), 2F); -121.6 (m, CF_2(g,h), 4F).

Synthesis 1-dibutylaminoeptadecafluoroundecan-2-ol ($A_{8,4}$)

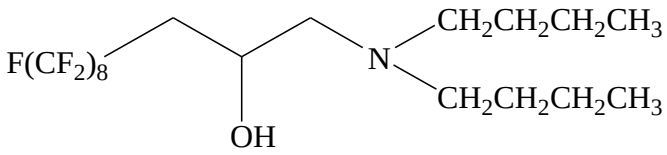

30.0 g (0.063 mol) of 3-perfluorooctyl-1,2 epoxypropane was added to a stirred solution of 8.9 g (0.069 mol) of dibutylammine in 50 mL of methanol. The mixture was refluxed for 10 h at 60 °C. After the solvent were evaporated under reduced pressure, the residue was washed three times by 100 mL of deionized water. Then, the organic phase was washed with diethyl ether, dried over anhydrous Na_2SO_4 to give a red liquid. Purification of the residue by column chromatography on silica gel (dichloromethane: methanol= 99:1) gave compound as a yellow liquid. The yield was 81 %.

spectral data: MS *m/z* (rel. ab. %): 605 ($[M]^{+\bullet}$, 5 %); 172 ($[M\text{-}CF_3(CF_2)_7, \text{-}CH_2]^+$, 8 %), 142 ($[M\text{-}CF_3(CF_2)_8CHOHCH_2]^+$, 100 %), 57 $[CH_2CH_2CH_2CH_3]^+$ 10 %;

^{1}H NMR (CD_3OD): δ = 2.18 (m, CH_2(a), 1H); 2.49 (m, CH_2(a), 1H); 4.2 (d-d, CH(b), 1H); 2.49 (m, CH_2(c,d,), 6H); 1.38 (m, CH_3(e,f), 8H); 1.04 (d-d, CH_3(g), 6H); 4.1 (d-d, OH(h), 1H).

^{19}F NMR (CD_3OD): δ = -80.9 (t, CF_3(a), 3F); -111.7 (m, CF_2CH_2(b), 2F); -126.2 (m, CF_2(c), 2F); -123.3 (m, CF_2(d), 2F);-122.8 (m, CF_2(e), 2F);-121.9 (m, CF_2(f), 2F); -121.6 (m, CF_2(g,h), 4F).

Synthesis 1-dihexylamminoeptadecafluoroundecan-2-ol ($A_{8,6}$)

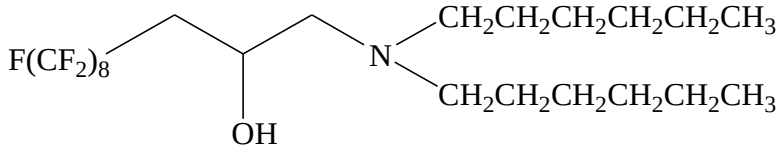

23.8 g (0.05 mol) of 3-perfluoroctyl-1,2 epoxypropane was added to a stirred solution of 10.2 g (0.055 mol) of dihexylammine in 40 mL of methanol. The mixture was refluxed for 14 h at 60 °C. After the solvent were evaporated under reduced pressure, the residue was washed three times by 100 mL of deionized water. Then, the organic phase was washed with diethyl ether, dried over anhydrous Na_2SO_4 to give a red liquid. Purification of the residue by column chromatography on silica gel (dichloromethane: methanol= 96:4) gave compound as a yellow liquid. The yield was 67 %.

spectral data: MS *m/z* (rel. ab. %): 661 ($[M]^{+\bullet}$, 5 %); 576 ($[M-CH_2CH_2CH_2CH_2CH_2CH_3]^+$, 5 %), 228 ($[M-CF_3(CF_2)_7, -CH_2]^+$, 20 %), 198 ($[M-CF_3(CF_2)_8CHOHCH_2]^+$, 100 %);

^{1}H NMR (CD_3OD): δ = 2.18 (m, CH_2(a), 1H); 2.49 (m, CH_2(a), 1H); 4.2 (d-d, CH(b), 1H); 2.49 (m, CH_2(c,d,), 6H); 1.38 (m, CH_3(e,f,g,h), 16H); 1.04 (d-d, CH_3(i), 6H); 4.1 (d-d, OH(l), 1H).

^{19}F NMR (CD_3OD): δ = -80.9 (t, CF_3(a), 3F); -111.7 (m, CF_2CH_2(b), 2F); -126.2 (m, CF_2(c), 2F); -123.3 (m, CF_2(d), 2F);-122.8 (m, CF_2(e), 2F);-121.9 (m, CF_2(f), 2F); -121.6 (m, CF_2(g,h), 4F).

Synthesis 1-dioctylamminoeptadecafluoroundecan-2-ol ($A_{8,8}$)

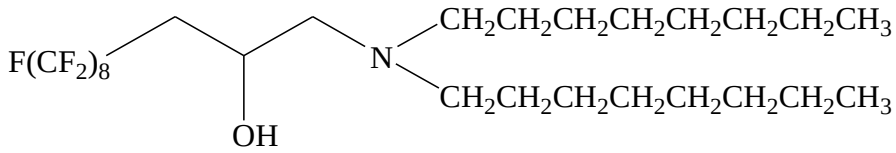

23.8 g (0.05 mol) of 3-perfluorooctyl-1,2 epoxypropane was added to a stirred solution of 14.4 g (0.055 mol) of dioctylammine in 50 mL of methanol. The mixture was refluxed for 20 h at 60°C. After the solvent was evaporated under reduced pressure, the residue was washed several times by 100 mL of deionized water. Then, the organic phase was washed with diethyl ether, dried over anhydrous Na_2SO_4 to give a red liquid. Purification of the residue by column chromatography on silica gel (dichloromethane: methanol= 99 : 1) gave compound as a yellow liquid. The yield was 74 %.

spectral data: MS *m/z* (rel. ab. %): 717 ($[M]^{+\bullet}$, 5 %); 604 ($[M\text{-}CH_2CH_2CH_2CH_2CH_2CH_2CH_2CH_3]^+$, 5 %), 284 ($[M\text{-}CF_3(CF_2)_7, \text{-}CH_2]^+$, 10 %), 254 ($[M\text{-}CF_3(CF_2)_8CHOHCH_2]^+$, 100 %);

^{1}H NMR (CD_3OD): δ = 2.18 (m, CH_2(a), 1H); 2.49 (m, CH_2(a), 1H); 4.2 (d-d, CH(b), 1H); 2.49 (m, CH_2(c,d,), 6H); 1.38 (m, CH_3(e,f,g,h,i,l), 24H); 1.04 (d-d, CH_3(m), 6H); 4.1 (d-d, OH(n), 1H).

^{19}F NMR (CD_3OD): δ = -80.9 (t, CF_3(a), 3F); -111.7 (m, CF_2CH_2(b), 2F); -126.2 (m, CF_2(c), 2F); -123.3 (m, CF_2(d), 2F);-122.8 (m, CF_2(e), 2F);-121.9(m, CF_2(f), 2F); -121.6 (m, CF_2(g,h), 4F).

Synthesis 1-methylamminotridecafluoroundecan-2-ol ($A_{6,1}$)

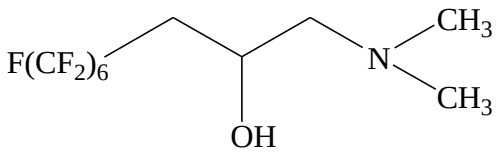

10.0 g (0.026 mol) of 3-perfluorohexyl-1,2 epoxypropane was added to a stirred solution of 15.4 g (0.05 mol) of dimethylammine in methanol 2 M. The mixture was refluxed for 10 h at 60 °C. After the dimethylammine in excess and solvent were evaporated under reduced pressure, the residue was washed several times time by deionized water to yield 1-dymethylaminotridecafluoroundecan-2-ol in form of colorless liquid. The yield was 94 %.

spectral data: MS *m/z* (rel. ab. %): 421 ($[M]^{+\bullet}$, 5 %); 406 ($[M\text{-}CH_3]^+$, 20 %), 88 ($[M\text{-}CF_3(CF_2)_7, \text{-}CH_2]^+$, 100 %), 58 ($[M\text{-}CF_3(CF_2)_8CHOHCH_2]^+$, 100 %);

^{1}H NMR (CD_3OD): δ = 2.39 (m, CH_2(a), 2H); 2.6 (m, CH(b), 1H); 2.49 (d, CH_2(c), 2H); 2.29 (t, CH_3(d), 6H); 4.2 (d, OH(e), 1H).

^{19}F NMR (CD_3OD): δ = -80.9 (t, CF_3(a), 3F); -111.7 (m, CF_2CH_2(b), 2F); -126.2 (m, CF_2(c), 2F); -123.3 (m, CF_2(d), 2F);-122.8 (m, CF_2(e), 2F);-121.8 (m, CF_2(f), 2F).

Synthesis 1-ethylamminotridecafluoroundecan-2-ol($A_{6,2}$)

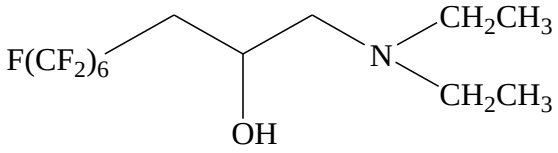

20.0 g (0.053 mol) of 3-perfluorohexyl-1,2 epoxypropane was added to a stirred solution of 4.2 g (0.058 mol) of diethylammine in 30 mL of methanol. The mixture was refluxed for 15 h at 60 °C. After the diethylammine in excess and the solvent were evaporated under reduced pressure, the residue was washed three time by 100 mL of deionized water. Then,

the organic phase was washed with diethyl ether, dried over anhydrous Na_2SO_4 to give a color red liquid. Purification of the residue by column chromatography on silica gel (dichloromethane: methanol= 99:1) gave compound as a yellow liquid. The yield was 89 %.

spectral data: MS *m/z* (rel. ab. %): 449 ($[M]^{+\bullet}$, 5 %); 116 ($[M\text{-}CF_3(CF_2)_7, \text{-}CH_2]^+$, 30 %), 86 ($[M\text{-}CF_3(CF_2)_8CHOHCH_2]^+$, 100 %);

^{1}H NMR (CD_3OD): δ = 2.18 (m, CH_2 (a), 1H); 2.49 (m, CH_2 (a), 1H); 4.2 (d-d, CH(b), 1H); 2.49 (m, CH_2(c,d,), 6H); 1.04 (t, CH_3(e), 6H); 4.1 (d-d, OH(f), 1H).

^{19}F NMR (CD_3OD): δ = -80.9 (t, CF_3(a), 3F); -111.7 (m, CF_2CH_2 (b), 2F); -126.2 (m, CF_2(c), 2F); -123.3 (m, CF_2 (d), 2F);-122.8 (m, CF_2 (e), 2F);-121.8 (m, CF_2 (f), 2F).

Synthesis 1-dipropylamminotridecafluoroundecan-2-ol ($A_{6,3}$)

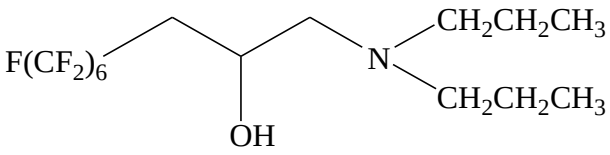

30.0 g (0.08 mol) of 3-perfluorohexyl-1,2 epoxypropane was added to a stirred solution of 8.9 g (0.088 mol) of dipropylammine in 30 mL of methanol. The mixture was refluxed for 18 h at 60 °C. After the dipropylammine in excess and solvent were evaporated under reduced pressure, the residue was washed three time by 100 mL of deionized water. Then, the organic phase was washed with diethyl ether, dried over anhydrous Na_2SO_4 to give a red liquid. Purification of the residue by column chromatography on silica gel (dichloromethane: methanol= 98:2) gave compound as a yellow liquid. The yield was 75 %.

spectral data: MS *m/z* (rel. ab. %): 477 ($[M]^{+\bullet}$, 5 %); 448 ($[M\text{-}CH_2CH_3]^+$, 20 %), 144 ($[M\text{-}CF_3(CF_2)_7, \text{-}CH_2]^+$, 20 %), 114 ($[M\text{-}CF_3(CF_2)_8CHOHCH_2]^+$, 100 %);

^{1}H NMR (CD_3OD): δ = 2.18 (m, CH_2(a), 1H); 2.49 (m, CH_2(a), 1H); 4.2 (d-d, CH(b), 1H); 2.49 (m, CH_2(c,d,), 6H); 1.38 (m, CH_3(e), 4H); 1.04 (d-d, CH_3(f), 6H); 4.1 (d-d, OH(g), 1H).

^{19}F NMR (CD_3OD): δ = -80.9 (t, CF_3(a), 3F); -111.7 (m, CF_2CH_2(b), 2F); -126.2 (m, CF_2(c), 2F); -123.3 (m, CF_2(d), 2F);-122.8 (m, CF_2(e), 2F);-121.8 (m, CF_2(f), 2F).

Synthesis 1-dibutylamminotridecafluoroundecan-2-ol ($A_{6,4}$)

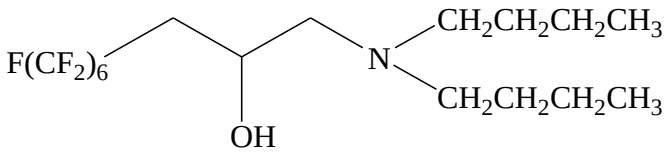

20 g (0.053 mol) of 3-perfluorohexyl-1,2 epoxypropane was added to a stirred solution of 7.8 g (0.060 mol) of dibutylammine. The mixture was refluxed for 17 h at 60 °C. After the solvent were evaporated under reduced pressure, the residue was washed three time by 100 mL of deionized water. Then, the organic phase was washed with diethyl ether, dried over anhydrous Na_2SO_4 to give a red liquid. Purification of the residue by column chromatography on silica gel (dichloromethane: methanol= 99:1) gave compound as a yellow liquid. The yield were 81 %.

spectral data: MS *m/z* (rel. ab. %): 505 ($[M]^{+\bullet}$, 5 %); 448 ($[M\text{-}CH_2CH_2CH_2CH_3]^+$, 5 %), 172 ($[M\text{-}CF_3(CF_2)_7, \text{-}CH_2]^+$, 20 %), 142 ($[M\text{-}CF_3(CF_2)_8CH_2OHCH_2]^+$, 100 %);

^{1}H NMR (CD_3OD): δ = 2.18 (m, CH_2(a), 1H); 2.49 (m, CH_2(a), 1H); 4.2 (d-d, CH(b), 1H); 2.49 (m, CH_2(c,d,), 6H); 1.38 (m, CH_3(e,f), 8H); 1.04 (d-d, CH_3(g), 6H); 4.1 (d-d, OH(h), 1H).

^{19}F NMR (CD_3OD): δ = -80.9 (t, CF_3(a), 3F); -111.7 (m, CF_2CH_2(b), 2F); -126.2 (m, CF_2(c), 2F); -123.3 (m, CF_2(d), 2F);-122.8 (m, CF_2(e), 2F);-121.8 (m, CF_2(f), 2F).

Synthesis 1-dihexylamminotridecafluoroundecan-2-ol ($A_{6,6}$)

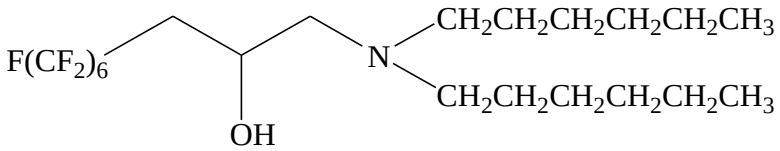

18.8 g (0.05 mol) of 3-perfluorohexyl-1,2 epoxypropane was added to a stirred solution of 11.1 g (0.06 mol) of dihexylammine in 30 mL of methanol. The mixture was refluxed for 17 h in 50 mL of methanol. After the solvent were evaporated under reduced pressure, the residue was washed three time by 100 mL of deionized water. Then, the organic phase was washed with diethyl ether, dried over anhydrous Na_2SO_4 to give a red liquid. Purification of the residue by column chromatography on silica gel (dichoromethane: methanol= 97:3) gave compound as a yellow liquid. The yield was 72 %.

spectral data: MS *m/z* (rel. ab. %): 561 ($[M]^{+\bullet}$, 5 %); 476 ($[M\text{-}CH_2CH_2CH_2CH_2CH_2CH_3]^+$, 10 %), 228 ($[M\text{-}CF_3(CF_2)_7, \text{-}CH_2]^+$, 20 %), 198 ($[M\text{-}CF_3(CF_2)_8CHOHCH_2]^+$, 100 %);

^{1}H NMR (CD_3OD): δ = 2.18 (m, CH_2(a), 1H); 2.49 (m, CH_2(a), 1H); 4.2 (d-d, CH(b), 1H); 2.49 (m, CH_2(c,d,), 6H); 1.38 (m, CH_3(e,f,g,h), 16H); 1.04 (d-d, CH_3(i), 6H); 4.1 (d-d, OH(l), 1H).

^{19}F NMR (CD_3OD): δ = -80.9 (t, CF_3(a), 3F); -111.7 (m, CF_2CH_2(b), 2F); -126.2 (m, CF_2(c), 2F); -123.3 (m, CF_2(d), 2F);-122.8 (m, CF_2(e), 2F);-121.8 (m, CF_2(f), 2F).

Synthesis 1-dioctylamminotridecafluoroundecan-2-ol ($A_{6,8}$)

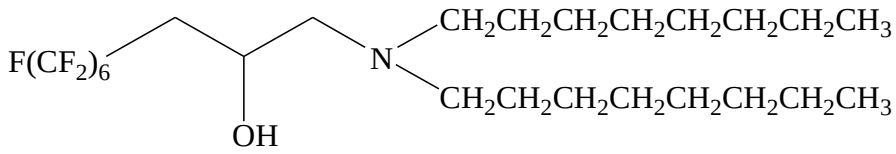

18.8 g (0.05 mol) of 3-perfluorohexyl-1,2 epoxypropane was added to a stirred solution of 14.4 (0.06 mol) of dioctylammine in 50 mL of methanol. The mixture was refluxed for 14 h at 60 °C. After the solvent was evaporated under reduced pressure, the residue was washed three time by 100 mL of deionized water. Then, the organic phase was washed with diethyl ether, dried over anhydrous Na_2SO_4 to give a color red liquid. Purification of the residue by column chromatography on silica gel (dichloromethane: methanol= 99 : 1) gave compound as a yellow liquid. The yield was 77 %.

spectral data: MS *m/z* (rel. ab. %): 617 ($[M]^{+\bullet}$, 5 %); 504 ($[M-CH_2CH_2CH_2CH_2CH_2CH_2CH_2CH_3]^+$, 5 %), 284 ($[M-CF_3(CF_2)_7, -CH_2]^+$, 10 %), 254 ($[M-CF_3(CF_2)_8CHOHCH_2]^+$, 100 %);

^{1}H NMR (CD_3OD): δ = 2.18 (m, CH_2(a), 1H); 2.49 (m, CH_2(a), 1H); 4.2 (d-d, CH(b), 1H); 2.49 (m, CH_2(c,d,), 6H); 1.38 (m, CH_3(e,f,g,h,i,l), 24H); 1.04 (d-d, CH_3(m), 6H); 4.1 (d-d, OH(n), 1H).

^{19}F NMR (CD_3OD): δ = -80.9 (t, CF_3(a), 3F); -111.7 (m, CF_2CH_2(b), 2F); -126.2 (m, CF_2(c), 2F); -123.3 (m, CF_2(d), 2F);-122.8 (m, CF_2(e), 2F);-121.8 (m, CF_2(f), 2F).

Synthesis 1-methylamminononafluoroundecan-2-ol ($A_{4,1}$)

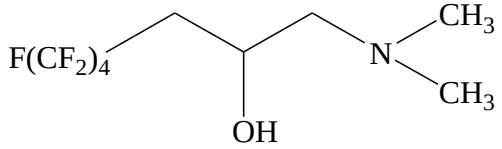

15.0 g (0.054 mol) of 3-perfluorobutyl-1,2 epoxypropane was added to a stirred solution of 20.6 g (0.06 mol) of dimethylammine in methanol 2 M. The mixture was refluxed for 10 h. After the dimethylammine and the solvent were evaporated under reduced pressure, the

residue was washed several times by deionized water to yield 1-dymethylaminononafluoroundecan-2-ol in form of colorless liquid. The yield was 93 %.

spectral data: MS *m/z* (rel. ab. %): 321 ($[M]^{+\bullet}$, 5 %); 306 ($[M\text{-}CH_3]^+$, 20 %), 88 ($[M\text{-}CF_3(CF_2)_7, \text{-}CH_2]^+$, 100 %), 58 ($[M\text{-}CF_3(CF_2)_8CHOHCH_2]^+$, 100 %);

^{1}H NMR (CD_3OD): δ = 2.39 (m, CH_2(a), 2H); 2.6 (m, CH(b), 1H); 2.49 (d, CH_2(c), 2H); 2.29 (t, CH_3(d), 6H); 4.2 (d, OH(e), 1H).

^{19}F NMR (CD_3OD): δ = -80.9 (t, CF_3(a), 3F); -111.7 (m, CF_2CH_2(b), 2F); -126.2 (m, CF_2(c), 2F); -123.3 (m, CF_2(d), 2F);-122.8 (m, CF_2(e), 2F);-121.8 (m, CF_2(f), 2F).

Synthesis 1-ethylamminononafluoroundecan-2-ol ($A_{4,2}$)

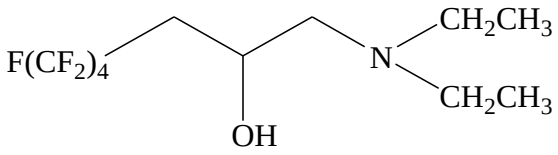

20.0 g (0.07 mol) of 3-perfluorobutyl-1,2 epoxypropane was added to a stirred solution of 5.6 g (0.077 mol) of diethylammine in 30 mL of methanol. The mixture was refluxed for 14 h at 60 °C. After the diethylammine in excess and the solvent were evaporated under reduced pressure, the residue was washed three times by 100 mL of deionized water. Then, the organic phase was washed with diethyl ether, dried over anhydrous Na_2SO_4 to give a red liquid. Purification of the residue by column chromatography on silica gel (dichloromethane: methanol= 99 : 1) gave compound as a yellow liquid.

The yield was 82 %.

spectral data: MS *m/z* (rel. ab. %): 349 ($[M]^{+\bullet}$, 10 %), 116 ($[M\text{-}CF_3(CF_2)_7, \text{-}CH_2]^+$, 30 %), 86 ($[M\text{-}CF_3(CF_2)_8CH_2OHCH_2]^+$, 100 %);

^{1}H NMR (CD_3OD): δ = 2.18 (m, CH_2(a), 1H); 2.49 (m, CH_2(a), 1H); 4.2 (d-d, CH(b), 1H); 2.49 (m, CH_2(c,d,), 6H); 1.04 (t, CH_3(e), 6H); 4.1 (d-d, OH(f), 1H).

^{19}F NMR (CD_3OD): δ = -80.9 (t, CF_3(a), 3F); -111.7 (m, CF_2CH_2(b), 2F); -126.2 (m, CF_2(c), 2F); -123.3 (m, CF_2(d), 2F).

Synthesis 1-propylamminononafluoroundecan-2-ol ($A_{4,3}$)

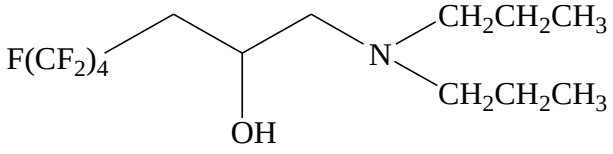

70.0 g (0.25 mol) of 3-perfluorobutyl-1,2 epoxypropane was added to a stirred solution of 27.3 g (0.27 mol) of dipropylammine in 100 mL of methanol. The mixture was refluxed for 20 h at 60 °C. After the dipropylammine in excess and the solvent were evaporated under

reduced pressure, the residue was washed three times by deionized water. Then, the organic phase was washed with diethyl ether, dried over anhydrous Na_2SO_4 to give a red liquid. Purification of the residue by column chromatography on silica gel (dichloromethane: methanol= 99 : 1) gave compound as a yellow liquid. The yield was 81 %.

spectral data: MS *m/z* (rel. ab. %): 377 ($[M]^{+\bullet}$, 5 %); 348 ($[M\text{-}CH_2CH_3]^+$, 30 %), 144 ($[M\text{-}CF_3(CF_2)_7, \text{-}CH_2]^+$, 20 %), 114 ($[M\text{-}CF_3(CF_2)_8CH_2OHCH_2]^+$, 100 %);

^{1}H NMR (CD_3OD): δ = 2.18 (m, CH_2(a), 1H); 2.49 (m, CH_2(a), 1H); 4.2 (d-d, CH(b), 1H); 2.49 (m, CH_2(c,d,), 6H); 1.38 (m, CH_3(e), 4H); 1.04 (d-d, CH_3(f), 6H); 4.1 (d-d, OH(g), 1H).

^{19}F NMR (CD_3OD): δ = -80.9 (t, CF_3(a), 3F); -111.7 (m, CF_2CH_2(b), 2F); -126.2 (m, CF_2(c), 2F); -123.3 (m, CF_2(d), 2F).

Synthesis 1-dibutylamminonafluoroundecan-2-ol ($A_{4,4}$)

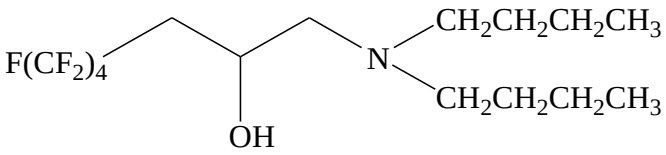

20.0 g (0.07 mol) of 3-perfluorobutyl-1,2 epoxypropane was added to a stirred solution of 10 g of dibutylammine in 30 mL of methanol. The mixture was refluxed for 20 h at 60 °C. After the solvent was evaporated under reduced pressure, the residue was washed several times by deionized water. Then, the organic phase was washed with diethyl ether, dried over anhydrous Na_2SO_4 to give a red liquid. Purification of the residue by column chromatography on silica gel (dichloromethane: methanol= 99 : 1) gave compound as a yellow liquid. The yield was 75 %.

spectral data: MS *m/z* (rel. ab. %): 405 ($[M]^{+\bullet}$, 5 %); 362 ($[M\text{-}CH_2CH_2CH_3]^+$, 20 %), 172 ($[M\text{-}CF_3(CF_2)_7, \text{-}CH_2]^+$, 15 %), 142 ($[M\text{-}CF_3(CF_2)_8CH_2OHCH_2]^+$, 100 %);

^{1}H NMR (CD_3OD): δ = 2.18 (m, CH_2(a), 1H); 2.49 (m, CH_2(a), 1H); 4.2 (d-d, CH(b), 1H); 2.49 (m, CH_2(c,d,), 6H); 1.38 (m, CH_3(e,f), 8H); 1.04 (d-d, CH_3(g), 6H); 4.1 (d-d, OH(h), 1H).

^{19}F NMR (CD_3OD): δ = -80.9 (t, CF_3(a), 3F); -111.7 (m, CF_2CH_2(b), 2F); -126.2 (m, CF_2(c), 2F); -123.3 (m, CF_2(d), 2F).

Synthesis 1-dihexylamminononafluoroundecan-2-ol ($A_{4,6}$)

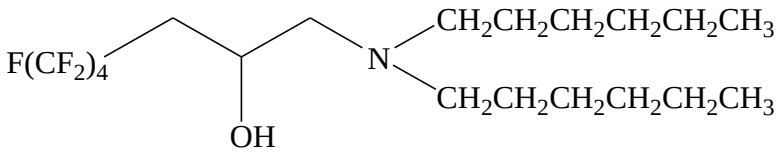

10.0 g (0.036 mol) of 3-perfluorobutyl-1,2 epoxypropane was added to a stirred solution of 7.3 g (0.039 mol) of dihexylammine in 30 mL of methanol. The mixture was refluxed for 24 h at 60 °C. After the solvent were evaporated under reduced pressure, the residue was washed three times by 100 mL of deionized water. Then, the organic phase was washed with diethyl ether, dried over anhydrous Na_2SO_4 to give a red liquid. Purification of the residue by column chromatography on silica gel (dichloromethane: methanol= 97 : 3) gave compound as a yellow liquid. The yield was 65 %.

spectral data: MS *m/z* (rel. ab. %): 461 ($[M]^{+\bullet}$, 5 %); 376 ($[M\text{-}CH_2CH_2CH_2CH_2CH_3]^+$, 20 %), 228 ($[M\text{-}CF_3(CF_2)_7, \text{-}CH_2]^+$, 10 %), 198 ($[M\text{-}CF_3(CF_2)_8CH_2OHCH_2]^+$, 100 %);

^{1}H NMR (CD_3OD): δ = 2.18 (m, CH_2(a), 1H); 2.49 (m, CH_2(a), 1H); 4.2 (d-d, CH(b), 1H); 2.49 (m, CH_2(c,d,), 6H); 1.38 (m, CH_3(e,f,g,h), 16H); 1.04 (d-d, CH_3(i), 6H); 4.1 (d-d, OH(l), 1H).

^{19}F NMR (CD_3OD): δ = -80.9 (t, CF_3(a), 3F); -111.7 (m, CF_2CH_2(b), 2F); -126.2 (m, CF_2(c), 2F); -123.3 (m, CF_2(d), 2F).

Synthesis 1-dioctylamminononafluoroundecan-2-ol ($A_{4,8}$)

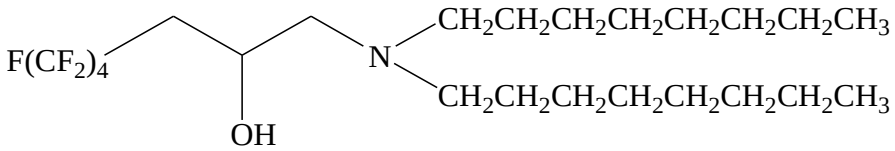

10.0 g (0.036 mol) of 3-perfluorobutyl-1,2 epoxypropane was added to a stirred solution of 9.5 g (0.039 mol) of dioctylammine. The mixture was refluxed for 24 h at 60 °C. After the solvent were evaporated under reduced pressure. The residue was washed several times by deionized water. Then, the organic phase was washed with diethyl ether, dried over anhydrous Na_2SO_4 to give a red liquid. Purification of the residue by column chromatography on silica gel (dichloromethane: methanol= 98:2) gave compound as a yellow liquid. The yield were 73 %.

spectral data: MS *m/z* (rel. ab. %): 517 ($[M]^{+\bullet}$, 5 %); 418 ($[M\text{-}CH_2CH_2CH_2CH_2CH_2CH_2CH_3]^+$, 10 %), 284 ($[M\text{-}CF_3(CF_2)_7, \text{-}CH_2]^+$, 15 %), 254 ($[M\text{-}CF_3(CF_2)_8CHOHCH_2]^+$, 100 %);

^{1}H NMR (CD_3OD): δ = 2.18 (m, CH_2(a), 1H); 2.49 (m, CH_2(a), 1H); 4.2 (d-d, CH(b), 1H); 2.49 (m, CH_2(c,d,), 6H); 1.38 (m, CH_3(e,f,g,h,i,l), 24H); 1.04 (d-d, CH_3(m), 6H); 4.1 (d-d, OH(n), 1H).

^{19}F NMR (CD_3OD): δ = -80.9 (t, CF_3(a), 3F); -111.7 (m, CF_2CH_2(b), 2F); -126.2 (m, CF_2(c), 2F); -123.3 (m, CF_2(d), 2F).

6.2 Preparation of the partially quaternary ammonium salts (F_nH_m)

Synthesis N,N-dimethylammino-heptadecafluoro-2-hydroxy-N,N,N- trimethyl undecan-1-ammonium iodide (F_8H_1)

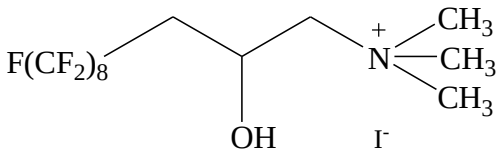

5.0 g (0.009 of 1-dimethylaminoeptadecafluoroundecan-2-ol and 2.7 g (0.02 mol) of iodomethane were refluxed in acetonitrile at 60 °C for over 15 h. After iodomethane and solvent are removed by evaporation, the residue was washed twice times by ether anhydrous et recrystallized by mixture of methanol-ether anhydrous and dried under reduced pressure to give N,N-diethylamino-heptadecafluoro-2-hydroxy-N,N,N-trymethylundecan-1-ammonium iodide in form of white solid. The yield was 91 %.

^{1}H NMR (CD_3OD): δ = 2.24 (m, CH_2(a), 2H); 4.6 (m, CH(b), 1H); 3.51 (t, CH_2(c), 2H); 3.26 (m, CH_3(d), 9H); 4.7 (m, OH(e), 1H).

^{19}F NMR (CD_3OD): δ = -80.9 (t, CF_3(a), 3F); -111.7 (m, CF_2CH_2(b), 2F); -126.2 (m, CF_2(c), 2F); -123.3 (m, CF_2(d), 2F).

Synthesis N,N-diethylamino-heptadecafluoro-2-hydroxy-N,N,N-trymethylundecan-1-ammonium iodide (F_8H_2)

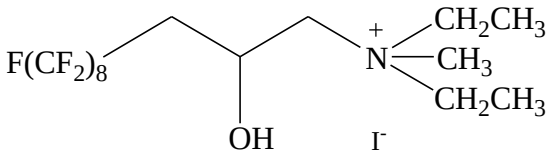

15 g (0.027 mol) of 1-diethylaminoeptadecafluoroundecan-2-ol and 5.7 g (0.054 mol) of iodomethane were refluxed in acetonitrile at 40°C for over 24 h. After iodomethane and solvent were removed by evaporation, the residue was washed 2 times by ether anhydrous et recrystallized by several times ether anhydrous and dried under reduced pressure to give N,N-diethylamino-heptadecafluoro-2-hydroxy-N,N,N-trymethylundecan-1-ammonium iodide in form of yellow solid. The yield was 88 %.

^{1}H NMR (CD_3OD): δ = 2.46 (m, CH_2(a), 2H); 4.6 (m, CH(b), 1H); 3.52 (m, CH_2(c,d), 6H); 3.14 (s, CH_3(e), 3H); 4.7 (m, CH(f), 1H); 1.37 (t, CH_3(g), 6H).

^{19}F NMR (CD_3OD): δ = -80.9 (t, CF_3(a), 3F); -111.7 (m, CF_2CH_2(b), 2F); -126.2 (m, CF_2(c), 2F); -123.3 (m, CF_2(d), 2F);-122.8 (m, CF_2(e), 2F);-121.9 (m, CF_2(f), 2F); -121.6 (m, CF_2(g,h), 4F).

Synthesis N,N-dipropylamino-heptadecafluoro-2-hydroxy-N,N,N-trymethylundecan-1-ammonium iodide (F_8H_3)

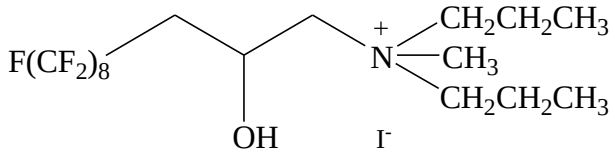

25.0 g (0.05 mol) of 1-dipropylaminoeptadecafluoroundecan-2-ol and 14.8 g (0.1 mol) of iodomethane were refluxed in acetonitrile at 40 °C for over 24 h. After iodomethane and solvent are removed by evaporation, the residue was washed twice by ether anhydrous et recrystallized several times by mixture of methanol-ether. The white solid was filtrated and washed with fresh diethyl ether anhydrous and then dried under reduced pressure to give N,N-dipropylamino-heptadecafluoro-2-hydroxy-N,N,N-trymethylundecan-1 ammonium iodide in form of white solid. The yield was 73 %.

^{1}H NMR (CD_3OD): δ = 2.46 (m, CH_2(a), 2H); 4.6 (m, CH(b), 1H); 3.52 (m, CH_2(c,d,e), 10H); 3.14 (s, CH_3(f), 3H); 4.7 (m, CH(g), 1H); 1.37 (t, CH_3(h), 6H).

^{19}F NMR (CD_3OD): δ = -80.9 (t, CF_3(a), 3F); -111.7 (m, CF_2CH_2(b), 2F); -126.2 (m, CF_2(c), 2F); -123.3 (m, CF_2(d), 2F);-122.8 (m, CF_2(e), 2F);-121.9 (m, CF_2(f), 2F); -121.6 (m, CF_2(g,h), 4F).

Synthesis N,N-dibutylamino-heptadecafluoro-2-hydroxy-N,N,N-trymethylundecan-1-ammonium iodide (F_8H_4)

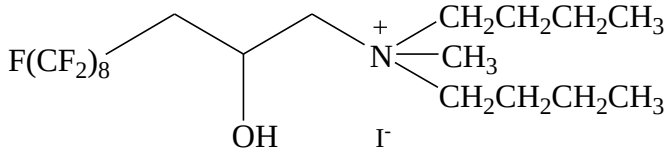

30.0 g (0.05 mol) of 1-dibutylaminoeptadecafluoroundecan-2-ol and 14.0 g (0.1 mol) of iodomethane were refluxed in acetonitrile at 40 °C for over 24 h. After iodomethane and solvent are removed by evaporation, the residue was washed twice by ether anhydrous et recrystallized several times by mixture of methanol-ether. The yellow solid was filtrated and washed with fresh diethyl ether anhydrous and then dried under reduced pressure to give

N,N-dibutylamino-heptadecafluoro-2-hydroxy-N,N,N-trymethylundecan-1-ammonium iodide in form of yellow solid. The yield was 74 %.

^{1}H NMR (CD_3OD): δ = 2.46 (m, CH_2(a), 2H); 4.6 (m, CH(b), 1H); 3.52 (m, CH_2(c,d,e,f), 14H); 3.14 (s, CH_3(g), 3H); 4.7 (m, CH(h), 1H); 1.37 (t, CH_3(i), 6H).

^{19}F NMR (CD_3OD): δ = -80.9 (t, CF_3(a), 3F); -111.7 (m, CF_2CH_2(b), 2F); -126.2 (m, CF_2(c), 2F); -123.3 (m, CF_2(d), 2F);-122.8 (m, CF_2(e), 2F);-121.9 (m, CF_2(f), 2F); -121.6 (m, CF_2(g,h), 4F).

Synthesis N,N-dihexyl-heptadecafluoro-2-hydroxy-N,N,N-trymethylundecan-1-ammonium iodide (F_8H_6)

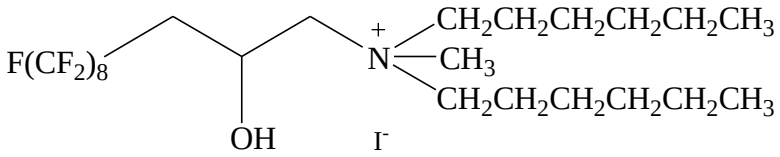

20.0 g (0.03 mol) of 1-dihexyleptadecafluoroundecan-2-ol and 8.5 g (0.06 mol) of iodomethane were refluxed in acetonitrile at 40 °C for over 24 h. After iodomethane and solvent are removed by evaporation, the residue was washed by ether anhydrous et recrystallized several times by mixture of methanol-ether. The yellow solid was filtrated and washed with fresh diethyl ether anhydrous and then dried under reduced pressure to give N,N-dihexylamino-heptadecafluoro-2-hydroxy-N,N,N-trymethylundecan-1-ammonium iodide in form of yellow gel. The yield was 74 %.

^{1}H NMR (CD_3OD): δ = 2.46 (m, CH_2(a), 2H); 4.6 (m, CH(b), 1H); 3.52 (m, CH_2(c,d,e,f,g,h), 22H); 3.14 (s, CH_3(i), 3H); 4.7 (m, CH(l), 1H); 1.37 (t, CH_3(m), 6H).

^{19}F NMR (CD_3OD): δ = -80.9 (t, CF_3(a), 3F); -111.7 (m, CF_2CH_2(b), 2F); -126.2 (m, CF_2(c), 2F); -123.3 (m, CF_2(d), 2F);-122.8 (m, CF_2(e), 2F);-121.9 (m, CF_2(f), 2F); -121.6 (m, CF_2(g,h), 4F).

Synthesis N,N-dioctyl-heptadecafluoro-2-hydroxy-N,N,N-trymethylundecan-1-ammonium iodide (F_8H_8)

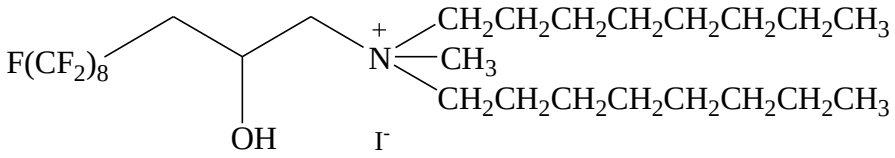

10.0 g (0.014 mol) of 1-dioctyleptadecafluoroundecan-2-ol and 4.0 g (0.028 mol) of iodomethane were refluxed in acetonitrile at 40 °C for over 24 h. After iodomethane and

solvent are removed by evaporation, the residue was washed by ether anhydrous et recrystallized several times by mixture of methanol-ether and washed by petroleum ether. The yellow solid was filtrated and washed with fresh diethyl ether anhydrous and then dried under reduced pressure to give N,N-dioctylamino-heptadecafluoro-2-hydroxy-N,N,N-trymethylundecan-1-ammonium iodide in form of white solid. The yield was 74 %.

^{1}H NMR (CD_3OD): δ = 2.46 (m, CH_2(a), 2H); 3.32 (m, CH(b), 1H); 3.40 (m, CH_2(c,d), 6H); 1.27 (t, CH_2(e,f,g,h,i), 20H); 1.70 (m, CH_2 (l), 4H); 0.86 (t, CH_3(m), 6H); 3.14 (m, CH(n), 3H); 4.7 (t, CH_3(o), 1H).

^{19}F NMR (CD_3OD): δ = -80.9 (t, CF_3(a), 3F); -111.7 (m, CF_2CH_2(b), 2F); -126.2 (m, CF_2(c), 2F); -123.3 (m, CF_2(d), 2F);-122.8 (m, CF_2(e), 2F);-121.9 (m, CF_2(f), 2F); -121.6 (m, CF_2(g,h), 4F).

Synthesis N,N-diethylamino-tridecafluoro-2-hydroxy-N,N,N-trymethylundecan-1-ammonium iodide (F_6H_1)

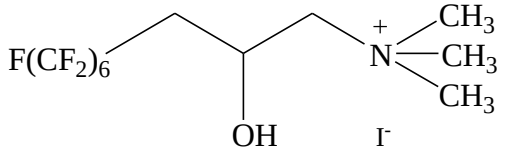

5.0 g (0.01 mol) of 1-dimethylaminotridecafluoroundecan-2-ol and 3.16 g (0.02 mol) of iodomethane were refluxed in acetonitrile at 60 °C for over 4 h. After iodomethane and solvent are removed by evaporation, the residue was washed several times by diethyl-ether et recrystallized by ether petroleum and dried under reduced pressure to give N,N-dimethylamino-tridecafluoro-2-hydroxy-N,N,N-trymethylundecan-1-ammonium iodide in form of white solid. The yield was 94 %.

^{1}H NMR (CD_3OD): δ = 2.24 (m, CH_2(a), 2H); 4.6 (m, CH(b), 1H); 3.51 (t, CH_2(c), 2H); 3.26 (m, CH_3(d), 9H); 4.7 (m, OH(e), 1H).

^{19}F NMR (CD_3OD): δ = -80.9 (t, CF_3(a), 3F); -111.7 (m, CF_2CH_2(b), 2F); -126.2 (m, CF_2(c), 2F); -123.3 (m, CF_2(d), 2F);-122.8 (m, CF_2(e), 2F);-121.8 (m, CF_2(f), 2F).

Synthesis N,N-diethylamino-tridecafluoro-2-hydroxy-N,N,N-trymethylundecan-1-ammonium iodide (F_6H_2)

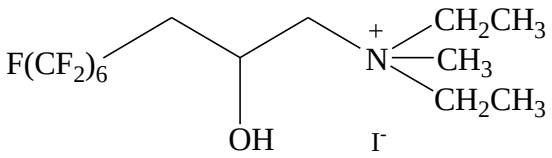

15.0 g (0.025 mol) of 1-diethylaminotridecafluoroundecan-2-ol and 7.2 g (0.05 mol) of iodomethane were refluxed in acetonitrile at 60 °C for over 24 h. After iodomethane and chloroform are removed by evaporation, the residue was washed twice by ether anhydrous et recrystallized by mixture of methanol-ether and dried under reduced pressure to give N,N-diethylamino-tridecafluoro-2-hydroxy-N,N,N-trymethylundecan-1-ammonium iodide in form of color red gel. The yield was 89 %.

^{1}H NMR (CD_3OD): δ = 2.46 (m, CH_2(a), 2H); 4.6 (m, CH(b), 1H); 3.52 (m, CH_2(c,d), 6H); 3.14 (s, CH_3(e), 3H); 4.7 (m, CH(f), 1H); 1.37 (t, CH_3(g), 6H).

^{19}F NMR (CD_3OD): δ = -80.9 (t, CF_3(a), 3F); -111.7 (m, CF_2CH_2(b), 2F); -126.2 (m, CF_2(c), 2F); -123.3 (m, CF_2(d), 2F);-122.8 (m, CF_2(e), 2F);-121.8 (m, CF_2(f), 2F).

Synthesis N,N-dipropylamino-tridecafluoro-2-hydroxy-N,N,N-trymethylundecan-1-ammonium iodide (F_6H_3)

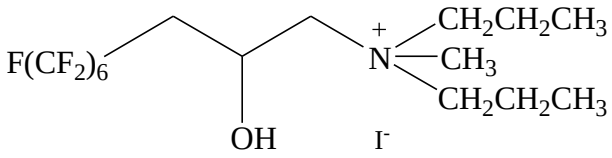

20.0 g (0.03 mol) of 1-dipropylaminotridecafluoroundecan-2-ol and 9.1 g (0.06 mol) of iodomethane were refluxed in acetonitrile at 60 °C for over 24 h. After iodomethane and solvent are removed by evaporation, the residue was washed twice by ether anhydrous et recrystallized several times by mixture of methanol-ether and dried under reduced pressure to give N,N-dipropylamino-tridecafluoro-2-hydroxy-N,N,N-trymethylundecan-1-ammonium iodide in form of color red gel. The yield was 73 %.

^{1}H NMR (CD_3OD): δ = 2.46 (m, CH_2(a), 2H); 4.6 (m, CH(b), 1H); 3.52 (m, CH_2(c,d,e), 10H); 3.14 (s, CH_3(f), 3H); 4.7 (m, CH(g), 1H); 1.37 (t, CH_3(h), 6H).

^{19}F NMR (CD_3OD): δ = -80.9 (t, CF_3(a), 3F); -111.7 (m, CF_2CH_2(b), 2F); -126.2 (m, CF_2(c), 2F); -123.3 (m, CF_2(d), 2F);-122.8 (m, CF_2(e), 2F);-121.8 (m, CF_2(f), 2F).

Synthesis N,N-dibutylamino-tridecafluoro-2-hydroxy-N,N,N-trymethylundecan-1-ammonium iodide (F_6H_4)

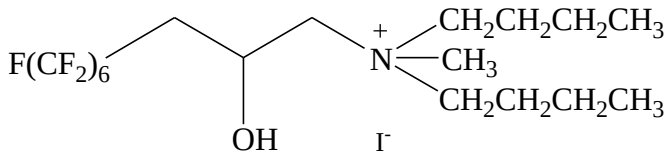

20.0 g (0.03 mol) of 1-dibutylaminotridecafluoroundecan-2-ol and 4.3 g (0.06 mol) of iodomethane were refluxed in acetonitrile at 60 °C for over 24 h. After iodomethane and solvent are removed by evaporation, the residue was washed twice by ether anhydrous et recrystallized several times by mixture of methanol-ether and dried under reduced pressure to give N,N-dibutylamino-tridecafluoro-2-hydroxy-N,N,N-trymethylundecan-1-ammonium iodide in form of color red gel. The yield was 73 %.

^{1}H NMR (CD_3OD): δ = 2.46 (m, CH_2(a), 2H); 4.6 (m, CH(b), 1H); 3.52 (m, CH_2(c,d,e,f), 14H); 3.14 (s, CH_3(g), 3H); 4.7 (m, CH(h), 1H); 1.37 (t, CH_3(i), 6H).

^{19}F NMR (CD_3OD): δ = -80.9 (t, CF_3(a), 3F); -111.7 (m, CF_2CH_2(b), 2F); -126.2 (m, CF_2(c), 2F); -123.3 (m, CF_2(d), 2F);-122.8 (m, CF_2(e), 2F);-121.8 (m, CF_2(f), 2F).

Synthesis N,N-dihexylamino-tridecafluoro-2-hydroxy-N,N,N-trymethylundecan-1-ammonium iodide (F_6H_6)

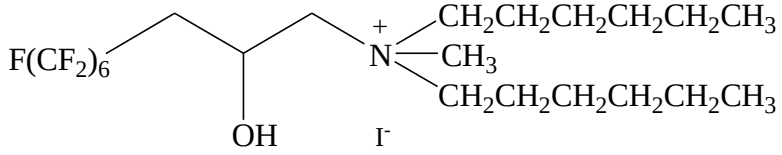

10.0 g (0.014 mol) of 1-dihexylaminotridecafluoroundecan-2-ol and 4.0 g (0.028 mol) of iodomethane were refluxed in acetonitrile at 60 °C for over 24 h. After iodomethane and solvent are removed by evaporation, the residue was washed twice by ether anhydrous et recrystallized several times by mixture of methanol-ether and dried under reduced pressure to give N,N-dihexylamino-tridecafluoro-2-hydroxy-N,N,N-trymethylundecan-1-ammonium iodide in form of color red gel. The yield was 73 %.

^{1}H NMR (CD_3OD): δ = 2.46 (m, CH_2(a), 2H); 4.6 (m, CH(b), 1H); 3.52 (m, CH_2(c,d,e,f,g,h), 22H); 3.14 (s, CH_3(i), 3H); 4.7 (m, CH(l), 1H); 1.37 (t, CH_3(m), 6H).

^{19}F NMR (CD_3OD): δ = -80.9 (t, CF_3(a), 3F); -111.7 (m, CF_2CH_2(b), 2F); -126.2 (m, CF_2(c), 2F); -123.3 (m, CF_2(d), 2F);-122.8 (m, CF_2(e), 2F);-121.8 (m, CF_2(f), 2F).

Synthesis N,N-dioctylamino-tridecafluoro-2-hydroxy-N,N,N-trymethylundecan-1-ammonium iodide (F_6H_8)

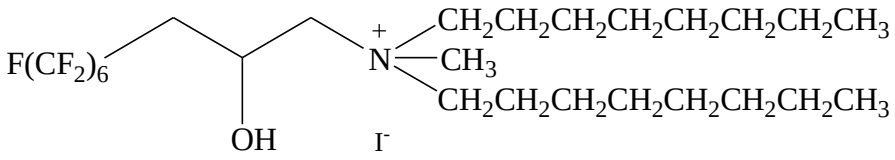

10.0 g (0.016 mol) of 1-dioctylaminoeptadecafluoroundecan-2-ol and 4.6 g (0.032 mol) of iodomethane were refluxed in acetonitrile at 60 °C for over 24 h. After iodomethane and solvent are removed by evaporation, the residue was washed 2 times by ether anhydrous et recrystallized several times by mixture of methanol-ether. Then, the residue was washed several times by petroleum ether. The yellow solid was filtrated and washed with fresh diethyl ether anhydrous and then dried under reduced pressure to give N,N-dibutylamino-tridecafluoro-2-hydroxy-N,N,N-trymethylundecan-1-ammonium iodide in form of white solid. The yield was 83 %.

^{1}H NMR (CD_3OD): δ = 2.46 (m, CH_2(a), 2H); 3.33 (m, CH(b), 1H); 3.40 (m, CH_2(c,d), 6H); 1.27 (t, CH_2(e,f,g,h,i), 20H); 1.70 (m, CH_2 (l), 4H); 0.86 (t, CH_3(m), 6H); 3.14 (m, CH(n), 3H); 4.7 (t, CH_3(o), 1H).

^{19}F NMR (CD_3OD): δ = -80.9 (t, CF_3(a), 3F); -111.7 (m, CF_2CH_2(b), 2F); -126.2 (m, CF_2(c), 2F); -123.3 (m, CF_2(d), 2F);-122.8 (m, CF_2(e), 2F);-121.8 (m, CF_2(f), 2F).

Synthesis N,N-diethylamino-tridecafluoro-2-hydroxy-N,N,N-trymethylundecan-1-ammonium iodide (F_4H_1)

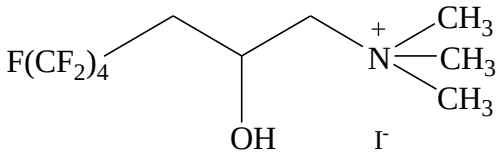

3.0 g (0.009 mol) of 1-dimethylaminononafluoroundecan-2-ol and 2.65 g (0.018 mol) of iodomethane were refluxed in acetonitrile at 60 °C for over 4 h. After iodomethane and solvent are removed by evaporation, the residue was washed twice by ether anhydrous et recrystallized several times by mixture of methanol-ether. The white solid was filtrated and washed with fresh diethyl ether anhydrous and then dried under reduced pressure. The yield was 93 %.

^{1}H NMR (CD_3OD): δ = 2.24 (m, CH_2(a), 2H); 4.6 (m, CH(b), 1H); 3.51 (t, CH_2(c), 2H); 3.26 (m, CH_3(d), 9H); 4.7 (m, OH(e), 1H).

^{19}F NMR (CD_3OD): δ = -80.9 (t, CF_3(a), 3F); -111.7 (m, CF_2CH_2(b), 2F); -126.2 (m, CF_2(c), 2F); -123.3 (m, CF_2(d), 2F).

Synthesis N,N-diethylamino-nonafluoro-2-hydroxy-N,N,N-trymethylundecan-1-ammonium iodide (F_4H_2)

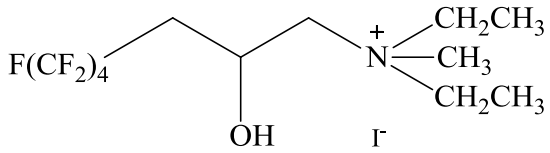

10.0 g (0.028 mol) of 1-diethylaminononadecafluoroundecan-2-ol and 8.1 g (0.057 mol) of iodomethane were refluxed in acetonitrile at 60 °C for over 24 h. After iodomethane and solvent are removed by evaporation, the residue was washed twice by ether anhydrous et recrystallized several times by mixture of methanol-ether. The white solid was filtrated and washed with fresh diethyl ether anhydrous and then dried under reduced pressure. The yield was 73 %.

^{1}H NMR (CD_3OD): δ = 2.46 (m, CH_2(a), 2H); 4.6 (m, CH(b), 1H); 3.52 (m, CH_2(c,d), 6H); 3.14 (s, CH_3(e), 3H); 4.7 (m, CH(f), 1H); 1.37 (t, CH_3(g), 6H).

^{19}F NMR (CD_3OD): δ = -80.9 (t, CF_3(a), 3F); -111.7 (m, CF_2CH_2(b), 2F); -126.2 (m, CF_2(c), 2F); -123.3 (m, CF_2(d), 2F).

Synthesis N,N-propylamino-nonafluoro-2-hydroxy-N,N,N-trymethylundecan-1-ammonium iodide (F_4H_3)

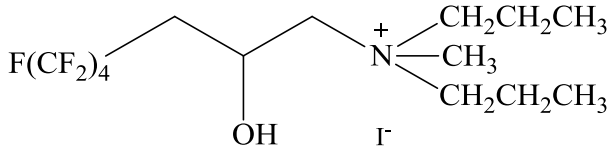

10.0 g (0.026 mol) of 1-dipropylaminoeptadecafluoroundecan-2-ol and 7.5 g (0.052 mol) of iodomethane were refluxed in acetonitrile at 60 °C for over 24 h. After iodomethane and solvent are removed by evaporation, the residue was washed twice by ether anhydrous et recrystallized several times by mixture of methanol-ether. The yellow solid was filtrated and washed with fresh diethyl ether anhydrous and then dried under reduced pressure. The yield was 73 %.

^{1}H NMR (CD_3OD): δ = 2.46 (m, CH_2(a), 2H); 4.6 (m, CH(b), 1H); 3.52 (m, CH_2(c,d,e), 10H); 3.14 (s, CH_3(f), 3H); 4.7 (m, CH(g), 1H); 1.37 (t, CH_3(h), 6H).

^{19}F NMR (CD_3OD): δ = -80.9 (t, CF_3(a), 3F); -111.7 (m, CF_2CH_2(b), 2F); -126.2 (m, CF_2(c), 2F); -123.3 (m, CF_2(d), 2F).

Synthesis N,N-dibutylamino-nonafluoro-2-hydroxy-N,N,N-trymethylundecan-1-ammonium iodide (F_4H_4)

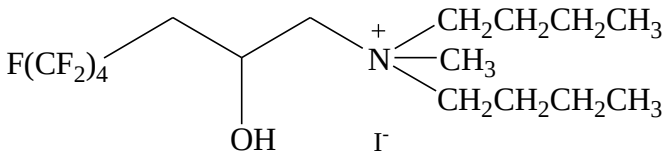

10.0 g (0.024 mol) of 1-dibutylaminononafluoroundecan-2-ol and 7.0 g (0.048 mol) of iodomethane were refluxed in acetonitrile at 60 °C for over 24 h. After iodomethane and solvent are removed by evaporation, the residue was washed twice by ether anhydrous et recrystallized several times by mixture of methanol-ether. The yellow solid was filtrated and washed with fresh ether petroleum and then dried under reduced pressure.

The yield was 73 %.

^{1}H NMR (CD_3OD): δ = 2.46 (m, CH_2(a), 2H); 4.6 (m, CH(b), 1H); 3.52 (m, CH_2(c,d,e,f), 14H); 3.14 (s, CH_3(g), 3H); 4.7 (m, CH(h), 1H); 1.37 (t, CH_3(i), 6H).

^{19}F NMR (CD_3OD): δ = -80.9 (t, CF_3(a), 3F); -111.7 (m, CF_2CH_2(b), 2F); -126.2 (m, CF_2(c), 2F); -123.3 (m, CF_2(d), 2F).

Synthesis N,N-dihexylamino-tnonafluoro-2-hydroxy-N,N,N-trymethylundecan-1-ammonium iodide (F_4H_6)

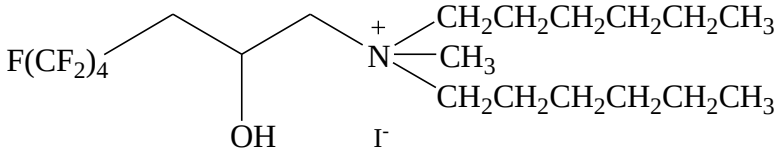

10.0 g (0.021 mol) of 1-dihexylaminononafluoroundecan-2-ol and 6.1 g (0.042 mol) of iodomethane were refluxed in acetonitrile at 60 °C for over 24 h. After iodomethane and solvent are removed by evaporation, the residue was washed twice by ether anhydrous et recrystallized several times by mixture of methanol-ether and dried under reduced pressure to give N,N-dihexylmino-nonafluoro-2-hydroxy-N,N,N-trymethylundecan-1-ammonium iodide in form of color red gel. The yield was 73 %.

^{1}H NMR (CD_3OD): δ = 2.46 (m, CH_2(a), 2H); 3.34 (m, CH(b), 1H); 3.52 (m, CH_2(c,d,e,f,g,h), 22H); 3.14 (s, CH_3(i), 3H); 4.7 (m, CH(l), 1H); 1.37 (t, CH_3(m), 6H).

^{19}F NMR (CD_3OD): δ = -80.9 (t, CF_3(a), 3F); -111.7 (m, CF_2CH_2(b), 2F); -126.2 (m, CF_2(c), 2F); -123.3 (m, CF_2(d), 2F).

Synthesis N,N-octylamino-nonafluoro-2-hydroxy-N,N,N-trymethylundecan-1-ammonium iodide (F_4H_8)

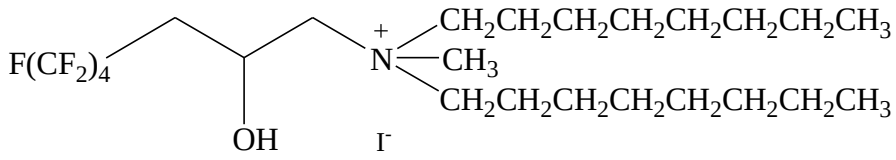

5.0 g (0.009 mol) of 1-dioctylaminononafluoroundecan-2-ol and 2.7 g (0.019 mol) of iodomethane were refluxed in acetonitrile at 60 °C for over 24 h. After iodomethane and solvent are removed by evaporation, the residue was washed twice by ether anhydrous et recrystallized several times by mixture of methanol-ether and dried under reduced pressure to give N,N-dioctylamino-nonafluoro-2-hydroxy-N,N,N-trymethylundecan-1-ammonium iodide in form of color red gel. The yield was 73 %.

^{1}H NMR (CD_3OD): δ = 2.46 (m, CH_2(a), 2H); 3.34 (m, CH(b), 1H); 3.40 (m, CH_2(c,d), 6H); 1.27 (t, CH_2(e,f,g,h,i), 20H); 1.70 (m, CH_2 (l), 4H); 0.86 (t, CH_3(m), 6H); 3.14 (m, CH(n), 3H); 4.7 (t, CH_3(o), 1H).

^{19}F NMR (CD_3OD): δ = -80.9 (t, CF_3(a), 3F); -111.7 (m, CF_2CH_2(b), 2F); -126.2 (m, CF_2(c), 2F); -123.3 (m, CF_2(d), 2F).

7 Experimental section 2

The second group of quaternary ammonium salts is characterized using the variation of fluorinated and hydrocarbon chains and a constant alkylating agent with the same number of carbon of hydrocarbon moiety (iodomethane and iodoethane). Then, counter-ion iodide was change in bromide to analysis its influence on the physico-chemical properties.

The preparation of the second group of synthetic perfluoroalkyl quaternary ammonium salts was performed following to the two-step reaction reported in Scheme 12. It was used the tertiary ammines obtained in the first step of the Scheme 1. Intermediates were subsequently reacted (Step 2) with iodomethane or iodoethane, alkylating agents, in acetonitrile at 60 °C, obtaining the corresponding 3 quaternary ammonium salts (F_nH_mI).

Therefore, they were passed throw a column Amberlite IRA96 (anion exchange resin Br- form) to ion exchange to obtaining the corresponding quaternary ammonium salts (F_nH_mBr) (step 3).

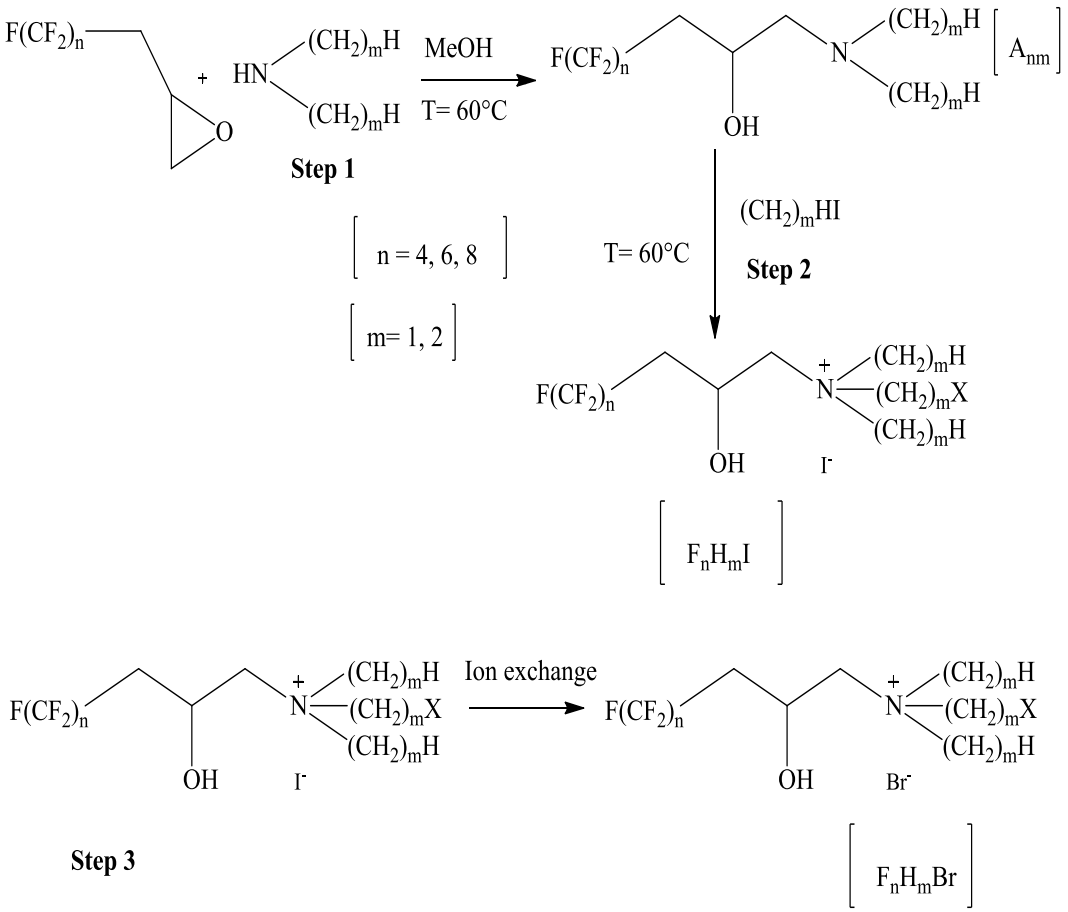

Scheme 12 synthesis of fluorinated quaternary salts F_nH_mX

Synthesis N,N-diethylamino-eptadecafluoro-2-hydroxy-N,N,N-tryethylundecan-1-ammonium iodide (F_8H_2I).

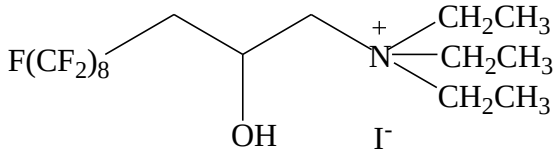

4.0 g (0.007 mol) of 1-diethylaminoeptadecafluoroundecan-2-ol and 10.2 g (0.021 mol) of iodoethane were refluxed in 10 mL of acetonitrile at 60 °C for over 24 h. After iodoethane and solvent are removed by evaporation, the residue was washed several times by diethyl-ether and recrystallized several times by mixture of methanol-ether and dried under reduced pressure to give N,N-ethylamino-eptadecafluoro-2-hydroxy-N,N,N-tryethylundecan-1-ammonium iodide in form of white solid. The yield was 84 %.

^{1}H NMR (CD_3OD): δ = 2.57 (m, CH_2(a), 2H); 3.62 (m, CH(b), 1H); 3.31 (s, CH_2 (c,), 1H); 3.24 (s, CH_2 (c), 1H); 3.62 (m, CH_2(d), 6H); 1.36 (t, CH_3(e), 9H); 4.80 (m, OH (f), 1H).

^{19}F NMR (CD_3OD): δ = -80.9 (t, CF_3(a), 3F); -111.7 (m, CF_2CH_2(b), 2F); -126.2 (m, CF_2(c), 2F); -123.3 (m, CF_2(d), 2F);-122.8 (m, CF_2(e), 2F);-121.9 (m, CF_2(f), 2F); -121.6 (m, CF_2(g,h), 4F).

Synthesis N,N-diethylamino-tridecafluoro-2-hydroxy-N,N,N-tryethylundecan-1-ammonium iodide (F_6H_2I).

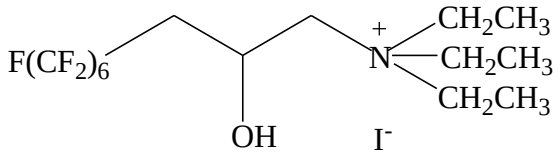

10.0 g (0.022 mol) of 1-diethylaminotridecafluoroundecan-2-ol and 10.2 g (0.066 mol) of iodoethane were refluxed in 10 mL of acetonitrile at 60 °C for over 24 h. After iodoethane and solvent are removed by evaporation, the residue was washed several times by diethyl ether and recrystallized several times by mixture of methanol-ether and dried under reduced pressure to give N,N-ethylamino-tridecafluoro-2-hydroxy-N,N,N-tryethylundecan-1-ammonium iodide in form of white solid. The yield was 79 %.

^{1}H NMR (CD_3OD): δ = 2.57 (m, CH_2(a), 2H); 3.62 (m, CH(b), 1H); 3.31 (s, CH_2 (c,), 1H); 3.24 (s, CH_2 (c), 1H); 3.62 (m, CH_2(d), 6H); 1.36 (t, CH_3(e), 9H); 4.80 (m, OH (f), 1H).

^{19}F NMR (CD_3OD): δ = -80.9 (t, CF_3(a), 3F); -111.7 (m, CF_2CH_2(b), 2F); -126.2 (m, CF_2(c), 2F); -123.3 (m, CF_2(d), 2F);-122.8 (m, CF_2(e), 2F);-121.8 (m, CF_2(f), 2F).

Synthesis N,N-diethylamino-nonafluoro-2-hydroxy-N,N,N-tryethylundecan-1-ammonium iodide (F_4H_2I).

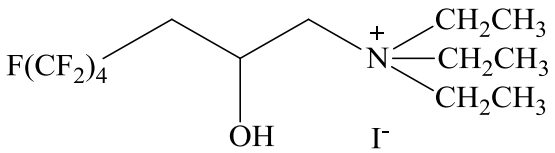

5.0 g (0.014 mol) of 1-diethylnonafluoroundecan-2-ol and 6.5 g (0.042mol) of iodoethane were refluxed in 10 mL of acetonitrile at 60 °C for over 24 h. After iodoethane and solvent are removed by evaporation, the residue was washed several times by diethyl ether and recrystallized several times by mixture of methanol-ether and dried under reduced pressure to give N,N-ethylamino-nonafluoro-2-hydroxy-N,N,N-tryethylundecan-1-ammonium iodide in form of yellow solid. The yield was 78 %.

^{1}H NMR (CD_3OD): δ = 2.57 (m, CH_2(a), 2H); 3.62 (m, CH(b), 1H); 3.31 (s, CH_2 (c,), 1H); 3.24 (s, CH_2 (c), 1H); 3.62 (m, CH_2(d), 6H); 1.36 (t, CH_3(e), 9H); 4.80 (m, OH (f), 1H).

^{19}F NMR (CD_3OD): δ = -80.9 (t, CF_3(a), 3F); -111.7 (m, CF_2CH_2(b), 2F); -126.2 (m, CF_2(c), 2F); -123.3 (m, CF_2(d), 2F).

7.1 Preparation of column ion exchange

Solution (50 : 50) methanol-water was introduced through Amberlite IRA96. Therefore, it was performed a regeneration of column with carbonate sodium. The column was washed several times with a solution of methanol-water (50 : 50) to neuter pH. Then, it was washed by concentrate water solution of NaBr. The pH was resulted basic if there was a good ion exchange. Then, it was washed by water solution of NaBr to neuter pH. Finally, it was washed by methanol water solution (50 : 50) [227].

Ion ExchangeF_8H_1Br

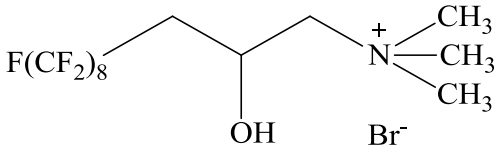

2 g of F_8H_1I, obtained as reported in Scheme 11, was dissolved in methanol and passed through a column of Amberlite IRA96 (anion exchange resin, Br form, 50 - 100 mesh) as reported. After the eluted solution was evaporated under reduced pressure, the residue was recrystallized from diethyl-ether and dried under reduced pressure, yielding 1.8 g (F_nH_1Br) in form of white solid.

Ion Exchange F_6H_1Br

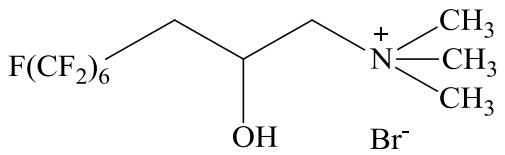

1.5 g of F_6H_1I, obtained as reported in Scheme 11, was dissolved in methanol and passed through a column of Amberlite IRA96 (anion exchange resin, Br form, 50 - 100 mesh) as reported. After the eluted solution was evaporated under reduced pressure, the residue was recrystallized from diethyl ether and dried under reduced pressure, yielding 1.45 g (F_nH_1Br) in form of white solid.

Ion Exchange F_4H_1Br

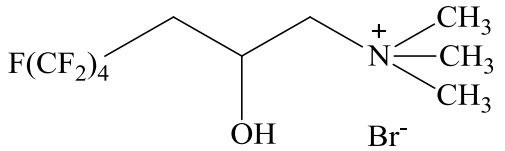

1.5 g of F_4H_1I, obtained as reported in Scheme 11, was dissolved in methanol and passed through a column of Amberlite IRA96 (anion exchange resin, Br form, 50 - 100 mesh) as reported. After the eluted solution was evaporated under reduced pressure, the residue was recrystallized from diethyl ether and dried under reduced pressure, yielding 1.45 g (F_4H_1Br) in form of white solid.

Ion Exchange F_8H_2Br

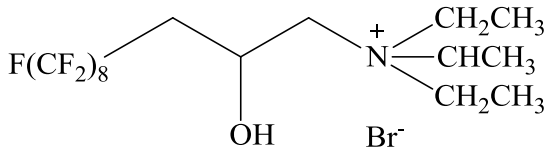

1.5 g of F_8H_2I was dissolved in methanol and passed through a column of Amberlite IRA96 (anion exchange resin, Br form, 50 - 100 mesh). After the eluted solution was evaporated under reduced pressure, the residue was recrystallized from diethyl ether and dried under reduced pressure, yielding 1.4 g (F_8H_2Br) in form of white solids.

Ion Exchange F_6H_2Br

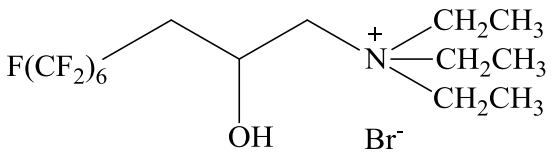

1.5 g of F_6H_2I was dissolved in methanol and passed through a column of Amberlite IRA96 (anion exchange resin, Br form, 50 - 100 mesh). After the eluted solution was evaporated under reduced pressure, the residue was recrystallized from diethyl ether and dried under reduced pressure, yielding 1.4 g (F_6H_2Br) in form of white solid.

Ion Exchange F_4H_2Br

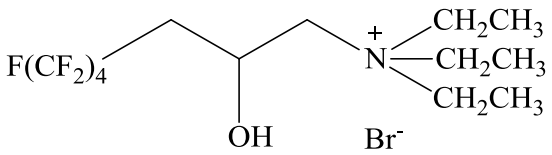

1.5 g of F_4H_2I was dissolved in methanol and passed through a column of Amberlite IRA96 (anion exchange resin, Br form, 50 - 100 mesh). After the eluted solution was evaporated under reduced pressure, the residue was recrystallized from diethyl ether and dried under reduced pressure, yielding 1.4 g (F_4H_2Br) in the form of white solid.

8 Physico-chemical characterization

8.1 Introduction

Surfactants are among the most versatile products of the chemical industry, appearing in several industrial application such as motor oils, pharmaceutical, detergency, petroleum recovery, electronic printing, magnetic recording, biotechnology, etc.

In cationic fluorinated surfactants the fluorinated hydrophobic part is attached directly to a quaternary ammonium group, a protonated amino group. Cationic surfactants dissociate in water, forming a surface-active positively charged ion and a negatively charged counter-ion.

The physical, chemical, and electrical properties of matter confined to phase boundaries are often profoundly different from those of the same matter in bulk.

The amphipathic structure, consisting of a structural group that has very little attraction for the solvent (lyophobic group) and a group that has strong attraction for the solvent (lyophilic group), determines a distortion of the structure of the solvent (in particular of the water), increasing the free energy of the system. The system responds in order to minimize the contact between the lyophobic group and the solvent: in surfactant dissolved in water the lyophobic/hydrophobic group distorts the structure of the water breaking hydrogen bonds between water molecules and structuring the water in the vicinity of hydrogen group.

As a result of this distortion, some surfactant molecules are expelled to the interfaces of the system, with their hydrophobic groups oriented so as to minimize contact with the water molecules. They also concentrate them at the surface, orienting themselves so that their hydrophobic groups are directed away from the solvent to minimize the free energy of the solution.

Therefore, the amphipathic structure of the surfactant causes not only concentration of the surfactant at the surface and reduction of the surface tension of the water, but also orientation of the molecule at the surface with its hydrophilic group in the aqueous phase and its hydrophobic group oriented away from it.

However, there is another mean of minimizing the free energy in these systems. The distortion of the solvent structure can also be decreased (and the free energy of the solution reduced) by the aggregation of the surface-active molecules into clusters (micelles) with their hydrophobic groups directed toward the interior of the cluster and their hydrophilic groups directed toward the solvent. Micellization is also an alternative mechanism to adsorption at the interfaces for removing hydrophobic groups from contact with the water,

thereby reducing the free energy of the system. When there is little distortion of the structure of the solvent by the lyophobic group (e.g., in water, when the hydrophobic group of the surfactant is short), then, there is a little tendency for micellization to occur.

Although removal of the lyophobic group from contact with the solvent may result in a decrease in the free energy of the system, the surfactant molecules, in transferring the molecules from solution in the solvent, may experience some loss of freedom in being confined to the micelle or from electrostatic repulsions of other similarly charged surfactant molecules in the micelle (in the case of ionic surfactants). These forces increase the free energy of the system and thus oppose micellization. Whether micellization occurs in a particular case and, if so, at what concentration of monomeric surfactant, therefore depends on the balance between the factors promoting micellization and those opposing it.

The study of physico-chemical properties is important to understand how surfactants function and to select a surfactant for a specific purpose.

Hence, in order to investigate the influence of

- effects of the hydrophobic group
- increase in the length of the hydrophobic groups
- the introduction of branching of different chain length
- counter-ion

on physico-chemical properties, some measurements carried out.

For the first group (F_nH_m) of surfactants synthesized

- surface tension (γ), surface excess (Γ), area per molecule (A)
- concentration micelle critic (cmc), ΔG^0_{ads}, ΔG^0_{mic}
- temperature of Krafft (T_K)
- micellar structure and shape
- antimicrobial activity

were investigated as function of fluorinated and alkyl chains.

Then, the capacity of some surfactants (F_8H_1 and F_8H_2) to form an hydrogel in aqueous medium leaded to investigate the rheological properties as function of some physico-chemical parameters including concentration, temperature, viscosity, strain and frequency.

8.1.1 Physico-chemical characterization of F_nH_mX

For the second group of surfactants synthesized (F_nH_mX)

- surface tension (γ), surface excess (Γ), area per molecule (A)
- concentration micelle critic (cmc),
- antimicrobial activity

were studied in order to investigate the role of counter-ion.

8.2 Surface tension

8.2.1 Wilhelmy plate method

The surface tensions of the aqueous solutions of the fluorinated surfactants were measured using a Kruss K100 tensiometer by the Wilhelmy plate technique. The apparatus is an electrobalance with a computer-controlled lifting system.

A thin plate made from platinum foil is either detached from the interface (non-equilibrium condition) or its weight is measured statically using an accurate microbalance. In the detachment method, the total force F_T is given by the weight of the plate W and the interfacial tension force,

$$F_T = W + \gamma p \qquad 4$$

where p is the ‘‘contact length’’ of the plate with the liquid, i.e., the plate perimeter. When the contact angle of the liquid is zero, no correction is required. The static technique may be applied to follow the interfacial tension as a function of time (to follow the kinetics of adsorption) till equilibrium is reached. In this case, the plate is suspended from one arm of a microbalance and allowed to penetrate the upper liquid layer (usually the oil) until it touches the interface, or alternatively the whole vessel containing the two liquid layers is raised until the interface touches the plate. The increase in weight ΔW is given by the following equation (eq. 5),

$$\Delta W = \gamma p \cos \vartheta \qquad 5$$

where ϑ is the contact angle. If the plate is completely wetted by the lower liquid as it penetrates, $\vartheta = 0$ and γ may be calculated directly from ΔW. Care should always be taken

that the plate is completely wetted by the aqueous solution. For that purpose, a roughened platinum plate is used to ensure a zero contact angle.

However, if the oil is denser than water, a hydrophobic plate is used so that when the plate penetrates through the upper aqueous layer and touches the interface it is completely wetted by the oil phase.

8.2.2 Procedure

The measurements were carried out by wisystematically adding a concentrated surfactant solution to water. Some partially fluorinated quaternary ammonium salts show a bad water solubility in water and for these case, a 10 % methanol aqueous solution was used. It was demonstrated that the surface tension varies only slightly with 10 % of methanol in water [228].

All of the measurements were performed at 25 °C.

8.2.3 Results F_nH_m

Figure 31 shows the curves of surface tension as function of the logarithm ofconcentration of F_nH_m for n= 4, 6, and 8, m=1, 2, 3, 4, 6, and 8. The surface tension values at the cmc (γ_{cmc}) are summarized in Table 2.

Figure 32 shows the curve of surface tension as a function of carbon's number in fluorinated chain for the surfactants F_nH_m synthesized.

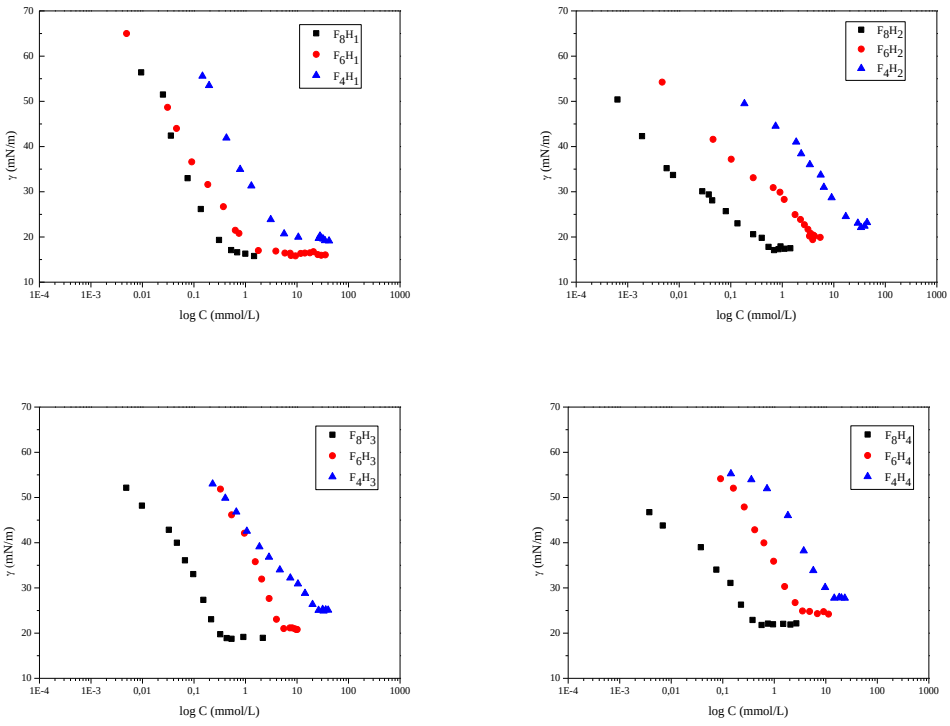

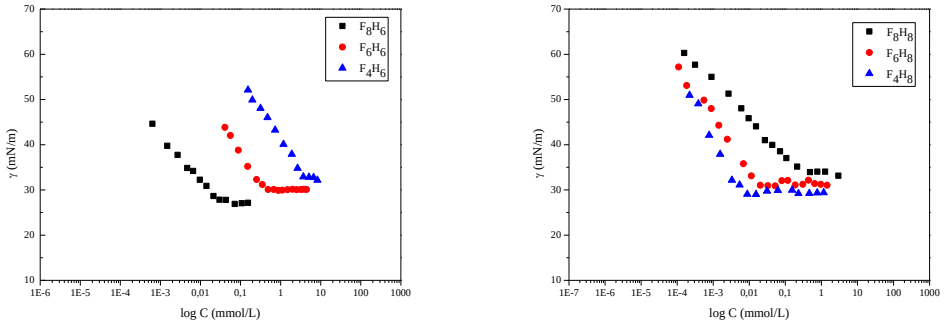

Figure 31: Surface tension as function of the concentration of F_nH_m for n= 4, 6, and 8, m=1, 2, 3, 4, 6, and 8

The effectiveness of reducing the surface tension for the fluorinated surfactants is significantly greater than that for the hydrocarbon surfactants; this is attributed to the presence of fluorocarbon chain in the molecule, which makes a positive contribution to the adsorption at the air/water interface.

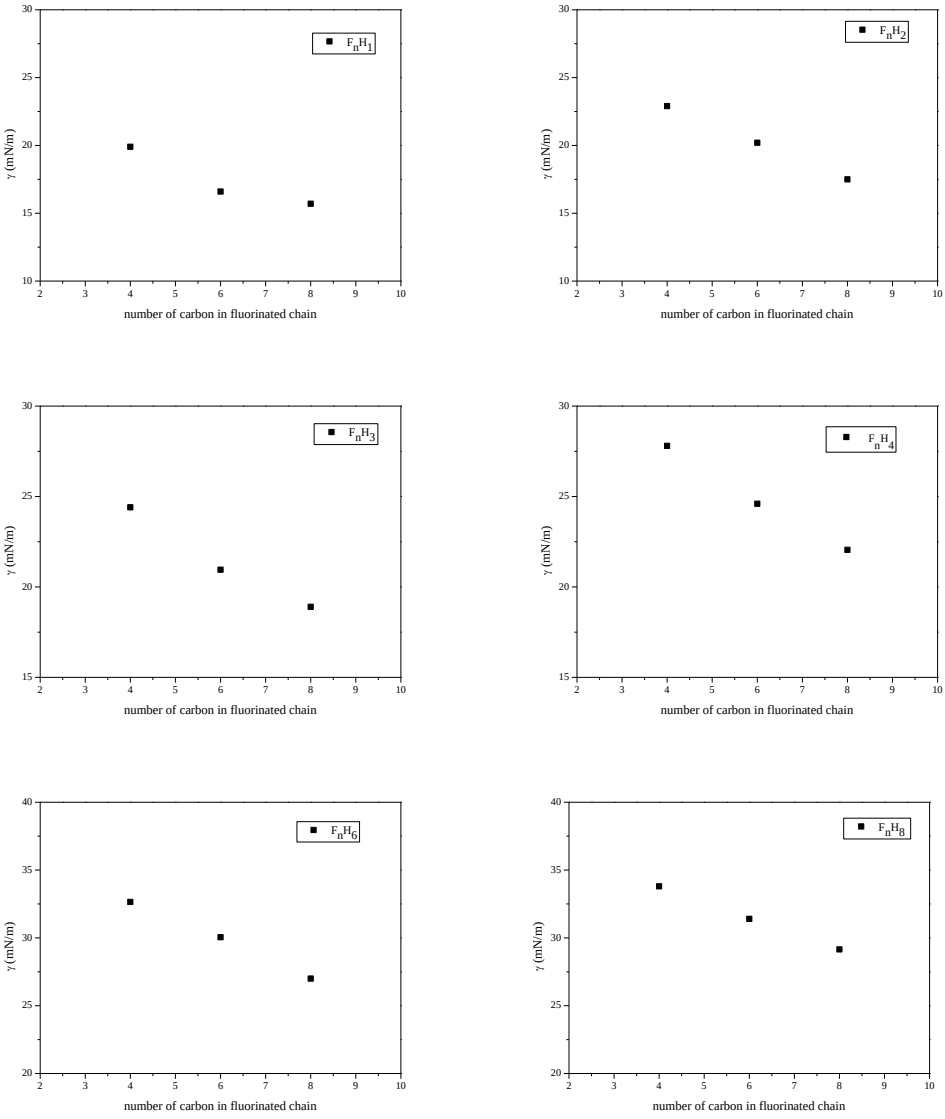

Figure 32: surface tension as a function of carbon's number in fluorinated chain of F_nH_m

The observed trend in the surface tension shows that with decreasing of fluorocarbon chain length the surfactant becomes less surface active. Figure 33 shows the values of surface tension as function of alkyl chain of F_nH_m. The observed trend in the surface tension shows that with increasing of alkyl chain length, the surfactant becomes less surface active. Therefore, the fluorocarbon chain enhances the amphiphilic character of the surfactants and increases the surface activity. However, the efficiency of the fluorinated surfactant in terms of surface tension reduction increases with fluorinated chain length. Also, the hydrocarbon chain enhances the hydrophobicity of surfactant but without to contribute on the reduction of surface tension.

Replacement of the usual hydrocarbon-based hydrophobic group by a fluorocarbon-based hydrophobic group appears to provide only a small increase in the effectiveness of adsorption at the aqueous solution–air interface, in contrast to its large effect on most other interfacial properties.

When the number of carbon atoms in a hydrocarbon branched group increases, at either the aqueous solution hydrocarbon interface, a significant decrease in the effectiveness of adsorption occurs, which can be attributed to coiling of the long chain, with a consequent increase in the cross–sectional area of the molecule at the interface.

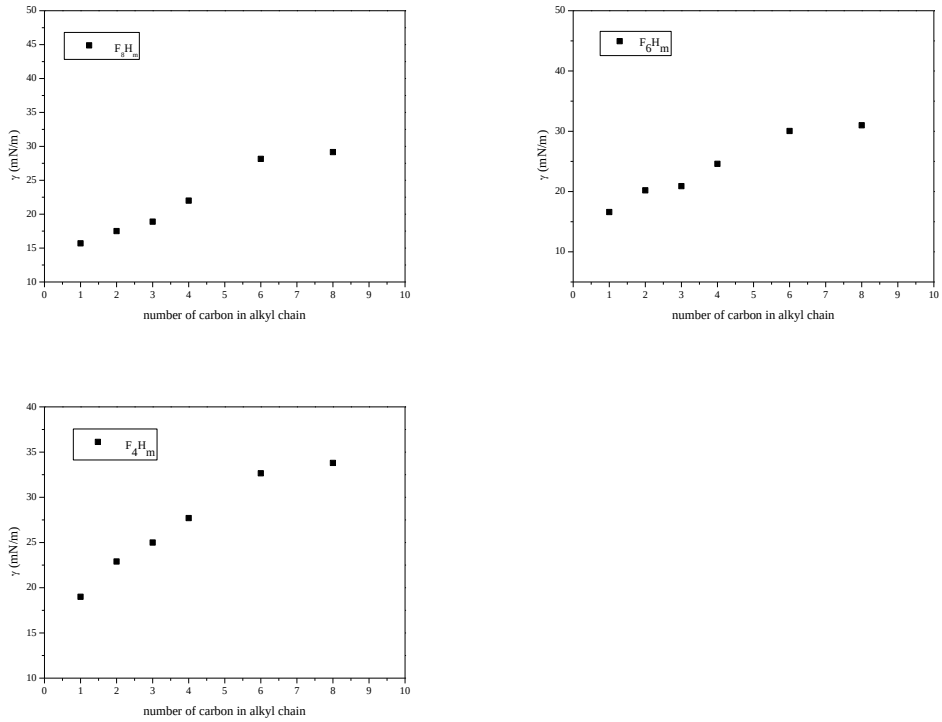

Figure 33: surfaces tension as function of alkyl chain of F_nH_m

8.3 Surface excess (Γ), Surface pressure (π), Area per molecule (A)

By the slope of surface tension curves as function of concentration the surface excess (Γ) was calculated.

The surface excess concentration at surface saturation Γ_m is a useful measure of the effectiveness of adsorption of the surfactant at the L / G or L / L interface, since it is the maximum value that adsorption can attain. The effectiveness of adsorption is an important factor in determining such properties of the surfactant as foaming, wetting, and emulsification, since tightly packed, coherent interfacial films have very different interfacial properties than loosely packed, non coherent films. It is apparent that the hydrophobic chains of surfactants adsorbed at the aqueous solution–air or aqueous solution hydrocarbon interfaces are generally not in the close-packed arrangement normal to the interface at saturation adsorption.

The adsorbed amount of a surfactant (Γ) can be calculated according to the Gibbs adsorption equation 6 [229]:

$$\Gamma = -\frac{1}{4.606\ \mathrm{RT}}\left(\frac{\partial\gamma}{\partial \log \mathrm{C}}\right)_{\mathrm{T}} \qquad 6$$

For surfactants with a single hydrophilic group, either ionic and nonionic, the area occupied by a surfactant molecule at the surface appears to be determined by the area occupied by the hydrated hydrophilic group rather than by the hydrophobic group. The area occupied by a surfactant molecule (A_{cmc}) at the air/water interface (in squareangstroms) is obtained from the value of saturation adsorption at the cmc by using the expression (eq. 7):

$$\mathrm{A}_{cmc} = \frac{1}{\mathrm{N}\Gamma_{\mathrm{cmc}}} \qquad 7$$

where N is Avogadro's number. The greater effectiveness of adsorption means that the area occupied by a surfactant molecule becomes smaller.

The area per molecule (A_{cmc}) at the interface provides information on the degree of packing and the orientation of the adsorbed surfactant molecule when compared with the dimensions of the molecule as obtained by using of molecular models.

8.3.1 Results F_nH_m

Furthermore, the Γ_{cmc} and A_{cmc} values of the partially fluorinated surfactants F_nH_m are listed in Table 10. It observed that greater is effectiveness of adsorption, smaller is the area occupied by the surfactant molecules.

The A_{cmc} values for the fluorinated surfactants obtained are close to the values for three times the molecular area of the fluorinated monomeric surfactants (0.41 - 0.55 nm^2 per molecule). In addition, the A_{cmc} values of F_nH_m are also greater to those of the corresponding quaternary ammonium salt hydrocarbon surfactants with indicating that the adsorption at the air/ water interface is dependent of the nature of hydrophobic chains .

The branching of the alkyl chain results in an increase in the area per molecule at the liquid/air interface probably due to the strong interaction of the alkyl chains.

Figure 34 shows the increase of area per molecule as function of hydrocarbon chain for F_8H_m, F_6H_m, F_4H_m. The reduction in the area values with the decreasing of fluorinated chain length is explained by the chain localization changes at the interface as a result of the intramolecular head group distance decrease.

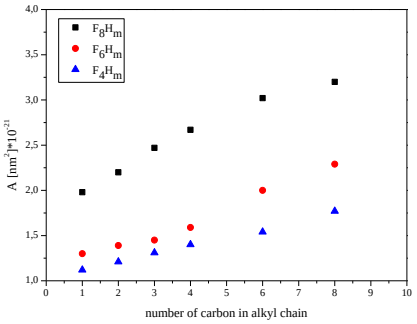

Figure 34: area per molecule as function of hydrocarbon chain

Table 10: surface tension (γ), surface excess (Γ), area per molecule (A) and surface pressure (π) of F_nH_m

surfactants	γ_{cmc} [mN/m]	Γ_{cmc} [mol/m^2]	A_{cmc} [nm^2]10^{-21}	π [mN/m]
F_8H_1	15.7	8.40E-04	1.98	56.9
F_8H_2	17.5	7.56E-04	2.20	55.1
F_8H_3	18.9	6.72E-04	2.47	53.7
F_8H_4	22	6.22E-04	2.67	50.6
F_8H_6	28.15	5.50E-04	3.02	44.45
F_8H_8	29.15	5.19E-04	3.20	43.45
F_6H_1	16.6	1.28E-03	1.30	56
F_6H_2	20.2	1.20E-03	1.39	52.4
F_6H_3	20.9	1.14E-03	1.45	51.7
F_6H_4	24.6	1.04E-03	1.59	48
F_6H_6	30.05	8.29E-04	2.00	42.55
F_6H_8	31	7.25E-04	2.29	41.6
F_4H_1	19	1.47E-03	1.12	52.7
F_4H_2	22.9	1.36E-03	1.21	49.7
F_4H_3	25	1.27E-03	1.31	47.6
F_4H_4	27.7	1.19E-03	1.40	44.8
F_4H_6	32.65	1.07E-03	1.54	39.95
F_4H_8	33.8	9.40E-04	1.77	38.8

8.3.2 Results F_nH_mX

Figure 35 shows the curves of surface tension as function of the concentration of F_nH_mX for n= 4, 6, and 8, m= 1, 2, and X= I, Br. Figure 36 shows the curve of surface tension as function of carbon's number in fluorinated chain.

The surface tension (γ_{cmc}), the Γ_{cmc} and A_{cmc} values at the cmc are summarized in Table 11.

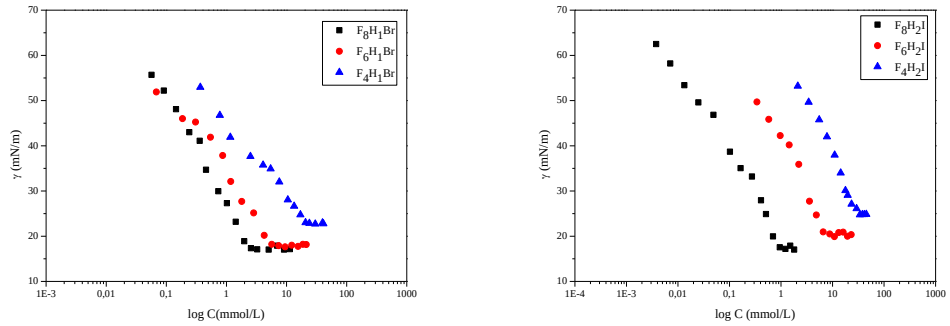

Figure 35: surface tension as function of the concentration of F_nH_mX

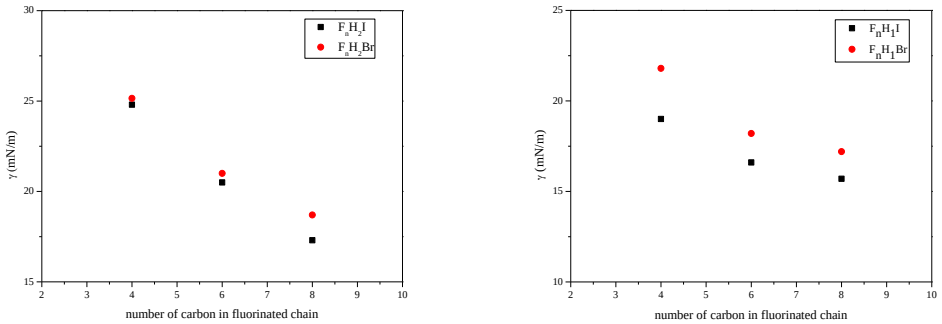

Figure 36: surface tension as function of carbon's number in fluorinated chain of F_nH_mX

As the previous group (F_nH_m) the increase of fluorinated chain leads to an increase of surfactants properties. Then, the increase of alkyl chain, in particular the branching of molecule, increases the solubility of surfactant but decreases his effectiveness.

The observed trend (shown in Figure 36) in the surface tension shows that the change of bromide by iodide causes a decrease of the surface tension values in comparison with the values of the same fluorocarbon and hydrocarbon chain lengths. The steric hindrance of the iodide counter-ion enhances the hydrophobicity of molecule F_nH_mI leading to a decrease of the surface tension value.

The iodide counter-ion increases slowly the value of the area per molecule (A) and the value of surface pressure π, probably due to the stronger interactions of F_nH_mI than to the molecules with bromide as counter-ion, leading to an enhance of surface properties.

Table 11: surface tension (γ), surface excess (Γ), area per molecule (A) and surface pressure (π), cmc of F_nH_mX

surfactants	γ_{cmc} [mN/m]	Γ_{cmc} [mol/m^2]	A_{cmc} [nm^2]10^{-21}	π [mN/m]	cmc [mol/L]
F_8H_1I[a]	15.7	8.40E-04	1.98	56.9	2.00E-04
F_6H_1I[a]	16.6	1.28E-03	1.30	56.0	7.00E-04
F_4H_1I[a]	19	1.47E-03	1.12	52.7	3.00E-03
F_8H_1Br	17.2	1.21E-03	1.37	55.4	2.1E-03
F_6H_1Br	18	1.40E-03	1.18	54.6	4.77E-03
F_4H_1Br	22.8	1.81E-03	0.916	49.8	1.93E-02
F_8H_2I	17.3	1.61E-03	1.03	55.3	7.74E-04
F_6H_2I	20.5	2.49E-03	1.02	52.1	6.13E-03
F_4H_2I	24.80	1.83E-03	0.909	47.8	2.92E-02
F_8H_2Br	18.7	1.99E-03	0.833	53.9	1.02E-03
F_6H_2Br	21	3.22E-03	0.516	51.6	6.37E-03
F_4H_2Br	25.15	1.86E-03	0.895	47.45	3.08E-02

[a] These values are obtained by the first group of surfactants synthesized and they are reported here to a better visualization of results in comparison with the others.

8.4 Critical micelle critic (cmc)

The values of the cmc for the surfactants synthesized were obtained by break points of the surface tension as function of concentration of obtained as shown in Figure 35.

8.4.1 Results F_nH_m

The values of cmc are summarized in Table 12.

Figure 37 shows the plot of the number of carbon atoms in the fluorocarbon chain against the logarithm of the cmc of the fluorinated surfactants F_nH_m.

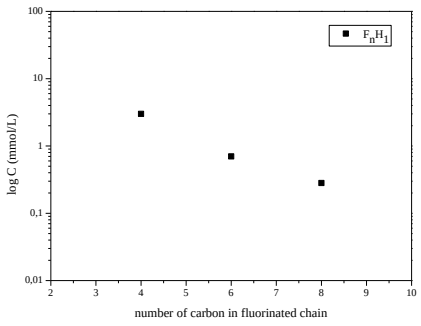

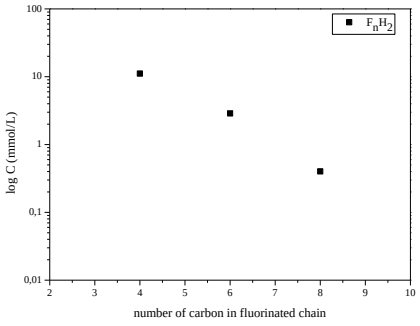

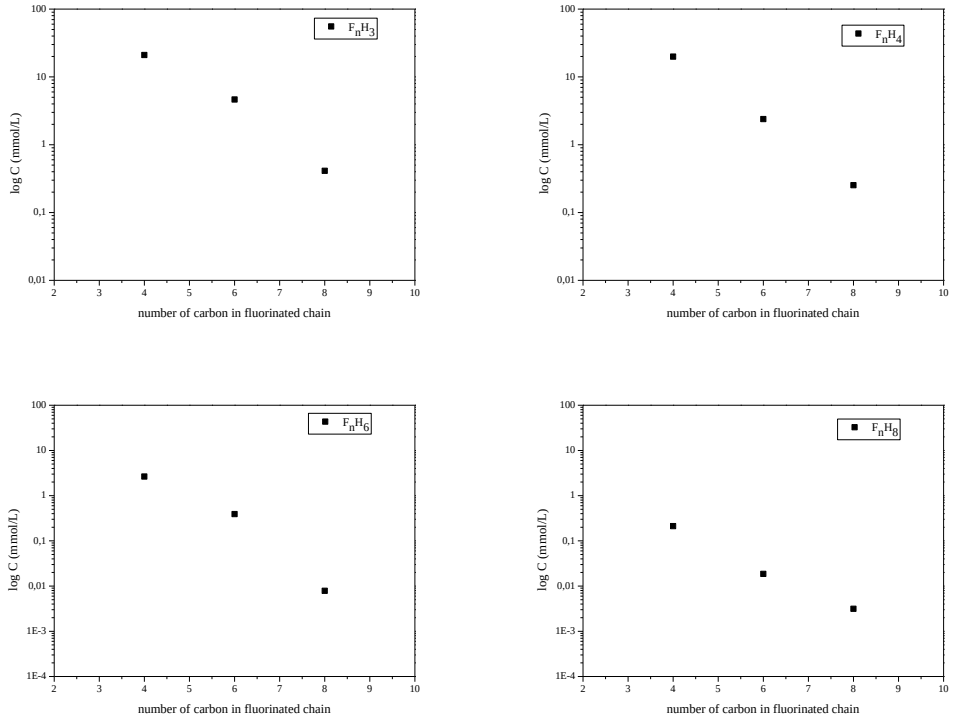

Figure 37: number of carbon atoms in the fluorocarbon chain against the logarithm of the cmc

The cmc of partially fluorinated surfactants decreases exponentially with increasing of the number of carbon atoms, according to the empirical equation of Klevens reported in the paragraph 3.1 of chapter 2. This equation is based on the assumption that the *N* value is equal to the sum of carbons in hydrophobic chain. In this case, there are n carbons in the fluorocarbon chain plus 3 carbon lengths in the 2-hydroxypropyl chain. The values of A and B are -0.54 and 0.29 respectively. They are constant for the particular ionic head at a given temperature.

Figure 38 shows the values of log (cmc) for F_nH_m with n= 4, 6, 8 and m= 1, 2, 3, 4, 6, 8 as function of number of carbon in alkyl chain.

The value of cmc increases as increasing of number of carbon in alkyl chain to reach a maximum; the long hydrocarbon chains contribute to decrease the value of cmc.

A short chain (< 2 carbons) or a long-chain (> 6 carbons) alkyl substituent reduces the efficiency of the surfactant, although the effect on effectiveness is small than the fluorinated chain. Alkyl groups of a length in the range of 2 - 4 carbon atoms give almost the same value of cmc.

When the hydrophilic group is branched, the carbon atoms on the branches appear to have about one-half the effect of carbon atoms on a fluorinated chain.

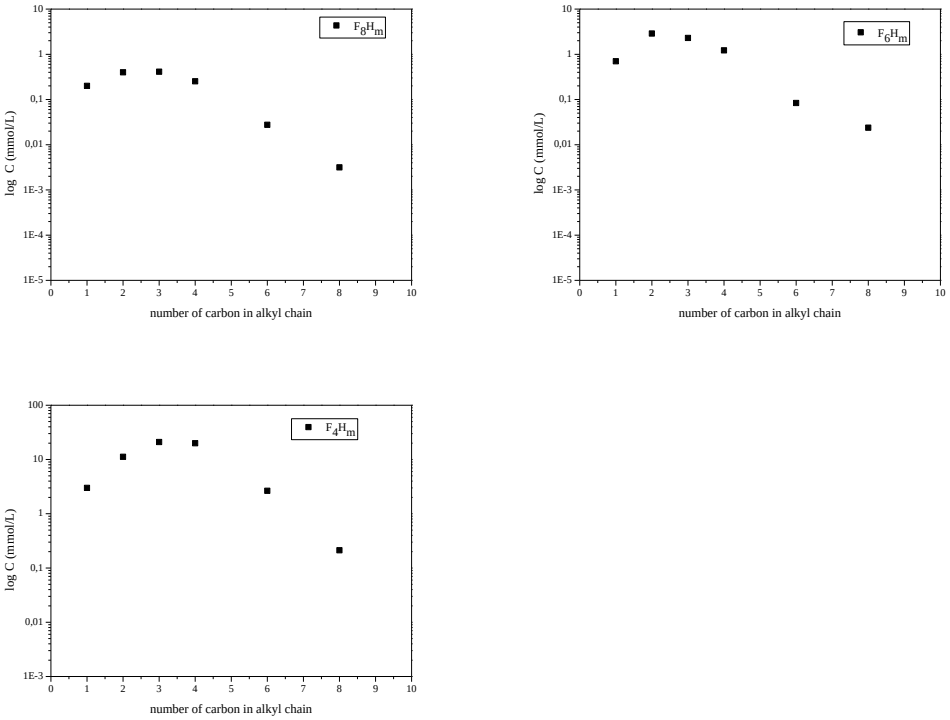

Figure 38: Values of log (cmc) for F_nH_m with n= 4, 6, 8 and m= 1, 2, 3, 4, 6, 8 as function of number of carbon in alkyl chain.

8.4.2 Results F_nH_mX

As in previous results for F_nH_m, the values of cmc, shown in Figure 39, decrease with increasing of fluorinated chain. The values of F_nH_mI are lower than F_nH_mBr leading to an influence of couter-ion to reduce the cmc values. The iodide counter-ion probably enhances the hydrophobic character of surfactants leading to an increase of amphiphilic properties. Then, while the surfactants F_8H_1I and F_8H_2I form hydrogel at concentration twice cmc, the homologues F_8H_1Br and F_8H_2Br do not present this property.

The values of cmc are summarized in Table 12.

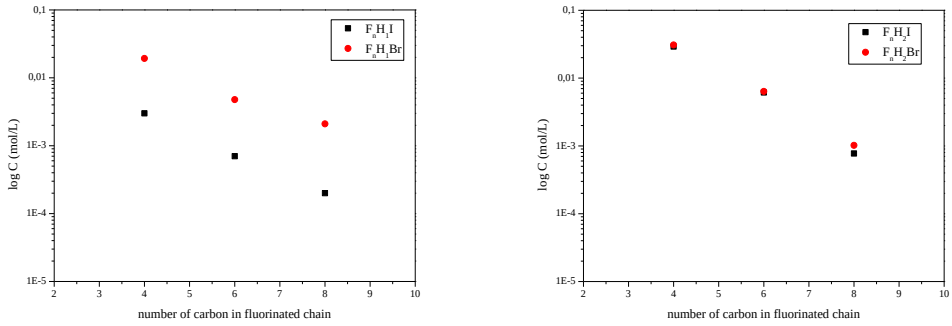

Figure 39: values of log cmc as function of number of carbon in fluorinated chain for F_nH_mX

8.5 Krafft temperature

Many ionic surfactants show dramatic temperature-dependent solubility. The solubility may be very low at low temperatures and then increases by orders of magnitude in a relatively narrow temperature range. This phenomenon generally denoted as the Krafft phenomenon [229], with the temperature for the onset of increasing solubility being known as the Krafft temperature.

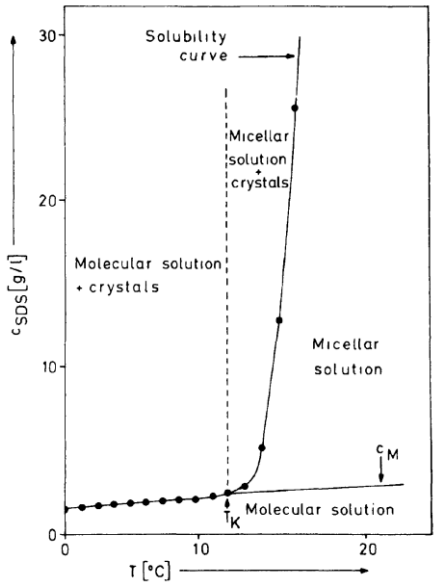

Figure 40: Krafft's temperature diagram

The latters may vary dramatically with subtle changes in the surfactant's chemical structure. In general, the Krafft temperature increases rapidly as the alkyl chain length of the surfactant increases. It also depends on the head group and counter-ion.

Krafft temperature and cmc of the surfactants provide informations about the conditions at which a compound acts as surfactant. Surfactants with a high Krafft's temperature are very efficient at lowering surface tension [230]. The Krafft's temperature is defined as the melting point of hydrated surfactant. It was observed that at low temperature, the conductance of pure as well as mixed hydrated surfactant mixture increases slowly because the solubility of the ionic surfactants are quite limited.

Cationic surfactants are generally water soluble when there is only one long alkyl chain group. In contrast, cationics with two or more long alkyl chains and with iodide counter-ion are soluble in hydrocarbon solvents, but they become only dispersible in water, sometimes forming bilayer vesicle type structures [231].

During the temperature transition stage, the conductance increases sharply with increasing temperature, due to larger dissolution of the surfactant until the T_k. Then, after T_k, the conductance increases slowly due to the increase in ionic mobility with increasing temperature (see Figure 40).

8.5.1 Procedure of measurements Krafft's temperature

Aqueous solutions were prepared at concentration of twice the cmc and kept at 5 °C during 24 h, where precipitation of surfactant hydrated crystals occurred. The temperature of the precipitated system was raised [232] and conductivity measured.

Table 12: values of Krafft's temperature (T_k) and cmc of surfactants synthesized

Surfactants	T_K [°C]	cmc [mol/L]
F_8H_1	<5	2.0E-04
F_8H_2	<5	4.0E-04
F_8H_3	insoluble	4.12E-04
F_8H_4	insoluble	2,53E-04
F_8H_6	insoluble	7.87E-06
F_8H_8	insoluble	3.15E-06
F_6H_1	<5	7.00E-04
F_6H_2	<5	2.88E-03
F_6H_3	insoluble	4.64E-03
F_6H_4	insoluble	2.39E-03
F_6H_6	insoluble	3.91E-04
F_6H_8	insoluble	1.86E-05
F_4H_1	<5	3.00E-03
F_4H_2	<5	1.10E-02
F_4H_3	<5	2.10E-02
F_4H_4	<5	2.00E-02
F_4H_6	insoluble	2.65E-03
F_4H_8	insoluble	2.12E-04

8.5.2 Results F_nH_m

The solubility of fluorinated surfactants depends on the hydrophilic part of the surfactant and decreases with increasing chain length [121]. However, it is evident from Table 12 that the influence of long hydrocarbon moieties and iodide counter-ion limit the solubility of surfactants, so the majority of surfactants are insoluble in pure water.

8.6 Thermodynamic Parameters of Micellization

8.6.1 Free energy of micellization and free energy of adsorption

The thermodynamic behavior of surface active compounds provides detailed understanding of the micellization phenomenon. The formation of micelles is generally understood in terms of hydrophobic effect, which is the main driving force behind the formation of micelles in solution. The micellization tendency rises with increasing fluorinated chain and the cmc aqueous solution generally decreases with increasing hydrophobic character of amphiphilic surfactant. The study of the micellization processes requires complete thermodynamic characterization. For ionic surfactants, a standard free energy change micellization ΔG_{mic}^{0} can be calculated (eq. 8) by taking into account the degree of binding of the counter-ion to the micelle, 1 - α. Thus, for ionic surfactants of the 1:1 electrolyte type [233, 234]:

$$\Delta G_{mic}^{0} = RT[1 + (1 - \alpha)] \ln x_{cmc} = 2.3\, RT(2 - \alpha) \ln x_{cmc} \qquad 8$$

where α is the degree of ionization of the surfactant, measured by the ratio of the slopes of the specific conductivity versus C plotted above and below the cmc and x_{cmc} is the mole fraction of the surfactant in the liquid phase at the cmc. Then, energy of adsorption is obtained by eq. 9

$$\Delta G_{ads}^{0} = \Delta \mathrm{G}_{mic}^{0} - \frac{\pi_{cmc}}{\Gamma} \qquad 9$$

where $\pi_{cmc} = \gamma_0 - \gamma_{cmc}$ is the surface pressure at cmc, where γ_0 is the surface tension of the water and γ_{cmc} the surface tension of surfactant's solution at the cmc and Γ is the surface excess.

Table 13 shows the ΔG_{mic}^{0} values for micellization of F_nH_n. All values of ΔG_{mic}^{0} are negative. This means that the micellization process for these surfactants is spontaneous. ΔG_{mic}^{0} values decrease increasing fluorinated chain. This pattern could be related to water lyophobic interactions, group interactions, or interactions between the lyophobic groups at the interior of the micelle. The standard free energies of adsorption (ΔG_{ads}^{0}), reported in Table 13 of the synthesized surfactants were found to have lower values than those of the micellization process; this means that the adsorption process of surfactant molecules was favorable. Moreover, the values of ΔG_{mic}^{0} and ΔG_{ads}^{0} increase with the fluorinated chains length because of the interaction between the fluorinated chains is strengthened when the chain lengths increase.

Table 13: values of standard free energy change of micellization and standard free energies of adsorption

surfactants	ΔG^0_{mic} **[kJ/mol]**	ΔG^0_{ads} **[kJ/mol]**
F_8H_1	-97.81	-164.66
F_8H_2	-89.17	-158.97
F_8H_3	-86.91	-166.81
F_8H_4	-92.34	-170.15
F_8H_6	n.d[a]	n.d[b]
F_8H_8	n.d[a]	n.d[b]
F_6H_1	-80.99	-124.77
F_6H_2	-66.67	-110.46
F_6H_3	-63.25	-108.44
F_6H_4	-67.30	-113.29
F_6H_6	-88.82	-140.13
F_6H_8	n.d[a]	n.d[b]
F_4H_1	-64.77	-110.52
F_4H_2	-51.4	-87.49
F_4H_3	-42.40	-79.87
F_4H_4	-69.29	-106.95
F_4H_6	-94.09	-131.25
F_4H_8	-98.66	-139.95

a: the conductivity is too close to the value of pure water, then it is not possible to calculate the micellization energy value
b: the value of micelizzation energy is not disponible

8.6.2 Kinetic of adsorption

For practical purposes, it is not only important to know how much of a fluorinated surfactant is needed to reduce surface tension to a desired value. The time required to decrease surface tension is also highly significant. Many industrial processes do not allow sufficient time to a surfactant to attain equilibrium and depend on the kinetics of surfactant adsorption.

The time required for surface tension reduction depends on the diffusion processes involved in surfactant adsorption. The first step is the transport of the surfactant to the subsurface, driven by a concentration gradient or hydrodynamic forces. The second step is the transfer of the surfactant molecule from the subsurface to the adsorbed state. Usually, the second step is rapid and the first step determines the adsorption rate, especially when the transport of the surfactant molecule is a diffusion process. The kinetics of surfactant adsorption depend on the surfactant structure. Fluorinated chains increase the rate $(d\gamma\, dt^{-1})$ of adsorption, but the time needed to attain equilibrium may not be affected considerably. Minutes or even hours may be required for the surface film to be reorganized. Increasing temperature accelerates the diffusion processes and the equilibrium surface tension is attained in a shorter time. Cationic surfactants dissociate in water, forming a surface-active positively charged ion and a negatively charged counter-ion. The rate at which a surfactant reaches equilibrium surface tension also depends on its counter-ion.

The effectiveness of reducing the surface tension for fluorinated surfactants is known to be significantly greater than that for hydrocarbon surfactants; this is attributed to the presence of fluorocarbon chains in the molecule, which makes a positive contribution to the adsorption at the air/water interface.

The kinetics of adsorption at the interface of the surfactants synthesized decrease with an increase in the fluorocarbon chain lengths and with the concentration. Then, the surfactants F_nH_m with the long alkyl chains take a long time to reach thermodynamic equilibrium in aqueous solution. The large molecular aggregates fluctuate in size amongst themselves through transfer of monomeric species in the bulk with time leading to an exchange very slow between monomeric and aggregate states of longer alkyl chains.

The time to reach thermodynamic equilibrium in aqueous solution increases with increasing of fluorinated and hydrocarbon chains.

8.7 Size of micelles

Micelles and other self-assembling amphiphile structures have a wide variety of scientific, engineering, and technical uses. The effectiveness of such applications of micelles may depend on their size and composition or their effect on solution properties, e.g., viscosity. Any technique for tailoring micelle size or structure thus have an extensive range of potential applications and the effect of small solute molecules on micelle size and aggregation number has long been a topic of study. Dynamic light scattering (DLS) is frequently used to measure diffusion in solutions of surfactant micelles. The measurements can be made rapidly (in minutes) and conveniently on small samples of solution (0.7 mL) into a disposable sizing cuvette (Figure 41). The analysis of micelle diffusion data provides information about of sizes, shape, hydrodynamic radii, micelle-micelle interactions [233].

8.7.1 Dynamic light measurements

DLS experiments were performed at surfactants concentration equal to 2 cmc. The reason for choosing a surfactant concentration close to the cmc in the light scattering experiments was to reach the state of isolated, non interacting aggregates to allow the application of cumulants method and calculation of equivalent hydrodynamic micelle size based on the Stokes-Einstein formula (eq. 10) [235]:

Figure 41: disposable sizing cuvette

$$D = \frac{k_B T}{6\pi\eta r} \qquad 10$$

where k_B Boltzmann constant, T temperature, η viscosity and r radius.

The Z-average diameter is the mean hydrodynamic diameter and polydispersity index is an estimate of width of distribution. Both of these parameters are calculated according to the International standard on dynamic light scattering ISO13321. Samples were cleaned by passage through 0.45 μm pore diameter microporous filters.

Particle size measurements on aggregates of fluorinated surfactants were carried out with a dynamic light scattering measuring apparatus (Malvern Instruments Zetasizer Nano-S model 1600). A He-Ne laser with a power of 4 mW was used as a light source. All the measurements were done at a scattering angle of 90 ° and a temperature of 25 °C, which was controlled by means of a thermostat. Measurements were carried out by the dynamic light scattering method of the particle size of surfactant aggregates to examine the state of aggregation in aqueous solution.

8.7.2 Results F_nH_m

Figure 42 and 43 show the diameter of the population of aggregates against the number of concentration solutions for F_4H_1 and F_4H_2. We can see that R increases with increasing of concentration and the value of R is higher for F_4H_2 suggesting the influence of hydrocarbon chain to lead larger aggregates. Also, the increasing interactions of hydrophobic alkyl tails with increasing carbon number in the alkyl chain, can lead to a decrease of the mean between the polar head and tail and hence to an increase in size.

Figures 44 and 45 show R as function of fluorinated chain: it can observed that higher values of R with large fluorinated chain. It reflects the ability of fluorinated surfactant to give aggregates micelles with lengths as large as several micrometers (as shown by Cryo – SEM images).

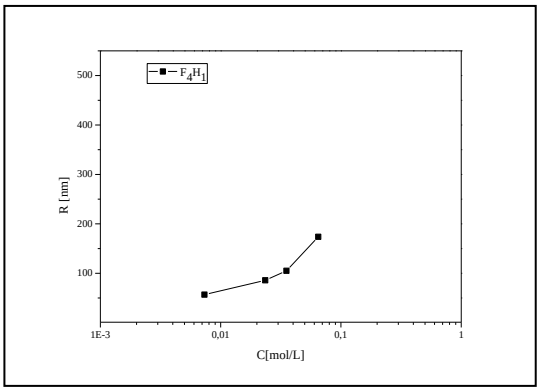

Figure 42: R as function of concentration of F_4H_1

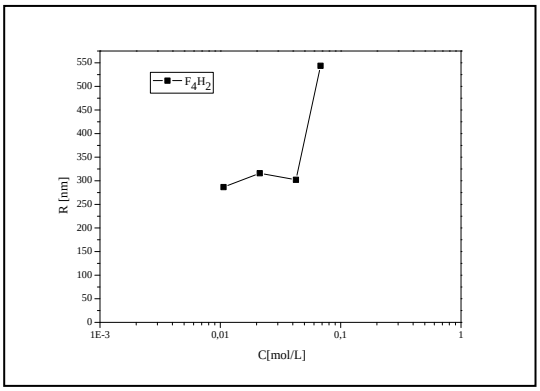

Figure 43: R as function of concentration of F_4H_2

These findings are consistent with the earlier observation by Zana and co-workers [236] with hybrid surfactants having a very strong propensity for micellar growth and formation of micelles of very low curvature. Then, the presence of big counter-ions I^- near to the polar heads of the surfactant molecules decreases the repulsion force between the head-groups. This reduction in the repulsion makes it possible for the surfactant molecules to approach each other more closely and form larger aggregates, which requires much more space for the long hydrophobic fluorinated chains. However, the electrostatic effect of the I^-

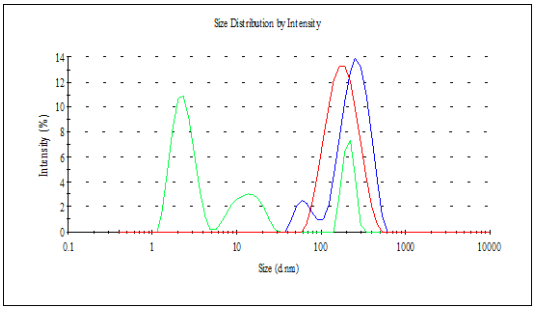

Figure 44: Variation in diameter as function of fluorinated chain. Blue colour for F_8H_1, Red colour for F_6H_1, green colour for F_4H_1.

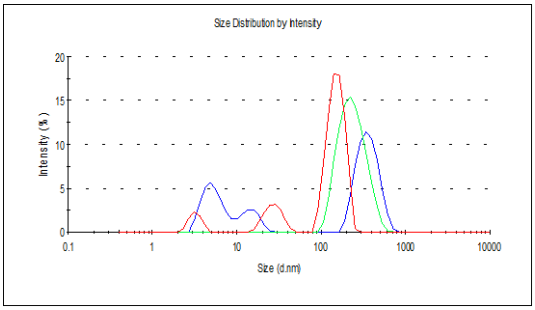

Figure 45: Variation in diameter as function of fluorinated chain. Blue colour for F_8H_2,Red colour for F_6H_2, green colour for F_4H_2.

counter-ion binding on ionic micelles and the change in the hydrocarbon-bonded structure of water cause hydrophobic interactions between surfactant molecules [180]. Also, due to Ostwald ripening [237], aggregates of larger curvature realized themselves into single species due to their higher chemical potential and the liberated single species adsorb to the aggregates of smaller curvature to make them further larger in size. As clearly shown in the Figures 44 - 45, the presence in the solution of different sizes of aggregates.

Figure 44 and 45 show also R as function of fluorinated chain, which clearly see the transition from monomodal to bimodal structure with increasing of fluorinated chain.

The effect of long fluorinated chain on packing of surfactant is expected to affect strongly the curvature of surfactant layer and the incorporation of fluorinated chain into the core provides to a bimodal distribution for the long fluorinated chains (F_8H_m and F_6H_m). Figure 46 shows the value (R_1) of the most abundant population (%) as function of hydrocarbon chain for F_8H_m, F_6H_m and F_4H_m respectively. Figure 46 shows also that with increasing of number of carbon in alkyl chain the values of size increase; this means there is also an influence of hydrocarbon chain on the structuring of the aggregates. The minor populations (%) of diameter R_2 and R_3 have a diameter in the range of 10 - 800 nm.

Table 14: Values of R_1, R_2, R_3 for the surfactants synthesized.

Surfactants	**R_1 (nm)**	**R_2 (nm)**	**R_3 (nm)**
F_8H_1	49.95	417	-
F_8H_2	100.32	48.2	3.2
F_8H_3	156.8	6.3	-
F_8H_4	241.2	302.1	-
F_8H_6	395.4	809	2.7
F_8H_8	497.7	50.3	-
F_6H_1	12.77	2.5	-
F_6H_2	33	169.4	3.6
F_6H_3	70.87	780.8	-
F_6H_4	106	34.3	-
F_6H_6	164.9	22.1	-
F_6H_8	195.6	33.2	2.4
F_4H_1	181.2	-	-
F_4H_2	261.5	-	-
F_4H_3	342	-	-
F_4H_4	420	-	-
F_4H_6	547.4	-	-
F_4H_8	605.2	-	-

An increase in flexibility with decreasing of fluorinated chain, in particular for F_4H_m, may permit a closer approach of chains to reduce the tendency to transform a sphere into cylindrical aggregates providing a monomodal distribution and the higher values of spherical aggregates (Figure 46). In fact, it may be assumed that with increasing number of carbon atoms in alkyl chain, the hydrophobic interactions become more intensive and large aggregates with diameter 200 – 500 nm can be observed. The values of R_1, R_2, R_3 for the surfactants synthesized are listed in Table 14. Also, Table 14 shows that the smallest

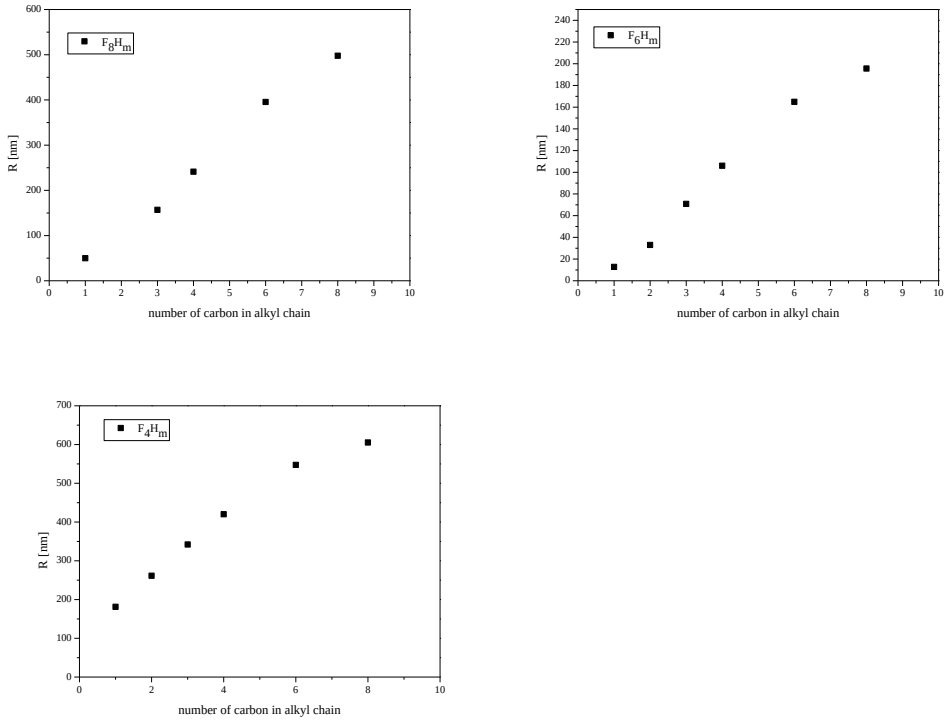

Figure 46: R_1 of F_8H_m, F_6H_m and F_4H_m as function of alkyl chain

populations detected were in the range of 2 - 40 nm diameter, the biggest populations 300 - 800 nm that, in most cases, largely exceeds what expected for spherical micelles (above 20 nm). These measurements suggest a spontaneous organization in large aggregates (vesicles or cylinders) for all of the surfactants synthesized. Then, the strong interaction between multiple hydrocarbon chains causes an increase of micelle's size. Therefore, the interaction of head group alkyl chains between two surfactant molecules may also cause the formation of large aggregates.

9 Self-assembled structures

9.1 Introduction

Surfactant solutions represent a well-documented class of self-assembled structures providing a powerful tool in several applications of pharmaceutical and cosmetics industries. Under certain conditions such as concentration, ionic strength (salinity), temperature, pH, presence of counter-ions, the globular micelles of surfactants may undergo uniaxial growth and form very long and highly flexible aggregates. Also, the addition of an inorganic [238] or a strongly binding organic salt [239], or addition of an oppositely charged surfactant lead to the growth of aggregates. This growth generally leads to highly viscous solutions and the formation of an entangled network made of flexible worm-like micelles, often referred to as thread-like micelles. The length of these aggregates can reach 1 μm, but the diameters are only a few times the length of the constituent molecules. Prud'homme and Warr investigated the behavior of solutions of tetradecyltrimethylammonium salicylate [240] and they observed a rheological behavior for wormlike micelles in the surfactant solution similar to that for flexible polymers. Above a critical concentration c*, few weight percent, wormlike micelles entangle into a transient network similar to a solution of flexible polymers; they behave in exactly the same way as the equivalent macromolecules and entangle with each other to form transient networks, which display remarkable viscoelastic properties in a manner analogous to semi-dilute polymer solutions. Also, the wormlike micelles are dynamic systems and the aggregates are constantly breaking and recombining (Figure 47), making them 'living polymers' and proving an increase in viscosity with shear rate [236, 241].

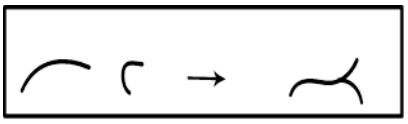

Figure 47: living polymer

The polymer analogy has been the catalyst for recent theoretical advances in understanding the properties of anisometric micellar solutions. By incorporating the dynamic nature of micelles into polymer solution theories, Cates [242] has been able to predict scaling laws for both equilibrium and dynamic properties of these systems. Because the micelles are in thermodynamic equilibrium with the surrounding solvent, they are not geometrically fixed like polymer molecules. As a consequence, the connecting or branching points of the micelles are able to move along the primary axis of the micelles.

These living polymers have one extra property that the normal polymer system lack, and hence their name, as we now show. If either polymer chains or surfactant worm-like

micelles are subjected to a high extensional force, they can be snapped in half. While polymer fragments always remain thereafter at this lower (halved) molecular weight, the broken surfactant micelles can reform under more quiescent conditions, since they are thermodynamic objects held together by reversible bonds. If elastic liquids are needed to withstand continual damage, and yet survive, then these micellar systems are much more mechanically robust.

Micellar microstructures have a strong influence on the rheological properties of aqueous surfactant solutions. The transition to a shear-thickened fluid is commonly attributed to the formation of shear-induced structures, where phase separation takes place between a surfactant-rich and a surfactant-poor phase. Their unique viscoelastic behavior is exploited to tune the rheology in numerous applications with or without the use of polymers or additives. For this reason they have been suggested for drag reducing fluids in central-heating systems [243]. Like all fibrous microstructures, the viscosity is high when the system is randomly dispersed in space and highly entangled, but once the flow has aligned the microstructures, the viscosity is quite low.

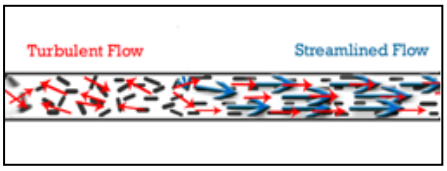

Figure 48: Drag reduction fluid

This change from very high to very low viscosity takes place over a narrow range of stress or temperature. These self-assembled structures may reduce friction energy loss in turbulent flow by up to 90 % at relatively low surfactant concentrations under appropriate flow and temperature conditions. This phenomenon is called drag reduction (DR) and it has significant potential impacts on fluid transport (Figure 48) and on the environment [244]. The self-assembly of surfactant DR additives (DRAs) permits them to be used in recirculation applications such as in district heating/cooling systems [245, 246]. Cationic surfactants have been extensively investigated and it seems that they are the most effective surfactant drag reducers providing the proper conditions (such as the chemical structure and concentrations of surfactant and counter-ion). Some cationic surfactants can spontaneously pack into cylindrical structures without any additives at room temperature. Often the addition of inorganic salts to ionic surfactants can promote micellar growth and viscoelastic properties [247]. The mechanism involved is primarily the screening of the electrostatic repulsions between the charged head-groups, which results into a reduction of the optimal molecular area at the hydrocarbon–water interface, leading to an increase in the end-cap energy [248]. Rather, little is known about fluorosurfactants, in particular cationic fluorosurfactants, despite the technical interest of their potential usefulness, with the large hydrophobicity and strong surface activity. Solutions of these surfactants have a number of

peculiarity properties because their micellar chains are formed due to weak non-covalent interactions and easily change their structures in response to external actions. The introduction of fluorinated chains in surfactants is very promising, thanks to their high hydrophobicity, stiffness, for the formation of structures with relatively little curvature, such as cylindrical micelles. In order to investigate the viscoelastic properties of the surfactants F_8H_1 and F_8H_2 that form hydrogel without any additives Zeta potential and rheological measurements, Cryo-SEM and optical polarize microscopy images were carried out. However, concentrated solutions of hybrid surfactants as function of temperature, stress and strain are carried out.

9.2 Zeta potential

The development of a net charge at the particle surface affects the distribution of ions in the surrounding interfacial region, resulting in an increased concentration of counter-ions (ions of opposite charge to that of the particle) close to the surface.

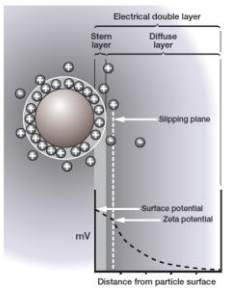

The liquid layer surrounding the particle exists as two parts; an inner region, called the *Stern layer*, where the ions are strongly bond and an outer, diffuse region where they are less firmly attached; thus an *electrical double layer* exists around each particle. Within the diffuse layer there is a notional boundary inside which the ions and particles form a stable entity. When a particle moves (e.g. due to gravity), ions within the boundary move with it, but any ions beyond the boundary do not travel with the particle. This boundary is called the surface of hydrodynamic shear or slipping plane. The potential that exists at this boundary is known as the Zeta potential.

Zeta potential (ζ) is measured using a combination of measurement technique as electrophoresis and laser doppler velocimetry. This last method measures how fast a particle moves in a liquid when an electrical field is applied (its velocity). Once we know the velocity of the particle and the electrical field applied we can, by using two other known constants of the sample, viscosity and dielectrical constants, work out the Zeta potential. Since surfactant binding to proteins at high concentrations is primarily associative in nature and governed by the properties of the surfactant, a reasonable estimate of the charge density of the aggregate can be taken to be that of the surfactant micelle under identical solution conditions [237].

The Zeta potential ζ was calculated from the electrophoretic mobilities (μ_E) using the Henry equation [249] (eq. 11):

$$\zeta = \frac{3\mu_E \eta}{2\varepsilon_0 \varepsilon_r} \frac{1}{f(ka)} \qquad 11$$

where ε_0 is the permittivity of vacuum, ε_r and η are the relative permittivity and viscosity of the medium, respectively, a the particle radii, k the Debye length. The function $f(ka)$ depends on the particle shape and for our systems was determined by eq. 12

$$f(ka) = 1.5 - \frac{9}{2ka} + \frac{75}{2k^2a^2} - \frac{330}{k^3r^3} \qquad 12$$

The Henry function appraises 1 for small *kr* and 1.5 for large *kr*. Hence, for larger aggregates of relatively small potential, eq (1) can be used to determine the Zeta potential of particle. k is related to the ionic strength of electrolyte solution according to eq. 13.

$$k = (2000\mathrm{F}^2)/(\varepsilon_0 \varepsilon_r R\mathrm{T})^{1/2} \mathrm{I}^{1/2} \text{ (3)} \qquad 13$$

where F is the Faraday constant, ε_0 the permittivity of a vacuum, ε_r the relative permittivity, *R* the gas constant, T the temperature, I the ionic strength of the electrolyte solution [250].

9.2.1 Zeta potential measurements

In this study, the charge density of the micelles of F_nH_m with n= 4, 6, 8 and m= 1, 2 were estimated from measurements of the Zeta potential of micelles using a laser Doppler light-scattering technique.

Zeta potential measurements of surfactant complex were made using a Malvern Instruments Ltd. NanoZs by taking the average of three measurements at the stationary level. The cell used was a 5 mm × 2 mm rectangular quartz capillary (Figure 49). The temperature of the experiments was 298.15 ± 0.01 K controlled by proportional temperature controller HETO.

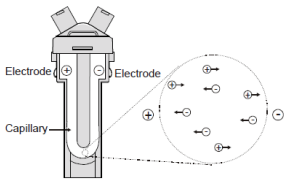

Figure 49: zeta potential cuvette

9.2.2 Results F_nH_m

Figures 50 and 51 show Zeta potential ζ for F_8H_1 and F_8H_2 as function of concentration 20, 30, 40 times over cmc; these concentrations were chosen to observe the behavior until to maximal solubility of surfactants synthesized. In this case, the formation of self-assembled structures can be presumed because of the surfactants form hydrogel in pure water. So, the interactions of these large structures can be studied. The concentration 40 times over cmc of F_8H_1 was not realized because the surfactant is insoluble at this concentration.

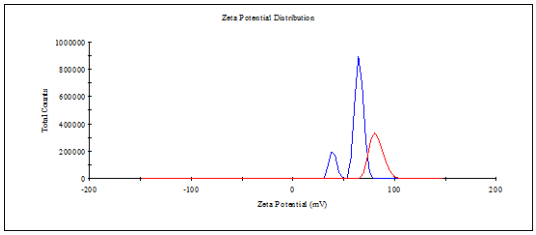

Figure 50: Zeta potential, red F_8H_1 at C_1, blue F_8H_1 at C_2

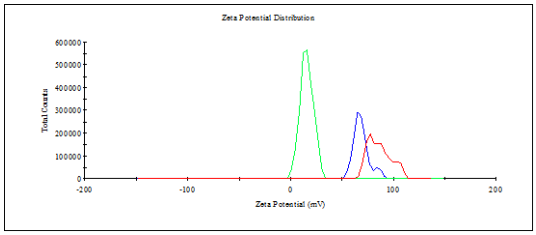

Figure 51: Zeta potential, red F_8H_2 at C_1, blue F_8H_2 at C_2, green F_8H_2 at C_3

We can see that the main peak was found to be positive and it corresponds with the positive change of head group in hybrid surfactants.

The main positive peak is probably attributed to the large aggregates with a low degree of curvature and a weak adsorption of I^- counter-ions at the micelles surface.

Here, Figures 50 and 51 show also the positive Zeta potential of F_8H_1, F_8H_2 decreases with increasing surfactant concentration due to the formation of entangled networks of wormlike micelles caused by higher hydrophobic interactions.

Also, Zeta potential measurements were carried out at concentration twice to cmc of F_nH_m with n= 4, 6, 8 and m= 1, 2 in order to study the influence of fluorinated chain. Therefore, Figure 52 shows the Zeta potential of F_4H_2, F_6H_2, F_8H_2 as function of fluorinated chain length. All values are positive, due to head group, and the values increase as increasing of fluorinated chain. The same results were found for F_4H_1, F_6H_1, F_8H_1.

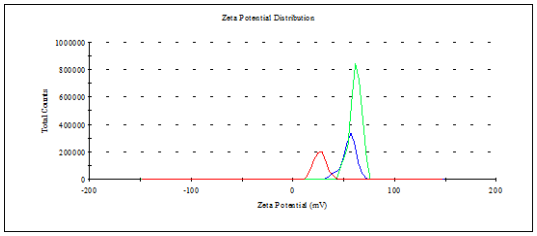

Figure 52: Zeta potential F_8H_2 (green), F_6H_2 (blue), F_4H_2 (red).

The fluorinated chain enhances the hydrophobic interactions leading to increase the value of Zeta potential. The values of surfactants synthesized are summarized in Table 15.

Table 15: values of Zeta potential of surfactants F_nH_m

surfactants	**ζ (mV)**	**surfactant**	**ζ (mV)**
F_8H_1	65.9	F_8H_2	58.3
F_6H_1	24.4	F_6H_2	38.9
F_4H_1	11.3	F_4H_2	9.5

9.3 Rheological measurements

The stiffness of the fluorocarbon chain has an effect on the packing [247] leading fluorinated surfactants, in aqueous solutions, to form cylindrical micelles with lengths as large as several micrometers, under solution conditions where hydrocarbon analogous would form spherical aggregates. The packing constraints of the perfluoroalkyl chain is responsible for the formation of flexible aggregates in water at low concentrations and low temperatures. Surfactant solutions commonly exhibit viscoelastic properties only at low temperatures because heating enhances thermal vibrations in micelles and the chains are more frequently breaking and their average length decreases. Some surfactants reach a maximum of viscosity at specific temperature and then decrease with increasing temperature [238]. These surfactants are called thermo-responsive viscoelastic surfactants.

The surfactants synthesized F_8H_1 and F_8H_2 and F_6H_2 form hydrogel in pure water. Then, to investigate the importance of fluorocarbon and hydrocarbon chain to give viscoelastic properties, rheological measurements were carried out.

No peculiar hydrogel behavior was observed on the solutions of F_nH_m with n= 4, 6 and m= 1, 2. Only F_8H_1, F_8H_2, F_6H_2 show the tendency to form hydrogels in pure water after cmc but only F_8H_1 and F_8H_2 show high viscosity. However, to investigate concentrated solutions of F_8H_1 and F_8H_2 rheological measurements at different conditions were carried out.

9.3.1 Kelvin-Voigt model

If we connect the single elastic and viscous elements in parallel, we end up with the simplest representation of a viscoelastic solid, represented by Kelvin-Voigt model.

The model describes the rheological properties, which constitute a single spring connected in parallel to a viscous element. In shear experiments the storage (or elastic) modulus (G') and the loss modulus (G'') are given by eq. 14

$$G' = G_0$$
$$G'' = \eta\omega \qquad 14$$
$$\eta' = \eta$$

here G_0 is the plateau modulus, η the viscosity and ω the frequency.

9.3.2 Procedure

The rheological properties of samples were measured with a Anton Parr Physica MCR-301 rheometer. Cone geometry was used in each case (50 mm diameter, 1 angle). The gap was 0.05 mm. A solvent trap was used to minimize water evaporation. Frequency sweep measurements were performed at a given stress in the frequency region varying from 0.01 to 100 rad s^{-1}. Experiments were performer at 20, 30, 40, 50 ± 1 °C. The viscosity of the sample was obtained from steady-shear measurements with the shear ranging from 0.3 to 500 s^{-1}. All the rheology/viscosity data given in this project are average values of two measurements, the deviations were in the range of ± 0.01 Pa·s. Due to instrumental limitation we were not able to measure at the lower shear rate.

9.3.3 Temperature-viscosity results of F_nH_m

Figure 53 and 54 show viscosity as function of temperatures for F_8H_1 and F_8H_2 at concentrations 20, 30, 40 times over cmc. We can observe a thermo-responsive viscoelasticity for all the concentrations. Also, the value of the maximal viscosity and the temperature at which there is maximal viscosity appear be dependent on surfactant concentration and hydrocarbon chain length [238]. In particular, the value of maximum is T= 19 °C at C_1 = 20 times cmc, T = 26 °C at C_2 = 30 times cmc for F_8H_1, and T = 32 °C at C_1 = 20 times cmc, T = 42 °C at 40 times cmc, T = 37 °C times cmc at 40 times cmc for F_8H_2.

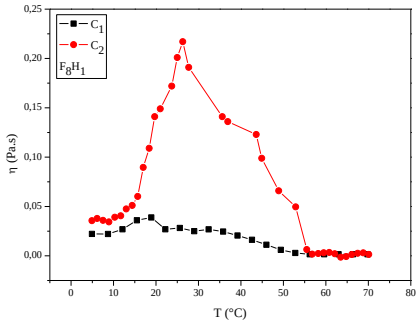

Figure 53: viscosity as function of temperature at concentration 20 and 30 times cmc for F_8H_1

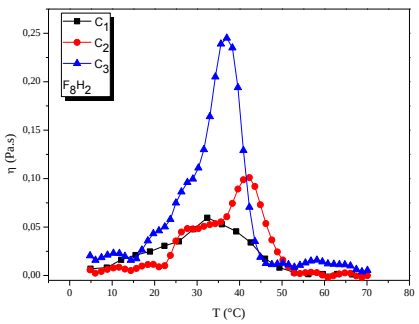

Figure 54: viscosity as function of temperature at concentration 20, 30, 40 times cmc for F_8H_2

There is a thermodynamic explanation usually proposed for this increasing-decreasing in viscosity. The increase of viscosity with temperature can be understood in terms of a decrease in the mean size of the micelles or the formation of cross-linked micellar networks [239]. Considering reptation model of Cates [251], relaxation of chain conformations occurs by the gradual disengagement of any given chain, by curvilinear diffusion along its own

contour [241] from a tube-like environment. Cates also deduced the rheological properties of flexible surfactant micelle. In particular, the normalized number density *C(L)* of micelles of length L is given by eq. 15:

$$C(L) = e^{\frac{L}{\bar{L}}} \qquad 15$$

where *C(L)* normalized number density of micelle of length L and the mean length $\bar{L}$ is related to the volume fraction φ and to temperature T by eq. 16:

$$\bar{L}(\varphi, T) = \varphi^{\frac{1}{2}} e^{(E_{break/2k_BT})} \qquad 16$$

where E_{break} is the scission Energy required to break a micelle in two part.

This temperature dependence of micellar length produces a decrease in micellar size and thus a greater resistance to the flow.

However, networks have to be in some way similar to flexible polymers with their stress relaxation partly controlled by motion of micelles along its own contour and by reversible scission of micelles. The formation of a inter-micellar junction may be viewed as a fusion reaction between the end cap of one cylindrical micelle with the main body of another, forming a Y-like joint [236] (Figure 47). Hence, the variation of viscosity as function of temperature in the surfactants synthesized is due to the formation of inter-micellar junctions. Also, Figures 53 and 54 show that the trend of viscosity-temperature curve is similar with increasing surfactant concentration, but the temperature for viscosity maximum gradually shift to lower value. Then, they show that highly viscoelastic solutions are formed at low temperature and high surfactant concentration. In fact, Figure 53 shows the value of maximal viscosity for F_8H_2 at C_3 is higher than the value at C_1 and C_2 because the viscosity increases with surfactant concentration due to an increase in the mean micellar length. As the contour length decreases, the viscosity is predicted to decrease because of a reduction in the extent of entanglement of micelles. Therefore, changes to solution concentration can lead to the formation of other self-assembled structures and the formation of micellar network takes place at lower temperature. Also, as shown in Figure 54 the maximal viscosity is higher for F_8H_2 for all concentrations to lead to think that an increase of hydrocarbon chains of hybrid surfactants forms larger molecular assemblies in solution; in fact, if the aggregates are located in the vicinity of micelle surface they are likely to actively participate in the hydrophobic intermicellar interaction, thereby forming large molecular assemblies through the gathering of small molecular assemblies. The distance between cross-links, which is a decreasing function of surfactant concentration, replaces the contour length as the appropriate micellar length scale. For a saturated network the reptation model

breaks down, which suggests that the system becomes very fluid and so F_8H_1 at C_3 shows a low viscosity and no hydrogel behavior.

9.3.4 Frequency-Temperature

The storage modulus (G') and the loss modulus (G") as function of temperature at frequency of 1 Hz and 20 % strain for the concentrations C_1, C_2, C_3 were also analyzed. The results at low frequencies are somewhat scattered because the rheometer was out of its measuring range. In the range of temperature used (T= 10 - 70 °C) the plots are linear and the value of G' is always larger than of G" (range 0.01-10 Hz); then, the storage modulus shows no frequency dependency in the range 10-70 °C. Figure 55 and 56 show examples of measurements. In this range analyzed the surfactants F_8H_1 and F_8H_2 have a viscoelastic behavior.

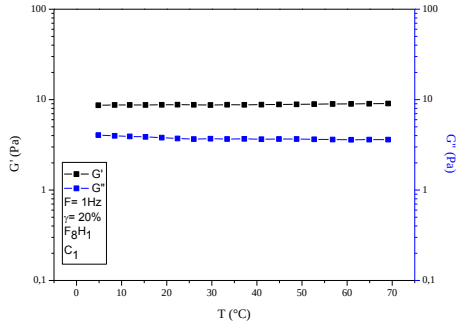

Figure 55: storage and loss modulus at C_1 as function of temperature for F_8H_1

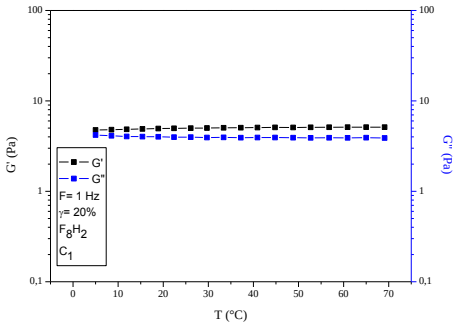

Figure 56: storage and loss modulus at C_1 as function of temperature for F_8H_2

9.3.5 Frequency- strain

The storage modulus (G') and the loss modulus (G") as function of frequency at 20, 30, 40 and 50 °C and 20 % strain were analyzed to calculate relaxation times as function of temperature. Figure 57 and 58 show examples of measurements. The values are plotted in the Figures 59-63.

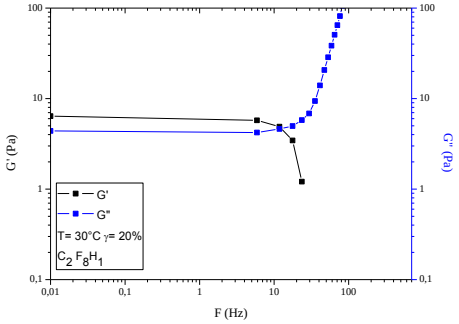

Figure 57: G' and G" as function of frequency for F_8H_1 at C_1

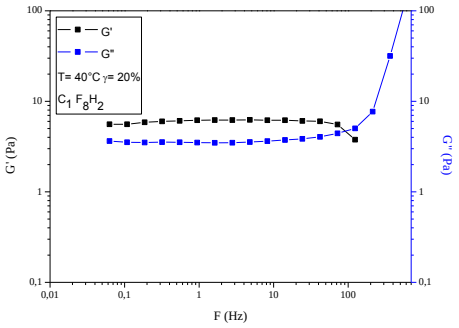

Figure 58: G' and G" as function of frequency for F_8H_2 at C_2

9.3.6 Reptation and breaking time

The relaxation time can be correlated with *reptation time* τ_{rep} and *breaking time* τ_b of Cates's model. In fact, the relaxation time is the geometric mean of two characteristic times, for micellar breaking-recombination and for micellar reptation, as proposed by the reptation-reaction model. However, reptation time (τ_{rep}) is defined in eq. 17:

$$\tau_{rep} = \bar{L}\varphi^{3/2} \qquad 17$$

it is the time required to form a worm-micelle of contour length $\bar{L}$ to pass through a hypothetical tube, with $\varphi^{3/2}$ volume fraction. At τ_{rep} the formation of the aggregate is associated with the creation of an interface between its hydrophobic domain and water. The surfactant head-groups are brought to the aggregate surface, giving rise to steric repulsions between them.

Then, breaking time is defined in eq. 18

$$\tau_b = (k_r\bar{L})^{-1} \qquad 18$$

it is the average time necessary for a chain of average length to break into two pieces by a reversible scission characterized by a temperature-dependent rate constant k_r per unit of time and per unit arc length, which is the same for all elongated micelles and is independent of time and of volume fraction [251].

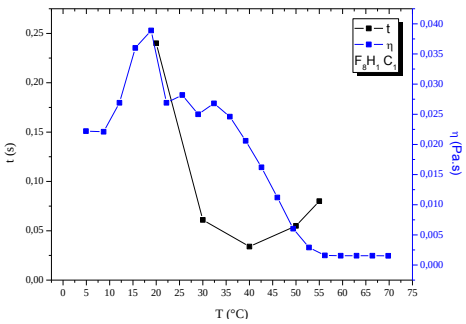

Figure 59: correlation between viscosity and relaxation time of F_8H_1 at C_1

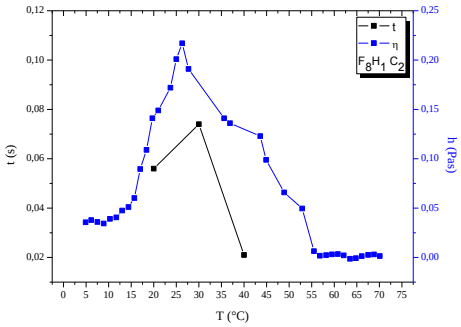

Figure 60: correlation between viscosity and relaxation time of F_8H_1 at C_2

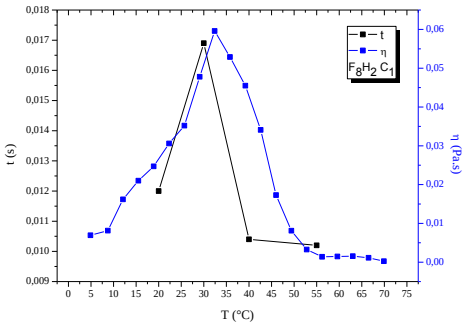

Figure 61: correlation between viscosity and relaxation time of F_8H_2 at C_2

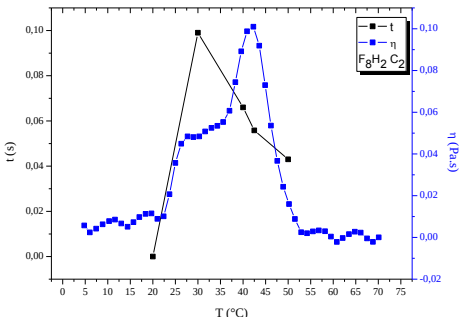

Figure 62: correlation between viscosity and relaxation time of F_8H_2 at C_2

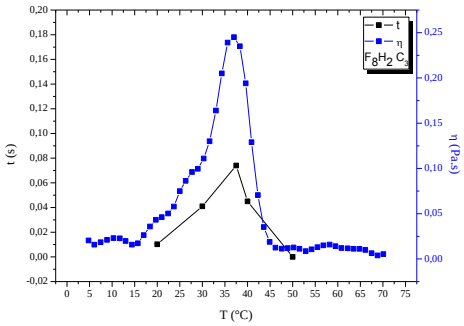

Figure 63: correlation between viscosity and relaxation time of F_8H_2 at C_3

Figure 59 - 63 show a correlation between relaxation time and change of viscosity as function of temperature. At low temperatures either not all of the surfactants into the solution form wormlike micelles, or not all of the wormlike micelles were long enough to entangle. Therefore, relaxation time is very low at low temperatures because surfactants micelles exchange slowly at lower temperatures and they have strong hydrophobic interactions of single micelles. Then, with an increase of the temperature a very small reduction of repulsion between the head-groups and the hydrophobic micellar aggregates (interactions between the hydrophobic chains located near to the micelle surface) determines the increase of molecular aggregates. Then, the aggregates accomplish a cylinder to worm-like micelles (Figure 64) increasing the viscosity and allowing to the system to release the stress quickly [252]. Similarly, an increase of the micelle length often leads to lower viscosity due to faster relaxation, because the triggering tricks consist essentially in reducing the preferred curvature of the micelles.

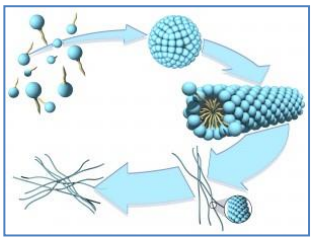

Figure 64: worm micelles

Moreover, for an entangled network of wormlike micelles, junctions provide a mean relax stress such to increase viscosity. Hence, at maximum of viscosity, fluorocarbon chains are removed from contact with water and are subjected to packing constraints because of the polar head group requirements that should remain at the aggregate–water interface and the micelle core should have the hydrocarbon chains into the liquid [236]. Consequently, they are incorporated into the micelle core and the surfactant forms compact micelles with increasing of the relaxation time. Then, an increase of temperature determines degradation process of micelles leading an decrease of viscosity and decreasing of relaxation time.

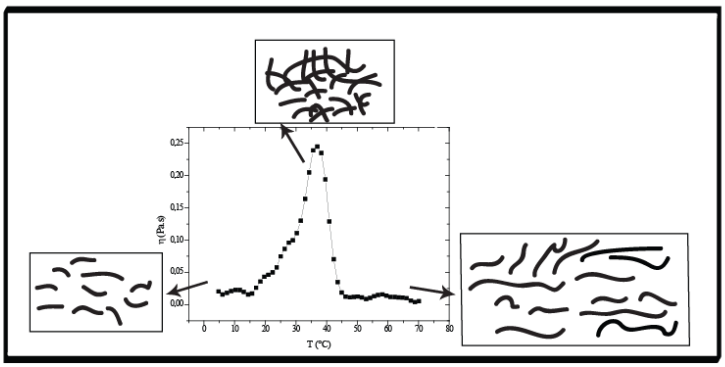

Figure 65: micelles transition as function of viscosity

Also, the decrease in time relaxation with increasing of temperature was attributed to the shift in worm-like to cylinder transition (Figure 65), yielding shorter cylinder at higher temperatures. The decreased counter length was thought to cause a transition from an entangled network to a semi-dilute solution in which the shorter aggregates no longer overlap. However, the decreasing in viscosity at τ_b with increasing of temperature is due an high free-energy cost of hemispherical ends formation and consequently one-dimension growth is favored due to the very strong interactions of chains, so relaxation time is low.

The temperature dependence of relaxation time can be obtained by Arrhenius law [236] in eq. 19:

$$\tau = \text{Aexp}\,(-\frac{E_t}{T}) \qquad 19$$

where A is characteristic constant of the system and E_t is the activation energy of flow and the viscosity, function of $\bar{L}$. However, the activated state in the process of stress relaxation is not the formation of two ends, but the formation of junctions, which correspond to smaller curvature than ends or cylinders.

Kato et al. attribute the decrease in the activation barrier with temperature to the continuous transition from an entangled to a branched micellar network.

9.3.7 Strain-frequency

The storage modulus (G') and the loss modulus (G") as function of strain at 20, 30, 40 and 50 °C and frequency (1 Hz) for all concentrations were analyzed. Examples of measurements are shown in Figures 66 and 67.

G' and G" are independent of the strain from 0.01 - 30 %, indicating that the sample is an elastic hydrogel in this range of strain.

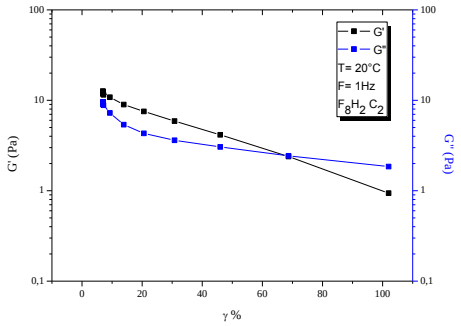

Figure 66: G' and G" of F_8H_1 as function of strain at C_2

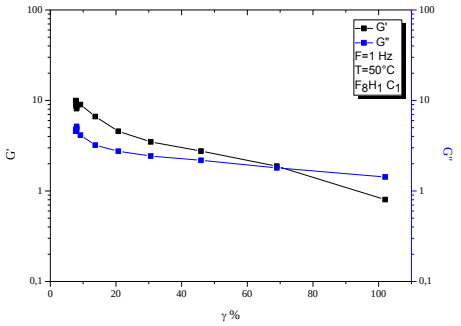

Figure 67 :G' and G" of F_8H_2 as function of strain at C_1

After setting frequency of 1 Hz and strain to 20 % the storage modulus (G') and the loss modulus (G") as function of temperature were studied: G' are always larger than G" suggesting that the gels are stable in the range 5 - 70 °C, F= 1 Hz and strain 20 %.

However, the thermo-responsive viscoelastic fluid as function of temperature, strain or frequency can be reversibly repeated simply by heating or cooling giving the same results. It is very important because generally the structure of polymer solutions can be irreversibly destroyed at rather large changes in temperature or strong stresses. This is the confirmation that these surfactants are "*living polymer systems"*.

9.3.8 Conclusion

By the analyses of the loss and the storage modulus as function of frequency and strain, temperature, concentrations, the surfactants synthesized have had viscoelastic properties. Then, the analyses of loss and storage modulus as function of temperature (5 - 70 °C), strain (20 %) and frequency (1 Hz), provide the stability of the hydrogels in the range analyzed.

Also they show a change of viscosity as function of temperature due to the formation and breaking of entangled micelles.

9.4 Polarizing Optical Microscopy (POM)

The solutions of surfactants F_8H_1 and F_8H_2 show rubber-like behavior (Figures 68 - 69). Polarizing optical microscopy images were carried out to investigate the behavior of these hydrogels structures as function of temperature.

Figure 68: rubber-like behaviour of solution of F_8H_1

Figure 69: rubber-like behaviour of solution of F_8H_2

9.4.1 Measurements

A microscope (Olympus BX60) equipped with a heating stage was used to observe the texture of samples during the heating and the cooling processes. Samples kept between cover slips were heated from 20 to 200 °C and their changes were monitored. The samples were illuminated with linearly polarized light and analyzed through a crossed polarizer. To capture images at different critical temperatures, a video camera and a PC were used.

9.4.2 Results

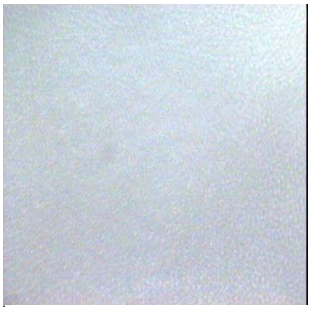

Figure 70: POM image F_8H_1 at C_2 mol/L (20°C)

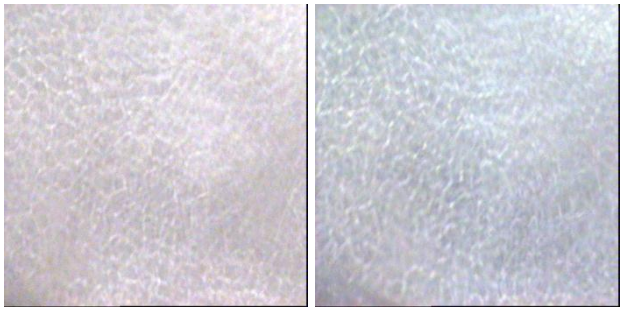

Figure 71: POM image of F_8H_2 at C_2 (37°C)

Figure 70 shows the POM image of F_8H_1 at 20 °C (near to the temperature of maximal viscosity). The structural feature in this image is little spherical nodules with several junctions. Instead, Figure 71 shows POM images of F_8H_2 at 37 °C (temperature of viscosity maximum), where cylinder aggregates linked together at junctions can be observed.

9.5 Cryo-SEM images

The surfactant F_nH_m with n= 4, 6, 8 and m= 1, 2 were further characterized using cryogenic scanning electron microscopy (Cryo-SEM), a powerful microscopy technique capable of imaging nanometer scale topographical features in concentrated fluids and soft solids.

Contrast is obtained with this technique by subliming water from the surface layer of a cryo-fractured specimen, leaving behind the frozen material originally dispersed in the aqueous medium.

9.5.1 Procedure

Cryogenic scanning electron microscopy (Cryo-SEM) images were obtained with a FESEM 6700F JEOL microscope (Japan). One drop of the sample was rapidly frozen in nitrogen slush at - 220 °C and transferred under vacuum in the cryo-fracture apparatus (Alto

2500 GATAN UK) chamber where it was fractured at -100 °C approximately 2E-9 bar and maintained at this temperature during 7 min for sublimation to expose the less volatile structure while avoiding recrystallization of the remaining vitrified water. It was then metalized with AuPd and introduced into themicroscope chamber where it was maintained at -100 °C during the observation. The high pressure lowers the supercooling limit of water and greatly elevates its viscosity, thereby yielding fast-frozen samples with negligible freezing artifacts. To ensure reproducibility, the selection of micrographs presented in this chapter was chosen from a fifty number of negatives.

9.5.2 Results F_nH_m

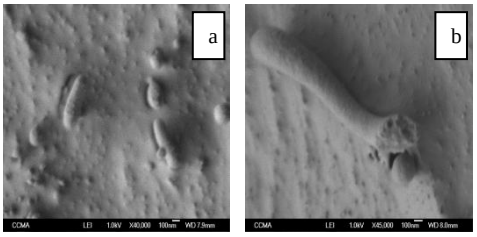

Figure 72: Representative Cryo-SEM micrographs of F_8H_1

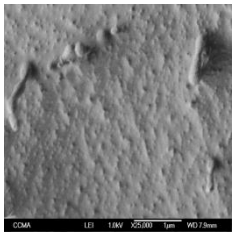

Figure 73: Representative Cryo-SEM micrographs of F_8H_1

Cryo-SEM selected images were presented to establish the morphologies associated with mixtures. Figure 72 a shows a Cryo-SEM image (100 nm) of F_8H_1 mixture in water. The predominant structural feature in this image is spherical nodules, with little evidence of branches or cylindrical aggregates. Figure 72 b shows a giant cylinder micelle in medium of a little spherical nodulus. Figure 73 (1 μm) shows little cylinder aggregates linked together at junctions.

Figure 74 a and b (1 μm) show little cylinder aggregates branches. The basic structural element of the random network appears to be approximately cylindrical, with a diameter of 50 – 100 nm, consistent with the dimension extracted from the form factor scattering.

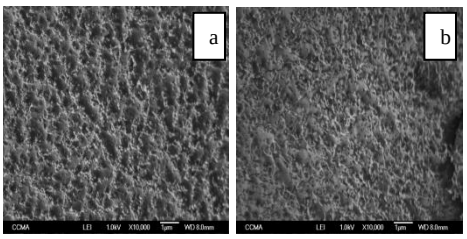

Figure 74: Representative Cryo-SEM micrographs of F_8H_2

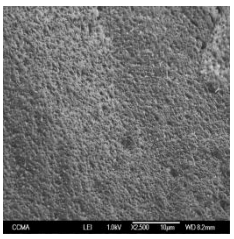

Figure 75 Representative Cryo-SEM micrographs of F_6H_2

Although it is impossible to determine the aspect ratio with any certainty, these cylinders appear to be rather long, with length-to-radius exceeding at least 30 - 40 nm. This image reveals a densely connected, random, network morphology. Strands of surfactants, roughly

40 - 50 nm in length, are linked together at junctions that range from simple 3- fold unions to larger, flat, multifunctional connections (probably the same connections that we can see in the POM images). The same results were found for F_6H_2 shows in Figure 75 (10 μm).

In contrast to spheres, cylinders, and vesicles, there is no way to continuously expand (dilate) a three-dimensional network formed from bulk (hydrophobic) cylindrical struts and multifunctional branches. The preferred local structure is dominated by Y-junctions, thus leading to the formation of a dense network under equilibrium conditions.

Branching in cylindrical micelles is less obvious at low hydrocarbon chain due to the chain packing constraints associated with the formation of Y-junctions.

10 Antibacterial tests

The antimicrobial activity tests of some surfactants synthesized were performed in collaboration with *Centre de Transfert de Technologie du Mans -Pôle Ingénierie Biologique et Médicale* (Le Mans, France).

Antibacterial and antifungal activities were evaluated using measurement of the Minimal Inhibitory Concentration (MIC). Four microorganisms were used: *Pseudomonas Aeruginosa* (ATCC 10145), *Staphylococcus Aureus* (ATCC 6538), *Aspergillus Niger* (ATCC 6275), *Candida Albicans* (ATCC 10231).

10.1 Cultures of microorganisms

The bacteria were grown on agar Mueller-Hilton (pH = 7.3) at T= 37 °C, while the yeasts on agar Saboraud (pH = 6) at 25 °C. After 18 - 24 h of incubation, a suspension of bacteria was realized in a broth and the optical density was measured at λ = 600 nm. The initial concentration of bacteria was 1.10^8 UFC^2 mL^{-1}. The mushrooms were incubated for 5 days at T= 25 °C.

10.2 Preparation of antimicrobial solutions

All the synthesized compounds were weighed (40 mg), diluted with water (10 mL) and cleaned by pass through 0.2 μm pore diameter microporous filters to prepare the stock solutions of 200 mg mL^{-1}.

The serial dilution from 50 to 50000 μL were made in a 96 - wells plate. Each well 20 μL of a bacterial suspension, obtained from 24 h culture, contained ~1.10^6-1.10^8CFU mL^{-1}. The

plates were incubated at 37° C for 24 h for *Pseudomonas Aeruginosa* ATCC 10145 (PA), *Staphylococcus Aureus* ATCC 6538 (SA), *Candida Albicans* ATCC 10231 (CA), and 48 h for *Aspergillus Niger* ATCC 6275 (AN) at T= 25 °C. These experiments were carried out in triplicate.

10.3 Antimicrobial evaluation

Antibacterial activity of surfactants was evaluated by the measure of Minimal Inhibitory Concentration (MIC) expressed in μmol L^{-1}. The MIC were determined by broth micro-dilution methods according to NCCLS standards [253].

The growth of microorganisms was estimated by the measure of absorbance λ= 620 nm for the bacteria and yeasts and by visual observation for the mould.

10.4 Results

The MIC values obtained for all the synthesized molecules are reported in Table 16. For all the synthesized surfactants no growth towards Aspergillus Niger was observed after 24 h of incubation. Hence, the value of MIC was determinate after 48 h of incubation.

For the first group of surfactants synthesized (F_nH_m) it observed:

- The surfactants F_8H_1 and F_8H_2 showed only an activity towards Staphylococcus Aureus and Candida Albicans.
- The surfactants F_6H_1 and F_6H_2 were active towards any of four microorganisms with the exception of F_6H_1 towards Aspergillus Niger.
- The surfactant F_4H_1 was no active toward the four microorganisms. The surfactant F_4H_2 showed only an activity towards Staphylococcus Aureus.
- All the second group of surfactants synthesized (F_nH_mX) were active towards four microorganisms studied.

Table 16: MIC results obtained for the synthesized surfactants

Surfactants	MIC PA [μmol L^{-1}] (24 hours)	MIC SA [μmol L^{-1}] (24 hours)	MIC CA [μmol L^{-1}] (24 hours)	MIC AN [μmol L^{-1}] (24 hours)	MIC AN [μmol L^{-1}] (48 hours)
F_8H_1	>148.6	37.1	148.6	a	>148.6
F_8H_2	>303.9	38	152.0	a	>303.91
F_6H_1	603.9	151.0	603.9	a	>603.9
F_6H_2	2019	252.4	2019	a	2019
F_4H_1	>2504.9	>2504.9	>2504.9	a	>2504.9
F_4H_2	>10003.1	10003.1	>10003.1	a	>10003.1
F_8H_1Br	125.3	15.7	125.3	a	250.5
F_8H_2Br	919.5	14.4	57.5	a	229.9
F_8H_2I	177.4	11.1	44.4	a	177.4

a: no growth was observed after 24 h of incubation

10.4.1 Influence of the fluorinated and alkyl chains

The values of MIC of Staphyloccocus Aureus (SA) and Candida Albicans (CA) as function of fluorinated chain are represented in Figure 76. The antimicrobial activity was influenced by fluorinated chains length leading to lowest values for the surfactants F_8H_m. Then, the hydrocarbon chain had only a weak influence on the values of MIC.

Also, Figure 77 shows the values of MIC of SA as function of fluorinated chain for F_nH_2. There is a linear relation between the value of MIC and the number of carbon in fluorinated chain.

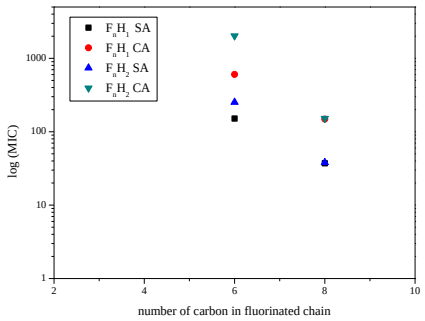

Figure 76:SA and CA values of MIC as function of fluorinated chain for F_nH_2

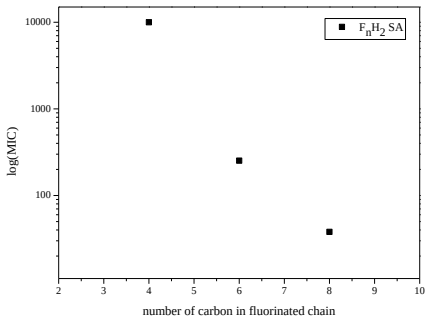

Figure 77:SA values of MIC as function of fluorinated chain for F_nH_2

Figure 78 shows the values of PA, SA, CA, AN MIC for F_8H_mBr. The increase of alkyl chain has a little influence on the biological activity. Only in the case of PA there is a abrupt decrease of antimicrobial activity as a rise of hydrocarbon chain length.

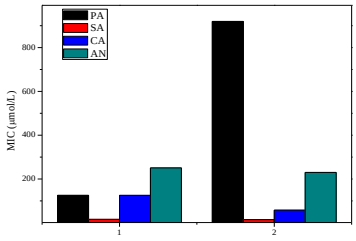

Figure 78: MIC of F_8H_mBr as function of alkyl chain

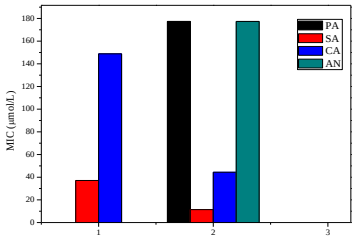

Figure 79: MIC of F_8H_mI as function of alkyl chain

Figure 79 shows MIC values for F_8H_mI as function of alkyl chain. The surfactant F_8H_1I is no active towards PA and AN. In this case, the increase of alkyl chain contribute to enhance the solubility of surfactant and also to enhance probably the adsorption on bacteria cell in order to affect in a favorable manner on the microbial activity.

10.4.2 Influence of counter-ion

The surfactant F_8H_1Br is active towards the four microorganisms studied while the surfactants F_8H_1I is active only SA and CA. In this case, the only change of iodide counter-ion into bromide provides the antimicrobial activity, probably because the surfactant become more soluble in water medium and the adsorption is favorite.

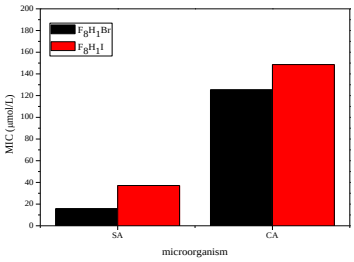

Figure 80: MIC of F_8H_1Br and F_8H_1I

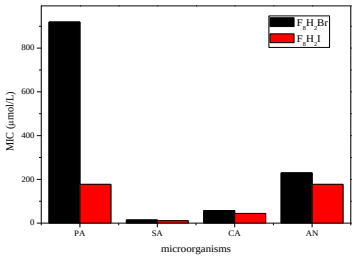

Figure 81: MIC of F_8H_2Br and F_8H_2I

Figure 80 shows the values of MIC of SA and CA for F_8H_1Br and F_8H_1I. The surfactant F_8H_1Br is more active than F_8H_1I. Figure 81 shows the values of MIC of PA, SA, CA and AN for F_8H_2Br and F_8H_2I. The surfactants F_8H_2I is more active than F_8H_2Br, in particular towards PA probably because the increase of hydrocarbon chain enhances the amphiphilic properties of surfactant and affects in a unfavorable manner on the biocidal activity.

11 Conclusion

Two groups of partially quaternary ammonium salts were synthesized according with two-step reaction.

A first series of hybrid surfactants (F_nH_m) with general formula $F(CF_2)_nCH_2CH(OH)CH_2N(CH_2)_mHCH_3I^-$ (with n= 4, 6, 8 and m= 1, 2, 3, 4, 6, 8), obtained by reaction of semifluorinated tertiary ammine with iodomethane in acetonitrile as solvent, was synthesized.

A second series hybrid surfactants (F_nH_mX) with general formula $F(CF_2)_nCH_2CH(OH)CH_2N(CH_2)_mH(CH_2)_mI^-$ (with n= 4, 6, 8 and m= 1, 2), obtained by reaction of semifluorinated tertiary ammine with iodoalkane in acetonitrile as solvent, was synthesized. Then, a change of counter-ion into a column resin was carried out to obtain the F_nH_mBr pairs.

In order to select the surfactants for specific purposes physico-chemical properties were investigated.

In the first group of surfactants synthesized of general formula F_nH_m, the length of the fluorinated chain (hydrophobic group)

- decreases the solubility of the surfactant in water and decreases the values of surface tensions and cmc.
- causes closer packing of the surfactant molecules at the interface increasing the tendency of the surfactant to adsorb at an interface ($\Delta G^0_{ads} > \Delta G^0_{mic}$).
- affects strongly the curvature of surfactant's layer forming bimodal distribution of sizes and large aggregates (R= 400 - 700 nm) (worm-like micelles) with several junctions, as observed in the Cryo-SEM and POM images.
- increase the positive values of zeta potential that correspond with the positive change of head group
- contributes to form hydrogels for the surfactants completely soluble in water

The introduction of long hydrocarbon branchings into the molecules

- increases the area per molecule (A) at the liquid/air interface reducing the effectiveness of adsorption and thus obtaining higher values of surface tensions.
- decreases strongly the solubility of the surfactant in water leading to the insolubility of several surfactants.
- contributes to increase the hydrophobicity of surfactant leading to lower values of cmc.

- causes strong interactions of chains increasing the micelle's size and proving bigger values what expected for spherical aggregates

Rheological measurements to investigate the viscoelastic properties of F_nH_m solutions with n=8 and m=1, 2 by oscillatory-shear measurements were carried out. A change of viscosity (in particular a maximal value) as function of temperature was observed showing a thermo-responsive behavior of these surfactants. It is due to the formation and the breaking of entangled micelles as function of temperature. The value of maximal viscosity changes as function of concentration because of the formation of other self-assembled structures. Then, the micellar networks can be takes place to lower temperature.

Then, the maximal viscosity values are higher for F_8H_2 for all concentrations to have a positive contribute of hydrocarbon chains to form larger molecular aggregates. The analyses of the viscoelastic properties as function of frequency and strain leaded to a storage modulus (G') always larger of the loss modulus (G") suggesting that the hydrogels are stable in the range analyzed. These worm-likes micelles are dynamic systems (living polymers) with a reversible breaking / recombination of the aggregates. Then, their unique viscoelastic thermo-responsive behavior suggests the use in central-heating systems as DRAG redactions fluid mixtures.

Hence, antimicrobial tests were performed to evaluate the Minimal Inhibitory Concentration (MIC) on four microorganism of some surfactants synthesized (in particular the surfactants that are soluble in water medium).

The fluorinated chain length influences the antimicrobial activity leading to lower values of MIC for the long chains. Then, the surfactants with a short fluorinated chain are no activities toward a several microorganisms. Instead, the hydrocarbon chain has only a weak contribute to reduce the antimicrobial effect.

In the second group of surfactants synthesized of general formula F_nH_mX the effect of the counter-ion on physico-chemical properties was investigated.

The change of iodide by bromide:

- causes a increase of the surface tension values in comparison with the values of the same fluorocarbon and hydrocarbon chain lengths.
- reduces the hydrophobicity character.
- enhances the cmc values.
- decreases the values of area per molecule enhancing the kinetic of adsorption.
- causes the lost of hydrogel behavior.
- increases the antimicrobial activity, due to a better adsorption on bacteria cells.

INDEX

1 List of Abbreviations

AN: Aspergillus Niger

ARMD: age related macular degeneration

CA: Candida Albicans

CEC: cation exchange capacity

cmc: concentration micellar critic

Cryo-SEM: cryogenic scanning electron microscopy

DLS: Dynamic light scattering

DPPC: dipalmitoylphosphatidylcholines

FMRI: fluoro magnetic resonance imaging

GC-MS: Gas chromatography-mass spectrometry

IOP: intraocular pressure

HIV: human immunodeficiency virus

MIC: minimal inhibitory concentration

MRI: magnetic resonance imaging

MS: mass spectrometry

NCCLS: National Committee for Clinical Laboratory Standards

n.f.o: no foam observed

n.g.o: no gel observed

NMR: nuclear magnetic resonance

n.s: phase separation (non soluble)

NRDS: neonatal respiratory distress syndrome

o: opalescent

PA: Pseudomonas Aeruginosa

PDR: regmotous retinal detachment

PLGA: poly(lactic-*co*-glycolic acid)

PEG: polyoxyethylen glycol

PFOB: perfluorooctylbromide

PFEs: Partially fluorinated ethers

$PFE_{n,m}$: partially fluorinated ether n,m

PFCs: perfluorocarbons

PFCLs: perfluorocarbon liquids

PMMA: poly methyl methacrylate

POE: polyoxyethylene

POM: polarize optical microscopy

PS: pulmonary surfactant

PVR: proliferative vitreous retinopathy

Quats: quaternary ammonium salts

s: soluble

SA: Staphylococcus Aureus

SRT: standard refrigeration temperature

STP: standard temperature pressure

USCa: ultrasounds contrast agents

2 List of Symbols

α = degree of ionization of the surfactant

a = particle radii

A= area per molecule

γ= surface tension

γ_0= surface tension of the water

γ_{cmc}= surface tension at cmc

γ_i= interfacial tension

γ_f= surface tension of the foam

γ_h= surface tension hydrocarbon burning fuel

γ_{hf}= interfacial tension between burning fuel and foam

Γ= surface excess

Γ_m= surface excess concentration at saturation

C= concentration

C(L)= normalized number density of micelles of length L

ΔG^0_{ads}= free energy of micellization

ΔG^0_{mic}= free energy of adsorption

D= diffusion coefficient

E_{break} = scission energy required to break a micelle in two part

E_p= free penalty energy

E_t = activation energy

ε_0= permittivity of vacuum

ε_r= relative permittivity

F= Faraday

F_T= total force

f (φ)= volume fraction

G_0 = plateau modulus

G'= elastic modulus

G''= loss modulus

H_0= monolayer curvature

I= ionic stretch

θ= contact angle

ζ= zeta potential

η= viscosity

k= monalayer bending

k= Debye length

k_B= Boltzmann constant

$\bar{L}$= mean length

μ_E= electrophoretic mobilities

N= number of Avogadro

P= pressure

p = contact length

π= surface pressure

R= size of particle (nm)

R= gas constant

r= radium

S_{spr}= spreading coefficient

τ_b = breaking time

τ_{rep}= reptation time

T= temperature

T_k= temperature of Krafft

x_{cmc}= the mole fraction of the surfactant in the liquid phase at the cmc

φ = volume fraction

V_m= mole volume

W= weigh of plate

ΔW= variation weight

ω= frequency

3 List of Figures

4 List of Tables

5 List of Schemes

6 References

1. J. H. Fried, E. F. Sabo, *J. Am. Chem. Soc.*, **1953**, 75, p: 2273-2274.
2. J. H. Fried, E. F. Sabo, *J. Am. Chem. Soc.*, **1954**, 76, p: 1455-1456.
3. R. E. Banks, B. E. Smart, J.C. Tatlow, *Organofluorine Chemistry: Principles and Commercial Applications*, **1994**, Plenum Press, New York, p: 57-88.
4. J. G. Riess, *Tetrahedron*, **2002**, 58, p: 4113-4131.
5. S. Pastorekova, D. Vullo, A. Casini, A. Scozzafava, J. Pastorek, I. Nishimori, T. Supuran, *J. Enzyme Inhib. Med. Chem*, **2005**, 20, p: 211-217.
6. W. K. Hagmann, *J. Med. Chem.*, **2008**, 51, p: 4359-4369.
7. J. C. Tatlow, M. Stacey, *Adv. Fluorine Chem.*, **1960**, 1, p: 166-198.
8. P. Kirsch, *Modern fluoroorganic chemistry*, ed. Wiley-Vch, **2004,** p: 25-35.
9. R. Kirk, L. Kenneth, *J. Fluorine Chem.*, **2006**, 127, p: 1013-1029.
10. Peters, *Proceedings of the Ciba Foundation Symposium on Carbon- Fluorine Compounds: Chemistry, Biochemistry, and Biological Activities*, ed. Elsevier, **1972**, Amsterdam, p: 55-76.
11. J. C. Tatlow, M. Stacey, *Adv. Fluorine Chem.*, **1960**, 1, p: 166-198.
12. R. D. Fowler, W. B. Burford III, J. M. Hamilton, H. C. Anderson, C. E. Weber, R. G. Sweet, *Ind. Eng. Chem*, **1947**, 39, p: 319-329.
13. A. Zaggia, L. Conte, G. Padoan, R. Bertani, *J. Surfact. Deterg.*, **2010**, 13, p: 33-40.
14. J. M. Corpart, M. Pabon, *J Fluorine Chem.*, **2002**, 114, p: 149-156.
15. F. Guittard, S. Geribaldi, *J. Fluorine Chem.*, **2001**, 107, p: 363-374.
16. B. Ameduri, B. Boutevin, F. Guida-Pietrasanta, A. Rousseau, *J. Fluorine Chem.*, **2001**, 107, p: 397-409.
17. P. Thebault, E. Taffin de Givenchy, S. Géribaldi, R. Levy, Y. Vandenberghe, F. Guittard, *J. Fluorine Chem.*, **2010**, 131, p: 592-596.
18. J. G. Riess, *Curr. Opin. Colloid Interface Sci.*, **2003**, 8, p: 259-266.
19. M. J. Colthurst, P. S. Hiscott, R. L. Williams, I. Grierson, *Biomaterials*, **2000**, 21, p: 649-665.
20. M. Q. Huang, P. H. Basse, Q. Yang, J. A. Horner, T. K. Hichens, Ho Chien, *Magn. Reson. Imaging*, **2004**, 22, p: 645-652.
21. E. Tsuchida, *Blood Stubstitutes: present and future perspectives*, Elsevier, Lausanne Switzerland, **1998**, p: 327-338.
22. K. C. Lowe, *Blood Reviews*, **1999**, 13, p: 171-184.

23. L. Kresie, *Bunc Proceedings*, **2001**, 14, p: 158-161.
24. M. P. Krafft, J. G. Riess, *Biomaterials*, **1998**, 19, p: 1529-1539.
25. B. Remy, G. Deby-Dupont, M. Lamy, *Br Med Bull*, **1999**, 55, p: 277-298.
26. S. A. Dulchavsky, W. Schwarz, A. Silbergleit, *Curr. Sur.*, **2002**, 59, p: 378-383.
27. F. Golan, L. C. Clark, *Science*, **1966**, 152, p: 1755- 1756.
28. D. R. Spahn, *Critical Care*, **1999**, 3, p: 91-92.
29. R. Winslow, *Blood Substitutes*, **2006**, Elsevier, Great Britain, p: 259-275.
30. J. G. Weerst, J. G. Riess, *Curr. Opinion Colloid Interf Sci.*, **1996**, 1, p: 652-659.
31. J. C. Riess, C. Cornelus, R. Follana, M. P. Krafft, A. M. Mahe, M. Postel, L. Zarif, *Adv Exp Med Biol.*, **1994**, 345, p: 227-234.
32. K. C. Lowe, *Blood Reviews*, **1999**, 13, p: 171-184.
33. J. G. Riess, *Tetrahedron*, **2002**, 58, p: 4113-4131.
34. D. R. Spahn, *Critical Care*, **1999**, 3, p: 91-92.
35. O. M. Moiseenko, I. Vorobev, B. L. Belyaev, V. A. Srednyakov, Yu. V. Luzganov, *Pharmaceutical Chemistry Journal*, **2009**, 43, p: 263-266.
36. P. Cabrales, A. G. Tsai, M. Intaglietta, *J. Am. Coll. Surg.*, **2007**, 204, p: 225-235.
37. H. P. Wiedemann, *Clinics in Chest Medicine*, **2000,** 21, p: 543-554.
38. M. S. Conrad,Y. V. Chang, *J. Magn. Reson.*, **2006**, 181 p: 191-198.
39. B. Uslu, N. Aydogan, H. Tanaci, *J. Colloid Interface Sci.*, **2011**, 360, p: 163-174.
40. J. C. Fitzpatrick, B. S. Jordan, N. Salman, J. Williams, W. G. Cioffi, B. A. Pruitt, *J. Pediatric Surgery*, **1997**, 32, p: 192-196.
41. R. Herold, U. Pison, S. Schfirch, *Colloids Surf. A*, **1996**, 114 p: 165-184.
42. J. Deschamps, M. F. Costa-Gomez, D. H. Menz, *J. Fluorine Chem.*, **2004**, 125, p: 1325-1329.
43. K. N. Makarov, A. S. Kabalnov, O. V. Shcherbakova, *J. Fluorine Chem.*, **1990**, 50, p: 271-284.
44. R. H. Notter, *Lung surfactants: Basic science and clinical applications 149th ed.;* ed. M. Dekker, **2000**, New York, p: 1-444.
45. J. Johansson, B. Robertson, T. Curstedt, *Med. Mol.Today*, **2000**, 6, p: 119-124.
46. M. Goldmann, M. P. Krafft, *Curr. Opin. Colloid Interface Sci.*, **2003**, 8, p: 243-250.
47. F. Gerber, T. F. Vandamme, M. P. Krafft, *Comptes Rendus Chim.*, **2009**, 12 p: 180-187.
48. F. Gerber, M. P Krafft; T. F. Vandamme, M. Goldmann, P. Fontaine, *Biophys. J.*, **2006**, 90, p: 3184-3192.

49. M. F. Paige, A. F. Eftaiha, *J. Colloid Interface Sci.*, **2011**, 353, p: 210-219.
50. O. Shibata, M. P. Krafft, *Langmuir*, **2000**, 16, p: 10281-10286.
51. T. F. Vandamme, H. M. Courrier, M. P. Krafft, S. Nakamara, O. Shibata, *Colloids Surf. A*, **2003**, 215, p: 33-41.
52. S. Nakamura, M. Rusdi, O. Shibata, Y. Moroi, Y. Abe, T. Takahashi, *J. Colloid Interface Sci.*, **2001**, 243, p: 370-381.
53. S. Lee, H. Nakahara, M. P. Krafft, O. Shibata, *Langmuir*, **2010,** 26, p: 18256-18265.
54. J. G. Riess, M. P. Krafft, A. Chittofrati, *Curr. Opin. Colloid Interface Sci.*, **2003**, 8, p: 251-258.
55. J. Krebs, C. Tsagogiorgas, M. Pukelsheim, G. Beck, B. Yard, B. Theisinger, M. Quintel, T. Luecke, *Eur. J. Pharm. Biopharm.*, **2010**, 76, p: 75-82.
56. J. G. Riess, *Curr. Opin. Colloid Interface Sci.*, **2003**, 8, p: 259-266.
57. D. M. Long, M. S. Liuand, *Radiology*, **1977**, 122, p: 71-76.
58. J. Cherif, J. L. Cohen, D. S. Segar, L. D. Gillam, J. S. Gottdiener, E. Hausnerova, D. E. Bruns, *J. Am. Cardiol.*, **1998**, 32, p: 746-752.
59. P. L. Allan, P. S. Sidhu, F. Cattin, D. O. Cosgrove, A. H. Davies, D. Do, S. Karakagil, J. Langholz, D. A. Legemate, A. Martegani, J-B. Llull, C. Pezzoli, A. Spinazzi, *Br. J. Radiol.*, **2006**, 79, p: 44-51.
60. J. Weer, A. Kabalnov, *Langmuir*, **1996**, 12, p: 1931-1935.
61. N. Tsapis, R. Diaz-Lopez, E. Fattal, *Pharm. Res.*, **2010**, 27, p: 1-16.
62. L. J. Cruz, M. Srinivas, F. Bonetto, A. Heerschap, C. G. Figdor, I. J. M. de Vries, *Biomatiarials*, **2010**, 31, p: 7070-7077.
63. K. D. Wallace, G. M. Lanza, M. J. Scott, W. P. Cacheris, D. R. Adendschein, D. H. Christy, *Circulation*, **1996**, 94, p: 3334-3340.
64. J. M. Janjic, M. Srinivas, D. K. K. Kadayakkara, E. T. Ahrens, *J. Am. Chem. Soc.*, **2008**, 130, p: 2832-2841.
65. M. Minami, Y. Imamura, M. Ueki, B. Satoh, T. Ikeda, *Br. J. Ophthalmol.*, **2003**, 87, p: 563-566.
66. J. A. Schulman, G. A. Peyman, B. Sullivan, *Surv. Ophthalmol*, **1995**, 39, p: 375-395.
67. C. Sheridan, P. Hiscott, R. M. Magee, I. Grierson, *Prog. Retin. Eye Res.*, **1999**, 18, p: 167-190.
68. O. Lundquist, S. Osterlin, *Graefes Arch. Clin. Exp. Ophthalmol.*, **1994**, 232, p: 71-74.
69. The Retina Society Terminology Commitee, *Ophthalmology*, **1983**, 90, p: 121-125.

70. D. J. D'Amico, *New Enl. J. Med.*, **1994**, 331, p: 95-106.
71. S. R.Wilkes, *J. Natl. Med. Assoc.*, **1993**, 85, p: 841-847.
72. E. Feuer, W. E. Smiddy, W. D. Irvine, H. W. Flynn, G. W. Blankenship, *Ophthalmology*, **1995**, 102, p: 1688-1695.
73. J. R. Sparrow, S. Chang, T. Iwamoto, A. Gershbein, R. Ross, R. Ortiz, *Retina*, **1991**, 11, p: 367-374.
74. F. Claudi, G. M. Cingolani, M. Massi, F. Venturi, *Eur. J. Med. Chem.*, **1990**, 25, p: 709-712.
75. T. Y. Wong, T. Ho, *Int. Ophthalm.*, **1997**, 20, p: 293-294.
76. U. Stolba, M. Velikay, A. Wedrich, Y. Li, P. Datlinger, S. Binder, *Graefes Arch. Clin. Exp. Ophthalmol.*, **1995**, 233, p: 26-30.
77. H. Meinert, *Semifluorinated alkanes and their use thereof*, **1996,** US814493.
78. T. T. Kleinberg, R. T. Tzekov, L. Stein, N. Ravi, S. Kaushal, *Surv. Ophthalm.*, **2011**, 56, p: 300-323.
79. T. V. Chirila, Y. Hong, P. D. Dalton, I. J. Constable, M. F. Refojo, *Prog. Polym. Sci.*, **1998**, 23, p: 475-508.
80. M. F. Refojo, G. G. Giordano, *Prog. Polym. Sk.*, **1998**, 23, p: 509-532.
81. D. P. Curran, J. A. Gladysz, I. T. Horvath, *Handbook of Fluorous Chemistry*, ed. Wiley, **2004**, Germany, p: 571-573.
82. N. L. Cutler, *Trans. Am. Acad. Ophthalmol. Otolaryngol.*, **1947**, 52, p: 253-259.
83. M. W. Dumm, K. H. Stenzel, A. L. Rubin, T. Miyata, *T. Arch. Ophthalmol.*, **1969**, 82, p: 840-844.
84. R. L. Williams, M. J. Colthurst, P. S. Hiscott, I. Grierson, *Biomaterials*, **2000**, 21 p: 649-665.
85. C. T. Pollak, N. E. Larsen, K. Reiner, E. Leshchiner, E. A. Balazs. *J. Biomed. Mater. Res.*, **1993**, 27, p: 1129-1134.
86. E. R. Berman, G. M. Gombos, *Acta Ophthalmol.*, **1967**, 45, p: 794-804.
87. G. A. Calabria, R. C. Pruett, C. L. Schepens, *Arch Ophthalmol Experimental study*, **1972**, 88, p: 540-543.
88. G. A. Peyman, C. P. Liang, P. Serracarbassa, N. Calixto, A. A. Chow, P. Rao, *Int. Ophthalmol.*, **1998**, 22, p: 13-18.
89. J. A. Oosterhuis, *Arch. Ophthalmol.*, **1966**, 76, p: 374-377.
90. J. Y. Lai, *J. Mater. Sci. Mater. Med.*, **2010**, 21, p: 1899-1911.
91. E. W. D. Norton, *Trans. Am. Acad. Ophthalmol. Otolaryngol.*, **1973**, 77, p: 85-98.

92. J. Mardirossian, H. A. Lincoff, A. Lincoff, P. Ligget, T. Iwamoto, F. Jakobiec, *Arch. Ophthalmol.*, **1980**, 98, p: 1610-1611.
93. H. Lincoff, S. Chang, D. J. Coleman, W. Fuch, M. Farber, *Ophthalmology*, **1985**, 92, p: 651-656.
94. H. Lincoff, A. Lincoff, C. Solorzano, T. Iwamoto, *Arch. Opthalmol.*, **1982**, 100, p: 996-997.
95. C. Baumal, R.W. Kim, *Ophthalmol. Clin. North Am.*, **2004**, 17, p: 569-576.
96. M. R. Wilson, D. A. Lee, M. O. Yoshizumi, M. Hall, *Arch. Ophthalmol.*, **1991**, 109, p: 571-575.
97. P. A. Cibis, *Vitreoretinal Pathology and Surgery in Retinal Detachment*, St Louis, CV. Mosby Pub Co, **1965**, p:116-133.
98. W. J. Foster, *Expert Rev. Ophthalmol.*, **2008**, 3, p: 211-218.
99. F. Baino, *Acta Biomaterialia*, **2011**, 7, p: 921-935.
100. T. M. Aarberg, H. Lewis, *Am. J. Ophthalmol.*, **1991**, 111, p: 15-19.
101. J. M. Zarco, J. C. Pastor, M. J. Delnozal, A. Pampliega, P. Marinero, *Eur. J. Ophthalmol.*, **1998**, 8, p: 179-183.
102. M. F. Refojo, M. Doi, *Exp. Eye Res.*, **1995**, 61, p: 469-478.
103. M. F. Refojo, M. Doi, *Exp. Eye Res.*, **1994**, 59, p: 737-746.
104. J. S. Guyton, E. G. Grafton, *Am. J. Ophthalmol.*, **1948**, p: 299-303.
105. L. C. Clark, S. J. Haidt, J. Ginsberg, *Invest. Ophthalmol. Vis. Sci.*, **1991**, 32, p: 2382-2397.
106. D. Faris, N. J. Zimmerman, *Invest. Ophthalmol. Vis. Sci.*, **1984**, 25, p: 258-265.
107. K. Kobuch, I. H. Menz, H. Hoerauf, J. Hans Dresp, V. Gabel, *Graefe's Arch. Clin. Exp. Ophthalmol.*, **2001**, 239, p: 635-642.
108. A. Morgillo, F. Malchiodi-Albedi, G. Formisano, S. Paradisi, R. Perilli, G. C. Scalzo, G. Scorcia, S. Caiazza, *J. Biomed. Mater. Res.*, **2002**, 60, p: 548-555.
109. F. Baino, *Polymers*, **2010**, 2, p: 286-322.
110. M. Napoli, L. Conte, C. Fraccaro, P. Alessi, *Chimica Oggi*, **1988**, p: 61-63.
111. C. R. Keese, I. Giaever, *Proceedings of the National Academy of Sciences*, **1983**, 80, p: 5622-5626.
112. J. Becker, D. Zeana, R. Kuckelkorn, B. Kirchhof, *Int. Ophthalmol.*, **1999**, 23, p: 17-24.
113. D. Guillon, W. Mahler, A. Skoulios, *Mol. Cryst. Liq. Cryst. Lett.*, **1985**, 2, p: 111-119.

114. M. Napoli, *J. Fluorine Chem.*, **1996**, 79, p: 59-69.
115. T. Roy, H. Meinert, *Eur. J. Ophthalmol.*, **2000**, 10, p: 189-197.
116. M. Napoli, L. Krotz, L. Conte, R. Seraglia, P. Traldi, *Rapid Commun. Mass Spectrom.*, **1993**, 7, p: 1012-1016.
117. J. E. Brady, M. P. Turberg, *J. Am. Chem. Soc.*, **1988**, 110, p: 7797-7801.
118. L. Conte, M. Napoli, A. Guerrato, *J. Fluorine Chem.*, **2001**, 110, p: 47-58.
119. P. Dynarowicz-Łatka, M. Broniatowski, W. Witko, *J. Fluorine Chem.*, **2005**, 126, p: 79-86.
120. P. Lo Nostro, *Current Opinion in Colloid and Interface Science*, **2003**, 8, p: 223-226.
121. E. Kissa, *Fluorinated Surfactants and Repellents second ed.*, ed. M. Dekker, **2001**: New York, p: 1-615.
122. P. Lang, P. Marczuk, M. Moller, *Colloids Surf. A*, **2000**, 163, p: 103-113.
123. P. D. I. Fletcher, B. P. Binks, S. N. Kotsev, R. L. Thompson, *Langmuir*, **1997**, 13, p: 66-69.
124. R. D. Dunlap, R. G. Bedford, *J. Am. Chem. Soc.*, **1958**, 80 p: 282-285.
125. M. V. Aspiotis, M. I. Stefaniotou, G. D. Kitsos, C. D. Kalogeropoulos, I. C. Asproudis, K. G. Psilas, *Eur. J. Ophthalmol.*, **2002**, 12, p: 518-522.
126. B. Kirchhof, D. Wong, J. V. Meurs, R. D. Hilgers, M. Macek, N. Lois, N. F. Schrage., *Am. J. Ophthalmol.*, **2002**, 133, p: 95-101.
127. A. Kolck, H. Gerding, *Ophthalmologe*, **2004**, 101, p: 255-262.
128. Y. El-Shabrawi, B. Schatz, A. Haas, G. Langmann, *Retina*, **2004**, 24, p: 567-573.
129. X. Benouaich, V. Pagot-Mathis, A. Mathis, I. Rico-Lattes, A. Dumoulin, *J. Fr. Ophtalmol.*, **2006**, 29, p: 137-145.
130. W. W. Lai, D. Wong, K. K. Li, P.L. Leow, *Graefes Arch. Clin. Exp. Ophthalmol.*, **2008**, 246, p: 1633-1635.
131. F. Genovesi-Ebert, S. Rizzo, C. Belting, A. Vento, F. Cresti, *Graefes Arch. Clin. Exp. Ophthalmol.*, **2005**, 243, p: 1153–1157.
132. T. Stappler, M. R. Romano, J. Marticorena, C. Groenewald, I. Pearce, S. K. Gibran, I. Pearce, S. K. Gibran, D. Wong, H. Heimann, *Graefes Arch. Clin. Exp. Ophthalmol.*, **2008,** 246, p: 1541-1546.
133. A. Lappas, A. M. H. Foerster, B. Kirchhof, *Acta Ophthalmol.*, **2009**, 87, p: 866-870.
134. F. Genovesi-Ebert, S. Rizzo, A. Vento, F. Cresti, E. Di Bartolo, C. Belting, *Retina*, **2007**, 27, p: 613-620.

135. A. Sekiya, K. Ueda, *Chem. Lett.*, **1990**, 6, p: 609-612.
136. D. F. Persico, H. S. Huang, R. J. Lagow, *J. Org. Chem.*, **1988**, 53, p: 78-85.
137. P. L. Coe, M. Brandwood, C. S. Ely, J. C. Tatlow, *J. Fluorine Chem.*, **1975**, 5, p: 521-535.
138. E. Hayashi, T. Abe, H. Baba, K. Kodaira, S. Nagase, *J. Fluorine Chem.*, **1980**, 15, p: 353-380.
139. R. H. Mobbs, R. D. Chambers, *Adv. Fluorine Chem.*, **1965**, 4, p: 50-112.
140. P. Tarrant, J. A. Young, *J. Am. Chem. Soc.*, **1950**, 72, p: 1860-1861.
141. M. A. Smook, A. L. Henne, *J. Am. Chem. Soc.*, **1950**, 72, p: 4378-4380.
142. S. Langner, P. Rollinson, **1959**, US814493.
143. O. Scherer, H. Millauer, B. Wojetch, *Verfahren zur herstelung von polymeren fluoroalkyl-vinyl-aether*, **1968**, DE 1720799A1.
144. M. Tamura, J. Murata, A. Sekiya, *Green Chem.*, **2002**, 4, p: 60-63.
145. I. L. Knunyants, A. V. Fokin, A. I. Shchekotikhin, *Izv. Akad. Nauk.*, **1953**, 282, 2.
146. W. M. Sweeney, J. D. Park, S. L. Hopwood, J. R. Lacher, *J. Am.. Chem. Soc.*, **1956**, 78, p: 1685-1686.
147. G.K.S. Prakash, J. Hu, A. Clah, *Arkivoc*, **2003**, 3, p: 104-119.
148. J. March, M. B. Smith, *Advanced organic Chemistry reactions: mechanism and structures Sixth edition*. ed. Wiley, **2007**: Hoboken, New Jersey, p: 529-531.
149. N.O. Brace, *J. Fluorine Chem.*, **1999**, 96, p: 1-25.
150. R. Miethchen, M. Hein, *Tetrahedron Letters*, **1998**, 39, p: 6679-6682.
151. R. Polak, V. Cirkva, O. Paleta, K. Kefurt, J. Moravcova, M. Kodıcek, S. Forman, *Carbohydr. Res.*, **2004**, 339, p: 2177-2185.
152. Y. Fujii, E. Tamuba, S. Yano, H. Furugaki, *Fluorine-containing ether compounds*, **2000**, US6060626.
153. C. Jin, W. Huang, D. K. Derzon, T.A. Huber, J. A. Last, P. P. Provencio, A.S. Gopalan, M. Dugger, D. Y. Sasaki, *J. Colloid Interf. Sci.*, **2004**, 272, p: 457-464.
154. L. Conte, A. Zaggia, M. Beccaro, E. Bettini, P. Signori, *Fluoroalkiloxy alkanes, process for production and uses thereof*, **2009**, WO133575A1.
155. A. Leszczyńska, J. Njuguna, K. Pielichowski, J. R. Banerjee, *Thermochimica Acta*, **2007**, 454, p: 1-22.
156. Q. Zhou, S. Deng, Q. Yu, Q. Zhang, G. Yu, J. Huang, H. He, *Chemosphere*, **2010**, 78, p: 688-694.
157. G-L. Li, L-Q. Zheng, J-X. Xiao, *J. Fluorine Chem.*, **2009**, 130, p: 674-681.

158. P. Lo Nostro, C. Cardelli, S-H. Chen, *Polym. Prepr.*, **1999**, 40, p: 1101-1107.
159. J-M. Thomassin, C. Pagnoulle, D. Bizzari, G. Caldarella, A. Germain, R. Jérôme, *Solid State Ionics*, **2006**, 177, p: 1137-1144.
160. R. E. Grim, *Clay Mineralogy*. ed. Mcgraw-Hill, **1953**: New York, p: 1-422.
161. P. Praus, M. Turicová, S. Študentová, M. Ritz, *J. Colloid Interf. Sci.*, **2006**, 304, p: 29-36.
162. J. P. Sterte, J. E. Otterstedt, *Stud. Surf. Sci. Catal.*, **1987**, 31, p. 631-648.
163. J-H. Chang, Y. Uk An, D. Cho, E. P. Giannelis, *Polymer*, **2003**, 44, p: 3715-3720.
164. D. H. S. Souza, K. Dahmouche, C. T. Andrade, M. L. Dias, *Appl. Clay Sci*., **2011**, 54, p: 226-234.
165. A. K. Mishra, S. Bose, T. Kuila, N. H. Kim, J. H. Lee, *Progress in Polymer Science*, **2011** (*In Press*).
166. C.-W. Chiu, C-C. Chu, W-T. Cheng, J-J. Lin, *Eur. Polym. J.*, **2008**, 44, p: 628-636.
167. R. Gosalawit, S. Chirachanchai, S. Shishatskiy, S. P. Nunes, *Solid State Ionics*, **2007**, 178, p: 1627-1635.
168. N. Marquet, E. Grunova, E. Kirillov, M. Bouyahyi, C. M. Thomas, J-F. Carpentier, *Tetrahedron*, **2008**, 64, p: 75-83.
169. G. Dogmak, *Dtsch Med Wochenschr*, **1935**, 61, p: 829-832.
170. G. Billard, L. Dieulafe, *L. Compt. Rend. Soc. Biol.*, **1904,** 56, p: 146-150.
171. Y. Lacko, M. Pavlikova, F. Devinsky, D. Mlynarcik, *Coll. Czech. Chem. Comm*, **1995**, 60, p: 1213-1227.
172. Y. Lacko, M. Pavlikova-Moricka, F. Devinsky, L. Masarova, D. Mlynarcik., *Folia Microbiol.*, **1994**, 39, p: 176-180.
173. M. Diz, A. Manresa, A. Pinazo, P. Erra, M. R. Infante, *J. Chem. Soc. Perkin Trans. 2*, **1994**, 2, p: 1871-1879.
174. J. P. Bell, A. K. Doyle, R. F. Farmer, J. F. Gadberry, D. Lukas, R. B. Mirviss, *Biocidal preservatives*, **1999**, WO9943212.
175. E. Arrieta, J. M. Parel, M. C. Aguilar, E. Lee, F. Ponce, E. Hernandez, T. Albini, S. Dubovy, M. Beccaro, C. Mariotti, Fort Lauderdale, FL, USA. p. May 2-6, **2010**.
176. E. A. Quintero, M. C. Aguilar, C. Medina, E. Hernandez, S. Dubovy, J. M. Parel, *ARVO Annual Meeting*, **2009.**
177. C. Mariotti, *Use of HeavySIL 1500, a new heavier than water endotamponade in complicated retinal detachment surgery*, The annual meeting of the Retina Society, September 22-25, **2011,** Rome, Italy.

178. M. R. Romano, *Density, viscosity and surface tension for the choice of new tamponades*, Mediterretina, April 14-15, **2011**, Ravenna, Italy.
179. S. Zenoni, *Heavier than water: HeavySIL 1500-injection technique*, Present and Future challenges in severe retinal disease, February 4-5, **2011**,Verona, Italy.
180. D. Weihs, D. Danino, R. Zana, G. Orädd, G. Lindblom, M. Abe, Y. Talmon, *J. Colloid Interface Sci.*, **2003**, 259, p: 382-390.
181. F. Claudi, G. Giorgioni, L. Scoccia, R. Ciccocioppo, I. Panocka, M. Massi, *Eur. J. Med. Chem.*, **1997**, 32, p: 651-659.
182. L. B. Rice, *Clin. Infect. Dis.*, **2006**, 43, p: 100-105.
183. M. Shinoda, K. Hato, T. Hatashi, *J. Phys. Chem.*, **1972**, 76, p: 909-914.
184. A. Gonzales-Perez, E. Blanco, J. M. Ruso, R. Pedrido, G. Prieto, F. Sarmiento, *J. Colloid Interface Sci.*, **2005**, 288, p: 247–260.
185. B. Pitts, T. F. Mah, B. Pellock, G. C. Walker, P. S. Stewart, G. A. O'Toole, *Nature*, **2003**, 246, p: 306-310.
186. D. Myers, *Surfaces, Interfaces and Colloids: Principles and Applications*. ed. Wiley-Vch, **1999**, Weinheim, p: 358-396.
187. E. A. Ghazyb, M. Z. Mohamed, A. M. Badawia, N. G. Kandilc, *J. Surfactants Deterg.*, **2005**, 8, p: 181-185.
188. R. Bertocchio, A. Lantz, *Prog. Colloid Polym. Sci*, **1987**, 81, p: 136-139.
189. S. Hartland, *Surface and interfacial tension: measurement, theory and applications*, M. Ekkerin, **2004**, New York, p: 1-1500.
190. J. F. McBride, C. S. Simmons, J. W. Cary, *J. Contam. Hydrol.*, **1992**, 11, p: 1-25.
191. G. Padoan, *Thesys: sintesi e impiego di tensioattivi fluorurati per la formulazione di schiume antincendio,* **2006,** University of Padua**.**
192. H. S. Fogler, K. R. Srinivasan, *Clay. Clay. Miner.*, **1990**, 38, p: 277-286.
193. A. Di Gianni, R. Bongiovanni, L. Conzatti, S. Turri, *J. Colloid Interface Sci.*, **2009**, 336, p: 455-461.
194. G. Lagaly, *Layer charge determination by alkylammonium ions,* ed. A.R. Mermut, **1994,** p: 2-46.
195. E. Manias, E. Hackett, E. P. Giannelis, *J . Chem. Phys.*, **1998,** 108, p: 7410-7415.
196. B. K. Theng, *The Chemistry of Clay-Organic Reactions*. ed.Wiley, **1974**: London, p: 1-343.
197. D. L. Sparks, Z. Z. Zhang, N. C. Scrivner, *Environ. Sci. Technol.*, **1993**, 27, p: 1625-1631.

198. W.A. Jacobs, *J. Exp. Med.*, **1916**, 23, p: 563-568.
199. W. A. Jacobs, M. Heidelberger, *J. Biol. Chem.*, **1915**, 20, p: 659-683.
200. G. Dogmak, *Dtsch. Med. Wochenschr*, **1935**, 61, p: 829-832.
201. O. T. Uneskans, M. S. Karabit, P. Lundgren, *Int. J. Pharm.*, **1988**, 46, p: 141-147.
202. B. Brycki, A. Skrzypczak, I. Mirska, J. Pernak, *Eur. J. Med. Chem.*, **1997**, 32, p: 661-668.
203. X-L. Qiu, J-Y. Sun, W-D .Meng, F-L Qing, *Tetrahedron*, **2006**, 62, p: 8702-8706.
204. I. Mirska, J. Pernak, R. Kmiecik, *Eur. J. Med. Chem.*, **1999**, 34, p: 765-771.
205. A. Saeed, U. Shaheen, A. Hameed, S. Z. Haider Naqvi, *J. Fluorine Chem.*, **2009**, 130, p: 1028-1034.
206. H. M. Choi, Y. H. Kim, J. H. Yoon, *Text Res. J.*, **1998**, 68, p: 428-434.
207. I. Perillo, E. Repetto, M. C. Caterina, R. Massa, G. Gutkind, A. Salerno, *Eur. J. Med. Chem.*, **2005**, 40, p: 811-815.
208. R. J. Ward, S. Krishnan, A. Hexemer, K. E. Sohn, K. L. Lee, E. R. Angert, D. A. Fischer, E. J. Kramer, C. K. Ober, *Langmuir*, **2006**, 22, p: 11255-11266.
209. J-Y. Sun, J. Li, X-L. Qui, F-L Qing, *J. Fluorine Chem.*, **2005**, 126, p: 1425-1431.
210. S-x L. Zhang, Y. Lin, C-s. Chi, *J. Fluorine Chem.*, **1991**, 54, p: 201-206.
211. L. Massi, F. Guittard, S. Géribaldi, R. Levy, Y. Duccini, *Int. J. Antimicrob. Agents*, **2003**, 21, p: 20-26.
212. L. Massi, F. Guittard, R. Levy, Y. Duccini, S. Géribaldi, *Eur. J. Med. Chem.*, **2009**, 44, p: 1615-1622.
213. L. Massi, F. Guittard, R. Levy, Y. Duccini, S. Géribaldi, *Eur. J. Med. Chem.*, **2003**, 38, p: 519-523.
214. L. Callier, E. Taffin de Givenchy, R. Levy, Y. Vandenberghe, S. Géribaldi, F. Guittard, *Eur. J. Med. Chem.*, **2009**, 44, p: 3201-3208.
215. J. Mao, *Process for the treatment of nonwoven with antimicrobial agents.*, **1999,** EP09377812A2.
216. W. B. Hugo, *Sterilization and Disinfection*, **1975**, p: 187–276.
217. J. J. Merianos, *Disinfection, Sterilization, and Preservation*, S. S. Block, Editor **2001**, Lea & Febiger: Philadelphia, p. 283-320.
218. M. Frier, W. B. Hugo, *Appl. Microbiol.*, **1969**, 17, p: 118-127.
219. S. P. Denyer, G. S. A. B. Stewart, *Int. Biodet. Biodegrad.*, **1998**, 41, p: 261-268.

220. W. B. Hugo, D. Russell, G. A. J. Ayliffe, *Principles and practice of disinfection, preservation and sterilization, 4rd ed.*, Blackwell Science, **2004**: Oxford, England, p: 1-361.
221. M. Frobisher, *J. Bacteriol.*, **1926**, 13, p: 163-182.
222. C. E. Kwartler, S. Ross, J. H. Bailey, *J. Colloid Sci.*, **1953**, 8, p: 385-401.
223. A. Kopecka-Leitmanova, F. Devinsky, F. Sersen, P. Balgavy, *J. Pharm. Pharmacol.*, **1990**, 42, p: 790-794.
224. S. Langsrud, G. Sundheim, E. Heir, A. L. Holck, *Int. Biodet. Biodegrad.*, **1998**, 41, p: 235-239.
225. C. Bassilana, B. Martin, A. Cambon, *J. Fluorine Chem.*, **1998**, 92, p: 109-117.
226. L. Conte, F. Maniero, A. Zaggia, R. Bertani, G. Gambaretto, A. Berton, R. Seraglia, *J. Fluorine Chem.*, **2005**, 126, p: 1274-1280.
227. T. Darmanin, *Thesis, structuration de surface par voie electrochimique:preparation et applications*, **2008,** University of Nice Sophia Antipolis.
228. S. Ogiri, K. Esumi, *Colloids Surf. A*, **1995**, 94, p: 107-110.
229. M. J. Rosen, *Surfactants and interfacial phenomena*. ed. Wiley-Vch, **2004**: Hoboken, New Jersey, p: 1-444.
230. C. Jungnickel, J. Łuczak, M. Joskowska, J. Thoming, J. Hupka, *J. Colloid Interface Sci.*, **2009**, 336, p: 111-116.
231. T. F. Tadros, *Applied surfactants: principles and applications*. ed. Wiley-Vch, **2005**: Weinheim, p: 1-634.
232. K. S. Sharma, P. A. Hassan, A. K. Rakshit, *Colloids Surf. A*, **2006**, 289, p: 17-24.
233. S. M. Mercer, E. Sutherland, M. Everist, D. G. Leaist, *J. Chem. Eng. Data*, **2009**, 54, p: 272-278.
234. A. Ohno, T. Yoshimura, K. Esumi, *Langmuir*, **2006**, 22, p: 4643-4648.
235. G. Ghosh, U. S. Siddiqui, Kabir-ud-Din, *Langmuir*, **2006**, 22, p: 9160-9168.
236. E. W. Kaler, R. Zana, *Giant Micelles. Properties and Applications*, **2007**, Taylor & Francis Group: New York, p: 1-554.
237. R. H. Ottewill, P. Taylor, *Colloids Surf. A*, **1994**, 88, p: 303-316.
238. E. Hirsch, S. J Candau, R. Zana, M. Adam, *J. Colloid Interface Sci.*, **1988**, 122, p: 430-440.
239. J. J. Cai, Z. Lin, L. E. Scriven, H. T. Davis, *J. Phys. Chem.*, **1994**, 98, p: 5984- 5993.
240. J. Eastoe, K. Trickett, *Adv. Colloid Interface Sci.*, **2008**, 144, p: 66-74.
241. S. J. Candau, M. E. Cates, *J. Phys. Condens. Matter*, **1990**, 2, p: 6869-6892.

242. M. E. Cates, *J. Phys. France*, **1988**, 49, p: 1593-1600.
243. M. Hellsten, *J. Surf. Detergents*, **2001**, 4, p: 65-70.
244. Y. Wang, H. Shi, B. Fang, Y. Talmon, W. Ge, S. R. Raghavan, J. L. Zakin, *Langmuir*, **2011**, 27, p: 5806-5813.
245. M. Hollamby, J. Eastoe, L. Hudson, *Adv. Colloid Interface Sci.*, **2006**, 128-130, p: 5-15.
246. G. C. Maitland, *Curr. Opin. Colloid Interface Sci.*, **2000**, 5, p: 301-311.
247. G. Waton, Cl. Oelschlaeger, E. Buhler, S. J. Candau, M. E. Cates, *Langmuir*, **2002**, 18, p: 3076-3085.
248. M. Schopferer, C. Oelschlaeger, F. Scheffold, N. Willenbacher, *Langmuir*, **2009**, 25, p: 716-723.
249. A. Ohno, T. Yoshimura, K. Esumi, *Langmuir*, **2006**, 22, p: 4643-4648.
250. I. W. Hamley, *Introduction to Soft Matter, 2nd ed.*, ed. Wiley, **2007**: New York, p: 200-204.
251. F. Lequeux, F. Kern, R. Zana, S. J. Candau, *Langmuir*, **1994**, 10, p: 1714-1723.
252. Y. Qiao, Y. Lin, Y. Yan, J. Huang, *Soft Matter*, **2009**, 5, p: 3047-3053.
253. National Committee on Clinical Laboratory Standards (NCCLS), **2003**.

7 Acnowledgements

It is a pleasure to thank many people who made this dissertation possible.

I am forever thankful to my father, my mother, my brother for their support and encouraging in these years.

I want to thank my Italian supervisor, Prof. Lino Conte to give me the possibility to conduct this doctoral work.

To Alessandro Zaggia, I would like to express my greatest gratitude and sincere thanks for all you have done especially for the great supervision during this work.

I also wish to express my warm gratitude to all the Italian graduate students who have worked and are still working in Italian lab. I wish to express special thank to Flavio Ceretta, my colleague PhD student, for their great help and patience in these years.

I wish to express my sincere thank to my French supervisor, Prof. Frederic Guittard, to receive me in his team. His understanding and encouraging guidance have provided a good basis for the present dissertation.

To Dr. Elisabeth Taffin de Givenchy, Dr. Sonia Amigoni, Dr. Thierry Darmanin, I am very grateful for their help. They have always been available all the time to help in every way to make things work, provide suggestions and ideas, chemicals, instruments form of my program research.

I wish to express special thank to Elena, Arnaud, Hervé, Mamadou, Alioune, Mélanie, Jeanne, Chahinez, Matthieu, Carine for the friendly work atmosphere and for their help in every way in my French stay. I want also to thank them to teach me French language and for the wonderful time always in a warm atmosphere.

I am very grateful to physical group “Fluides et Matériaux Complexes” (L.P.M.C) for their great help and assistance with the instruments.

I thank Dr. Geoges Bossis and Olga Volkova to give me the possibility to use the instruments of their laboratory.

To Audrey, Juan, Romain, Pavel, Pascal thank you very much for the wonderful time in the laboratory and outside.

To my grand-mother Giorgina that look at me by the sky, for her encouraging in all University's career.

To all my relatives, thank you for believing in me.

Many thanks to my Italian friends who have been so wonderful and supportive, thank you very much for the prayers and support throughout this work.

I wish to express my sincere thank to Prof. Alberto Bertucco, Chair of the Doctoral School of Chemical Engineering at Padua University, for his help with my problems during the change program.

I also thank Catherine Briet, French secretary staff, for her precious work and her warm friendship.

Thank you very much to M. C. Aguilar, J. M. Parel and al. of Department of Ophthalmology, Ophthalmic Biophysics Center, Bascom Palmer Eye Institute, University of Miami to have performed in vivo tests.

Thank you very much also to J. Brunneliere of Centre de Transfert de Technologie du Mans - Pôle Ingénierie Biologique et Médicale (Le Mans, France) to have performed antibacterial tests.